The Role of Leaf Senescence in Relation to Nitrogen Uptake and Translocation to the Reproductive Plant Organs for Cultivar Differences in Nitrogen Efficiency in Winter Oilseed-Rape (*Brassica napus* L.)

Von der Naturwissenschaftlichen Fakultät
der Gottfried Wilhelm Leibniz Universität Hannover

zur Erlangung des Grades
Doktor der Naturwissenschaften (Dr. rer. nat.)

genehmigte Dissertation
von

M. Sc. Fabian Köslin-Findeklee
geboren am 08. November 1984 in Hamburg

2015

Referent: Prof. Dr. Walter Johannes Horst

Korreferent: Prof. Dr. Nicolaus von Wirén

Korreferent: Prof. Dr. Thomas Roitsch

Tag der Promotion: 05.02.2015

Zusammenfassung

Winterraps (*Brassica napus* L.) ist die bedeutendste landwirtschaftlich genutzte Ölpflanze in den Ländern Nordeuropas sowie der kaltgemäßigten Klimazone weltweit. Winterraps ist jedoch eine der Feldkulturen mit sehr hohen Stickstoff (N)-Bilanzüberschüssen. Diese beruhen auf einer niedrigen N-Aufnahme während der reproduktiven Phase und hohe N-Mengen in den Ernterückständen, bedingt durch eine unvollständige N-Verlagerung in die Körner. Dies hat negative Folgen für die Umwelt, da nicht genutzter N zur erhöhten Freisetzung von umweltschädlichen reaktiven N-Verbindungen führt. Eine Reduktion der hohen Bilanzüberschüsse ist zunehmend Ziel restriktiver gesetzlicher Vorgaben. Aber auch aus ökonomischen Gründen (Kostenersparnis beim N-Düngereinsatz) ist eine Reduktion sinnvoll. Ein wirkungsvoller Ansatz, ohne negative Auswirkungen auf das aktuelle Ertragsniveau, ist die Reduzierung der N-Düngung durch die Kultivierung von N-effizienten Genotypen/Kultivaren mit hohem Kornertrag unter N limitierenden Bedingungen. Durch langjährige Vorarbeiten ist bekannt, dass die N-Effizienz von Winterraps Linienkultivaren hauptsächlich auf einer während der reproduktiven Phase, insbesondere während der Blüte, andauernden N-Aufnahme beruht (N-Aufnahmeeffizienz). Ein Charakteristikum solcher Kultivare ist eine verzögerte Seneszenz der älteren Blätter einhergehend mit einer aufrechterhaltenen photosynthetischen Aktivität (Functional Stay-Green).

Ziel dieser Arbeit war es **(I)** Unterschiede in der N-Effizienz zwischen Sortentypen (Linien, Hybride und Zwerge) zu identifizieren und die Bedeutung der N-Aufnahme und -Nutzungseffizienz sowie von Functional Stay-Green für Unterschied in der N-Effizienz zu bestimmen **(II)** Markergene zu selektieren, die nicht nur N-Mangel spezifisch reguliert sind, sondern auch geeignet sind, genotypische Unterschiede in der N-Mangel induzierten Blattseneszenz bereits zu frühen Seneszenzstadien zu detektieren **(III)** mittels reziproker Kreuzung zweier Sortenpaare, die sich in der N-Effizienz und der N-Mangel induzierten Blattseneszenz unterscheiden, zu klären, ob genotypische Unterschiede in Functional Stay-Green unter N-Mangel auf blattinhärenten Faktoren und/oder auf wurzelvermittelten Signalen beruhen **(IV)** den Beitrag der N-Retranslokation und -Aufnahme während der reproduktiven Phase zur N-Effizienz von Kultivaren mit unterschiedlichem Functional Stay-Green Phänotyp zu bestimmen als auch die Hauptquellen der N-Mengen in den Ernterückständen zu identifizieren.

Folgende zentrale Ergebnisse wurden erzielt:

(I) Die Hybriden waren den Linien- und Zwergsorten in der Ertragsbildung unabhängig vom N-Angebot überlegen. Der Anbau von Zwergsorten führte zu keiner Verbesserung der N-Effizienz von Winterraps. Die hohe N-Effizienz der Hybriden war verbunden mit einer hohen N-Aufnahme bis zur Reife, jedoch nicht mit Functional Stay-Green. Zudem zeichneten sich die Hybriden durch eine

effiziente N-Retranslokation von den vegetativen zu den generativen Pflanzenorganen in Kombination mit einer geringeren Proteinkonzentration im Korn aus. Somit waren für die hohe N-Effizienz der Hybriden sowohl N-Aufnahmeeffizienz als auch N-Verwertungseffizienz von Bedeutung.

(II) Die globale Genexpressionsanalyse der Blätter vier Tage nach Stressinduktion ergab ein N-Mangel spezifisches Programm im Vergleich zu durch Schattierung oder Abschneiden einzelner Blätter induzierter Blattseneszenz. Insbesondere Gene des N-Metabolismus, der Photosynthese und der Photorespiration wurden N-Mangel spezifisch größtenteils herunterreguliert. Hingegen N-Mangel spezifisch vorwiegend heraufreguliert wurden Gene der Flavonoidbiosynthese und der mitochondrialen Elektronentransportkette. Unter den N-Mangel spezifisch heraufregulierten Genen konnten sechs Markergene identifiziert werden, die bereits zu frühen Stadien genotypische Unterschiede in der Blattseneszenz anzeigten.

(III) Genotypische Unterschiede in der N mangelinduzierten Blattseneszenz beruhten auf blattinhärenten Faktoren. Übereinstimmend damit ergab die Analyse von Cytokininen unterschiedlicher biologischer Aktivität und die Regulation von Genen der Cytokininhomöostase, Bindung und Signaltransduktion, dass für genotypische Unterschiede in Functional Stay-Green während der N-Mangel induzierten Blattseneszenz die blattinhärente Inaktivierung von biologisch aktiven Cytokininen in früh seneszierenden und die Synthese und Wirkung biologisch aktiver Cytokinine in Functional Stay-Green Kultivaren von großer Bedeutung sind.

(IV) Bei stark limitiertem N-Angebot beruhten genotypischen Unterschiede in der N-Effizienz hauptsächlich auf der N-Aufnahme während der reproduktiven Phase (N-Aufnahmeeffizienz). Zudem wiesen Kultivare mit einer hohen N-Aufnahmekapazität nach der Vollblüte eine verzögerte Blattseneszenz auf. Die verbleibenden N-Mengen in den Ernterückständen beruhten unabhängig von der Höhe des N-Angebotes hauptsächlich auf den verbleibenden N-Mengen in den Schotenwänden und Stängeln. Darüber hinaus zeigte sich, dass nicht die N-Retranslokation von den vegetativen in die generativen Organe der begrenzende Faktor für die verbleibenden N-Mengen in den Ernterückstanden war, sondern die unvollständige Verlagerung von den Schotenwände in die Rapskörner innerhalb der Rapsschote.

Zusammengefasst kann aus den Ergebnissen gefolgert werden, dass die N-Aufnahmeeffizienz nicht nur generell von großer Bedeutung für genotypische Unterschiede in der N-Effizienz zwischen Sorten und Sortentypen ist, sondern diese auch bei ausgeprägter N-Limitierung zunimmt. Unter letzteren Bedingungen gewinnt die Bedeutung eines Functional Stay-Green Phänotypen für die N-Effizienz an Bedeutung. Bereits zu frühen Stadien der Seneszenz sind eine Vielzahl von Genen N-Mangel spezifisch reguliert, wobei genotypische Unterschiede in der N Mangel induzierten Blattseneszenz auf blattinhärenten Faktoren beruhen.

Schlagwörter: Winterraps, genotypische Unterschiede, Stickstoffeffizienz

Abstract

Winter oilseed-rape (*Brassica napus* L.) is the most important oil crop in the countries of northern Europe as well as the cold temperate climate zone worldwide. But winter oilseed-rape is a crop with high nitrogen (N)-balance surpluses, which result from a low N uptake during the reproductive phase and high N amounts remaining in the crop residues due to an incomplete N retranslocation into the grains. This has negative consequences for the environment because the not used N leads to increased release of environmentally harmful reactive N compounds. A reduction of the high surpluses is increasingly target of restrictive legal requirements. But also for economic reasons (cost savings in N fertilizer use) a reduction is meaningful. A promising approach without compromising the current yield level is the reduction of the N fertilization by the cultivation of N-efficient genotypes/cultivars with high grain yield under N-limited conditions. From previous work of many years it is known, that N efficiency of winter oilseed-rape line-cultivars primarily is based on a maintained N uptake during the reproductive phase, particularly during flowering (N uptake efficiency). A characteristic of such cultivars is a delayed senescence of the older leaves accompanied by maintained photosynthetic activity (functional stay-green).

The objective of the work was **(I)** to identify differences in the N efficiency between cultivar types (lines, hybrids and dwarfs) and to determine the contribution of N uptake and N utilization as well as functional stay-green to differences in N efficiency, **(II)** to identify and select marker genes, which are not only N starvation specifically regulated, but also suitable to detect cultivar differences in N starvation-induced leaf senescence at early senescence stages, **(III)** to clarify by reciprocal grafting of two cultivar pairs which differ in N efficiency and N starvation-induced leaf senescence, whether cultivar differences in functional stay-green under N starvation are based on leaf-inherent factors and/or governed by root-mediated signals, and **(IV)** to determine the contribution of N retranslocation and uptake during reproductive growth for the N efficiency of cultivars with different functional stay-green phenotype, and to identify the main sources for the remaining N amounts in the crop residues.

The following central results have been obtained:

(I) Hybrids were superior in yield formation to the line and dwarf cultivars independent of the N supply. The cultivation of dwarf cultivars did not enhanced the N efficiency of winter oilseed-rape. The greater N efficiency of the hybrids was related to a higher N uptake until maturity, but not to functional stay-green. Moreover, the hybrids were characterized by an efficient N retranslocation from vegetative to reproductive plant organs in combination with a lower grain-N (protein) concentration. Both, N uptake and N utilization efficiency were decisive for the superior N efficiency of the hybrids.

(II) The global transcriptomic analysis of the leaves four days after stress induction revealed an N starvation-specific program compared to leaf senescence induced by shading or detaching. In particular, genes assigned to the N metabolism, photosynthesis and photorespiration were N starvation specifically mostly down-regulated, whereas N starvation specifically mostly up-regulated were genes of the flavonoid biosynthesis and mitochondrial electron transport. Among the N starvation specifically up-regulated genes six genes could be identified which were suitable to detect cultivar differences in leaf senescence already at early stages.

(III) Cultivar differences in N starvation-induced leaf senescence were based on leaf-inherent factors. In accordance to this, the analysis of cytokinins differing in biological activity and the regulation of genes assigned to cytokinin homeostasis, perception and response revealed that for genotypic differences in functional stay-green during N starvation-induced leaf senescence, in the early-senescing cultivars the leaf-inherent inactivation and in the functional stay-green cultivars the synthesis and action of biologically active cytokinins were of major importance.

(IV) Under severely limiting N supply genotypic differences in N efficiency were primarily based on N uptake during the reproductive phase (N uptake efficiency). A characteristic of cultivars with a high N uptake capacity after full flowering was delayed leaf senescence. Independent of the N supply the N in the pod walls and stems mainly contributed to the N amounts remaining in the crop residues. Thus not the N retranslocation from the vegetative to generative organs was the limiting factor for the high N amounts remaining in the crop residues, but the incomplete retranslocation from the pod walls into the grains within the pods.

It can be concluded from the results, that N uptake efficiency is not only generally of major importance for genotypic differences in N efficiency between cultivars as well cultivar types, but also increases in importance with the severity of N limitation. Under the latter conditions a functional stay-green phenotype for N efficiency increases in importance. Already at early leaf senescence stages numerous genes were N starvation specifically regulated. Cultivar differences in N starvation-induced leaf senescence were based on leaf-inherent factors.

Keywords: winter oilseed-rape, genotypic differences, nitrogen efficiency

Table of Contents

Abbreviations

+	Statistically significant to p <0.10
*	Statistically significant to p <0.05
**	Statistically significant to p <0.01
***	Statistically significant to p <0.001
ABA	Absisic acid
aCK(s)	Biologically active cytokinin(s)
ANOVA	Analysis of variance
AMT	Ammonium transporter
ANS	Anthocyanidin synthase
BBCH	Biologische Bundesanstalt, Bundessortenamt und Chemische Industrie
CAO	Chlorophyll α oxygenase
Chl	Chlorophyll
CK(s)	Cytokinin(s)
CKX	Cytokinin oxidase
cv(s).	Cultivar(s)
cZ	*cis*-Zeatin
DAF	Days after flowering
DAFF	Days after full flowering
DAT	Days after start of treatment
DH	Doubled haploid
DHZ	Dihydrozeatin
DFCI	Dana-Farber cancer institute
DREB	Dehydration responsive element binding
DFR	Dihydroflavonol 4-reductase
ELF	Early flowering
FAOSTAT	Food and agriculture organization corporate statistical database
FC	Fold change
GARP	GOLDEN2, *Arabidopsis* response regulator proteins, *Chlamydomonas* Psr1 protein

HI	Harvest index
HK	Histidine kinase
HPLC	High performance liquid chromatography
iCK(s)	Biologically inactive but activatable cytokinin(s)
iP	Isopentenyladenin
IPT	Isopentenyltransferase
JA	Jasmonic acid
LOG	Lonely guy
MACE	Massive analysis of cDNA ends
MS	Mass spectrometer
MSD	Minimum significant difference
n	Group size
n	Number of biological replicates
NAC	No apical meristem / *Arabidopsis* transcription activation factor / Cup-shaped cotyledon)
NCBI	National center for biotechnology information
NHI	Nitrogen harvest index
NIRS	Near infrared reflectance spectroscopy
NPZ	Norddeutsche Pflanzenzucht Hans-Georg Lembke KG
NRT	Nitrate transporter
ns	Statistically non-significant
NUE	Nitrogen utilization efficiency
NUPT	Nitrogen uptake efficiency
PAR	Photosynthetic active radiation
PC	Principal component
PCA	Principal component analysis
PCD	Programmed cell death
PCR	Polymerase chain reaction
QTL	Quantitative trait locus
qRT	Quantitative real-time

r^2	Coefficient of determination
RAP	RNA-binding domain abundant in apicomplexans
RE	Relative expression
RQ	Relative quantification
RR	Response regulator
SA	Salicylic acid
SAG	Senescence-associated gene
SGR	Stay-green
SPAD	Soil and plant analyze developments
SPS	Sucrose-phosphate synthase
TAIR	The Arabidopsis information resource
TF	Transcription factor
tZ	*trans*-Zeatin
tZOG	*tran*s-Zeatin-*O*-glucosid
tZOGR	*trans*-Zeatin-*O*-glucosid-ribosid
tZR	*trans*-Zeatin-ribosid
UDP	Uridine diphosphate
UGT	UDP-glycosyltransferase
UPLC	Ultra high performance liquid chromatography
UPS	Ureide permease
USDA	United States department of agriculture

General Introduction

Winter oilseed-rape (*Brassica napus* L.)

Winter oilseed-rape (*Brassica napus* L.) belongs to the family of the *Brassicaceae* and is an allopolyploid hybrid (1n = 19) of a bastardization between turnip rape (*B. rapa* L. ; 1n = 10) and cabbage (*B. oleracea* L. ; 1n = 9) (Downey & Rimmer, 1993). For *B. napus* summer as well as winter cultivars existing. In temperate zones of Europe and China primarily the winter form is cultivated. Whereas in the dry areas of Australia and the cooler areas of Europe and Canada the summer form is most frequently grown (Berry & Spink, 2006). Due to its high oil content in the grains *B. napus* is grown as an oil crop. It is the most important oil crop in European agriculture. Winter oilseed-rape is a two years culture. In temperate zones of Western-Europe it is commonly sown in August to September and harvested in the following year in June to July. This crop is not only valuable for interrupting cereal-dominated crop-rotations but also a favorable crop to precede winter wheat in the rotation (Sieling *et al.,* 2005).

The harvested grain is crushed to give oil primarily for human consumption or the synthesis of biodiesel. The remaining protein-rich grain meal is a valuable animal feed (Wittkop *et al.,* 2009). But the attractiveness of cultivating *B. napus* was limited for a long time, due to the high erucic acid and glucosinolate contents of the grains. The extracted oil was hardly suitable for foodstuffs as well as the remaining rapeseed cake as animal feed. Therefore, the oil was primarily used as a lubricant or lamp oil. The high erucic acid content caused an abnormal number of heart lesions in animals. No such effects have been recorded in humans, but nevertheless the oil was considered to be harmful for human nutrition. The situation changed in the 1960s when Canadian researchers developed varieties with an altered grain fatty acid pattern showing low erucic acid contents. Today, cultivars with an erucic acid proportion less than two percent of the measured total fatty acids are referred as “single-low” or “0”. 0-varieties produce a healthy food oil of enhanced value. And in the 1980s cultivars with additionally low glucosinolate content were developed. The defatted meal of the so called “double-lows” or “00” is a valuable animal feed. Up to this time the meal could only be fed to livestock in small quantities, because the high glucosinolate content inter alia harmed the thyroid gland (Ward *et al.,* 1985; Booth & Gunstone, 2004).

Thus, *B. napus* is a good example for the opportunities and progress of breeding on quality. Until today further types of varieties have been developed for special purposes. The characteristics of the “Holli” varieties are a modified fatty acid pattern. Due to the high oleic and low linoleic acid content, the oil is highly heat-stable and consequently less harmful trans-fatty acids arise during heating (Barth, 2009).

Oilseed-rape production

The designation oilseed rape is not unambiguous. Worldwide four agronomically important *Brassica* species are cultivated as oilseed-rape crops: *B. napus*, *B. rapa*, *B. juncea* and *B. carinata* (Berry & Spink, 2006). Since between and within the species often no clear distinction is made the term oilseed rape comprises the four species in the following.

Oilseed-rape production worldwide increased by 18-fold over the past decades from the early 1960s until today (FAOSTAT, 2013). The current world production (grain harvest) accounted to 64,813 kt (Table 1). With worldwide oil production of 23,798 kt in 2012/13 oilseed-rape oil is currently the third most important vegetable oil (USDA, 2013). Although oilseed rape is cultivated on every continent the majority is produced in only few countries. The major producers are Canada (15,410 kt) and China (14,000 kt) with nearly half of the world production. In Europe the major oilseed rape producing countries are France (5,463 kt), Germany (4,821 kt) and the United Kingdom (2,557 kt) (Table 1). Currently oilseed rape is cultivated worldwide on 34,257,051 ha, led by Canada (8,379,900 ha) followed by China (7,300,000 ha) and India (5,920,000 ha) (Table 1). Principally the locations with the highest production quantities also have the greatest cultivation areas. But the grain yields reveal substantial differences between the continents and countries in their productivity. Particularly the grain yield of the major producers in Europa with 3.4 to 3.7 t ha^{-1} nearly doubles the world average. In Canada (1.8 t ha^{-1}) and China (1.9 t ha^{-1}) the productivity is equal to the world average or slightly lower (Table 1). The reasons for the variation in the productivity are manifold. Water and nutrient availability as well as chemical crop protection are undeniable important for exploiting the yield capacity (Ward *et al.,* 1985; Booth & Gunstone, 2004). But the most decisive factor for explaining the significant lower yields in Northern-America and Australia compared to Western-Europe is not the intensity of crop management, but rather the cultivated form. In general, the winter cultivars of *B. napus* have a higher yield capacity and actual yields than the summer cultivars or other *Brassica* species (Berry & Spink, 2006).

Hence, due to the high suitability of the oil for both human nutrition and for use as a biofuel oilseed-rape production will continue to increase in the future and thus become one of the major global oil crops.

Table 1 Oilseed-rape production (grain harvest), harvested area and average grain yield in 2012 worldwide, for each continent and selected countries with a proportion of more than 1% of the world production (FAOSTAT, 2013). The sorting is according to the production quantity.

Continent / Country	Production (grain harvest)		Harvested area		Grain yield	
	[kt]	[%]	[ha]	[%]	[t ha^{-1}]	[%]
World	**64,813**	**100.0**	**34,257,051**	**100.0**	**1.9**	**100.0**
Europe	**22,356**	**34.5**	**8,239,855**	**24.1**	**2.7**	**143.4**
France	5,463	*8.4*	1,607,186	*4.7*	*3.4*	*179.8*
Germany	4,821	*7.4*	1,306,200	*3.8*	*3.7*	*195.3*
United Kingdom	2,557	*3.9*	756,000	*2.2*	*3.4*	*179.0*
Asia	**21,928**	**33.8**	**14,262,139**	**41.6**	**1.5**	**81.5**
China	*14,000*	*21.6*	*7,300,000*	*21.3*	*1.9*	*101.5*
India	*6,776*	*10.5*	*5,920,000*	*17.3*	*1.1*	*60.6*
Northern-America	**16,522**	**25.5**	**9,080,460**	**26.5**	**1.8**	**96.3**
Canada	*15,410*	*23.8*	*8,379,900*	*24.5*	*1.8*	*97.3*
United States of America	*1,112*	*1.7*	*700,560*	*2.0*	*1.6*	*84.0*
Australia	**3427**	**5.3**	**2,358,735**	**6.9**	**1.5**	**76.7**
South-America	**374**	**0.6**	**201,215**	**0.6**	**1.9**	**98.4**
Africa	**203**	**0.3**	**111,967**	**0.3**	**1.8**	**95.8**

Nitrogen efficiency

The application of mineral N fertilizers has significantly contributed to the increased productivity of agriculture. About 50% of the yield increase during the last century was based on the application of chemical fertilizers (Borlaug & Dowswell, 1994). But a meaningful ongoing increase of crop yields will not be reachable by an increase of the amount applied. The doubling of the world food production from the 1960s until the turn of the millennium was accompanied by a nearly seven-fold increase in the global annual rate of N fertilization. But for doubling again the recent mineral N application has to triple (Tilman, 1999). Thus the breeding and cultivation of N-efficient crop plants will play a major role in increasing yields in the future. Above all, only less than half of the fertilized N is taken up by the crop plants (Craswell & Godwin, 1984; Raun & Johnson, 1999). The surplus N may cause environmental pollution mainly due to nitrate transport into ground and surface waters. Furthermore, enhanced nitrous oxide emission into the atmosphere contributes to global warming.

Genetic variation in N efficiency is known for almost 90 years (Hoffer, 1926). Nevertheless, today discussions about N efficiency are difficult, because there are different definitions and not only one valid overall accepted definition is available (Fageria *et al.,* 2008). In the present work N efficiency is defined according to Graham (1984) and Sattelmacher *et al.* (1994) as the ability of a genotype/cultivar to achieve a high grain yield under conditions of limited N supply. Nitrogen

efficiency is principally based on two components (I) the effectiveness of a cultivar in absorbing N from the soil (N uptake efficiency; NUPT) and/or (II) the efficiency with which the N are utilized to produce yield (N utilization efficiency; NUE). Due to the complexity of N efficiency the grain yield is a suitable and an often chosen agronomic trait to determine N efficiency (Sattelmacher *et al.,* 1994). The selection should be carried out under N-limited conditions, since N responsive cultivars are not necessarily N-efficient and vice versa (Blair, 1993). The ranking of cultivars for N efficiency depends on the severity of the N deficiency stress. Generally, with increasing strength of the N deficiency stress (percent yield decline under N deficiency compared to the N-sufficient control) the coefficient of genotypic correlation between deficient and sufficient N decreases (Bänzinger *et al.,* 1997; Bertin & Gallais, 2000; Presterl *et al.,* 2003; Worku *et al.,* 2007; Berry *et al.,* 2010; Schulte auf'm Erley *et al.,* 2011). Moreover, the relative contribution of NUPT and NUE to N efficiency depends on the severity of N limitation in additions to the crop species (Moll *et al.,* 1982; Wiesler *et al.,* 2001; Presterl *et al.,* 2003).

Nitrogen efficiency in winter oilseed-rape

Winter oilseed-rape crops require about 200 kg N ha^{-1} to obtain an optimum grain yield. (Rathke *et al.,* 2006). But even under best agronomic practice a grain yield of 4.5 t ha^{-1} causes a surplus of around 60 kg N ha^{-1}. The high crop-specific N balance surpluses are based on an incomplete depletion of plant available soil-N by the crop due to a terminated N uptake after transition into the reproductive phase and substantially amounts of N remaining in the crop residues owing to an incomplete retranslocation of N from vegetative plant organs into the grains (Aufhammer *et al.,* 1994; Lickfett *et al.,* 2001).

A promising approach to reduce the high crop-specific N balance-surpluses without compromising the current grain yields is the breeding and cultivation of N-efficient cultivars (Wiesler *et al.,* 2001; Sylvester-Bradley & Kindred, 2009). Genetic variation in N efficiency (high grain yield under N imitation) in winter oilseed-rape is well known (Wiesler *et al.,* 2001; Behrens, 2002; Kamh *et al.,* 2005; Schulte auf'm Erley *et al.,* 2007; Ulas, 2010; Schulte auf'm Erley *et al.,* 2011; Ulas *et al.,* 2012) and could be primarily attributed to maintained N uptake during reproductive growth, particularly during flowering (NUPT) (Behrens, 2002; Kamh *et al.,* 2005; Schulte auf'm Erley *et al.,* 2011; Ulas *et al.,* 2012). For a high NUPT in winter oilseed-rape a high root growth and consequently the formation of a large root system is of major importance (Kamh *et al.,* 2005; Ulas *et al.,* 2012). Particularly the exploitation of deeper soil layers enhancing the acquisition of subsoil nitrate appears to be decisive for improving NUPT (Kamh *et al.,* 2005).

In contrast the contribution of NUE to N efficiency in winter oilseed-rape is low (Berry *et al.,* 2010; Schulte auf'm Erley *et al.,* 2011). Moreover, from the crop N-balance and grain quality point of view a high N efficiency through improved NUE is not desired, because a physiological trait which may contribute to NUE is a low grain N concentration and thus low grain protein concentration. A lower N requirement for grain formation will not reduce the amount of N remaining in the crop residues, because a high N retranslocation from the vegetative plant organs into the grains is not necessary. Secondly a lower protein content of the remaining rapeseed-cake after oil extraction, which is used as animal feed, lowers the nutritional value. Hence, N-efficient cultivars should have a high efficiency in the allocation of N to the harvested grains, for which the N harvest index (NHI) is a measure. The NHI including the N losses with the shed leaves is very differently in oilseed rape. Aufhammer *et al.* (1994) reported a generally low NHI for oilseed rape with 0.3 to 0.5. Whereas Ulas *et al.* (2013) showed that N allocation to the grain can be highly efficient and reach up 80%.
However, the increase of the NHI trough breeding of N-efficient cultivars with high protein contents will be difficult. Because winter oilseed-rape is an oil crop and the oil and protein contents in the grain are negatively correlated (Würschum *et al.,* 2012). But, the identification of independent QTLs for both quality criteria (Zhao *et al.,* 2006) suggests that breeding of cultivars with high grain-oil and protein-contents could be possible in future.

Functional stay-green

Senescence is an integral part of plant development. It is the last developmental stage of a leaf leading to its death (Quirino *et al.,* 2000). Leaf senescence is one type of programmed cell death (PCD) occurring in plants, because leaf cells die at a predictable time and location, it has some beneficial effects on plant development and it is encoded in the hereditary material (Barlow, 1982). Senescence can be a natural event during development or prematurely induced by sub-optimal environmental conditions such as abiotic stresses such as nutrient limitation, particularly N starvation (Quirino *et al.,* 2000; Lim *et al.,* 2007). Leaf senescence is a highly coordinated process, in which the cells undergo changes in cell structure, metabolism and gene expression. The onset of leaf senescence is accompanied by transcriptional activation and repression of many genes (Smart, 1994). During senescence the photoassimilation is terminated and the metabolism shifted from anabolism to catabolism (Lim *et al.,* 2007). The most visibly hallmark of senescence is the yellow discoloration of the leaf by carotenoids which become visibly through chlorophyll breakdown (Christ & Hörtensteiner, 2014). Functionally, leaf senescence is not simply a degenerative process. It is rather a recycling process in which the senescing leaf becomes a net exporter (source) for phloem mobile nutrient elements, particularly N to young leaves, developing seeds, or storage tissues (Fischer, 2007; Masclaux-Daubresse *et al.,* 2008).

Stay-green is the general term for the retention of greenness through delayed leaf senescence, in which delayed leaf senescence accompanied with maintenance of photosynthetic capacity is referred to as functional stay-green (Thomas & Howart, 2000) Functional stay-green is an inheritable, mostly polygene-regulated quantitative trait (Wang *et al.,* 2012). Particularly in graminaceous crop-species, such as maize, rice and sorghum, several quantitative trait loci (QTLs) for the stay-green trait have been identified (Tao *et al.,* 2000; Xu *et al.,* 2000; Haussmann *et al.,* 2002; Jiang *et al.,* 2004; Wang *et al.,* 2012; Belícuas *et al.,* 2014).

But the undelaying mechanisms leading to a functional stay-green phenotype are currently poorly understood. Functional stay-green results from a delayed onset of senescence and/or a slower senescence course (Thomas & Howarth, 2000). Thus in contrast to cosmetic stay-green without any photosynthetic activity (Thomas & Howarth, 2000), functional stay-green requires more than the retention of green colour based on delayed or completely inhibited chlorophyll catabolism (Kusaba *et al.,* 2013).

Master-regulators of the gene-expression network during senescence are senescence-inducible transcription factors (TFs) (Balazadeh *et al.,* 2008b). Many of these TFs directly or indirectly control the activation or repression of down-stream senescence-associated genes (SAGs) and thus fine-tune the onset and rate of leaf senescence (Kusaba *et al.,* 2013). Among the senescence-inducible TFs are particularly members of the NAC and WRKY families, which positively or negatively act on leaf senescence (Balazadeh *et al.,* 2008b; Parlitz *et al.,* 2011). The NAC TF *JUB1* (Wu *et al.,* 2012) as well as the WRKY TFs *WRKY54* and *WRKY70* (Besseau *et al.,* 2012) are involved in retarding the onset of leaf senescence.

For functional stay-green the maintenance of functional chloroplasts is a prerequisite, which is under the control of nuclear as well as chloroplast-encoded genes. The chloroplast gene CAO encoding the enzyme chlorophyll *a* oxygenase is not only involved in chloroplast maintenance (Sakuraba *et al.,* 2012a) but also suppresses the expression of senescence-inducible nuclear transcription factors (Sakuraba *et al.,* 2012b). On the other hand, the nucleus NAC TF *ORE1* terminates chloroplast maintenance through repression of GARP nuclear TFs, which are involved in the regulation of chloroplast development (Rauf *et al.,* 2013).

Additional key regulators of leaf senescence are phytohormones (Lim *et al.,* 2007). Alterations in phytohormone, particularly cytokinin (CK), metabolism and signaling lead to functional stay-green phenotypes (Thomas & Ougham, 2014). Functional stay-green in cotton plants could be attributed to accumulation of root-derived CKs in mature leaves on the one hand (Dong *et al.,* 2008). On the other hand, modification of leaf inherent CK homeostasis in mature tobacco leaves (Gan & Amasino, 1995; del Mar Rubio-Wilhelmi *et al.,* 2014) as well as CK perception and signaling in mature *Arabidopsis*

thaliana leaves (Kim *et al.,* 2006) or downstream targets in tomato (Albacete *et al.,* 2014) or tobacco leaves (Lara *et al.,* 2004) lead to functional stay-green.

Functional stay-green and N efficiency

Nitrogen starvation prematurely induces leaf senescence (Pommel *et al.,* 2006) and compromises grain yield formation through enhanced crop maturation (Gregersen *et al.,* 2013). In many crop species stay-green phenotypes are superior in yield formation particularly under abiotic stress conditions such as drought or N limitation (Gregersen *et al.,* 2013). A characteristic of N-efficient winter oilseed-rape line-cultivars with high NUPT, particularly during flowering, is a functional stay-green phenotype, expressed through delayed leaf senescence of the older leaves accompanied with maintained photosynthetic activity (Schulte auf'm Erley *et al.,* 2007). Functional stay-green is a desirable crop trait to enhance N efficiency, because it will help to overcome yield limitation caused by insufficient availability of carbon (C) and N at the transition into the reproductive phase. Particularly under stress conditions delayed leaf senescence during grain filling enhanced the photosynthetic capacity of plants (Wolfe *et al.,* 1988). The total number of pods and grains in winter oilseed-rape is greatly depending on the availability of assimilates during the four weeks flowering period. The small photosynthetic active area at this time is the most source-limiting factor (Evans, 1984; Keiller & Morgan, 1988; Habekotté, 1993).

Moreover, post-flowering N uptake, which appeared decisive for genetic variation in N efficiency in winter oilseed-rape, (Berry *et al.,* 2010; Schulte auf'm Erley *et al.,* 2011), requires maintained root activity, for which a prolonged assimilate allocation to the roots is a prerequisite. Cultivars with delayed leaf senescence showed an enhanced root activity (Tollenaar & Wu, 1999) as well as N uptake during reproductive growth (Osaki, 1995; Mi *et al.,* 2003). Thus a maintained photosynthetic activity particularly of lower leaves through delayed leaf senescence will not only result in a better assimilate supply to the pods but also to the roots and thus enhances post-flowering N uptake.

However, a key function of senescence is the remobilization of particularly N from the vegetative plant parts to reproductive organs (particularly the grains) (Masclaux-Daubresse *et al.,* 2008). Thus for yield formation and low amounts of N remaining in the crop residues, which is desirable for environmental reasons resulting in lower N budget surplus, plant senescence, finally, is a prerequisite. In winter oilseed-rape more than 70% of pod N is derived from N remobilization (Malagoli *et al.,* 2005; Gombert *et al.,* 2010). Thus to fully utilize the advantages of functional stay-green for crop production the onset and rate of senescence must be finely synchronized with the development, particularly the beginning of flowering which marks the beginning of the reproductive growth phase (Gregersen *et al.,* 2013).

Hypothesis and Objectives

A promising approach to solve the large winter oilseed-rape crop-specific nitrogen (N) balance-surpluses is the breeding and cultivation of N-efficient genotypes/cultivars which have the ability to produce high grain yields under N-limited conditions.

N efficiency of winter oilseed-rape cultivars has been primarily attributed to maintained N uptake during reproductive growth (N uptake efficiency) (Wiesler *et al.,* 2001; Behrens, 2002; Kamh *et al.,* 2005; Schulte auf'm Erley *et al.,* 2007; Ulas, 2010; Schulte auf'm Erley *et al.,* 2011) in combination with delayed senescence of the older leaves accompanied with maintenance of photosynthetic capacity (functional stay-green) (Schulte auf'm Erley *et al.,* 2007). Based on these results a hypothetic N-efficient ideotype with a maximal use of the available soil-N was developed. This ideotype is characterized by a high N uptake during vegetative growth with a maintained high N uptake into reproductive growth and a functional stay-green phenotype, expressed through delayed senescence of the older leaves during this period. It is assumed that the prolonged photosynthetic activity leads to a better root growth and activity and thus enhanced N uptake owing to improved assimilate supply to the roots. But after induction of leaf senescence the N-efficient ideotype shows an accelerated senescence-course with a highly efficient N translocation to the grains.

However, firstly the previous studies comprised exclusively line cultivars, and currently it is not clear whether the same holds true for other cultivar types particularly hybrids which are increasingly cultivated. Secondly, it is not clear whether higher root growth and N uptake during early reproductive growth are causally related and if so, whether delayed leaf senescence of N-efficient cultivars is the cause or the consequence of maintained root growth/activity. Thus it needs to be clarified whether cultivar differences in N starvation-induced leaf senescence are due primarily to leaf-inherent factors or governed by root-mediated signals. Thirdly, facilitating and accelerating the breeding process of N-efficient cultivars requires not only the identification of secondary plant traits contributing to N efficiency but also the identification of N starvation-specific markers for functional stay-green because under field conditions other senescence inducers than N limitation may mask genotypic differences in functional stay-green. Therefore the study was divided into four main areas:

i. Investigation and comparison of the N efficiency of winter oilseed-rape cultivars belonging to different cultivar types (lines, hybrids and dwarfs) and the importance of delayed leaf senescence and maintained N uptake into the reproductive growth for differences in N efficiency between the cultivar types (Chapter I)

ii. Identification of marker genes which are specific for N starvation-induced leaf senescence and suitable to detect cultivar-specific differences at early leaf senescence stages prior to loss of chlorophyll (Chapter II)

iii. Clarification whether cultivar differences in N starvation-induced leaf senescence are due to leaf-inherent factors and/or governed by root-mediated signals (Chapter III)

iv. Dissecting the contribution of N uptake and retranslocation during reproductive growth to the N efficiency of winter oilseed-rape cultivars differing in leaf senescence (Chapter IV)

I The superior nitrogen efficiency of winter oilseed-rape (*Brassica napus* L.) hybrids is not related to delayed nitrogen starvation-induced leaf senescence

Fabian Köslin-Findeklee[1], Andreas Meyer[1], Andreas Girke[2], Katrin Beckmann[3] and Walter J. Horst[1]

[1]Institute of Plant Nutrition, Leibniz University of Hannover, Herrenhäuser Str. 2, D-30419 Hannover, Germany
[2]Norddeutsche Pflanzenzucht Hans-Georg Lembke KG, Hohenlieth-Hof 1, D-24363 Holtsee, Germany
[3]NPZ Innovation GmbH, AgroBioTechnikum, Thünenplatz 1, D-18190 Groß Lüsewitz, Germany

📖 Published in *Plant and Soil* (2014) 384: 347-362

Abstract

Winter oilseed-rape (*Brassica napus* L.) is the most important oil crop in cool temperate climates, but its cultivation causes high nitrogen (N) balance surpluses. The breeding and cultivation of N-efficient cultivars (high grain yield under low N supply) can contribute to reduce the crop-specific N balance surpluses. Genetic variation in N efficiency in winter oilseed-rape is predominantly attributed to N uptake efficiency. In particular maintained N uptake during reproductive growth related to delayed leaf senescence accompanied by maintained photosynthetic capacity (functional stay-green) appeared decisive for N efficiency. The aim of this study was to investigate and compare the N efficiency of winter oilseed-rape line-, hybrid- and dwarf-cultivars. Furthermore the hypothesis was tested if stay-green into the reproductive growth also contribute to the expected high N efficiency of hybrids and dwarfs.

The present two year field experiments with ten line, five hybrid and three dwarf cultivars revealed that the hybrids (but not the dwarfs) were superior in yield formation independent of the N supply. The greater N efficiency of the hybrids was related to a higher N uptake until maturity, but not to functional stay-green. This was in agreement with a hydroponic experiment in which the hybrids were particularly responsive in N starvation-induced leaf senescence of older leaves as revealed by SPAD, photosynthesis and the expression of the senescence-specific cysteine protease gene *SAG12-1*. Additionally, the hybrids were characterized by an efficient N retranslocation from vegetative to reproductive plant organs in combination with a lower grain-N (protein) concentration. Both, N uptake and N utilization efficiency were decisive for the superior N efficiency of the hybrids.

Keywords: genotypic differences, nitrogen deficiency, nitrogen uptake, nitrogen utilization, functional stay-green, *SAG12* expression

Introduction

Nitrogen is the element required in largest quantities for crop growth and is one of the most yield-limiting nutrients for annual crops in most soils worldwide (Huber & Thompson, 2007). The doubling of the world food production from the 1960s until the turn of the millennium was accompanied by a nearly seven-fold increase in the global annual rate of N fertilization (Tilman, 1999). Alarmingly, only less than half of the fertilized N is taken up by the crop plants (Craswell & Godwin, 1984; Raun & Johnson, 1999). The surplus N may cause environmental pollution mainly due to nitrate transport into ground and surface waters. Furthermore, enhanced nitrous oxide emission into the atmosphere contributes to global warming.

Winter oilseed-rape (*Brassica napus* L.) is the most important oil crop in European agriculture. The oil is used for human consumption or industrial purposes and furthermore an important source for the synthesis of biodiesel (Booth & Gunstone, 2004).

But winter oilseed-rape is a crop with a high N balance surplus. A grain yield of 4.5 t ha^{-1} causes a surplus of around 60 kg N ha^{-1}. A low acquisition of soil-N by the crop and particularly an incomplete retranslocation of N from vegetative into the reproductive harvested plant organs result in high N balance surpluses (Aufhammer *et al.,* 1994; Lickfett *et al.,* 2001). Therefore, for the reduction of the crop-specific N balance surplus the high fertilizer rates and the high N amounts remaining in the crop residues need to be reduced, but without yield reduction. A tool to achieve this goal is the breeding and cultivation of N-efficient cultivars (Sylvester-Bradley & Kindred, 2009). Genetic variation in N efficiency among cultivars of crop plants is known for more than 80 years (Hoffer, 1926; Smith, 1934). Nitrogen efficiency is defined as the ability of a cultivar to achieve a yield above average under conditions of suboptimal N supply (Graham, 1984; Sattelmacher *et al.,* 1994). Nutrient efficiency is complex and may be due to the effectiveness of a cultivar in absorbing nutrients from the soil (uptake efficiency) and/or the efficiency with which the nutrients are utilized to produce yield (utilization efficiency). The genetic improvement based on specific traits involved in nutrient efficiency is difficult and not trivial. Therefore, the determination of the yield under low nutrient supply is the most practicable selection trait for breeders (Sattelmacher *et al.,* 1994). There is great genotypic variation in yield potential of winter oilseed-rape and much progress has been made to increase the yield potential of landraces by breeding of line cultivars (Becker, 1987; Booth & Gunstone, 2004). In recent years, the breeding of hybrids which represent more than 50% of the cultivars used presently in German agriculture and which is increasing also in all other oilseed rape-producing countries worldwide, allowed a major further increase in oilseed rape yields (Gehringer *et al.,* 2007). The superior vigor and yield formation of hybrids compared to their parents were firstly reported as “heterosis” by Schull (1922). This is also characteristic of winter oilseed-rape hybrid-cultivars (Brandle & Mc Vetty, 1989; Léon 1991). Presently, only few studies investigated the

yield formation of hybrids compared to lines under limited N conditions (Friedt *et al.,* 2003; Gehringer *et al.,* 2007; Kessel *et al.,* 2012). These studies suggest that hybrids are superior to non-hybrids not only under sufficient but also under limiting N supply. The physiological reasons for the higher N efficiency of hybrids are not yet understood. Comparing line cultivars only, previous studies by our group (Wiesler *et al.,* 2001; Behrens, 2002; Kamh *et al.,* 2005; Schulte auf'm Erley *et al.,* 2007; Ulas, 2010; Schulte auf'm Erley *et al.,* 2011; Ulas *et al.,* 2012) showed that N efficiency was primarily related to N uptake efficiency particularly during the reproductive phase from the beginning until end of flowering. A characteristic of cultivars with a prolonged N uptake under N deficiency was a delayed leaf senescence of the older leaves accompanied by maintained photosynthetic capacity (functional stay-green). It is assumed that the prolonged assimilate supply to the roots enhances the N uptake into the reproductive phase because of extending leaf-photosynthesis duration. The aim of this study was to investigate and compare the N efficiency of oilseed rape cultivars belonging to different winter oilseed-rape types (lines, hybrids and dwarfs) and to test the hypothesis that a delayed leaf senescence and maintained N uptake into the reproductive growth is also contributing to the expected superior N efficiency of hybrids.

Material and Methods

Germplasm

A set of eighteen winter oilseed-rape cultivars was used for the field and nutrient solution experiments (Table I-1). The set was a compilation of ten lines, five hybrids and three dwarfs. The cultivars (cvs.) Apex, Capitol and the doubled haploid (DH) lines DH4, DH28 and DH42, derived from a cross between the cvs. Apex and Mohican, were selected based on previous field and nutrient solution experiments (Schulte auf'm Erley *et al.,* 2007). The hybrids cvs. NPZ-3 and NPZ-4 are crosses between the same mother and the pollinators cv. NPZ-1 or cv. NPZ-2. All other cultivars were selected based on observations by the breeder Norddeutsche Pflanzenzucht Hans-Georg Lembke KG (NPZ). The seeds of all cultivars were received from NPZ.

Table I-1 Description of the 18 winter oilseed-rape cultivars used for the field and hydroponic experiments

Description	Cross	Type	Properties
NPZ-1		Line	N-efficient
NPZ-2		Line	N-inefficient
NPZ-3	M1xNPZ-1	Hybrid	High yield
NPZ-4	M1xNPZ-2	Hybrid	High yield
NPZ-5	M2xNPZ-2	Hybrid	Very high yield
Oase		Line	Stay-green
NPZ-7		Line	
NPZ-8	M3xNPZ-7	Hybrid	High yield
Asgard		Line	N-efficient, early leaf senescence
Rohan	M1xAsgard	Hybrid	High yield under low N input
Apex		Line	N-efficient
Capitol		Line	N-inefficient
DH4		DH-Line	N-efficient
DH28		DH-Line	N-efficient
DH42		DH-Line	N-inefficient
NPZ-Dwarf-1	M4xNPZ-7	Dwarf-Hybrid	Dwarf with highest yield
NPZ-Dwarf-2		Dwarf-Hybrid	High yield
NPZ-Dwarf-3		Dwarf-Line	

Field experiments

Plant material and growing conditions

Field experiments were performed in the years 2009 and 2010 at the experimental station of NPZ on a loamy sandy soil in Malchow, Poel, Germany. In both experiments the complete set of 18 genotypes was grown under two N fertilizer rates, without mineral N (N0) and 150 kg ha^{-1} N (N150) as calcium ammonium nitrate. The soil mineral N content (N_{min}) in winter 2009 and 2010 was 20 kg ha^{-1} for a soil depth of 0.9 m. In 2009, additionally 40 t ha^{-1} (available N 50 kg ha^{-1}) cattle manure was added to both N treatments. The trials were laid out in a split-plot design with N

fertilization as main plot and cultivars as subplot in two replications. In 2009 the individual plot size was 7.5 m x 1.7 m (12.8 m²) and in 2010 6.5 m x 1.7 m (11.1 m²) with a plant density of approximately 40 plants m^{-2}.

Plant harvest and analysis

The developmental stage of the plants was determined using the BBCH-code (Biologische **B**undesanstalt, **B**undessortenamt und **Ch**emische Industrie) (Lancashire *et al.,* 1991). At maturity (BBCH89) grain and straw yields were determined on 3.5 m² of the center of each plot. Total N in the dried and ground plant material was analyzed using an elemental analyzer (Vario EL, Elementar Analysensysteme, Hanau, Germany). The oil concentration in the grain and the protein concentration in the grains and grain-meal were determined by near infrared reflectance spectroscopy (NIRS) according to the method of Tkachuk (1981). For characterizing the senescence status of individual leaves, at the developmental stages BBCH69 (end of flowering), BBCH78 (80% of the pods reached the cultivar-specific size) and BBCH82 (20% of the pods were mature) the chlorophyll contents of the leaves 2, 4 and 6 on the main stem counted from the inflorescence to the bottom of plant was assessed using a portable chlorophyll meter (SPAD-502, Konica Minolta, Tokyo, Japan) on three previously marked plants per plot. Three readings per leaf were taken. The senescence status of the whole plant was assessed for six previously marked plants per plot by counting the number of remaining green leaves on the main stem weekly from end of flowering until maturity. The agronomic relevant traits were calculated based on the following equations:

N uptake (NUPT) = N_{Straw} [kg ha^{-1}] + N_{Grain} [kg ha^{-1}]

$NUPT_{Total}$ = $NUPT_{BBCH89}$

N utilization efficiency (NUE) = Grain dry weight [kg ha^{-1}] / NUPT [kg ha^{-1}]

Nitrogen harvest index (NHI) = N_{Grain} [kg ha^{-1}] / NUPT [kg ha^{-1}]

Harvest index (HI) = Grain dry weight [kg ha^{-1}] / Shoot dry weight [kg ha^{-1}]

Straw represented the entire above-ground shoot including the pod walls. The shoot N uptake at maturity was only calculated for the year 2009, because of erroneously discarding the seeds before analysis in 2010.

Hydroponic experiment

Plant material and growing conditions

Twelve cultivars, the nine lines NPZ-1, NPZ-2, Oase, Asgard, Apex, Capitol, DH4, DH28 and DH42 and the three hybrids NPZ-3, NPZ-4 and NPZ-5, were grown in hydroponics to explore if cultivar differences in N deficiency-induced leaf senescence at early vegetative growth stages are representative for stay-green during the reproductive phase in the field experiments. Seeds were germinated in a climate chamber (Day/night 16/8 h; Temperature day/night 20/22°C; PAR 350 µmol m^{-2} s^{-1}) using a "sandwich" method arranging the seeds between filter paper sandwiched between sponges and PVC-plates on both sides. The "sandwiches" were placed into a box containing tap water. Seven days after germination the seedlings were transferred to continuously aerated nutrient solution in a greenhouse (assimilation light (16 klm) 16 h; heating/ventilation temperature 20/22°C; shading at 15 klx solar radiation; relative humidity 80%) and cultured from 15 December 2011 to 22 January 2012. Two seedlings were transferred to a 6-L plastic pot and the plants were pre-cultured for 28 days at optimal N supply (2.0 *mM*). The roots of the plants were daily separated by hand, to avoid intermingling of the root systems. The roots remained submerged during the separation to minimize root damage. The composition of the nutrient solution was 500 *µM* K_2S0_4, 250 *µM* KH_2PO_4, 325 *µM* $MgSO_4$, 50 *µM* NaCl, 8 *µM* H_3BO_3, 0.4 *µM* $MnSO_4$, 0.4 *µM* $ZnSO_4$, 0.4 *µM* $CuSO_4$, 0.1 *µM* Na_2MoO_4 and 40 *µM* Fe-EDDHA. During pre-culture $Ca(NO_3)_2$ and $(NH_4)_2SO_4$ were used as N sources in the ratio of nine to one, and 10 µ*M* $C_2H_4N_4$ (Dicyandiamide) was added to prevent nitrification. Prior to treatment begin one plant per pot was discarded. For N starvation the plants were grown at 0.1 *mM* N as $Ca(NO_3)_2$ and 1 *mM* $CaSO_4$ to allow for optimum Ca nutrition. For optimal N nutrition the plants were cultured at 4.0 *mM* N doubling the concentration used for pre-culture. After treatment begin the nutrient solution was changed every second day. The experiment was completely randomized with four replicates.

Plant harvest and analysis

The plants were harvested 10 days after treatment began (DAT) and separated into the shoot and root. Root-system length and surface were determined on representative subsamples using a modified method of Newman (1966). The root segments were spread on a flatbed optical scanner (Epson Expression STD 1600 + Regent Instruments Inc.) and their length and surface determined using a Root-Image Analysis-System Software (WinRHIZO Pro V. 2002c Regent Instruments Inc. Quebec, Canada). Based on the fresh weights of the subsamples and the total root system the length and surface was calculated for the whole root system. From the shoot three individual leaves were harvested: the youngest fully expanded leaf at the end of pre-culture and the two older leaves. The youngest fully expanded leaf was the 5^{th} leaf counted from the bottom to the top of the plant. Leaf

area of the individual harvested leaves was measured by a portable leaf area meter (LI-3100, LI-COR, Lincoln, USA). The leaves were divided along the midrib with a razor blade. One half was immediately frozen in liquid N and the other half was dried at 70°C until constant weight for dry weight determination. N concentrations of the dried and ground plant fractions were determined using an elemental analyzer (Vario EL, Elementar Analysensysteme, Hanau, Germany). The frozen leaf material was ground for total RNA isolation using a mixer mill (MM 400, Retsch, Haan, Germany). During the treatment the senescence status of the three leaves was measured using non-destructive methods. The chlorophyll contents of the leaves were assessed by a portable chlorophyll meter (SPAD-502, Konica Minolta, Tokyo, Japan). Photosynthesis rates of the same leaves were measured using a portable gas-exchange system (LI-6400, LI-COR, Lincoln, USA) with a photon flux-density of 1000 µmol m^{-2} s^{-1} and an incoming CO_2 concentration of 400 µmol m^{-2} s^{-1}.

RNA isolation and cDNA synthesis for qRT-PCR

For total RNA isolation 100 mg of frozen and ground leaf material was used. Total RNA was isolated with TRIsure™ (Bioline, London, UK) reagent according to the instructions of the manufacturer. RNA integrity was tested on 1% agarose gel electrophoresis and photometrically quantified (NanoPhotometer™, Implen, München, Germany). Two µg of total RNA were applied to synthesize cDNA with the RevertAid™ H Minus First Strand kit (Fermentas, Waltham, USA). For the reaction the supplied random hexamer primer were used to synthesize the first strand cDNA of the *m*RNA according to the instructions of manufacturer. Quality and quantity of cDNA was determined as for RNA.

Primer design

The *B. napus* sequences of the senescence-specific cysteine protease *SAG12-1* and the reference gene elongation factor 1-alpha *EF1-alpha* were used to design the primers for the qRT-PCR analysis. All sequences were obtained from the NCBI public database. The sequences were aligned and the most contrasting sequence regions were identified. The nucleotide alignment was performed using the Vector NTI® software (Invitrogen, Carlsbad, USA). Primer pairs (Table I-2) were designed using PrimerQuest software (Integrated DNA Technologies, Coralville, USA).

Table I-2 NCBI accession numbers and primer sequences of the gene of interest *SAG12-1* and the reference gene *EF1-alpha*.

NCBI accession number	Gene name	Forward primer sequence (5' → 3')	Reverse primer sequence (5' → 3')
AF089848	*SAG12-1*	TACGTGTAGGATGTTGTTGGGCGT	TGGCCATTATGTGCTCAAACGCAG
DQ312264	*EF1-alpha*	AGGTCCACCAACCTTGACTG	CCGTTCCAATACCACCAATC

qRT-PCR conditions

The 25 µL SYBR Green based mix included 2.5 µL 10x Hot-Start PCR buffer, 3.6 µL 25 *mM* $MgCl_2$, 0.25 µL of 1000-times diluted 1000x SYBR Green-I (Invitrogen GmbH, Darmstadt, Germany), 0.5 µL 10 *mM* dNTPs-mix, 0.63 µL of each 10 *µM* forward and reverse primer, 0.15 µL 5U μL^{-1} U DCS Hot Start DNA polymerase (DNA Cloning Service, Hamburg, Germany), 1 µL of 50 ng μL^{-1} cDNA template. The PCR reactions were performed in 96-well plates in a thermo cycler (CFX96™ Real-time system, BioRad Laboratories, Hercules, USA) and consisted of an initial denaturation at 95 °C (10 min), followed by 50 cycles at 95°C (15 s), 60°C (30 s), 72°C (30 s) and a final melting curve analysis from 60°C to 95°C with a 0.5°C (5 s^{-1}) increasing temperature gradient. The mean relative expression of the qRT-PCR results were calculated based on the $2^{-\Delta\Delta ct}$-method by Livak & Schmittgen (2001).

Statistical analysis

The statistical analysis was performed using the statistic software SAS® version 9.2 (SAS Institute, Cary, USA). The analysis of variance (ANOVA) for the field experiments was calculated using the PROC MIXED procedure. For the overall analysis cultivar, N rate, year and their interactions were set as fixed factors and replication, N rate, year and their interactions were set as random. For the ANOVA within a year cultivar, N rate and their interaction were set as fixed factors and replication, N rate and their interactions were set as random. For the comparison of the line (*n* = 10), hybrid (*n* = 5) and dwarf

(*n* = 3) cultivars within the N levels the LSMEANS statement was used. For each comparison the linear combinations were defined for the cultivar and the cultivar x N rate interaction using the ESTIMATE statement taking into account the unequal group sizes. For the nutrient solution experiment the ANOVA was calculated using the PROC GLM procedure. Multiple comparisons of means overall cultivars were made by the MEANS statement of the PROC GLM procedure. All-pairwise comparisons were calculated using the Tukey test at a p-value 0.05. For the comparison of the line (*n* = 9) and hybrid (*n* = 3) cultivars the LSMEANS statement was used. The linear combinations were defined for the cultivar using the ESTIMATE statement. For all tests of significance a p-value of 0.05 was used and the p-values were Bonferroni-Holm adjusted. In the tables and figures for the F-Test +, *, ** and *** indicate significance at the p <0.10, <0.05, <0.01 and <0.001 level, respectively. ns = non-significant. The same symbols were used to mark the significance for the correlations. For the comparison of means different letters on top of the columns indicate differences between the columns at p <0.05. The relative qRT-PCR data were analyzed using the %QPCR MIXED macro after Steibel *et al.* (2009) based on the PROC MIXED procedure. Curves were fitted using the graphic software SIGMA PLOT version 11 (Systat software, San Jose, USA).

Results

Field experiments

Straw biomass

The straw dry weight (shoot + pod walls) at maturity (BBCH89) was affected by the cultivar type (Figure I-1). Generally the straw dry weight was higher for the hybrids than for the other cultivar types, either significantly or in tendency, independent of the N fertilization level which did not significantly affect straw dry weight formation.

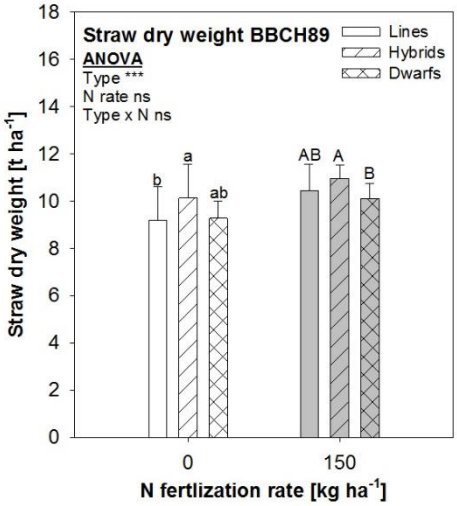

Figure I-1 Straw dry weight at maturity (BBCH89) of winter oilseed-rape lines (*n* = 10), hybrids (*n* = 5) and dwarfs (*n* = 3) as affected the by N fertilization rate (N0, N150) (n = 2). The data show the means of the field trials in 2009 and 2010. Different lower case and upper case letters on top of the columns indicate differences between the cultivar types within the N fertilizer rates (N0, N150) at p <0.05. For the ANOVA * indicate significant differences at p <0.001. ns = non-significant. The error bars represent the standard deviatons of the means.**

Grain yield

Under both N rates the hybrids reached a significantly higher grain yield compared to the line and dwarf cultivars (Figure I-2). The average grain yield across all cultivars was 4.2 and 4.9 t ha^{-1} at N0 and N150, respectively (Figure I-3). The grain yield was significantly affected by the N fertilization level across all cultivars but not for the hybrids alone. The cultivar differences in grain yield were consistent over the N supply (no significant cultivar x N interaction) (Table I-S2). At N0 among the line cultivars cv. NPZ-1 (4.0 t ha^{-1}) showed in tendency a higher yield than cv. NPZ-2 (3.7 t ha^{-1}); cv. Apex (3.8 t ha^{-1}) did not differ from cv. Capitol (3.8 t ha^{-1}) in yield formation. The N-efficient DH line cv. DH4 (4.3 t ha^{-1}) showed a significantly higher grain yield than the N-inefficient DH-line cv. DH42 (3.3 t ha^{-1}). Across all cultivars there was a significant correlation (r^2 = 0.78) between the grain yield under low N (N0) and high N supply (N150) (Figure I-3). The five hybrid cultivars as well as the dwarf cultivar NPZ-Dwarf-1 and the line cultivars NPZ-7 and DH4 can be classified as N-efficient and N-responsive.

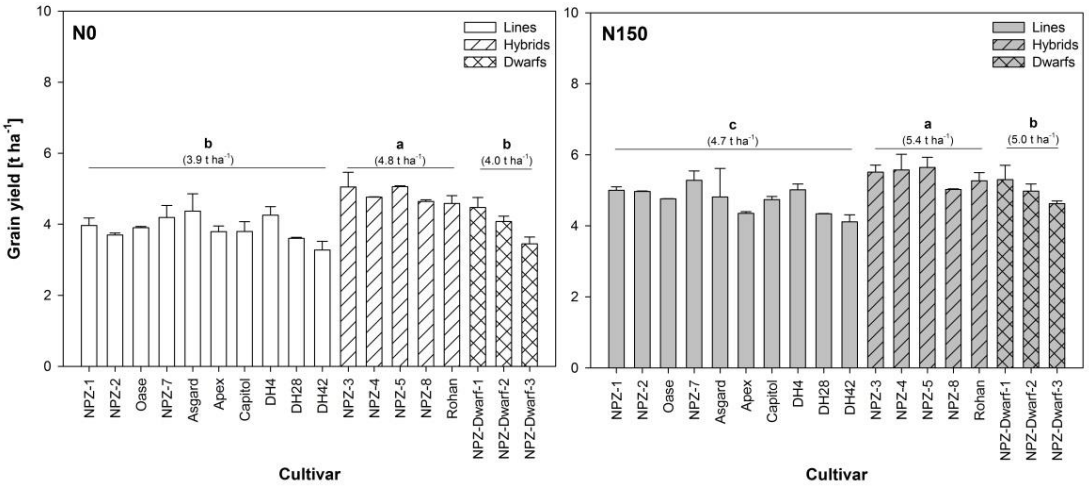

Figure I-2 Grain yield at maturity (BBCH89) of winter oilseed-rape lines (*n* = 10), hybrids (*n* = 5) and dwarfs (*n* = 3) as affected by the N fertilization rate (N0, N150). The data show the mean of the field trials in 2009 and 2010. () mean grain yield. Different letters on top of the columns indicate differences between the types of cultivars at p <0.05. The error bars represent the standard deviations of the means (n = 2).

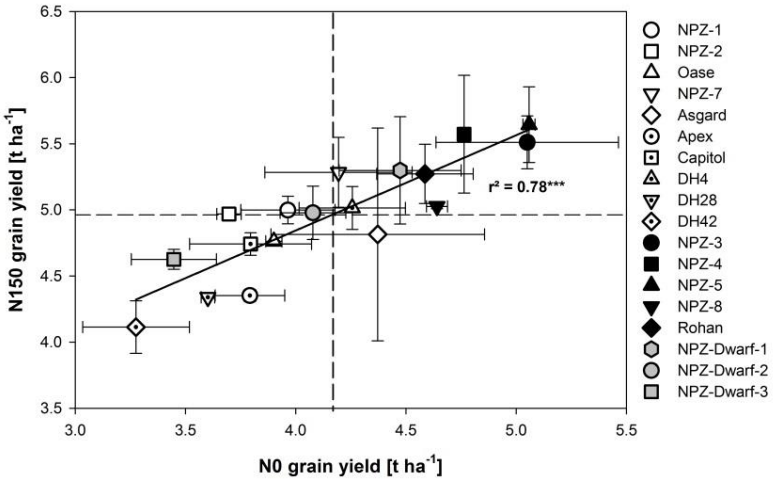

Figure I-3 Grain yield at maturity (BBCH89) of 18 winter oilseed-rape cultivars grown under field conditions without (N0) and with 150 kg N ha^{-1} (N150). The data show the mean of the years 2009 and 2010. The different types of cultivars are shown with following symbols: white = line, black = hybrid and grey = dwarf. The dashed lines show the average grain yield across all cultivars. For the correlation * indicate significance at p <0.001. The error bars represent the standard deviations of the means (n = 2).**

Thousand grain weight

For the thousand grain weight (TGW) no differences between the cultivar types occurred within both N supplies (Figure I-4). Also the N supply did not significantly affect the TGW (4.5 and 4.6 to 4.7 g at high and low N supply, respectively) (Table SI-3). Significant cultivar differences existed within the lines under low N ($p < 0.001$) and high N ($p < 0.01$) supply and within the dwarfs under low N ($p < 0.10$). The TGW and the grain yield were not correlated at either N supply (N0 $r^2 = 0.10^{ns}$; N150 $r^2 = 0.28^{ns}$).

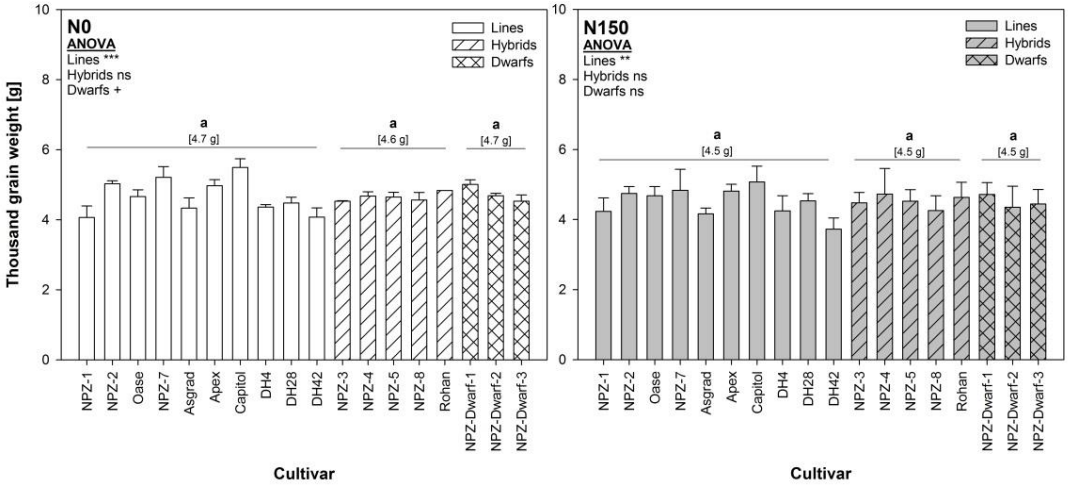

Figure I-4 Thousand grain weight at maturity (BBCH89) of winter oilseed-rape lines (*n* = 10), hybrids (*n* = 5) and dwarfs (*n* = 3) as affected by N fertilization rate (N0, N150) in 2009. () mean grain yield. Different letters on top of the columns indicate differences between the types of cultivars at p <0.05. For the ANOVA +, **, * indicate significant differences at p <0.10, <0.01, <0.001, respectively. ns = non-significant. The error bars represent the standard deviations of the means (n = 2).**

Grain N concentration

Grain N concentrations were only slightly higher at high (30.4 to 31.5 mg g^{-1} dry weight) compared to low N supply (27.1 to 29.5 mg g^{-1} dry weight) (Figure I-5, Table SI-4) and negatively related to grain yield (N0 r^2 = -0.47*; N150 r^2 = -0.50*). Whereas at N150 the cultivar types did not differ, at N0 hybrids (in tendency) and dwarfs (significantly) had lower grain-N concentrations than lines.

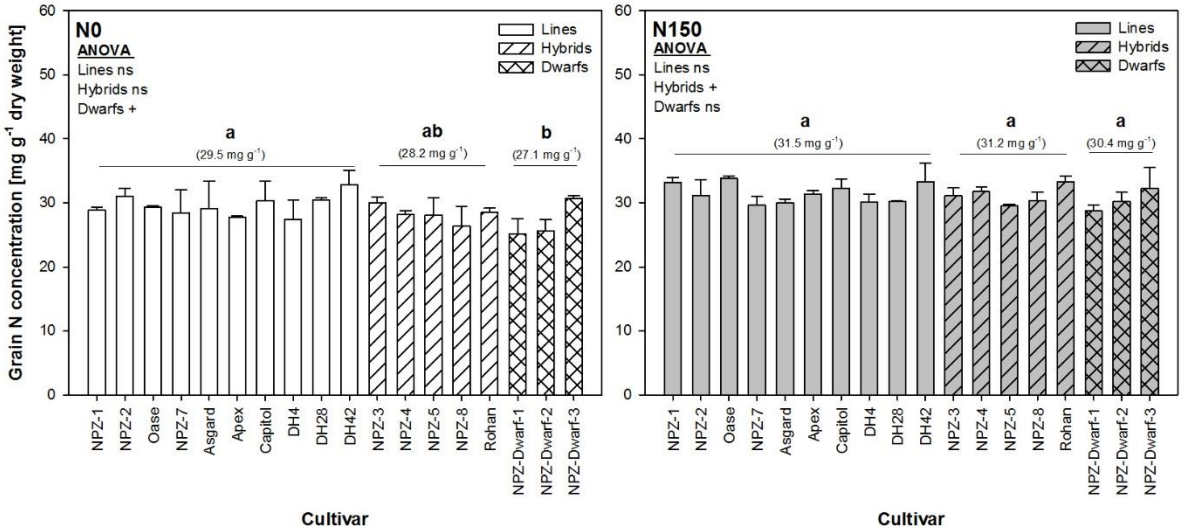

Figure I-5 Grain-N concentration at maturity (BBCH89) of winter oilseed-rape lines (*n* = 10), hybrids (*n* = 5) and dwarfs (*n* = 3) as affected by the N fertilization rate (N0, N150) in 2009. () mean N concentrations. Different letters on top of the columns indicate differences between the types of cultivars at p <0.05. For the ANOVA +, * indicate significant differences at p <0.10, <0.05, respectively. ns = non-significant. The error bars represent the standard deviations of the means (n = 2).

Grain-oil and grain-protein concentration

The N supply did not affect neither the oil (N0/N150 = 49.7/47.8% dry weight) nor the protein concentrations in the grains (N0/N150 = 171/188 mg g^{-1} dry weight) and the grain-meal (N0/N150 = 33.9/36.0% dry weight) (Figure I-6, Tables SI-5, SI-6). The dwarfs had lower oil concentrations than hybrids and lines independent of the N supply. The hybrids were generally significantly (only exception grain-protein concentration at low N supply) characterized by lower grain and grain-meal protein concentrations compared to the lines. Also the dwarfs had lower grain-meal protein concentrations than the lines.

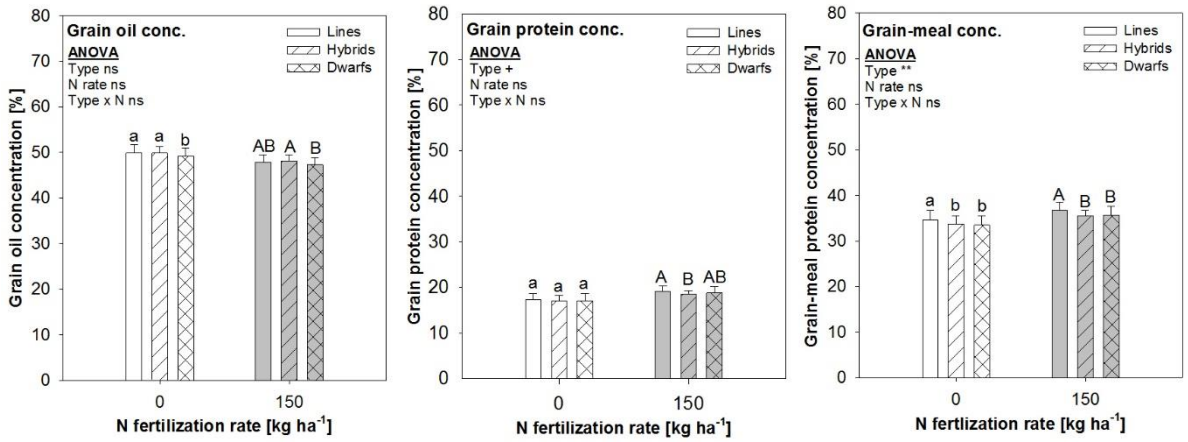

Figure I-6 Oil concentration and protein concentrations in the grains and grain-meal at maturity (BBCH89) of winter oilseed-rape lines (*n* = 10), hybrids (*n* = 5) and dwarfs (*n* = 3) as affected by the N fertilization rate (N0, N150) (n = 2). The data show the mean of the years 2009 and 2010. Different lower case and upper case letters on top of the columns indicate differences between the cultivar types within the N fertilizer rates at p <0.05. For the ANOVA +, ** indicate significant differences at p <0.10, <0.01, respectively. ns = non-significant. The error bars represent the standard deviations of the means.

Nitrogen uptake and utilization

At maturity the total N uptake could be divided into grain and straw N content (Figure I-7). The significantly higher total N contents of the hybrids at N0 compared to the lines and dwarfs exclusively relied on the hybrid cvs. NPZ-3, NPZ-4 and NPZ-5. For all cultivars the grain contributed most to the total N content at maturity ranging from 100.6 to 151.9 kg N ha^{-1} primarily depending on the cultivar type (significant type effect). The N content remaining in the straw varied across all cultivars from 40.7 to 90.2 kg N ha^{-1} and within the hybrid and dwarf cultivars but not between the lines significant differences occurred. Since there were no significant differences between the cultivars in straw N concentrations (Figure SI-1) the differences in N contents reflected the differences in biomass formation.

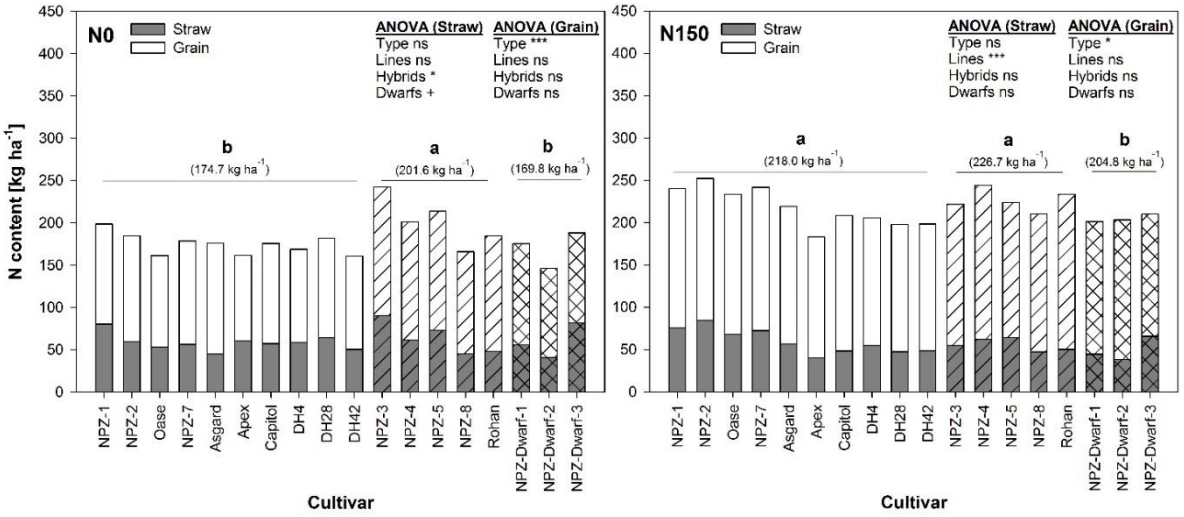

Figure I-7 Straw and grain N contents at maturity (BBCH89) of winter oliseed-rape lines (*n* = 10), hybrids (*n* = 5) and dwarfs (*n* = 3) as affected by the N fertlization rate (N0, N150) in 2009 (n = 2). () mean shoot N content (straw + grain). Different letters on top of the columns indicate differences between the types of cultivars at p <0.05. For the ANOVA +, *, * indicate significant differences at p <0.10, <0.01, <0.001, respectively. ns = non-significant.**

The separate determination of the dry weight and N contents of straw and grain allowed the calculation of N and biomass distribution efficiency for grain yield formation. The N utilization efficiency (NUE) did not differ between the N application rates but between the cultivar types within the N rates (Figure I-8). Independent of the N rate the hybrids and dwarfs had a higher NUE compared to the line cultivars. This difference between the cultivar types is also reflected by the harvest index (HI). Generally the HI ranged from 0.28 to 0.34 kg kg^{-1} of the total biomass. The nitrogen harvest index (NHI) which is a measure for the efficiency of the allocation of N to the grains (uptake and retranslocation) ranged from 0.66 to 0.76 kg kg^{-1} without significant type and N application effects. Although for the NHI cultivar differences existed within each type, only the NHI of the dwarfs was significantly affected by the N application (Table SI-8).

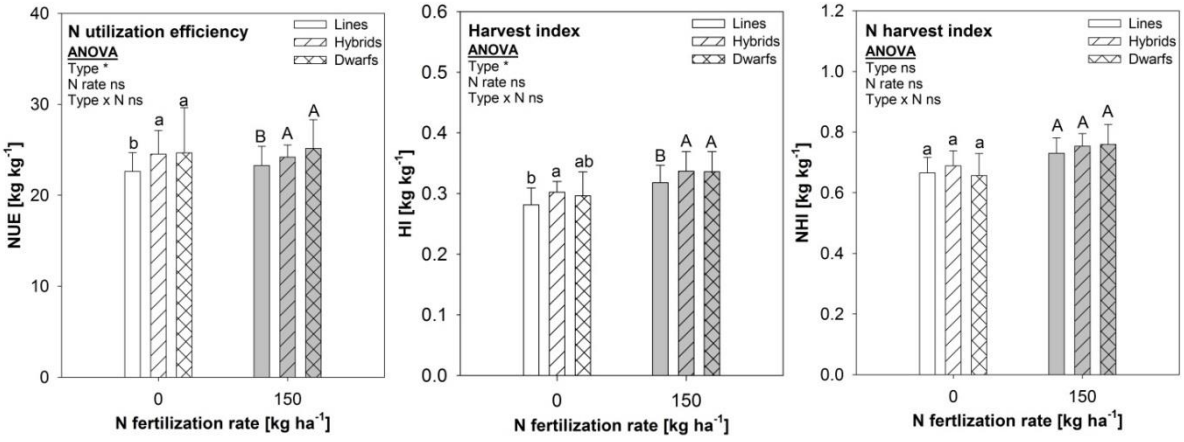

Figure I-8 NUE, NHI and HI at maturity (BBCH89) of winter oilseed-rape lines (*n* = 10), hybrids (*n* = 5) and dwarfs (*n* = 3) as affected by the N fertilization rate (N0, N150) in 2009 (n = 2). Different lower case and upper case letters on top of the columns indicate differences between the cultivar types within the N fertilizer rates at p <0.05. For the ANOVA * indicate significant differences at p <0.05. ns = non-significant. The error bars represent the standard deviatons of the means.

Leaf senescence

The higher N uptake of the hybrids could be due to delayed leaf senescence. Therefore, the number of green leaves remaining at the plant and the chlorophyll content (SPAD) of specific leaves were counted/measured from end of flowering until near maturity. For the SPAD measurement the leaves 2, 4 and 6 on the main stem counted basipetally from the inflorescence were selected. Leaf 6 was the oldest leaf which could reliably be measured until partially pod maturity (BBCH82), older leaves had been shed earlier. Leaf 6 SPAD value decreased across all cultivars by 50% from BBCH69 (end of flowering) to BBCH82 (data not shown). The overall statistical evaluation (Table SI-10) revealed for leaf 6 highly significant differences between the cultivars and a cultivar x developmental stage (BBCH) interaction particularly for the lines and the dwarfs. However, N supply did not affect the SPAD values. Comparing the SPAD values of leaf 6 of all cultivars at BBCH82 (Figure I-9) it is evident that although differences in SPAD within the cultivar types existed, there were no significant differences between the cultivar types neither at low nor at high N supply.

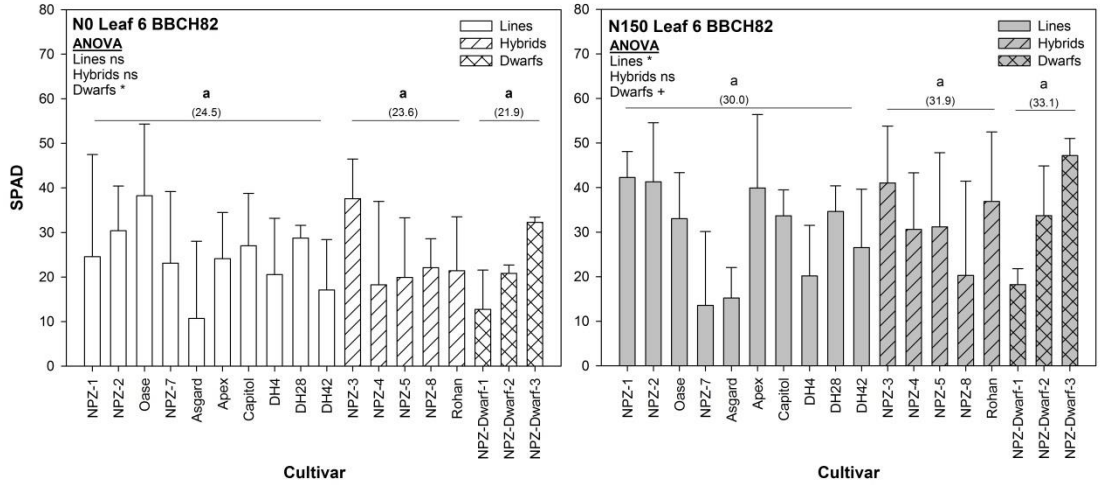

Figure I-9 SPAD of leaf six on the main stem of winter oilseed-rape lines (*n* = 10), hybrids (*n* = 5) and dwarfs (*n* = 3) at BBCH82. The plants were grown under field conditions without N fertilization (N0) or optimal N fertilization (N150). The data show the average for the years 2009 and 2010. () average for the lines, hybrids or dwarfs. Different letters on top of the columns indicate differences between the cultivar types at p <0.05. For the ANOVA +, * indicate significant differences at p <0.10, <0.05, respectively. ns = non-significant. The error bars represent the standard deviations of the means (n = 2).

The number of green leaves remaining at the main stem is a more comprehensive parameter of leaf senescence than the SPAD value of comparatively young leaves. Thus leaf counts were conducted in a weekly interval form end of flowering until near maturity (Figure I-10). Independent of the N supply the number of green leaves decreased substantially. The overall N effect was not significant (Table SI-11). Comparing the individual cultivars at the last counting date (Figure I-11) revealed that under N0 the line cultivars had significant higher numbers of green leaves that the dwarfs and in tendency also the hybrids. At high N supply clear differences existed only between hybrids and dwarfs. At this

sampling date it appeared that some cultivars maintained significantly more green leaves under high N (significant cultivar x N x DAF interaction, Table SI-11)

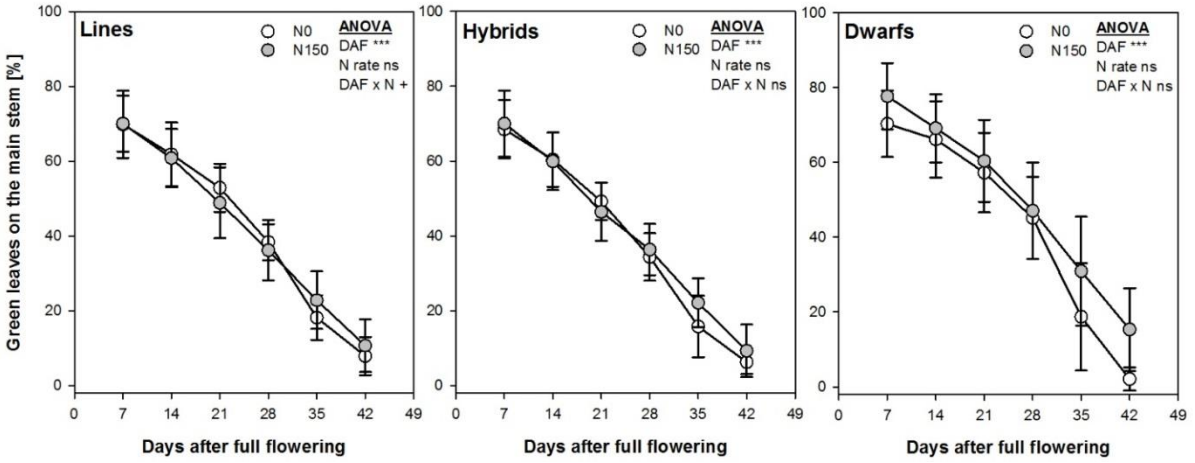

Figure I-10 Development of percentage of green leaves on the main stem during the reproductive phase under field conditions without N fertilization (N0) or optimal N fertilization (N150). The data show the average for the years 2009 and 2010 separately for the line (*n* = 10), hybrid (*n* = 5) and dwarf (*n* = 3) cultivars (n = 2). For the ANOVA +, * indicate significant differences at p <0.10, <0.001, respectively. ns = non-significant. The error bars represent the standard deviations of the means.**

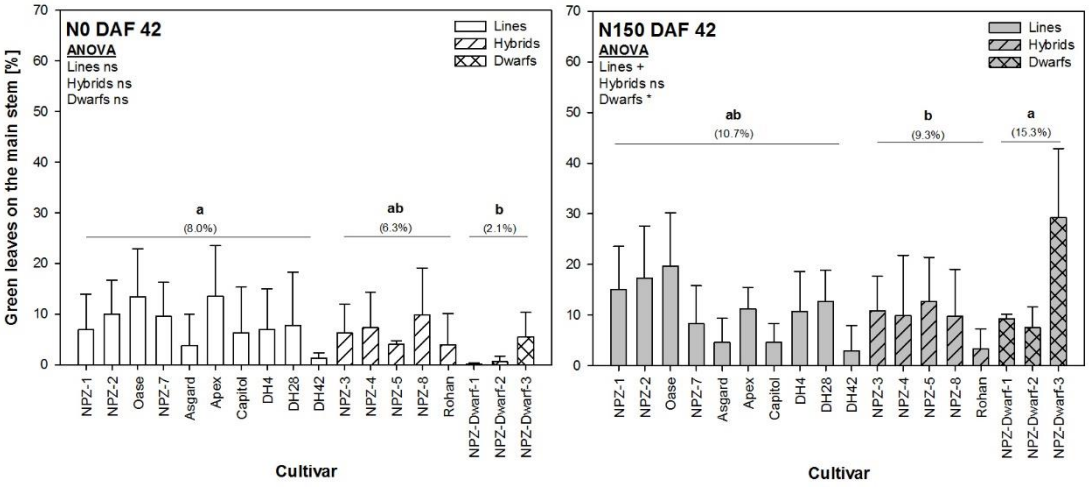

Figure I-11 Percentage of green leaves on the main stem at DAF 42 of winter oilseed-rape lines (*n* = 10), hybrids (*n* = 5) and dwarfs (*n* = 3) grown under field conditions without N fertilization (N0) or optimal N fertilization (N150). The data show the average for the years 2009 and 2010. () average for the lines, hybrids or dwarfs. Different letters on top of the columns indicate differences between the types of cultivars at p <0.05. For the ANOVA +, * indicate significant differences at p <0.10, <0.05, respectively. ns = non-significant. The error bars represent the standard deviations of the means (n = 2).

Hydroponic experiment

Line and hybrid cultivars were grown in an established hydroponic culture system which allowed studying the response of the cultivars to N starvation during early vegetative growth which is not possible under field conditions owing of the too high initial N supply of the soil of the field

experimental sites. Dwarfs were not considered in these studies because they did not meet the expectations in the field experiments.

Dry matter production

Shoot and root dry matter formation was significantly affected by the N supply and cultivar (Table SI-12). Independent of the N supply the three hybrids had a more vigorous shoot and root growth than the lines (Table I-3). N starvation decreased shoot growth but not or only slightly (hybrids) root growth, leading to a higher root/shoot ratio of N-starved plants for all cultivars. The root/shoot ratio was higher for hybrids than for lines at high but not at low N supply.

Table I-3 Variation ranges of shoot and root dry matter and root:shoot-ratio of winter oilseed-rape line (*n* = 9) and hybrid (*n* = 3) cultivars as affected by the N supply (n = 4). The plants were grown in hydroponics for 28 days at 2.0 *mM* N, followed by 10 days N starvation (0.1 *mM* N) or optimal N supply (4.0 *mM*). Different lower case and upper case letters indicate differences between the cultivar types at low and high N supply at p <0.05.

Cultivar	Shoot dry matter [g shoot^{-1}] x_{min} - x_{max}	Root dry matter [g root^{-1}] x_{min} - x_{max}	Root:Shoot [g g^{-1}] x_{min} - x_{max}
0.1 mM N			
Lines (*n* = 9)	7.9-12.8 b	1.1-1.6 b	0.11-0.16 a
Hybrids (*n* = 3)	14.9-16.0 a	1.6-1.9 a	0.11-0.13 a
4.0 mM N			
Lines (*n* = 9)	14.5-23.1 B	0.9-1.6 B	0.05-0.07 B
Hybrids (*n* = 3)	20.8-29.3 A	1.5-2.3 A	0.06-0.08 A

Nitrogen uptake

N starvation led to highly significantly decreased N concentrations in shoot and roots and thus N uptake in all cultivars (Table I-4, Table SI-13). However, the shoot and root N concentrations decreased more in the hybrids than in the lines. Nevertheless the N uptake of shoots and roots was higher for hybrid than for line cultivars. The high N uptake combined with high N utilization efficiency (NUE) led to the greater dry matter production of the hybrids at limited N supply (compare Table I-3). At high N supply shoot and root N concentrations of hybrids were the same or higher, respectively, than of lines leading to significantly higher shoot and root N uptake.

Table I-4 Variation ranges of shoot and root N concentrations and N uptake of winter oilseed-rape line (*n* = 9) and hybrid (*n* = 3) cultivars as affected by the N supply (n = 4). The plants were grown in hydroponics for 28 days at 2.0 *mM* N, followed by 10 days N starvation (0.1 *mM*) or optimal N supply (4.0 *mM*). Different lower case and upper case letters indicate differences between the cultivar types at low and high N supply at p <0.05.

Cultivar	Shoot				Root			
	N conc. [mg g^{-1}]		N uptake [mg $plant^{-1}$]		N conc. [mg g^{-1}]		N uptake [mg $root^{-1}$]	
	x_{min} - x_{max}		x_{min} - x_{max}		x_{min} - x_{max}		x_{min} - x_{max}	
0.1 mM N								
Lines (*n* = 9)	19-24	a	158-275	b	26-29	a	30-43	b
Hybrids (*n* = 3)	18-20	b	264-297	a	24-28	b	40-51	a
4.0 mM N								
Lines (*n* = 9)	62-68	A	985-1438	B	37-43	B	36-62	B
Hybrids (*n* = 3)	61-66	A	1368-1776	A	40-45	A	67-85	A

Root characteristics

Since for N uptake root morphological and physiological parameters rather than root biomass is decisive, the root length, specific root length (root length per weight) and specific root N uptake N uptake per unit of root length) were additionally determined at the end of the N treatment period. N starvation significantly decreased root length and the root length/weight ratio of lines but not the hybrids (Table SI-14). The specific root N uptake was significantly lower at low compared to high N supply in both cultivar types (Table I-5). In agreement with the root biomass, hybrids outranged lines also in root length. However, hybrids had lower specific root length (thicker roots) independent of N supply than the lines. Specific N uptake did not differ between the cultivar types neither at low N nor, at a much higher level, at high N supply confirming that root morphological characteristics are less important for N uptake in hydroponics than in soil.

Table I-5 Variation range of root characteristics of winter oilseed-rape line (*n* = 9) and hybrid (*n* = 3) cultivars as affected by the N supply (n = 4). The plants were grown in hydroponics for 28 days at 2.0 *mM* N, followed by 10 days N starvation (0.1 *mM*) or optimal N supply (4.0 *mM*). Different lower case and upper case letters indicate differences between the cultivar types at low and high N supply at p <0.05.

Cultivar	Root length [m]		Specific Root length [m g^{-1}]		Specific N uptake [mg m^{-1}]	
	x_{min} - x_{max}		x_{min} - x_{max}		x_{min} - x_{max}	
0.1 mM N						
Lines (*n* = 9)	316-368	b	206-322	a	0.7-1.0	a
Hybrids (*n* = 3)	360-411	a	195-249	b	0.8-1.0	a
4.0 mM N						
Lines (*n* = 9)	286-415	B	265-371	A	3.6-4.6	A
Hybrids (*n* = 3)	338-553	A	241-243	B	3.4-4.6	A

Nitrogen starvation-induced leaf senescence

The highly significant loss of chlorophyll (decreasing SPAD values) of an older leaf (leaf 3) confirms senescence induction by N starvation (Figure I-12). Cultivars responded differently in SPAD loss owing to N starvation (highly significant cultivar x N interaction). Among all cultivars two of the hybrids clearly had the lowest SPAD values after 10 days of N starvation. Among the lines, cvs. NPZ-1 and Apex had higher SPAD values (at least in tendency) than cvs. NPZ-2 and Capitol.

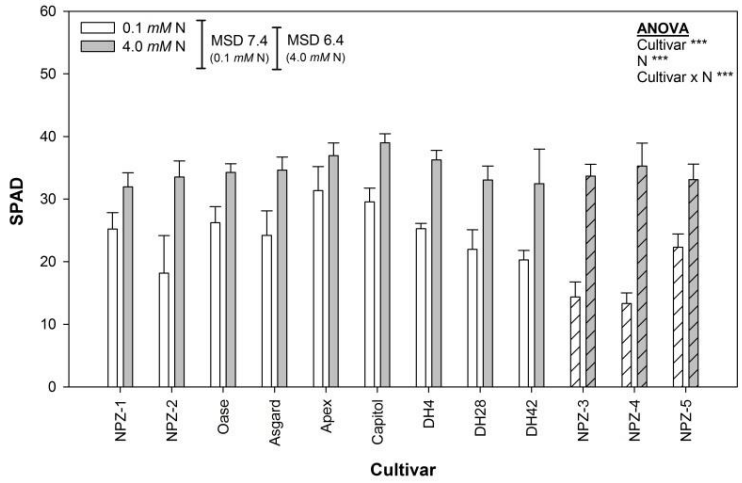

Figure I-12 SPAD values of leaf position three of winter oilseed-rape line (*n* = 9) and hybrid (*n* = 3) cultivars as affected by the N supply 10 DAT. The plants were grown in hydroponics for 28 days at 2.0 *mM* N, followed by 10 days of N starvation (0.1 *mM*) or optimal N supply (4.0 *mM*). Open columns show the lines, dashed columns show the hybrids. The error bars represent the standard deviations of the means (n = 3 to 4). MSD = Minimum significant difference (p <0.05). For the ANOVA * indicate significant differences at p <0.001.**

The photosynthesis rate was even a more sensitive but more variable indicator of leaf senescence induced by N starvation (Figure I-13). N supply and cultivar highly significantly affected the photosynthesis rate of leaf three at 10 DAT. However, owing to the high variability the cultivar x N interaction was not significant. Nevertheless, the cultivar differences described above for SPAD loss were confirmed: The hybrids had the highest reduction in photosynthesis rates after 10 days of N starvation, and the lines cv. NPZ-1 and cv. Apex were less affected by N starvation than their respective counterparts cv. NPZ-2 and cv. Capitol. The effectiveness in which leaf N is used for photosynthesis is described by the photosynthetic N use efficiency. The photosynthetic N use efficiency was generally higher under low N, but was neither significantly affected by N supply nor cultivar. Consequently no cultivar x N interaction existed.

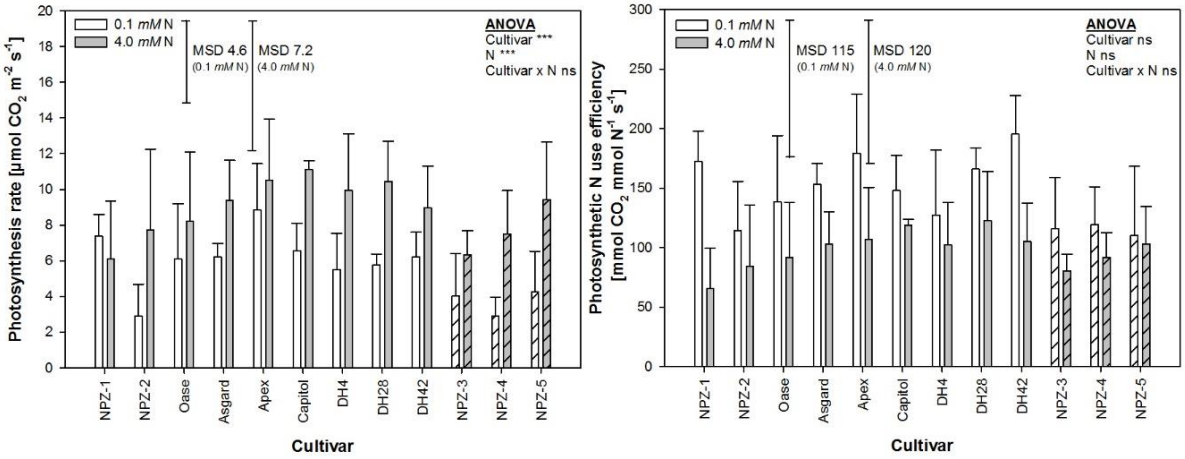

Figure I-13 Photosynthesis rates and photosynthetic N use efficiency of leaf position three of winter oilseed-rape line (*n* = 9) and hybrid (*n* = 3) cultivars as affected the by N supply. The plants were grown in hydroponics for 28 days at 2.0 *mM* N, followed by 10 days of N starvation (0.1 *mM*) or optimal N supply (4.0 *mM*). Open columns show the lines, dashed columns show the hybrids. The error bars represent the standard deviations of the means (n = 3 to 4). MSD = Minimum significant difference (p <0.05). For the ANOVA * indicate significant differences at p <0.001. ns = non-significant.**

As a further senescence marker the linear relative expression (RE) of the gene *SAG12-1* coding for a senescence-specific cysteine protease was determined (Figure I-14). *SAG12-1* expression proved to be a much more sensitive indicator than SPAD and photosynthesis (compare with figures 14 and 15). The ANOVA revealed highly significant N, cultivar and cultivar x N interaction effects. Most of the cultivars differentiated in *SAG12-1* expression induced by N starvation as expected on the basis of the SPAD loss and decrease in photosynthesis shown earlier. The hybrids NPZ-3 (RE 62,581) and NPZ-4 (RE 40,435) with a fast leaf senescence development were among the cultivars with the highest *SAG12-1* expression. The fast senescing line cultivar NPZ-2 (RE 132,425) showed the most dramatic increase in *SAG12-1* expression, nearly 10,000-times higher than of NPZ-1 (RE 185). Also the cvs. Apex and Capitol showed the expected cultivar-specific differences in expression. *SAG12-1* was 3.7-times higher up-regulated in cv. Capitol (RE 1450) than in cv. Apex (RE 394). Furthermore, the line cultivars cv. Oase (functional stay-green) and cv. Asgard (fast senescing) responded to N starvation with a low or high up-regulation of *SAG12-1*, respectively, in agreement with the senescence classification by the breeders (compare Table I-1).

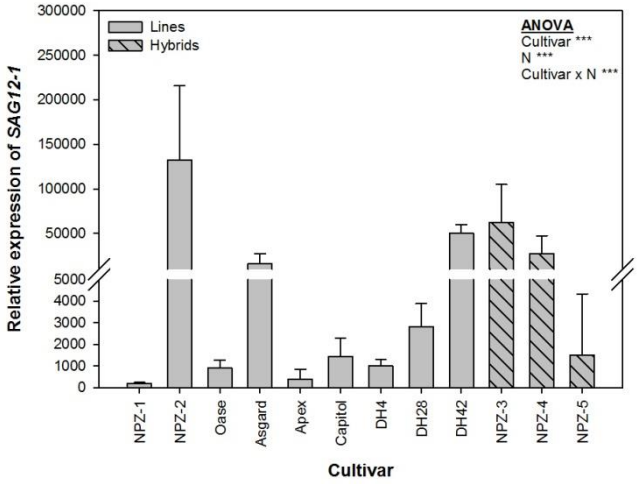

Figure I-14 Relative expression ($2^{-\Delta\Delta Ct}$) of *SAG12-1* in senescing leaves of leaf position three of winter oilseed-rape line (*n* = 9) and hybrid (*n* = 3) cultivars. The plants were grown for 28 days at 2.0 *mM* N followed by 10 days at N starvation (0.1 *mM*) supply or optimal N (4.0 *mM*) supply. Open symbols show the lines and the dashed symbols show the hybrids. The data are shown relative to the cultivar-specific control (4.0 *mM* N). The error bars represent the standard errors of the means (n = 3 to 4). For the ANOVA * indicate significant differences at p <0.001.**

In order to decide whether the cultivar-specific differences in N starvation-induced leaf senescence can be related to the N status of the leaf or rather depended on a lower sensitivity of the leaf to low N, the specific leaf N content has been related to the leaf-senescence indicators SPAD, photosynthesis rate and *SAG12-1* expression (Figure I-15). The indicators clearly showed that cultivar-specific differences in N starvation-induced leaf senescence were related to the N status of the leaf. All three parameters classify the two hybrids NPZ-3 and NPZ-4 as highly senescent in response to N starvation. This can be related to highly efficient retranslocation of N from the senescing leaves.

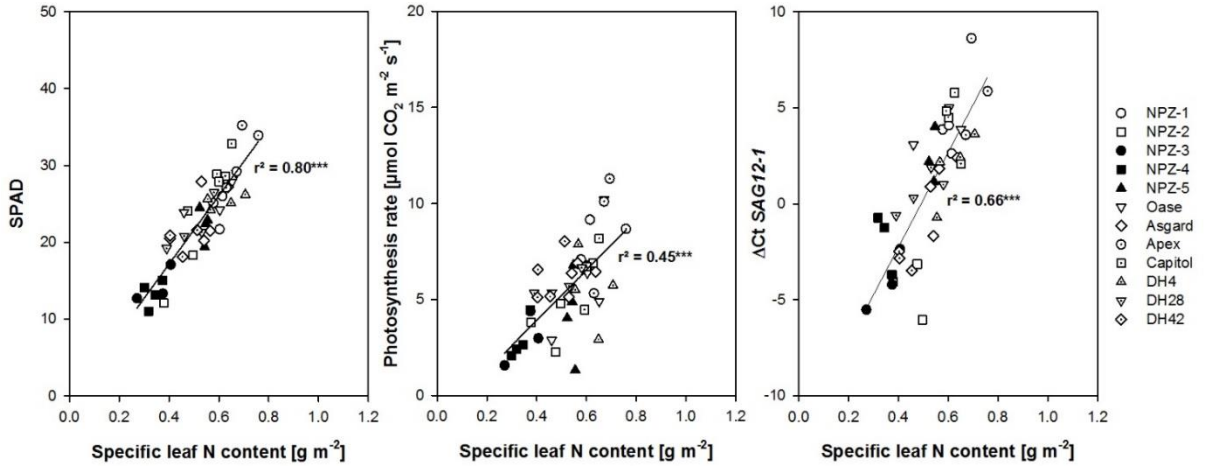

Figure I-15 Correlation between specific leaf N content and SPAD, photosynthesis rate and ΔC_t *SAG12-1* of leaf position three of winter oilseed-rape line (*n* = 9) and hybrid (*n* = 3) cultivars. The plants were grown for 28 days at 2.0 *mM* N followed by 10 days N starvation (0.1 *mM*). Open symbols show the lines and the filled symbols show the hybrids. For the correlation * indicate significance at p <0.001.**

Discussion

According to the definition of N efficiency, the ability of a genotype/cultivar to achieve a yield above average under conditions of limited N supply (Graham, 1984; Sattelmacher *et al.,* 1994), the hybrids were more N-efficient than the line and dwarf cultivars (Figures I-2, I-3). The dwarfs generally met the expectations of a lower biomass formation and N uptake until maturity, but without reducing the remaining N in the straw (Figures I-1, I-7). Also Sieling & Kage (2008) concluded from their comparison of commercial line cultivars with a semi-dwarf cultivar that the semi-dwarf was inferior in yield independent of N supply and despite its lower plant height did not provide the opportunity to reduce the risk of N leaching after growing winter oilseed-rape. Therefore, the following discussion will mainly concentrate on the comparison of hybrid and line cultivars.

The ranking of cultivars for N efficiency depends on the severity of the N deficiency stress. Generally, with increasing strength of the N deficiency stress (percent yield decline under N deficiency compared to the N-sufficient control) the coefficient of genotypic correlation between deficient and sufficient N decreases. This has been clearly shown for maize particularly by Presterl *et al.* (2003). Also Bänzinger *et al.* (1997), Bertin & Gallais (2000) and Worku *et al.* (2007) reported a change in the ranking of cultivars between limiting and sufficient N supply. There is no reason to assume that this not also holds true for oilseed rape as indicated by Berry *et al.* (2010) and Schulte auf'm Erley *et al.* (2011). In the present field experiments the N deficiency stress was mild with only 16% yield reduction across all cultivars (Figures I-2, I-3). Thus the correlation between the yield at low compared to high N was highly significant and close (r^2 = 0.78***, Figure I-3), and the cultivar x N supply interaction was not significant (Table SI-2). This may also explain why the line cultivars cvs. Apex versus Capitol and cvs. NPZ-1 versus NPZ-2 (N-efficient and N-inefficient, respectively) did not differ much in yield at limiting N supply (Figure I-2), whereas these cultivars differed greatly under more severe N deficiency stress (Behrens, 2002; Kamh *et al.,* 2005; Schulte auf'm Erley *et al.,* 2007; Chapter IV). Different from the line and dwarf cultivars the hybrids did not significantly differ in grain yield between N0 and N150 (Table SI-2). But not only at mild, such as in the experiments shown in this study, but also at more severe N deficiency stress hybrids proved to be superior to other cultivars (Gehringer *et al.,* 2007; Kessel *et al.*, 2012). It is increasingly clearly established that oilseed-rape hybrids are not only superior in grain yield at optimum growing conditions but particularly also under conditions of environmental stresses and are thus characterized by higher yield stability across years and locations (Friedt *et al.,* 2003; Gehringer *et al.,* 2007; Kessel *et al.,* 2012).

The main emphasis of the current work was on the identification of traits contributing to the higher N efficiency of the hybrids compared to the line cultivars. Since the N requirements for the formation of yield components are different it is first necessary to consider differences between hybrid and line

cultivars in yield structure although a complete yield structure analysis could not be performed in the filed experiments. The yield components of oilseed rape are number of plants per area, pods per plant, seeds per pod and thousand grain weight. Owing to severe inter-plant competition within a plant stand and a high compensation capacity for lower plant density by branching (Leach *et al.,* 1999) the most important yield component is the number of pods per area which is a combination of number of plant per area and number of pods per plant (Diepenbrock & Grosse, 1995). The final number of pods per plant is highly influenced by environmental conditions and is the most varying primary yield component (Hühn & Schuster, 1975; Richards & Thurling, 1979; Geisler & Henning, 1981a; Diepenbrock & Geisler, 1985a; Diepenbrock, 2000). The number of pods is principally based on the number of flower buds. However, the flower buds are located on the terminal raceme and the side shoots and, therefore, the branching of the plant is decisive for the number of pods. The potential number of pods seems not to be the limiting factor, because the number of flower buds (Habekotté, 1993; Tayo & Morgan 1975) and side shoots initials (Geisler & Henning, 1981b) is much higher than the final pod and side shoot numbers. For yield formation the number of pods located on the terminal raceme and on the uppermost first order side shoots is of major importance, because they carry the highest number of pods with the highest number of grains (Rakow, 1978; Geisler & Henning, 1981b). About 75% of the pods at maturity originated from flowers which opened within 14 days after anthesis and they are primarily located on the terminal raceme and the uppermost side shoots (Tayo & Morgan, 1975). Although the yield component grain number per pod varies between cultivars and within a single plant with the position of insertion (Rakow, 1978; Chay & Thurling, 1989a, b; Grosse *et al.,* 1992; Asare & Scarisbrick, 1995; Ulas, 2010), it was frequently observed that its contribution to grain yield formation of a canopy or an individual plant is low (Hühn & Schuster, 1982; Chay & Thurling, 1989a; Grosse *et al.,* 1992). Thus, the superior N efficiency of the hybrids was probably not based on number of grains per pod which is supported by several studies (Allen & Morgen, 1972; Scott *et al.,* 1973; Asare & Scarisbrick, 1995; Hocking *et al.*, 1997). Grosse *et al.* (1992) and Hocking *et al.* (1997) showed that the contribution of the yield component thousand grain weight (TGW) to grain yield is also low. The grain weight is influenced least from all yield components by environmental factors (Diepenbrock, 2000). Also in this study the thousand grain weight was affected neither by cultivar type nor by N supply (Figure I-4; Table SI-3). Consequently its contribution to variation in grain yield was low (N0 $r^2 = 0.10^{ns}$; N150 $r^2 = 0.28^{ns}$). Also Allen & Morgan (1972) and Asare & Scarisbrick (1995) reported that N application affected grain yield whereas the TGW was not affected. However, Hocking *et al.* (1997) and Ulas (2010) observed a significant N fertilization effect on the TGW, but the contribution to yield formation was still low. Genetic variation in TGW is well known (Rakow, 1978;

Asare & Scarisbrick, 1995; Berry *et al.,* 2010; Ulas, 2010; Schulte auf'm Erley *et al.,* 2011) and could be observed within the line cultivars also in the present study (Figure I-4). Overall it appears that the higher yielding capacity of the hybrids is mainly the result of the formation of more pods per area owing to a higher number of side shoots and a higher number of pods particularly on the terminal inflorescence and the uppermost side shoots.

For the expression of these yield components under N limitation a high N availability through uptake and retranslocation at branching and early pod formation appears to be decisive. The dry matter formation of winter oilseed-rape before winter is important for the exploitation of the yield potential (Stoy, 1982; Mendham & Scott, 1975). A high biomass formation before winter is important for yield formation independent of the later conditions, because improved growing conditions in the spring could not compensate an inferior development in the autumn (Stoy, 1982; Diepenbrock & Geisler, 1985b). This is particularly true under N-limiting conditions, because N accumulated before winter is protected from N leaching (Sieling & Kage, 2006) and contributes to growth and yield formation in spring. The growth of the plants until the rosette stage in the hydroponic experiment may be representative for the growth in the field at this growth stage. The hybrids showed a more vigorous shoot growth in hydroponics compared to the lines at high N supply but particularly also under N limitation (Table I-3). However, it is unlikely that in the present field experiments plant growth was N-limited at this growth stage because of the high availability of soil N. N efficiency of line cultivars has been attributed to prolonged N uptake during reproductive growth, (Wiesler *et al.,* 2001; Kamh *et al.,* 2005; Berry *et al.,* 2010; Schulte auf'm Erley *et al.,* 2011; Ulas *et al.,* 2013). Hence, Ulas *et al.* (2012) concluded that extended N uptake appears to be one of the most effective strategies to improve N efficiency. In the present field experiments N uptake during reproductive growth was not quantified. A superior N accumulation capacity of the hybrids in comparison with the line cultivars during vegetative growth is suggested by the results of the hydroponic experiment (Table I-4).

In other experiments comparing line cultivars, among them N-efficient cv. Apex and N-inefficient cv. Capitol, prolonged N uptake into the reproductive growth period was related to delayed leaf senescence (Wiesler *et al.*, 2001; Schulte auf'm Erley *et al.,* 2007, Chapter IV). Also in the field experiments recorded here, the line cultivars cvs. Apex compared to Capitol showed delayed leaf senescence according the number of green leaves remaining on the main stem in agreement with their N efficiency (Figure I-11). The line cultivars cvs. NPZ-1 and NPZ-2 did not differ in leaf senescence in the field experiments. But it must be considered that corresponding to the marginal N stress in these experiments, N starvation did not significantly enhanced senescence on the whole plant level (Table SI-11). The senescence status of individual leaves was only weakly affected by the N status and primarily depended of the position on the main stem (Table SI-9). The high N efficiency of

the hybrids was clearly not related to delayed leaf senescence (Figures I-9 to I-11). On the contrary most of the high yielding hybrid cultivars even showed an enhanced senescence course under low N supply. Thus owing to the rapid canopy development (leaf and pod area) during vegetative growth mutual- and self-shading was most likely the main senescence inducer. However, in the hydroponic experiment shading of the leaves was minimal and thus N starvation was the only leaf senescence inducer. These hydroponic experiments clearly confirmed and demonstrated the differences in N starvation-induced leaf senescence between cvs. NPZ-1 and Apex (late responding) and cvs. NPZ-2 and Capitol (rapid responding) based on SPAD value (Figure I-12), photosynthesis (Figure I-13) and particularly well *SAG12-1* expression (Figure I-14). *SAG12* has been frequently used as a suitable molecular leaf-senescence marker in winter oilseed-rape (Gombert *et al.,* 2006; Etienne *et al.,* 2007; Brunel-Muguet *et al.,* 2013). The encoded cysteine protease is involved in protein breakdown for N remobilization during senescence and is controlled on the transcription level (Grebic, 2003). Using the same parameters the early N deficiency-induced senescence of the high yielding N-efficient hybrid cultivars cvs. NPZ-3 and NPZ-4 could be confirmed.

A maintained photosynthetic capacity particularly of lower leaves through delayed leaf senescence will not only result in a better assimilate supply to the pods but also to the roots. A prolonged assimilate allocation to the roots maintain root growth and consequently N uptake (Osaki, 1995; Mi *et al.,* 2003). Kamh *et al.* (2005) showed for the line cultivars cvs. Apex and Capitol that improved N uptake efficiency was based on a higher root length in deeper soil layers enhancing the acquisition of subsoil nitrate. However, these results were not fully confirmed by Ulas *et al.* (2012). According to the studies of these authors, cv. Apex compared to cv. Capitol showed a generally higher total root length and a generally higher root-length density and more living fine roots in the plow layer without differences in the subsoil. In the present field experiments root growth was not studied. However, the potential root growth of the cultivars has been evaluated in the hydroponic experiment. In agreement with the shoot growth the hybrids also showed a more vigorous root growth than the line cultivars at limiting and non-limiting N supply, both on a dry weight (Table I-3) and on a root-length basis (Table I-5). In agreement with previous studies (Schulte auf'm Erley *et al.,* 2007) N starvation primarily impaired shoot growth, thus the root/shoot ratio nearly doubled, equally in both cultivar types (Table I-3). However, specific root length which is a measure of the root fineness differed significantly between the two cultivar types with hybrids showing coarser roots (Table I-5). Thicker roots might be beneficial for nitrate acquisition, because thicker roots have a higher soil penetration ability allowing to better exploiting deeper soil layers (Clark *et al.,* 2003). In contrast to the experimental results reported by Schulte auf'm Erley *et al.* (2007) the specific N uptake (N uptake per unit of root length) did not differ within the cultivar types and between hybrid and line cultivars (Table I-5), and thus seems not to play an important role in N

efficiency. However, it has to be considered that N uptake rate was calculated over the whole experimental period including pre-culture at sufficient N supply and thus might have masked differences between the cultivars during the N starvation period.

The second pillar of N efficiency is N utilization efficiency (NUE) (Sattelmacher *et al.,* 1994). Compared to N uptake efficiency (NUPT) under N-limiting conditions NUE plays a minor role for N efficiency of oilseed rape (Berry *et al.,* 2010; Schulte auf'm Erley *et al.,* 2011). These authors found that NUPT and grain yield were closely positively correlated whereas NUE was rather negatively or not correlated with grain yield under greatly limiting N supply. However, with increasing N supply NUE becomes increasingly more important than NUPT. This is in agreement with the present study where NUPT (r^2 = 0.34***) and NUE (r^2 = 0.25***) were equally important for grain yield formation under marginal N deficiency. Among the cultivars the hybrids and dwarfs showed a higher NUE compared to the lines (Figure I-8). Physiological traits that may contribute to N utilization efficiency are a low grain N concentration (low grain N requirement for grain formation), efficient retranslocation of N from vegetative plant organs to the grains and high photosynthetic N efficiency (low N requirement for maintaining photosynthesis). At low N supply grain N concentration of hybrids (in tendency) and dwarfs were lower than of the lines (Figure I-5), and an inverse relationship between the grain N concentrations and the N efficiency existed (r^2 = -0.22$^+$). This was consistent with lower grain protein (except seed protein at N0) and grain-meal protein concentrations of hybrids and dwarfs compared to the lines (Figure I-6). Lower protein concentrations of grains as contributing to N efficiency, however, is equivocal from the grain quality and crop N-balance point of view. Although winter oilseed-rape is an oil crop and the oil yield is the most important economic parameter (Funk & Mohr, 2010), the remaining oilseed meal is a valuable animal feedstuff and protein source (Wittkop *et al.,* 2009). Also, a lower N concentration in the grain might leave higher N amounts in crop residues contributing to high crop N balance-surpluses.

Therefore, a high retranslocation of N from vegetative plant organs to the grains, for which the N harvest index (NHI) is an overall indicator, is of greater importance as component of NUE. Generally N uptake after anthesis is not sufficient to meet the total N demand of the reproductive organs (Masclaux-Daubresse *et al.,* 2008). Thus N retranslocation particularly from leaves is crucial for grain formation (Ulas *et al.,* 2013; Chapter IV). The NHI was 0.67 and 0.75 for low and high N supply, respectively (Figure I-8) and thus in the range (or higher) than reported in other studies (Wiesler *et al.,* 2001; Friedt *et al.,* 2003; Sieling & Kage, 2008; Berry *et al.,* 2010). However, it has to be considered, that N in fallen leaves has not been included in total N uptake in this study leading to a slight overestimation of the NHI because the contribution of N in shed leaves particularly at N0 is small (Ulas *et al.,* 2013; Chapter IV). Although cultivar differences in NHI existed across all cultivars (Table SI-8) in agreement with Berry *et al.* (2010), the cultivar types did not significantly differ in NHI

(Figure I-8) suggesting that N retranslocation efficiency did not contribute to the higher N utilization efficiency of the hybrids. But the total N uptake at maturity was significantly higher in three of the hybrids in comparison to the line and dwarf cultivars at low N supply (Figure I-7). Thus given the same NHI the amount of N retranslocted was also higher. The high capacity of leaf N remobilization during N starvation-induced leaf senescence was clearly demonstrated in the hydroponic experiment, where the hybrids showed the lowest specific leaf N content after 10 days of N starvation (Figure I-15). It appears that the rapid and efficient remobilization of leaf N is the reason for the enhanced induction of senescence in the hybrids as clearly indicated by high *SAG12-1* expression (Figure I-14). The highly significant correlation between specific leaf N content and photosynthesis (Figure I-15) across all cultivars indicated that cultivar differences in photosynthetic N efficiency did not contribute to the superior NUE of the hybrids.

In conclusion, the greater N efficiency of hybrid compared to line cultivars was not related to delayed leaf senescence into the reproductive growth period. Rather a high biomass production (shoot and root) and thus N uptake during vegetative growth (NUPT) and a more efficient N retranslocation from vegetative to reproductive plant organs in combination with a lower grain-N (protein) concentration (NUE) were decisive for the superior N efficiency of the hybrids.

II Transcriptomic analysis of nitrogen starvation- and cultivar-specific leaf senescence in winter oilseed-rape (*Brassica napus* L.)

Fabian Köslin-Findeklee[1], Vajiheh Safavi Rizi[2], Martin A. Becker[1], Sebastian Parra-Londono[1], Muhammad Arif[3,4], Salma Balazadeh[3,4], Bernd Müller-Röber[3,4], Reinhard Kunze[2] and Walter J. Horst[1]

[1]Institute of Plant Nutrition, Leibniz University of Hannover, Herrenhäuser Str. 2, D-30419 Hannover, Germany
[2]Institute of Biology, Free-University Berlin, Albrecht-Thaer-Weg 6, D-14195 Berlin, Germany
[3]Max-Planck-Institute of Molecular Plant Physiology, Am Mühlenberg 1, 14476 Potsdam, Germany
[4]Institute of Biochemistry and Biology, University of Potsdam, Karl-Liebknecht-Str. 24-25, 14476 Potsdam, Germany

📖 Published in *Plant Science* (2015) doi: 10.1016/j.plantsci.2014.11.018

Abstract

High nitrogen (N) efficiency, characterized by high grain yield under N limitation, is an important agricultural trait in *Brassica napus* L. cultivars related to delayed senescence of older leaves during reproductive growth (a syndrome called stay-green). The aim of this study was thus to identify genes whose expression is specifically altered during N starvation-induced leaf senescence and that can be used as markers to distinguish cultivars at early stages of senescence prior to chlorophyll loss. To this end, the transcriptomes of leaves of two *B. napus* cultivars differing in functional stay-green characteristics and N efficiency were analyzed four days after the induction of senescence by either N starvation, leaf shading or detaching. In addition to N metabolism genes, N starvation mostly (and specifically) repressed genes related to photosynthesis, photorespiration and cell-wall structure, while genes related to mitochondrial electron transport and flavonoid biosynthesis were predominately up-regulated. A kinetic study over a period of 12 days with four *B. napus* cultivars differing in their functional stay-green characteristics confirmed the cultivar-specific regulation of six genes in agreement with their senescence behavior: the senescence regulator *ANAC029*, the anthocyanin synthesis-related gene *ANS* and the possibly anthocyanin synthesis-related gene *DFR-like1*, the ammonium transporter *AMT1;4*, the ureide transporter *UPS5*, and *SPS1* involved in sucrose biosynthesis. The identified genes represent markers for the detection of cultivar-specific differences in N starvation-induced leaf senescence and can thus be employed as valuable tools in *B. napus* breeding.

Keywords: *Brassica napus*, genotypic differences, leaf senescence, molecular marker, N efficiency, functional stay-green

Introduction

Production of winter oilseed-rape (*Brassica napus* L.) is characterized by high N balance surpluses of 60 kg N ha^{-1} even under the best agronomic practices. The high N surplus may cause environmental pollution due to nitrate leaching and volatilization of nitrous oxide. An important agricultural goal therefore is to reduce N surplus while at the same time ensuring high grain yield. An approach towards this goal is the breeding and cultivation of N-efficient cultivars producing high grain yield under conditions of N limitation.

Nitrogen efficiency may be primarily related to N uptake efficiency, particularly during flowering (Wiesler *et al.,* 2001; Kamh *et al.,* 2005; Berry *et al.,* 2010; Schulte auf'm Erley *et al.,* 2011; Ulas *et al.,* 2012). A characteristic of N-efficient cultivars is a functional stay-green phenotype during reproductive growth, expressed as delayed senescence of the older leaves, accompanied by maintenance of the photosynthetic capacity (Schulte auf'm Erley *et al.,* 2007). It is generally believed that prolonged assimilate supply to the roots together with extended leaf photosynthesis helps to maintain N uptake. However, it is currently not clear whether delayed leaf senescence of N-efficient cultivars is the cause or the consequence of maintained root growth (Kamh *et al.,* 2005). A key aspect of leaf senescence is the remobilization and retranslocation of N from aging to developing leaves and reproductive organs (Masclaux-Daubresse *et al.,* 2008). Accordingly, senescence strongly affects yield formation (Gregersen *et al.,* 2013). Besides being a developmental process, senescence can be induced by unfavorable environmental conditions such as suboptimal nutrient supply. Particularly N starvation induces and accelerates leaf senescence (Mei & Thimann, 1984). The onset of leaf senescence is accompanied by transcriptional activation of many genes which are directly or indirectly involved in the senescence-related biochemical and cellular changes. Numerous senescence-associated genes (SAGs) have been identified in *A. thaliana* (Buchanan-Wollaston *et al.,* 2005; van der Graaff *et al.,* 2006) and *B. napus* (Buchanan-Wollaston & Ainsworth, 1997; Lee *et al.,* 2014), of which many encode senescence-related transcription factors (TFs) (Balazadeh *et al.,* 20008b; Balazadeh *et al.,* 2010; Parlitz *et al.,* 2011; Ay *et al.,* 2013).

Nitrogen shortage leads to a significant shift in the transcriptome, in which the pattern of gene reprogramming depends on the intensity and duration of N deficiency. In particular, TFs of the AP2/ERF, WRKY, NAC and MYB families are involved in N starvation-related regulatory networks. Moreover, genes assigned to photosynthesis, protein biosynthesis, energy metabolism and nitrate assimilation are rapidly down-regulated in above-ground tissues, while genes involved in biotic and abiotic stress responses, related to secondary metabolism, or involved in N retrieval and retranslocation are up-regulated. Genes encoding for cysteine proteases (e.g. *SAG12*) involved in protein breakdown and genes involved in the reassimilation of ammonium released during protein degradation are specifically up-regulated. Furthermore, genes involved in anthocyanin biosynthesis

and their regulation (e.g. MYB TFs) are induced by N starvation, in accordance with the accumulation of anthocyanins (Scheible *et al.,* 2004; Diaz *et al.,* 2006; Bi *et al.,* 2007; Peng *et al.,* 2008; Krapp *et al.,* 2011; Misyura *et al.,* 2013; Nemie-Feyissa *et al.,* 2014).

Using ´stay-green´ as a selection parameter for breeding N-efficient cultivars is difficult owing to additional senescence inducers, particularly shading, that interact with N limitation. Similarly, metabolic processes are regulated and executed by many genes which complicate the identification of molecular leaf-senescence markers with high heritability.

The aim of the present study was to identify marker genes which are specific for N starvation-induced leaf senescence in *B. napus* and suitable for the detection of cultivar-specific differences at early leaf senescence stages prior to the loss of chlorophyll.

Material and Methods

Development and comparison of leaf senescence induced by different inductors

For comparing senescence induction by different inducers the two *B. napus* commercial cultivars cv. Apex (N-efficient) and cv. Capitol (N-inefficient) were selected, because previous field and long-term nutrient solution experiments classified cv. Apex as N-efficient accompanied by delayed senescence (´stay-green´) of the older leaves and cv. Capitol as N-inefficient accompanied by an accelerated senescence-course of the older leaves (Schulte auf'm Erley *et al.,* 2007). The plants were cultured in hydroponics in a greenhouse (assimilation light (16 klm) 16 h; heating/ventilation temperature 20/22°C; shading at 15 klx solar radiation; relative humidity 80%) from 10 March to 13 April 2010. Seven days after germination, the seedlings were transferred to 6-L plastic pots and pre-cultured for 28 days at optimal N supply in a continuously aerated nutrient solution composed of 2 *mM* N [9:1 ratio of $Ca(NO_3)_2$ and $(NH_4)_2SO_4$], 500 *µM* K_2S0_4, 250 *µM* KH_2PO_4, 325 *µM* $MgSO_4$, 50 *µM* NaCl, 8 *µM* H_3BO_3, 0.4 *µM* $MnSO_4$, 0.4 *µM* $ZnSO_4$, 0.4 *µM* $CuSO_4$, 0.1 *µM* Na_2MoO_4, 40 *µM* Fe-EDDHA and 10 µ*M* $C_2H_4N_4$ (dicyandiamide; to prevent nitrification). Three different treatments were applied to induce leaf senescence: (i) N starvation (0.1 *mM* N as $Ca(NO_3)_2$ and 1 *mM* $CaSO_4$ to allow for optimum Ca nutrition), (ii) shading of leaf 3 and 4 (counted from bottom to top of the plant) by covering the leaf blades with an upper unperforated and a lower perforated aluminum foil to allow gas exchange, while plants remained in 2 *mM* N nutrient solution, and (iii) by detaching leaves 3 and 4 and incubating them with their petioles submerged in 100 mL deionized water in Erlenmeyer flasks. After treatment start the nutrient solution and the deionized water were changed every second day. During treatment, the senescence status of the 3rd and 4th leaf was determined by assessing the chlorophyll content of the leaves with a portable chlorophyll meter (SPAD-502, Konica Minolta, Tokyo, Japan) and the photosynthesis rate using a portable gas exchange system (LI-6400, LI-COR, Lincoln, USA) with a photon flux density of 1000 µmol m^{-2} s^{-1} and an incoming CO_2 concentration of 400 µmol m^{-2} s^{-1}. The experiment was completely randomized with 3 to 5 replications.

Plants were harvested and separated into shoots and roots 0, 2, 4, and 6 days after treatment began (DAT). Leaves 3 and 4 were harvested separately. Leaf 4 was the youngest fully expanded leaf at the end of pre-culture. Since it reacted to the senescence inducers in exactly the same way as leaf 3, although delayed, only the results for leaf 3 are presented. Leaf material was immediately frozen in liquid N_2 and ground for total RNA isolation using a mixer mill (MM 400, Retsch, Haan, Germany). For the microarray analysis leaf 3 at 4 DAT was selected with three biological replicates.

Development of N starvation-induced leaf senescence

To investigate the kinetics of the development of N starvation-induced leaf senescence at early vegetative growth stages, in addition to the cultivar pair cvs. Apex and Capitol the cultivar pair cvs. NPZ-1 and NPZ-2 were selected. The cvs. NPZ-1 and NPZ-2 are breeding lines with a similar genetic background. Whereas cv. NPZ-1 shows a delayed senescence-course of the older leaves (stay-green) compared to cv. NPZ-2 under N starvation (Koeslin-Findeklee *et al.,* 2014). The plants were cultured from 23 September to 3 November 2010 in the greenhouse as described above. For N starvation the plants were grown at 0.1 *mM* N as $Ca(NO_3)_2$ and 1 *mM* $CaSO_4$ to allow for optimum Ca nutrition. For optimal N nutrition the plants were cultured at 4.0 *mM* N, doubling the N concentration used for pre-culture because of the longer treatment duration. After start of the treatment the nutrient solution was changed every second day. The experiments were completely randomized with three to four replications.

Plants were harvested after 3, 5, 7, 10 and 12 days of N starvation. Plants grown at optimal N supply were harvested at 7 and 12 DAT. The youngest fully expanded leaf at the end of pre-culture and two older leaves were harvested. In most cases the youngest fully expanded leaf was leaf 5, although sometimes it was the 4^{th} leaf due to differences between cultivars. Senescence status measurements during N starvation and harvest were performed as described above, but photosynthesis rate was measured at a photon flux density of 400 µmol m^{-2} s^{-1}.

RNA isolation and cDNA synthesis

For microarray and qRT-PCR analysis total RNA was extracted from 500 mg frozen and ground tissue according to Verwoerd *et al.* (1989). After extraction, 20 µg of total RNA were purified using the RNeasy Mini Kit and RNase free DNase set (Qiagen, Hilden, Germany). For qRT-PCR validation of the marker genes total RNA was isolated with TRIsure™ reagent (Bioline, London, UK) according to the manufacturer´s instructions. cDNA was synthesized from 2 µg of total RNA with the RevertAid™ H Minus First Strand kit (Fermentas, Waltham, USA). RNA and cDNA were photometrically quantified (NanoPhotometer, Implen, München, Germany) and their integrity was tested by 1% agarose gel electrophoresis.

Brassica napus custom microarray

A *B. napus* custom microarray was designed for the Agilent platform (Agilent Technologies, Santa Clara, CA, USA) by applying a probe-preselection strategy established by ImaGenes GmbH (Berlin, Germany; now Source BioScience, www.lifesciences.sourcebioscience.com) (Weltmeier *et al.,* 2011). Eventually, 60,955 probes representing 59,577 targets (EST clusters) were selected for the production of microarrays in the Agilent 8x60k format. Labelling of total RNA and microarray

processing were performed by ImaGenes GmbH. Briefly, the RNA quality was assayed on an Agilent 2100 Bioanalyzer. Cy3-labeled cRNA was synthesized with the Agilent Quick Amp Labeling Kit one-color and hybridized to *B. napus* custom microarrays fabricated by Agilent Technologies according to manufacturer's instructions. Microarrays were scanned on an Agilent High-Resolution Scanner G2505C and the images were processed with the Agilent Feature Extraction software using default settings. Microarray data are deposited in the NCBI Gene Expression Omnibus (GEO) repository (DataSet GSE60108).

Processing of the *Brassica napus* custom microarray data

The resulting processed signals of all individual hybridizations were quantile-normalized using the ranked median quantiles according to Bolstad *et al.* (2003). For principal component analysis (PCA) the statistic software SAS version 9.2 (SAS Institute, Cary, USA) was used. The normalized data were $\log_2$ transformed and the fold-change (FC) was calculated using the equation $FC = mean_{(control)} - mean_{(senescence\ inducer)}$. The PCA was performed using the PROC FACTOR procedure. The retaining principal components (PC) were extracted based on the Kaiser criterion (Kaiser, 1960), which retains any PC with an eigenvalue greater than 1.0 and the cumulative proportion of variance of the retained PCs should account for at least two-third of the total variance. Afterwards, the extracted PCs were rotated according to the varimax rotation using the ROTATE statement.

For the identification of significantly regulated targets by senescence inducer and cultivar and their interaction the two-factor ANOVA implemented in the Multi Experiment Viewer version 4.2 (Saeed *et al.,* 2003) was used. The two-factor ANOVA was calculated for each senescence inducer against the control to a p-value of 0.01. For the selection of the senescence inducer-specific regulated targets the significantly treatment-regulated targets and the significantly treatment x cultivar-regulated targets were compared between the senescence inducers.

To facilitate functional pathway analysis the *B. napus* targets were annotated to homologues of *A. thaliana* using TAIR10 (Lamesch *et al.,* 2012). The best hit based on E-value and query cover was chosen. Thus, in the following the microarray-selected genes are designated as homologues of *A. thaliana*. In case that several *B. napus* targets shared the same *TAIR* gene accession number, the FCs of the most closely related homologs were averaged. For functional pathway analysis MapMan (Thimm *et al.,* 2004) was used.

Primer design and qRT-PCR

Brassica napus gene sequences for PCR primer design were retrieved from GenBank (NCBI) and The Gene Index Project at the Dana-Farber Cancer Institute (DFCI; http://compbio.dfci.harvard.edu/tgi/). Primer pairs were designed using PrimerQuest (Integrated DNA Technologies, Coralville, USA) for

genes having NCBI accession numbers, or using QuantPrime (Arvidsson *et al.,* 2008) for genes having DFCI accession numbers (Table III-S1).

qRT-PCR for 95 microarray-selected potential marker genes and the three reference genes gibberellin receptor *GID1C* (DFCI accession number TC111745), nitrate transporter *Nrt1.1* (TC111660) and unknown protein (TC194033*)* (Table III-S2) was conducted in 384 well-plates as described by Balazadeh *et al.* (2008a). qRT-PCR for *SAG2* (Figure III-S3), *SAG12-1* (Figure II-4) and the validation of the marker genes (Figure II-11) was performed in 96 well-plates using a CFX96™ Real-time System (BioRad Laboratories, Hercules, USA). The thermal program consisted of an initial denaturation at 95°C (10 min), followed by 50 cycles at 95°C (15 s), 60°C (30 s), 72°C (30 s), and a final melting curve analysis from 60°C to 95°C with a 0.5°C 5 s^{-1} increasing temperature gradient. The gene *EF1-alpha* (NCBI accession number DQ312264) coding for an elongation factor was used as reference gene (Desclos *et al.,* 2008). The 25 µl SYBR Green-based mix included 2.5 µL 10x Hot-Start PCR buffer, 3.6 µL of 1000-times diluted 1000x SYBR Green-I (Invitrogen GmbH, Darmstadt, Germany), 0.5 µL 10 *mM* dNTP mix, 0.63 µL of each 10 *µM* forward and reverse primer, 0.15 µL 5U μL^{-1} U DCS Hot Start DNA polymerase (DNA Cloning Service, Hamburg, Germany), 1 µL of 50 ng μL^{-1} cDNA template. The mean relative expressions of the qRT-PCR results and their standard errors were calculated based on the $2^{-\Delta\Delta Ct}$-method by Livak & Smittgen (2001).

Microarray validation using qRT-PCR

For validation of the microarrays log_2 fold-changes between control and four days of N starvation (4 DAT), the expressions of 95 potential marker genes were determined in leaf three using qRT-PCR. The microarray Log_2 fold-change were highly significantly ($p < 0.001$) correlated ($r^2 = 0.69$) with the corresponding qRT-PCR data (Figure II-1).

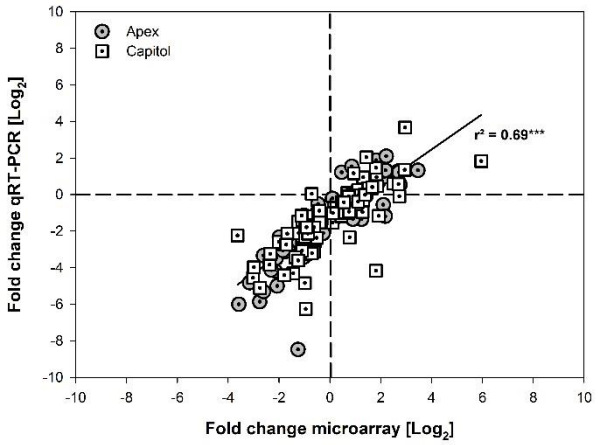

Figure II-1 Correlation of log_2-fold changes in expression of 95 microarray-selected genes between microarray and qRT-PCR analysis of leaf three of the winter oilseed-rape cultivars Apex and Capitol after four days of N starvation (4 DAT). The log_2-fold changes are calculated between N starvation and the 2.0 *mM* N control (n = 3). The plants were grown in hydroponics for 28 days at 2.0 *mM* N and were then treated for up to four days. For the correlation * indicate significance at p <0.001.**

Statistical analysis

The statistical analysis of the physiological and qRT-PCR data was performed using the statistics software SAS, version 9.2 (SAS Institute, Cary, USA). The analysis of variance (ANOVA) was calculated using the PROC GLM procedure. For testing the significance of effects the Type III sum of squares was applied, considering the unequal number of replicates. The relative qRT-PCR data were analyzed using the %QPCR MIXED macro after Steibel *et al.* (2009) based on the PROC MIXED procedure. For all tests of significance a p-value of 0.05 was used and the p-values were Bonferroni-Holm adjusted. In the tables and figures for the F-Test +, *, ** and *** indicate significance at the $p < 0.10$, < 0.05, < 0.01 and < 0.001 level, respectively. ns = non-significant. The same symbols were used to mark the significance for the correlations. For all tests of significance a p-value of 0.05 was used and the p-values were Bonferroni-Holm adjusted. Curves were fitted using the graphic software SIGMA PLOT version 11 (Systat software, San Jose, USA).

Results

Chlorophyll content in senescing leaves – SPAD

For comparing senescence induction by different inducers the cvs. Apex and Capitol were cultured in hydroponics. The SPAD value of the 3rd leaf was measured every second day (Figure II-2). At 4 DAT the SPAD values began to decrease significantly in detached and shaded leaves and continued to decline after 6 DAT in both cultivars. Nitrogen starvation did not significantly affect the SPAD values. However, a significant cultivar x DAT interaction at low N supply indicates that in cv. Capitol, in contrast to cv. Apex, the SPAD value decreased with the duration of N starvation (Figure SII-1).

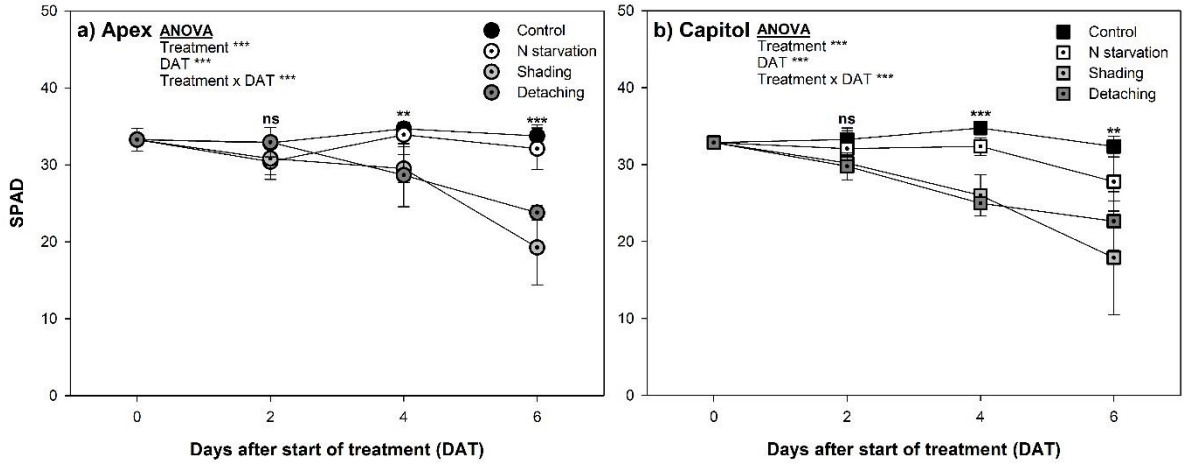

Figure II-2 SPAD values decrease in a senescence inducer-specific way. SPAD values of leaf three of the winter oilseed-rape cultivars Apex (a) and Capitol (b) in control (2.0 *mM* N) and treated plants (0.1 *mM* N, shading, detaching). The plants were grown in hydroponics for 28 days at 2.0 *mM* N and then treated for 6 days. Detached leaves were incubated in deionized water. For the ANOVA **, * indicate significant differences at p <0.01, <0.001, respectively. ns = non-significant. The error bars represent the standard deviations of the means (n = 3 to 5).**

Photosynthesis rate in senescing leaves

Photosynthesis reacted more sensitively than SPAD to the senescence-inducing treatments (Figure II-3). As early as 2 DAT, shading and particularly detaching significantly reduced the rate of photosynthesis which further declined to very low levels until 6 DAT. While both cultivars reacted similarly to shading, a significant cultivar x DAT interaction for detached leaves suggests an enhanced decline in photosynthesis in cv. Capitol compared to cv. Apex (Figure SII-2). Nitrogen starvation reduced photosynthesis significantly from 4 DAT onwards. Although there was a tendency of greater reduction in cv. Capitol than in cv. Apex, the cultivar x DAT interaction was not significant (Figure II-S2).

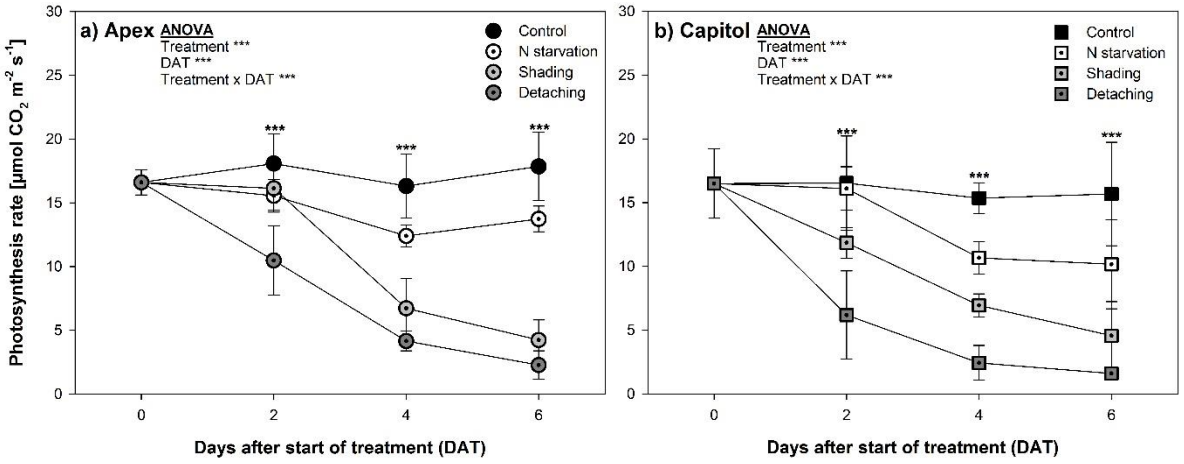

Figure II-3 Photosynthesis rate decreases in a senescence inducer-specific way. Changes in photosynthesis rate of leaf three of the winter oilseed-rape cultivars Apex (a) and Capitol (b) as affected by three different leaf senescence inducers (0.1 *mM* N, shading, detaching) and the 2.0 *mM* N control. The plants were grown in hydroponics for 28 days at 2.0 *mM* N and then treated for 6 days. Detached leaves were cultured in Erlenmeyer flasks containing deionized water. For the ANOVA, * indicate significant differences at p <0.001. The error bars represent the standard deviations of the means (n = 3 to 5).**

Expression of genes coding for the senescence-specific cysteine proteases SAG2 and SAG12 in senescing leaves

For a more sensitive monitoring of senescence induction the expression of the genes *SAG2* and *SAG12-1* coding for senescence-associated cysteine proteases was determined by qRT-PCR. In contrast to *SAG2* (Figure SII-3), *SAG12-1* proved to be very responsive to all senescence inducers (Figure II-4). In agreement with the strong decline of SPAD and photosynthesis by leaf shading and detaching *SAG12-1* was up-regulated in both cultivars by a factor of 100-1,000 at 4 DAT (Figure II-4a), and 1,000-10,000 at 6 DAT (Figure II-4b) by these senescence inducers. Whereas at 4 DAT the cultivars did not differ in shading- and detaching-induced *SAG12-1* expression, at 6 DAT the up-regulation was significantly higher in cv. Apex than in cv. Capitol. At day 4 of N starvation only slightly (factor 2), but significantly enhanced *SAG12-1* induction was observed in cv. Capitol but not in cv. Apex. At 6 DAT, *SAG12-1* was more strongly up-regulated in N-inefficient Capitol (factor 1,000) than in N-efficient Apex (factor 100). A highly significant cultivar x treatment interaction suggests that the genotype-specific differential response in *SAG12-1* expression only occurred under N starvation.

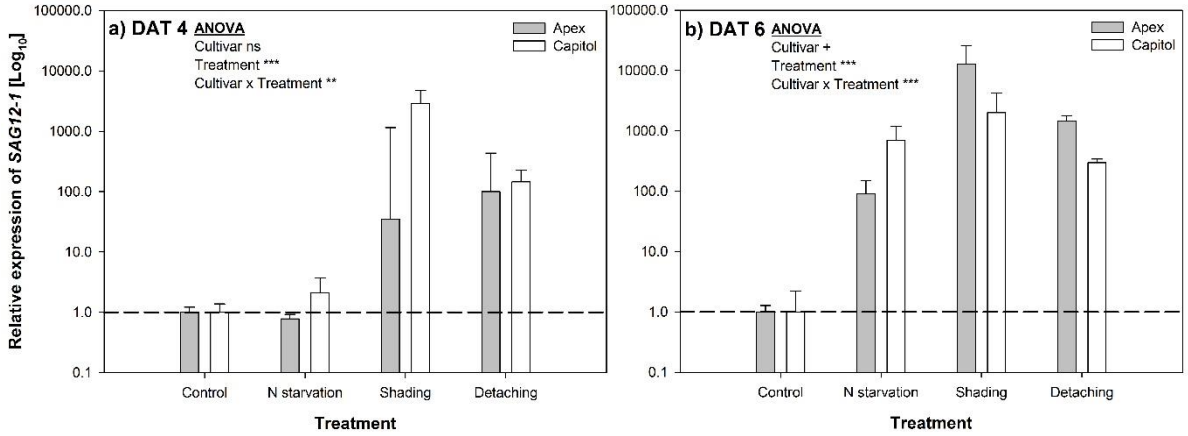

Figure II-4 Expression of *SAG12-1* increases in a senescence inducer- and cultivar-specific way. Relative expression ($2^{-\Delta\Delta Ct}$) of the senescence-specific cysteine protease gene *SAG12-1* in leaf three of the winter oilseed-rape cultivars Apex and Capitol as affected by three different leaf senescence inducers (0.1 *mM* N, shading, detaching) and the 2.0 *mM* N control after 4 (a) and 6 (b) days of treatment. The plants were grown in hydroponics for 28 days at 2.0 *mM* N and then treated for 4 or 6 days. Detached leaves were cultured in Erlenmeyer flasks containing deionized water. For the ANOVA, +, **, * indicate significant differences at p <0.10, <0.01, <0.001, respectively. ns = non-significant. The error bars represent the standard errors of the means (n = 3). The data are shown relative to the controls harvested at the same day.**

SAG12-1 expression responded to N starvation only slightly more sensitive than SPAD and photosynthesis rate. Consequently, the correlation between *SAG12-1* expression and SPAD ($r^2 = 0.69$) (Figure II-5a) or photosynthesis rate ($r^2 = 0.62$) (Figure II-5b) is highly significant ($p < 0.001$). With decreasing SPAD and photosynthesis rate transcription of *SAG12-1* increases. Although SAG12-1 expression was not N starvation-specific, *SAG12-1* proved to be a suitable marker for N starvation-induced leaf senescence in hydroponics where N starvation could be isolated as the only factor inducing senescence.

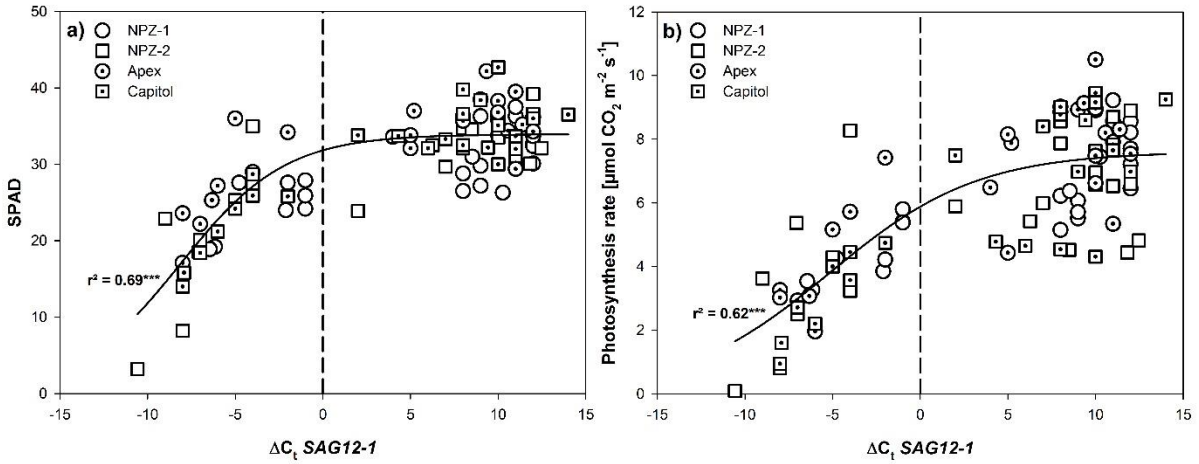

Figure II-5 *SAG12-1* expression and SPAD values or photosynthesis rate are correlated. Correlation between ΔC_t of *SAG12-1* and SPAD (a) or photosynthesis rate (b) of the second oldest harvested leaf of four winter oilseed-rape cultivars. Plants were grown for four weeks at 2.0 *mM* N followed by 3, 5, 7, 10, or 12 days of N starvation (0.1 *mM*). For the correlations * indicate significance at p <0.001.**

Microarray study

Principal component analysis (PCA)

Microarray data are of high dimensionality, but commonly redundancy occurs between the experimental variants in the obtained expression data. In a first step principal component analysis (PCA) was used in order to reduce the experimental variants into a smaller number of principal components (PC) which will account for most of the existing variance in expression of the targets. For the PCA the log_2-fold change compared to the control was used. The overall "eigenvalue" ($\lambda = 6$) is equal to the number of experimental variants. The calculated eigenvalue of each of the six PCs revealed, that the first PC (3.5) explained about 57.5%, the second PC (0.8) 13.7% and the third PC (0.7) 11.8% of the total variance (6.0) (Figure SII-4). Thus the first two principal components accounting for 71% of the total variance determined the variance in the data set: the senescence inducer > cultivar (Figure II-6). The senescence inducers separated into distinctive clusters. Cultivar differences existed particularly under N starvation.

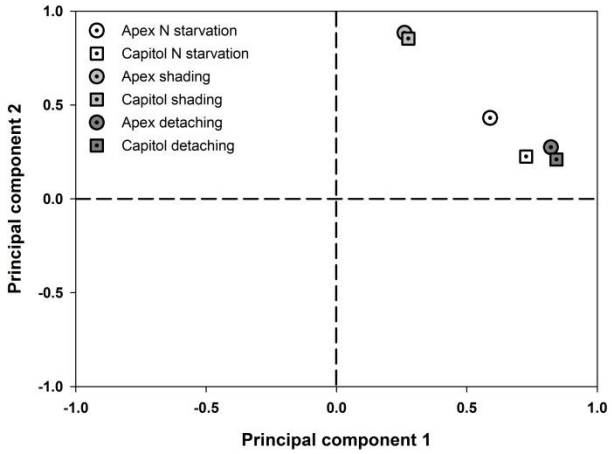

Figure II-6 Projection of the rotated principal factors loaded on the first two principal components for the six experimental variants. The different leaf senescence inducers (0.1 *mM* N, shading, detaching) are compared to the 2.0 *mM* N control (n = 3). The plants were grown in hydroponics for 28 days at 2.0 *mM* N and were then treated for four days.

Number of significantly differently expressed targets

In a second step the microarrays were evaluated in order to identify individual targets which responded in their expression sensitively and N starvation specifically after four days of exposure to the three senescence inductors (Table II-2). Among the 59,577 targets on the microarray, N starvation (14,832 targets) and detaching (13,116 targets) had a major effect on the leaf transcriptome by significantly changing target expression. On the other hand shading only affected 3,055 targets. Among the affected targets 5769, 4409 and 2706 showed a cultivar-specific response to the senescence inductors N starvation, detaching and shading, respectively. A much lower number

of targets showed a significant inductor x cultivar interaction: 4960 for N starvation, 424 for shading and 1052 for detaching.

Table II-2 Number [#] of significantly (p <0.01) differently expressed targets in leaf three of the winter oilseed-rape cultivars Apex and Capitol as affected by three different leaf senescence inducers (0.1 *mM* N, shading, detaching) and the 2.0 *mM* N control. The plants were grown in hydroponics for 28 days at 2.0 *mM* N and then treated for 4 days. Detached leaves were cultured in Erlenmeyer flasks containing deionized water. Each senescence inducer was tested against the 2.0 *mM* N control at 4 DAT. Percentage [%] refers to the total number of targets on the microarray (59577). Three biological replicates.

Factor	N starvation		Shading		Detaching	
	[#]	[%]	[#]	[%]	[#]	[%]
Cultivar	5,769	9.7	2,706	4.5	4,409	7.4
Inducer	14,832	24.9	3,055	5.1	13,116	22.0
Cultivar x Inducer	496	0.8	424	0.7	1,052	1.8

Identification of leaf senescence-inducer and cultivar-specific targets

The microarrays were evaluated to identify individual targets which responded in their expression significantly and N starvation-specifically after four days of exposure to the three senescence inducers (Figure II-7). Of the 59,577 targets represented on the microarray, N starvation (14,832) and detaching (13,116) had the strongest effect, whereas shading affected only 3,055 targets. Among the targets affected by a given senescence inducer 7,779 (52%) were specifically changed in expression by N starvation, 6,209 (47%) by detaching, and 1,050 (34%) by shading (Figure II-7a). For all senescence inducers most targets that showed a significant treatment x genotype interaction were treatment-specific (Figure II-7b): 407 (82%) for N starvation, 953 (91%) for detaching and 378 (89%) for shading.

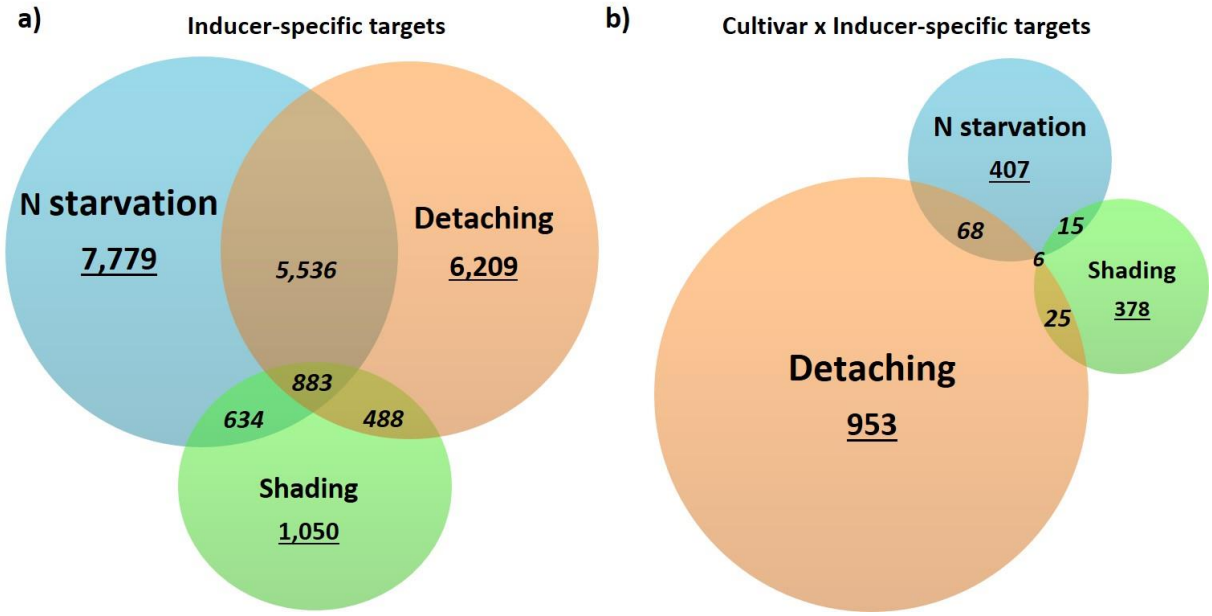

Figure II-7 V Venn diagrams visualizing the numbers of *Brassica napus* targets on the microarray significantly (ANOVA p <0.01) and specifically (underlined) regulated by the individual senescence inducers (a, main effects across cultivars) and showing additionally a cultivar x inducer interaction (b) in leaf three of the winter oilseed-rape cultivars Apex and Capitol 4 DAT. Each senescence inducer was tested against the control. Three biological replicates.

Relating gene expression to metabolic functions

We used the MapMan tool (Thimm *et al.,* 2004) to identify metabolic pathway genes affected by the three senescence inducers. As a *B. napus*-specific MapMan ontology is not yet available, we annotated the 59,577 *B. napus* targets to 20,457 homologous *A. thaliana* genes and used the corresponding ontology for data visualization. Figure 6 displays the mean fold changes of Apex and Capitol of the same set of 2,258 genes (maximal displayable number in MapMan) for each senescence inducer. The 2,258 genes pre-set by MapMan provide a good coverage of central metabolic pathways. Four days after stress induction primarily genes related to anabolic processes such as photosynthesis (light reaction, tetrapyrroles), the Calvin Benson cycle or amino acid biosynthesis as well as photorespiration were mostly down-regulated, independent of the inducer. Simultaneously, genes for catabolic processes such as nucleotide or amino acid degradation and mitochondrial electron transport were predominantly induced. Notably, however, we also observed senescence inducer-specific expression patterns. In particular, N starvation and detaching showed a more similar expression pattern than each of them to shading. This was not only the case for the number of affected genes (Figure II-7a), but also for the type of genes and their regulation (Figure II-8). Unlike shading (Figure II-8b), N starvation and detaching particularly induced genes related to sucrose and starch metabolism (synthesis/degradation), glycolysis, and flavonoid synthesis (Figures II-8a, c), while N starvation and shading mostly down-regulated a large number of cell wall-associated genes (compounds, modification, formation, degradation). In contrast, detaching induced particularly cellulose synthesis-related genes and genes involved in cell-wall modification (Figure II-8c).

Despite the large overlaps between senescence inducers, 7,779 *B. napus* targets annotated to 4,894 different *A. thaliana* homologous genes were specifically regulated by N starvation four days after stress induction (Figure II-7a). Of those, 606 genes could be visualized in the MapMan metabolic pathway analysis (Figure II-9). As expected, N metabolism-related genes were additionally affected by N starvation, including genes coding for glutamine-synthase and nucleotide degradation which were up-regulated (Figure II-9), and genes for amino acid synthesis which were down-regulated. However, also among the N starvation-specific genes (Figure II-9), particularly photosynthesis-, photorespiration- and cell wall-associated genes were mostly down-regulated, whereas genes related to mitochondrial electron transport and flavonoid biosynthesis were predominately up-regulated.

With respect to major carbohydrate metabolism more degradation- than synthesis-associated genes were specifically regulated by N starvation, suggesting that starch metabolism was shifted towards degradation rather than synthesis. The negative regulation by N starvation of the majority of genes of the sucrose degradation pathway and of most of the glycolysis-related genes suggests that starch

was degraded mainly for nitrogen retranslocation rather than for glycolysis. Many of the flavonoid biosynthesis-related genes were specifically changed in expression by N starvation. Genes involved in anthocyanin synthesis, a class of flavonoids contributing to protect the leaf tissue against photo-oxidative stress, were over-represented among the up-regulated genes.

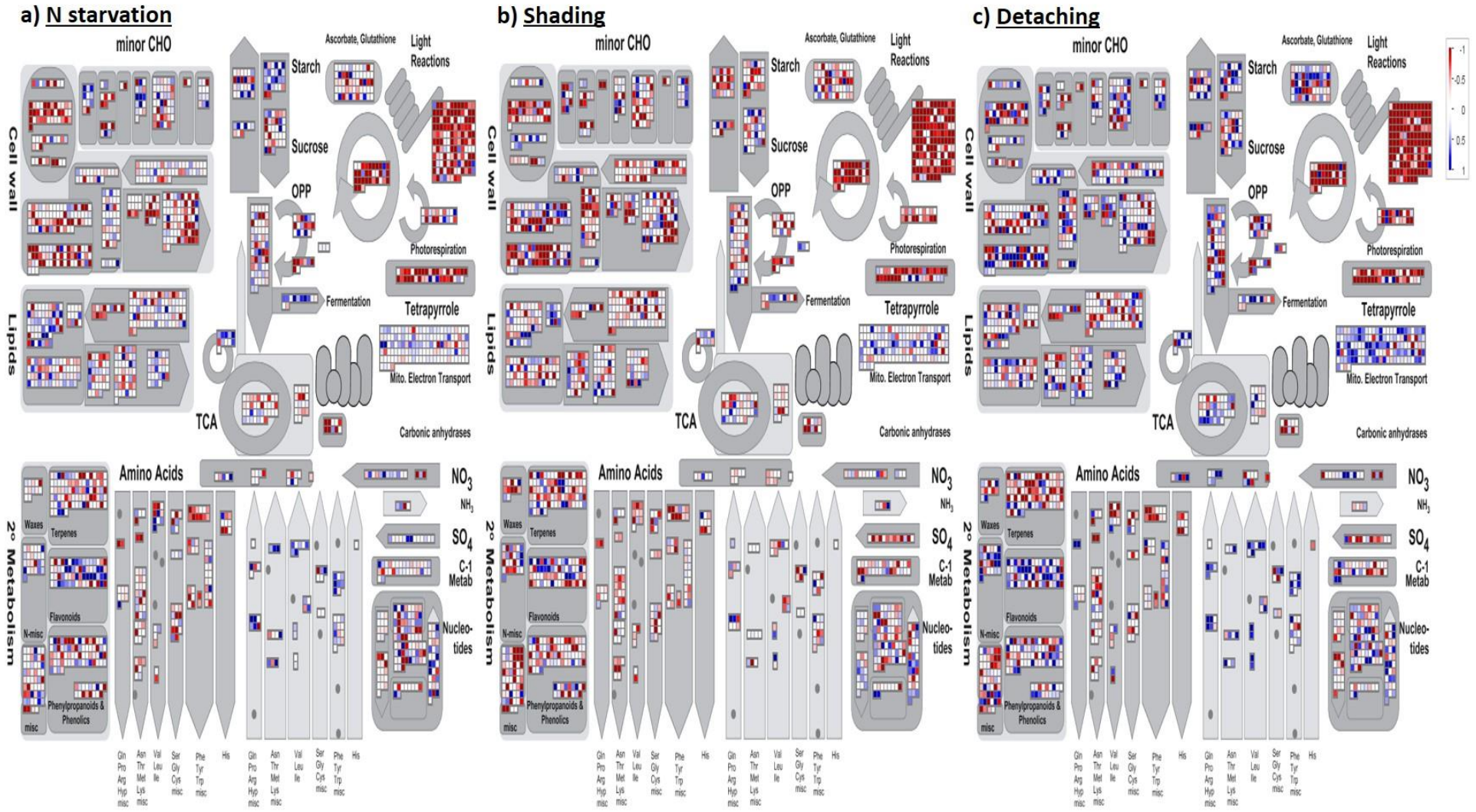

Figure II-8 Overall functional pathway analysis reveals differences between senescence inducers. MapMan metabolism overview of *Arabidopsis thaliana* genes homologous to the *Brassica napus* sequences on the custom microarray. For the inducers N starvation (a), shading (b) and detaching (c) the same 2,258 preset MapMan genes were mapped. Log_2-fold changes (FC) were calculated for each inducer against the control four days after treatment began for the winter oilseed-rape cultivars Apex and Capitol separately (n = 3) and then averaged. The false-color scale reflects the direction (FC of -1, red and +1, blue) and extent (faint to full saturation) of the expression.

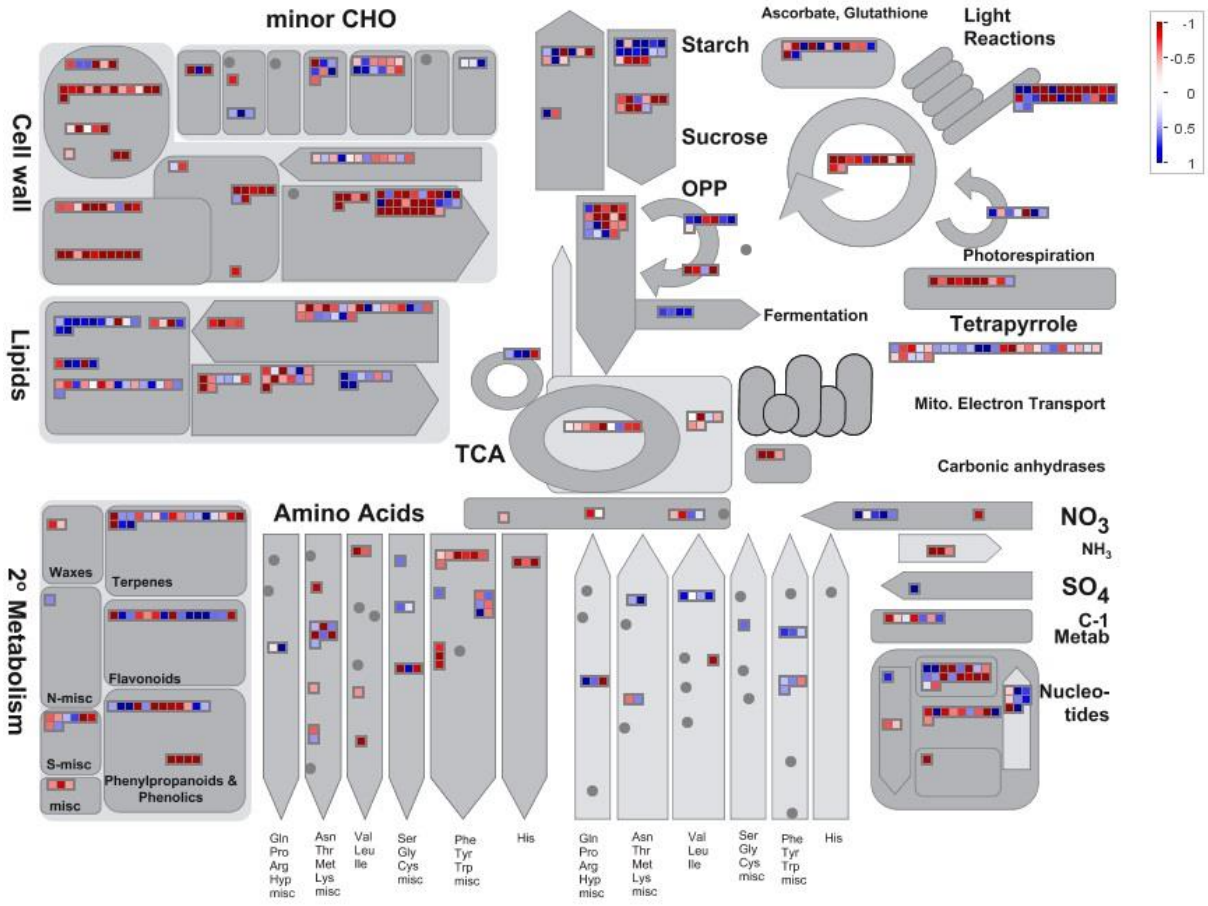

Figure II-9 Functional pathway analysis of N starvation-specific genes. MapMan metabolism overview of *Arabidopsis thaliana* genes homologous to the N starvation-specifically and significantly differentially expressed *Brassica napus* sequences on the custom microarray. Log_2-fold changes (FC) are calculated against the control four days after treatment began for the winter oilseed-rape cultivars Apex and Capitol separately (n = 3) and then averaged. The false-color scale reflects the direction (FC of -1, red and +1, blue) and extent (faint to full saturation) of the expression.

Nitrogen starvation-specific genes showing a significant cultivar x N starvation interaction

From the 59,577 *B. napus* targets on the microarray 407 were not only regulated specifically by N starvation but also differed significantly between the cultivars (see Figure II-7b). The 407 targets could be annotated to 370 different *A. thaliana* homologous genes (Table SII-3). The functional categorization, based on the 14 different gene ontology (GO) categories for biological processes, revealed that 4 days exposure to N starvation led to inter alia reprogramming of numerous genes involved in response to stress (91), response to abiotic or biotic stimulus (91), transport (57), DNA-dependent transcription (33) and signal transduction (28) (Figure II-10).

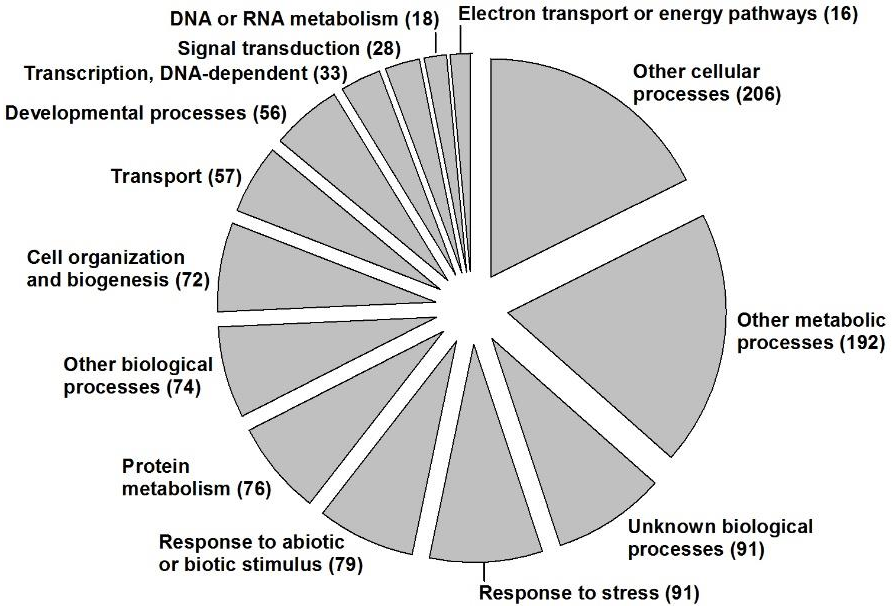

Figure II-10 Functional categorization of genes specific to N starvation and cultivar. Categorization of the 370 *Arabidopsis thaliana* genes homologous to the 407 *Brassica napus* sequences on the custom microarray specifically regulated by N starvation and showing a significant cultivar x treatment interaction in leaf three of the winter oilseed-rape cultivars Apex and Capitol four days after induction of N starvation (n = 3). The 14 categories were selected from the gene ontology (GO) identifier for biological processes based on TAIR gene accessions. The number of genes in each category is given in brackets. Individual genes might be mapped to several groups.

Final selection of leaf senescence marker genes

In a first step, from the 7,779 *B. napus* targets on the microarray specifically regulated by N starvation, 1,812 targets were selected because they met one of the following two criteria: (i) $\log_2$-fold change <-1 or >1 or (ii) $\log_2$-fold difference between the cultivars >0.5. In a second step, *the A. thaliana* homologues of these targets were functionally categorized. To further break down the number of selected genes the putative functions photosynthesis/chloroplasts,N transport/metabolism, sugar transport and C metabolism, phytohormone metabolism, and MYB, NAC, WRKY transcription factors were used as a third criterion. Ninety-five targets met at least two criteria (Table SII-2) and were thus selected as potential marker genes for re-evaluation by qRT-PCR using the same mRNA samples as for the microarrays (three senescence inducers, four DAT, leaf three). Only twelve genes met the criteria N starvation-specific and more than two-fold up-regulated in one of the two cultivars (Figure II-11). Among the five TFs only A*NAC029* showed a significantly higher expression in the faster senescing N-inefficient cv. Capitol. In contrast to the expectation, A*NAC102* and *RAP2-3* showed a higher expression in the late senescing cv. Apex. The ethylene-responsive TFs *DREB4A* and *ESE2* were two to three times up-regulated by N starvation but did not show a cultivar-specific differential response. However, the *DFR-like1* and *ANS* genes were highly up-regulated by N starvation and showed cultivar-specific differences with a higher up-regulation in the early senescing cv. Capitol. Different from the latter genes the *ammonia transporter 1;4* (*AMT1;4*)

coding for a high affinity ammonium transporter, *ureide permease 5* (*UPS5*) involved in the transmembrane transport of ureides and the *sucrose-phosphate synthase 1* (*SPS1*) involved in the biosynthesis of sucrose were not only up-regulated by N starvation but also showed a higher expression in cv. Apex. This suggests that these genes possibly contribute to a more efficient allocation of N and assimilates during senescence in the late senescing cv. Apex. However, in contrast to the expectations *Stay-green 1* (*SGR1)* involved in chlorophyll degradation was cultivar-specifically higher expressed in the late senescing cv. Apex, whereas the expression of the *early flowering 4* (*ELF4)* gene was only enhanced by N starvation in cv. Capitol.

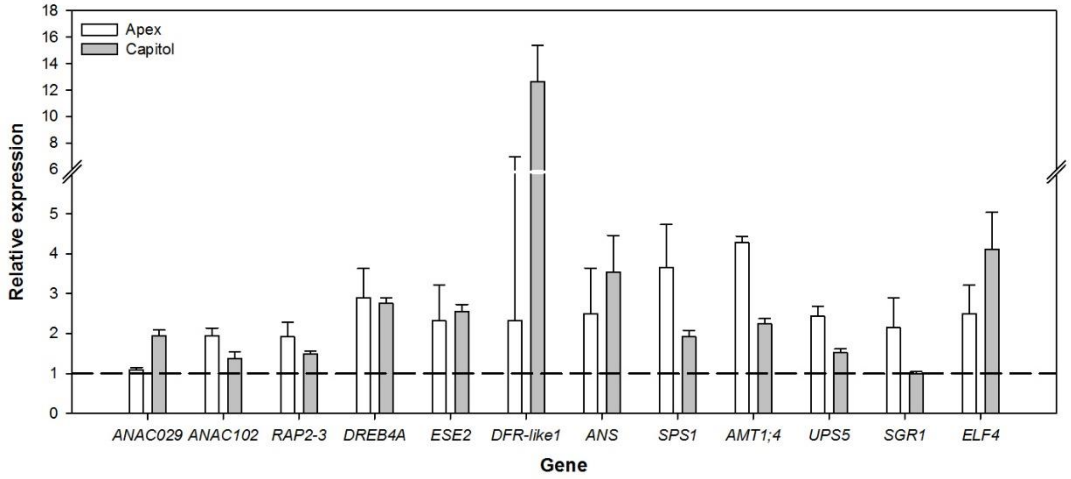

Figure II-11 Relative expression ($2^{-\Delta\Delta Ct}$) of 12 microarray-selected N starvation-specifically regulated and more than two-fold up-regulated in one of the both winter oilseed-rape cultivars Apex and Capitol potential marker genes in leaf three after four days of N starvation in hydroponics. The plants were pre-cultured for 28 days at 2.0 *mM* N. The designations of the genes are the *Arabidopsis thaliana* homologues of the *Brassica napus* sequences suggested by TAIR. The data are shown relative to the 2.0 *mM* N control harvested at the same day. The error bars represent the standard errors of the means (n = 3).

Kinetics of the expression of leaf senescence marker genes

For validation of the reliability of the twelve marker genes they were tested in the cvs. Apex and NPZ-1 (late senescing), and in their respective counterparts cvs. Capitol and NPZ-2 (early senescing) during development of N deficiency-induced leaf senescence from 3 to 12 DAT (Figure II-12). The TF *ANAC029* was increasingly and cultivar-specifically up-regulated by N starvation from DAT 3 onwards (Figure II-12a). The up-regulation was always lower in cvs. NPZ-1 and Apex than in their respective counterparts cvs. NPZ-2 and Capitol. At 5 and 7 DAT the relative expression levels in both, cvs. NPZ-2 and Capitol, were higher than in cvs. NPZ-1 and Apex. Also *ANAC102* was up-regulated by N starvation albeit at a lower level (Figure II-12b). The cultivar response to N starvation was less consistent, although the up-regulation in cv. NPZ-2 and in particularly cv. Capitol were mostly higher than in the later senescing counterparts cvs. NPZ-1 and Apex. Of the three *AP2/ERF* TFs only *RAP2-3* was consistently up-regulated by N starvation (Figure II-12c). *DREB4A* (Figure II-12d) and *ESE2*

(Figure II-12e) showed a peak expression at DAT 5 only in cv. Apex, but then the up regulation were even reduced with aggravating N starvation. None of the cultivars showed a gene regulation profile consistent with the senescence phenotype. The genes *DFR-like1* (already after 3 DAT; Figure II-12f) and *ANS* (after 7 DAT) (Figure II-12g) were strongly up-regulated by N starvation. In contrast to *DFR-like1*, *ANS* was higher up-regulated in the early senescing cvs. NPZ-2 and Capitol than in their respective late senescing counterparts, particularly at 7 DAT. Already three days after exposure to N starvation *SPS1* was up-regulated (Figure II-12h). While in the early senescing cvs. NPZ-2 and Capitol *SPS1* was only slightly up-regulated during extended N starvation, the late senescing cvs. NPZ-1 and Apex consistently showed a higher relative expression which was greatly enhanced at 12 DAT. Also *AMT1;4* was up-regulated as early as 3 DAT in all cultivars but cv. Capitol (Figure II-12i). However, in all cultivars its up-regulation decreased after longer duration of N starvation (10 to 12 DAT). Cultivar Apex always and cv. NPZ-1 mostly showed a higher up-regulation than their early senescing counterparts cvs. Capitol and NPZ-2. From 3 DAT onwards, *UPS5* was increasingly up-regulated in all cultivars with the duration of N starvation (Figure II-12j). From 5 DAT onwards, cv. NPZ-1 versus cv. NPZ-2, and cv. Apex versus cv. Capitol had higher *UPS5* up-regulation at most harvest dates. *SGR1* was generally up-regulated with ongoing N starvation in a cultivar-specific manner (Figure II-12k). Cultivar NPZ-2 showed a consistently higher up-regulation of *SGR1* in agreement with its earlier senescence compared to cv. NPZ-1. However, relative induction of *SGR1* was particularly strong in cv. Apex and always higher than in cv. Capitol, which conflicts with the later senescence of cv. Apex. The *ELF4* gene did neither show a consistent response to the duration of N starvation nor clear differences between the cultivars (Figure II-12l). However, in most cases there was a higher *ELF4* up-regulation in cvs. NPZ-1 and Apex compared to their early senescing counterparts cvs. NPZ-2 and Capitol.

In conclusion, among the studied genes *ANAC029, DFR-like1, ANS, SPS1, AMT1;4* and *UPS5* showed the most consistent and sensitive responses to N starvation, and separated the late senescing cvs. NPZ-1 and Apex from their respective early senescing counterparts cvs. NPZ-2 and Capitol.

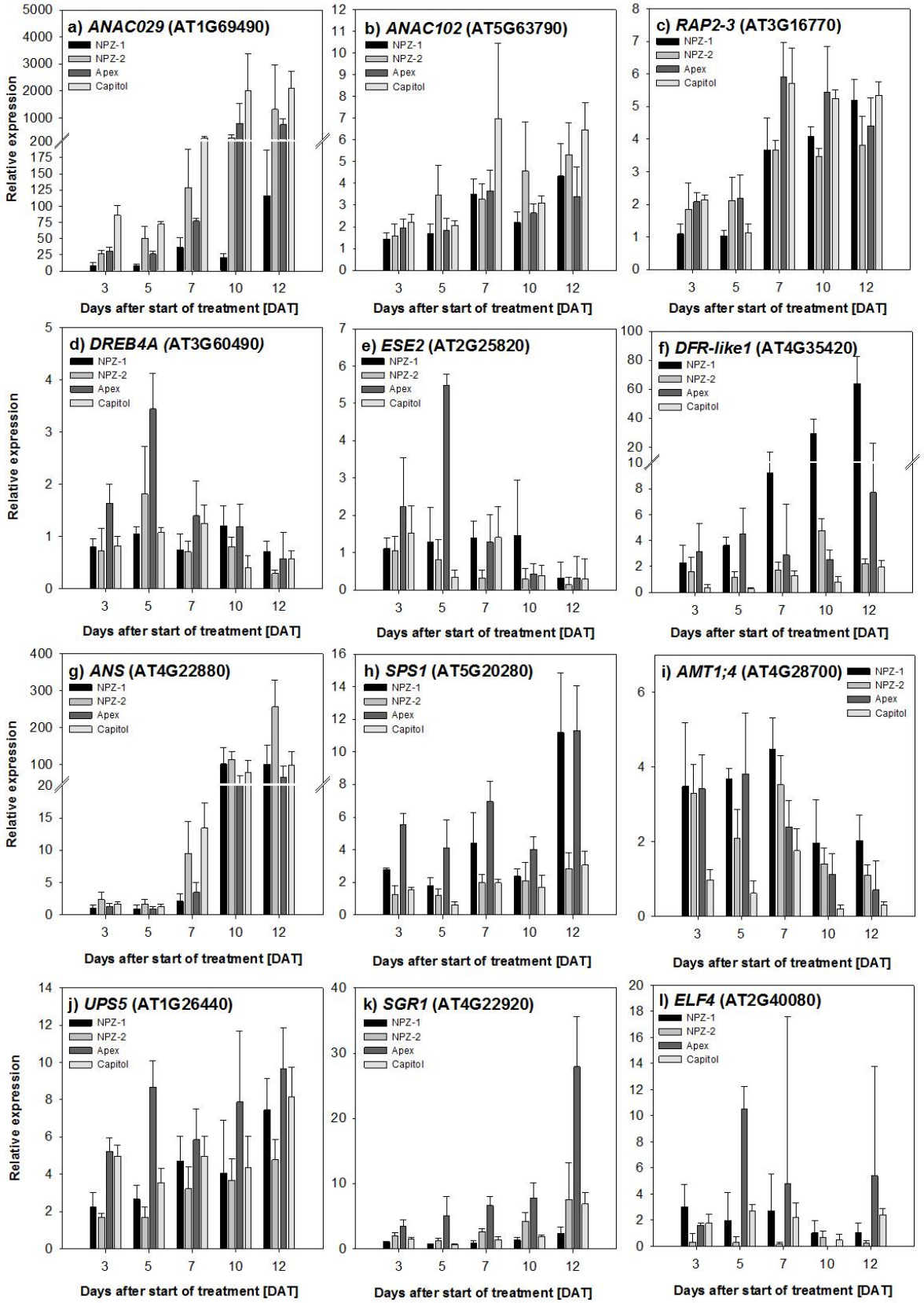

Figure II-12 Duration of N starvation and cultivar-dependent expression of selected genes. Relative expression ($2^{-\Delta\Delta Ct}$) of twelve selected N starvation- and cultivar-specifically regulated potential marker genes (a-l) of the second oldest leaf of four winter oilseed-rape cultivars grown in hydroponics for 12 days of N starvation (0.1 *mM*). The plants were pre-cultured for 28 days at 2.0 *mM* N. The data are shown relative to the controls harvested at DAT 0. The designations of the genes are the Arabidopsis thaliana homologues of the Brassica napus sequences suggested by TAIR. TAIR accession numbers are given in brackets. The error bars represent the standard errors of the means (n = 3 to 4).

Discussion

Under field conditions it is difficult to determine genotypic variation in N starvation-induced leaf senescence owing to additional interacting inducers, particularly shading of lower by upper leaves, inflorescences and pods and developmental senescence typically induced by the transition from the vegetative to the reproductive stage. Also dry spells during the growing period can lead to premature leaf senescence (Gregersen *et al.,* 2013). In hydroponics at rosette stage, N starvation-induced leaf senescence can be studied without interference by other inducers. Under such conditions genotypic variation in onset and development of leaf senescence (we use the expression 'stay-green' for genotypically delayed leaf senescence) has been recorded using SPAD and photosynthesis rate (Schulte auf'm Erley *et al.,* 2007) and could be confirmed in this study (Figures SII-6, SII-7). Schulte auf'm Erley *et al.* (2007) reported that genotypic differences in N starvation-induced leaf senescence at early vegetative growth stages in hydroponics were representative for the functional stay-green phenotype during reproductive growth under field conditions. However, leaf chlorophyll concentration (SPAD) and photosynthesis rate are suitable markers of leaf senescence only at rather advanced stages, are not N starvation-specific, and failed unraveling cultivar differences in functional stay-green characteristics at early senescence stages (< 7 DAT, Figures II-2, II-3). In *B. napus*, *SAG12-1* proved to be a suitable molecular leaf senescence marker (Gombert *et al.,* 2006; Brunel-Muguet *et al.,* 2013) and also for N starvation-induced leaf senescence (Koeslin-Findeklee *et al.,* 2014), which was confirmed here (Figures II-4, II-5, SII-8). However, also *SAG12-1* expression was not N starvation-specific either. This might be due to the fact that *SAG12-1* encodes a cysteine protease involved in degradation of the photosynthetic apparatus which takes place only at advanced stages of the senescence process. Therefore, there is a need for more sensitive and N starvation-specific leaf senescence marker genes capable of identifying cultivar differences in functional stay-green.

To identify N starvation-specific responsive genes we compared N starvation with leaf shading and detaching. Thus, N starvation-specific in the present context only relates to this comparison. Other senescence inducers (such as drought stress) might be relevant under field conditions. We chose leaf detaching although it has no implication for the induction of leaf senescence in intact plants. Yet, the comparison of genotypic differences in leaf senescence of intact and excised leaves was expected to allow conclusions about the role of roots in genotypic differences in functional stay-green and N efficiency.

Four days of stress led to the onset of leaf senescence, indicated by a decrease in SPAD (Figure II-2), photosynthesis rate (Figure II-3) and an increase in *SAG12-1* expression (Figure II-4) in shaded and detached but not in N-starved leaves. The transcriptome analysis revealed major changes triggered by all inducers with clear differences between the senescence inducers (Figure II-7a) in agreement

with Buchanan-Wollaston *et al.* (2005) and van der Graaff *et al.* (2006) who compared different senescence inducers in *A. thaliana*. Notably, a cultivar-specific response at the transcriptome level was only pronounced for N starvation (Figure II-6).

The functional pathway analysis of the senescence-regulated genes revealed that four days after treatment began the majority of the genes assigned to photosynthesis and chlorophyll synthesis were down-regulated (Figure II-8) clearly indicating that leaf senescence had already been initiated also by N starvation. At this stage the majority of the catabolic genes were not yet changed in expression in agreement with Breeze *et al.* (2011). In the present study only genes assigned to amino acid and nucleotide degradation were enhanced by all inducers. The majority of the genes related to mitochondrial electron transport increased in expression (Figure II-8), confirming that the mitochondria remain intact until late senescence (Hörtensteiner & Feller, 2002; Keech *et al.,* 2007) likely to provide metabolites and energy needed for N remobilization during senescence (Szal & Podgórska, 2012).

The global gene expression pattern after four days exposure to N starvation (Figure II-8) was similar to the reaction of *A. thaliana* leaves shortly after induction of N shortage (Balazadeh *et al.,* 2014). Additionally, the present study reveals that numerous genes were specifically regulated by N starvation (Figure II-9) in a way corresponding to the overall pattern of N starvation, but of course with a lower number of genes.

In the regulatory network of leaf senescence particularly NAC, MYB and WRKY TFs are involved (Buchanan-Wollaston *et al.,* 2005; Balazadeh *et al.,* 2008a; Parlitz *et al.,* 2011). Among the N starvation- and cultivar-specifically expressed genes five TFs were studied in more detail in a kinetic study using qRT-PCR (Figure II-12). *ANAC029* and *ANAC102,* but not the AP2/ERF TFs *RAP2-3*, *DREB4A*, and *ESE2* could be confirmed as highly sensitive molecular markers capable of identifying cultivar differences in N starvation-induced leaf senescence. In general, NAC TFs are positively or negatively acting on leaf senescence (Guo *et al.,* 2004; Kim *et al.,* 2009; Wu *et al.,* 2012). *ANAC029* (*AtNAP*) encodes a protein which enhances leaf senescence (Wu *et al.,* 2012). It is one of the most abundantly transcribed TF genes in leaves during developmental senescence, and its expression is closely associated with the progression of leaf senescence in rosette leaves of *A. thaliana* (Buchanan-Wollaston *et al.,* 2005; Guo & Gan, 2006). The present study revealed that *ANAC029* was a sensitive leaf senescence-marker capable of identifying winter oilseed-rape cultivar differences in N starvation-induced leaf senescence (Figure II-12a). Already at 3 DAT *ANAC029* was higher up-regulated in the early senescing cvs. NPZ-2 and Capitol compared to their functional stay-green counterparts cvs. NPZ-1 and Apex. *ANAC102* has been reported to be induced by low oxygen and to affect the viability of seeds (Christianson *et al.,* 2009), but nothing is known about its role in leaf senescence. The present study showed a higher relative induction in N-starved leaf tissue of the

faster senescing cvs. NPZ-2 and Capitol compared to their respective functional stay-green counterparts cvs. NPZ-1 and Apex (Figure II-12b). Thus, *ANAC102* may be a positive leaf senescence regulator like *ANAC029*. However, *ANAC102* was generally much less induced by N starvation and did not always detect cultivar differences.

In many plant species suboptimal N nutrition induces anthocyanin synthesis which is often used as indicator of the N status of the plant (Diaz *et al.,* 2006; Peng *et al.,* 2008; Misyura *et al.,* 2013). Also in winter oilseed-rape leaves we observed a rapid accumulation of anthocyanins upon N shortage (not shown), in accordance with the results of the metabolic pathway mapping which revealed that a large number of genes related to flavonoid metabolism including the anthocyanin pathway were up-regulated in N-starved leaves. We made a similar observation for detached but not for shaded leaves (Figure II-8). Nevertheless, several flavonoid metabolism-related genes such as *ANS* coding for an anthocyanin synthase catalyzing the last step in anthocyanin synthesis (Holton & Cornish, 1995) were specifically regulated by N starvation (Figure II-8). *ANS* was highly up-regulated by N starvation at 7 DAT and showed differences between the cultivars with higher up-regulation in the early senescing cvs. NPZ-2 and Capitol than in their functional stay-green counterparts cvs. NPZ-1 and Apex (Figure II-12g). Another gene (*DFR-like1*) with a putative function in anthocyanin metabolism was also very responsive to N starvation (Figure II-12f). Dihydroflavonol 4-reductase (DFR) catalyzes the reduction of dihydroflavonols to leucoanthocyanidins, which are the direct precursors of anthocyanidins (Holton & Cornish, 1995). In contrast to *ANS* the gene *DFR-like1* was not only consistently up-regulated in the functional stay-green cv. NPZ-1 compared to cv. NPZ-2, and in cv. Apex compared to cv. Capitol, but also responded to N starvation over the treatment duration (3 to 12 DAT) much more in functional stay-green cultivars than in their respective early senescing counterparts (Figures II-12f, g) suggesting that anthocyanin accumulation is not a sensitive indicator of N starvation-induced leaf senescence. However, a DFR-like protein (encoded by *BEN1*) has been reported to be involved in the catabolism of brassinosteroids (Yuan *et al.,* 2007) which may affect leaf senescence (Chung & Choe, 2013). The possible role of *DFR-like1* for cultivar differences in functional stay-green awaits molecular clarification.

Since anthocyanin accumulation often precedes leaf yellowing, it was assumed that its photo-protective function prevents the risk of photooxidation and enables a tightly controlled and efficient chlorophyll breakdown during leaf senescence (Diaz *et al.,* 2006). However, recent studies question this hypothesis (Misyura *et al.,* 2013). An increase in the internal sugar concentration could be the common trigger for the enhanced expression of genes involved in anthocyanin formation (Teng *et al.,* 2005; Solfanelli *et al.,* 2006) and leaf senescence induced by N starvation (Wingler *et al.,* 2006). Sugars strongly accumulate in detached leaves (Housley & Pollock, 1985) which could explain why detached leaves also showed anthocyanin accumulation and a similar gene

expression pattern compared to N-starved leaves (Figure II-8). The sucrose biosynthesis-related *SPS1* gene was specifically up-regulated by N starvation with a higher relative induction in the functional stay-green cvs. NPZ-1 and Apex than in their respective early senescing counterparts cvs. NPZ-2 and Capitol (Figure II-12h). For sucrose formation sucrose-phosphate synthase (SPS) is the rate-limiting key enzyme (Huber & Huber, 1996). Sucrose allocation from source leaves to sink tissues is essential for plant growth and yield formation (Worrell *et al.,* 1991; Galtier *et al.,* 1995). Hence, maintaining biosynthesis and allocation of sucrose to sink tissues will contribute to overcome yield limitation due to source limitation, particularly under stress conditions such as N starvation. SPS activity and *SPS1* gene transcription are closely feed-back regulated by the leaf sucrose level (Hesse *et al.,* 1995). Particularly the isoform encoded by *SPS1* plays a major role in leaf photosynthetic sucrose synthesis in *A. thaliana* (Sun *et al.,* 2011), though sucrose synthesis is not exclusively dependent on photosynthetic activity. In the absence of high sucrose and inorganic phosphorous levels SPS activity can be induced by the availability of energy and building blocks (Stitt *et al.,* 1983, 1988) which may explain that the ability of rice flag leaves to synthesize sucrose was not greatly reduced during senescence (Yoshiharu *et al.,* 1993). Already four days after induction of N starvation, expression of some glycolytic pathway genes was enhanced specifically by N starvation (Figure II-9), suggesting that the energy and building blocks needed for sucrose formation during senescence originate from glycolysis.

Ammonium (NH_4^+) transport across the plasma membrane is mediated inter alia by AMT1 high-affinity transporters (von Wirén *et al.,* 2004). Nitrogen starvation leads to enhanced transcription of several *AMT1* genes and enhances NH_4^+ influx in *A. thaliana* roots (Gazzarrini *et al.,* 1999). In *B. napus* leaves N starvation generally increased *AMT1;4* transcript abundance during the senescence course with a peak expression at 5 to 7 DAT (Figure II-12i). The higher up-regulation in the source leaves of the functional stay-green cultivars, particularly cv. NPZ-1, compared to their respective early senescing counterparts might reflect a higher NH_4^+ retrieval efficiency particularly during early stages of leaf senescence when NH_4^+ is produced owing to nitrate reduction and hydrolysis of proteins (Husted *et al.,* 1996). NH_4^+ accumulation in leaves starts only at rather advanced stages of leaf senescence (Masclaux *et al.,* 2000; Mattsson *et al.,* 2003) which coincides with a decrease in *AMT1;4* relative induction at >7 DAT when NH_4^+ production possibly exceeds the transport capacity.

With proceeding N starvation-induced leaf senescence heterocyclic N compounds such as ureide and purine degradation products become increasingly prominent (Desimone *et al.,* 2002). Purine degradation products originate from the turnover of nucleic acids (Zrenner *et al.,* 2006) and emerge massively after induction of senescence (Buchanan-Wollaston, 1997). Particularly this pathway was induced at the transcriptional level at DAT 4 under N starvation and several genes were specific to N starvation (Figure II-9). In *A. thalina* five ureide permeases (UPS) are involved in membrane transport

of ureides and purine degradation products (Desimone *et al.,* 2002; Schmidt *et al.,* 2006). This is also the case for the ureide transporter encoded by *UPS5* (Schmidt *et al.,* 2006) which was increasingly up-regulated by N starvation (Figure II-12j). The higher up-regulation in the functional stay-green cvs. NPZ-1 and particularly Apex compared to their respective counterparts cvs. NPZ-2 and Capitol, respectively, may also indicate a more efficient retrieval of these N compounds in these cultivars.

In conclusion, global analysis of gene expression in leaves revealed an N starvation-specific program different from that of leaf shading and detaching. Already after four days, N starvation coordinately repressed a majority of the genes assigned to photosynthesis and chlorophyll synthesis, the Calvin Benson cycle and photorespiration, but induced many genes related to the flavonoid pathway, ammonium assimilation, nucleotide and amino acid degradation, and reprogramming of mitochondrial electron transport. Among the N starvation-specific genes, six could be identified as highly sensitive molecular leaf-senescence markers suitable for revealing cultivar differences in N starvation-induced leaf senescence in *B. napus*. The general suitability of these marker genes for the identification of cultivar differences in functional stay-green cultivars and their role in N efficiency need to be validated using a larger and more diverse set of cultivars in the future.

III Differences between winter oilseed-rape (*Brassica napus* L.) cultivars in nitrogen starvation-induced leaf senescence are governed by leaf-inherent rather than root-derived signals

Fabian Köslin-Findeklee[1], Martin A. Becker[1], Eric van der Graaff[2], Thomas Roitsch[2,3] and Walter J. Horst[1]

[1]Institute of Plant Nutrition, Leibniz University of Hannover, Herrenhäuser Str. 2, D-30419 Hannover, Germany
[2]Department of Plant and Environmental Sciences, University of Copenhagen, Højbakkegård Allé 13, DK-2630 Taastrup, Denmark
[3]Global Change Research Centre, CzechGlobe AS CR, v.v.i., Drásov 470, Cz-664 24 Drásov, Czech Republic

📖 Submitted to *Journal of Experimental Botany*

Abstract

Nitrogen (N) efficiency of winter oilseed-rape (*Brassica napus* L.) line cultivars (cvs.), defined as high grain yield under N limitation, has been primarily attributed to maintained N uptake during reproductive growth (N uptake efficiency) in combination with delayed leaf senescence of the older leaves accompanied by maintained photosynthetic capacity (functional stay-green). However, it is not clear whether genetic variation in N starvation-induced leaf senescence is due to leaf-inherent factors and/or governed by root-mediated signals. Therefore, the N-efficient and late senescing cvs. NPZ-1 and Apex were reciprocally grafted with the N-inefficient and early senescing cvs. NPZ-2 and Capitol, respectively and grown in hydroponics. The senescence status of older leaves after twelve days of N starvation assessed by SPAD, photosynthesis and the expression of the senescence-specific cysteine protease gene *SAG12-1* revealed that the functional stay-green phenotype of the cvs. NPZ-1 and Apex under N starvation was under the control of leaf-inherent factors.

The same four cultivars were submitted to N starvation for up to twelve days in a time-course experiment. The specific leaf contents of biologically active and inactive cytokinins (CKs) and the expression of genes involved in CK homeostasis revealed that under N starvation leaves of early senescing cultivars are characterized by inactivation of biologically active CKs, whereas in functional stay-green cultivars synthesis, activation, binding of and response to biologically active CKs were favored.

These results suggest that the homeostasis of biologically active CKs is the decisive leaf-inherent factor for cultivar differences in N starvation-induced leaf senescence and thus N efficiency.

Keywords: *Brassica napus*, cytokinins, leaf senescence, genotypic differences, nitrogen efficiency, nitrogen starvation, reciprocal grafting, functional stay-green

Introduction

Nitrogen efficiency of winter oilseed-rape line-cultivars, defined as high grain yield under N limitation, has been primarily attributed to maintained N uptake during reproductive growth (N uptake efficiency) (Kamh *et al.,* 2005; Schulte auf'm Erley *et al.,* 2007; Berry *et al.,* 2010; Schulte auf'm Erley *et al.,* 2011). A characteristic of N-efficient cultivars is a functional stay-green phenotype during reproductive growth, expressed through delayed senescence of the older leaves accompanied by maintenance of photosynthetic capacity (Schulte auf'm Erley *et al.,* 2007). In many crop species, stay-green phenotypes are superior in yield formation particularly under abiotic stress conditions when senescence is prematurely induced for instance by drought or N limitation (Gregersen *et al.,* 2013). Functional stay-green results from a delayed onset of senescence and/or a slower senescence course (Thomas & Howarth, 2000). Thus in contrast to cosmetic stay-green without any photosynthetic activity (Thomas & Howarth, 2000), functional stay-green requires more than the retention of green colour based on delayed or completely inhibited chlorophyll catabolism (Kusaba *et al.,* 2013).

Functional stay-green is an inheritable, mostly polygene-regulated quantitative trait (Wang *et al.,* 2012). But the undelaying mechanisms are currently poorly understood. The onset of leaf senescence is accompanied by transcriptional activation and repression of many genes (Smart, 1994). Master-regulators of the gene-expression network during senescence are senescence-inducible transcription factors (TFs), which positively or negatively act on leaf senescence (Balazadeh *et al.,* 2008b; Parlitz *et al.,* 2011). Many of these TFs directly or indirectly control the activation or repression of down-stream senescence-associated genes (SAGs) and thus fine tune the onset and rate of leaf senescence (Kusaba *et al.,* 2013). A hallmark of leaf senescence is the termination of photoassimilation. For functional stay-green the maintenance of functional chloroplasts is a prerequisite, which is under the control of nuclear as well as chloroplast encoded genes (Sakuraba *et al.,* 2012a, b; Rauf *et al.,* 2013).

Additional key regulators of leaf senescence are phytohormones (Lim *et al.,* 2007). Alterations in phytohormone, particularly cytokinin (CK), metabolism and signaling lead to functional stay-green phenotypes (Thomas & Ougham, 2014). CKs are the most potent general antagonist of senescence (Zwack & Rashotte, 2013). Although currently nothing is known about the underlying mechanisms for genetic variation in stay-green under N starvation in winter oilseed-rape, leaf-inherent and/or root-mediated CKs might be important factors. Functional stay-green in cotton plants could be attributed to accumulation of root-derived CKs in mature leaves on the one hand (Dong *et al.,* 2008). On the other hand, modification of leaf inherent CK homeostasis in mature tobacco leaves (Gan & Amasino, 1995; del Mar Rubio-Wilhelmi *et al.,* 2014) as well as CK perception and signaling in

mature *A. thaliana* leaves (Kim *et al.,* 2006) or downstream targets in tomato (Albacete *et al.,* 2014) and tobacco leaves (Lara *et al.,* 2004) lead to functional stay-green.

To elucidate whether cultivar differences in N starvation-induced leaf senescence in winter oilseed-rape are due to leaf-inherent factors and/or governed by root-mediated signals, a reciprocal grafting approach was applied in the present study using two pairs of cultivars differing in N efficiency and N starvation-induced senescence. To clarify the role of phytohormones for genetic variation in stay-green, in a complementary time-course experiment comprising the same four cultivars used for the grafting approach, phytohormone levels were determined in roots, xylem sap and individual leaves. In addition, the expression of selected genes involved in the homeostasis, perception and signaling of CKs in the leaf tissue were analyzed.

Material and Methods

Grafting experiment

Plant material

Based on a previous experiment comparing N starvation and leaf detaching as inducers of leaf senescence of ten line-cultivars two pairs of cultivars (cvs.) were selected for the reciprocal grafting approach. The cvs. NPZ-1 & NPZ-2 are breeding lines with a similar genetic background and reacted differently to N starvation and detaching indicating root-derived factors. The commercial cultivars Apex & Capitol were selected, since they did not differ in leaf senescence independently of the senescence inducer suggesting leaf-inherent factors (Figure III-S1). Plants of both cultivar pairs were reciprocally-grafted or not-grafted and self-grafted as controls.

Grafting procedure

The seeds were germinated and the seedlings were grafted in a climate chamber (Day/night 16/8 h; Temperature day/night 20/22°C; PAR 350 µmol m^{-2} s^{-1}). The seeds were sown in substrate consisting of white peat, sand and perlite in the ratio of 3:1:2 (w:w:w). The substrate was limed to pH 6 using 4 g L^{-1} limestone (85% calcium carbonate, Otterbeinkalk) and macro- and micro-nutrients were added using 0.5 g L^{-1} Flory 3 (Euflor, Schrembeck, Germany) and 0.1 g L^{-1} Flory 10 (Euflor, Schrembeck, Germany). Seven days after germination the hypocotyl reached a diameter of 1 mm and the plants were grafted following a modified procedure described by Moroni (1997). The hypocotyls were horizontally cut and roots and shoots fixed to each other via a well-fitting PVC-tube (PVC-Standard diameters: 1.020; 1.143; 1.295; 1.422 mm, Spetec, Erding, Germany) (Figure III-1). The grafted plants were kept for five days under a wet tent. The humidification was gradually reduced to the ambient conditions in the climate chamber in daily steps. Afterwards the plants were acclimatized in the climate chamber for one day before they were transferred to hydroponics.

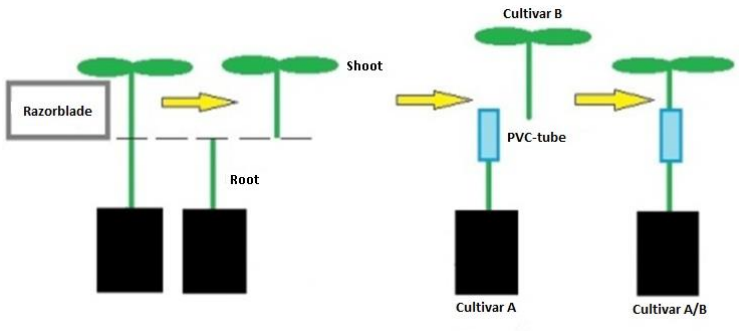

Figure III-1 Schematic diagram of the grafting procedure.

Hydroponic growing conditions

The plants were cultured in a greenhouse (assimilation light (16 klm) 16 h; heating/ventilation temperature 20/22°C; shading at 15 klx solar radiation; relative humidity 80%) from 24 February to 4 April 2012. The roots of the plants were washed out of the substrate using deionized water. Two plants were transferred to a 6-L plastic pot and pre-cultured for 28 days at optimal N supply (2.0 *mM*). The roots of the plants were daily separated by hand, to avoid intermingling of the root systems. The roots remained submerged during the separation to minimize root damage. The composition of the nutrient solution was 500 μM K_2S0_4, 250 μM KH_2PO_4, 325 μM $MgSO_4$, 50 μM NaCl, 8 μM H_3BO_3, 0.4 μM $MnSO_4$, 0.4 μM $ZnSO_4$, 0.4 μM $CuSO_4$, 0.1 μM Na_2MoO_4 and 40 μM Fe-EDDHA. During pre-culture $Ca(NO_3)_2$ and $(NH_4)_2SO_4$ were used as N sources in the ratio of nine to one, and 10 μM $C_2H_4N_4$ (dicyandiamide) was added to prevent nitrification. Prior to treatment begin one plant per pot was discarded, which allowed to select for homogeneity of the experimental plants. For N starvation the plants were grown at 0.1 *mM* N ($Ca(NO_3)_2$) and 1.0 *mM* $CaSO_4$ to allow for optimum Ca nutrition. For optimal N nutrition the plants were cultured at 4.0 *mM* N doubling the concentration used for pre-culture. After treatment began the nutrient solution was changed every second day. The experiment was completely randomized with four biological replications.

Non-destructive measurements, plant harvest and analysis

During the treatment the senescence status of the 4th leaf, counted from the bottom to the top of the plant, was measured using non-destructive methods. Leaf 5 was the youngest fully expanded leaf at the end of pre-culture. The chlorophyll content of the 4th leaf was assessed by a portable chlorophyll meter (SPAD-502, Konica Minolta, Tokyo, Japan). Photosynthesis rate of the same leaf was measured using a portable gas exchange system (LI-6400, LI-COR, Lincoln, USA) at a photon flux density of 1000 µmol m^{-2} s^{-1} and an incoming CO_2 concentration of 400 µmol m^{-2} s^{-1}. The plants were harvested 12 days after start of the treatment (DAT) and were separated into shoot and root, and the 4th leaf was harvested separately. The leaf area of the 4th leaf was measured by a portable leaf area meter (LI-3100, LI-COR, Lincoln, USA). The leaf was divided along the middle-rip with a razor blade. One half was immediately frozen in liquid N_2 and the other half was dried at 70°C until constant weight for dry weight determination. N concentrations of the dried and ground root, shoot and leaf material were determined using an elemental analyzer (Vario EL, Elementar Analysensysteme, Hanau, Germany). For RNA extraction, the frozen leaf material was ground using a mixer mill (MM 400, Retsch, Haan, Germany).

Kinetics of N deficiency-induced leaf senescence

Plant material and growing conditions

For investigating the kinetics of the development of N starvation-induced leaf senescence the same four cultivars cvs. NPZ-1, NPZ-2, Apex and Capitol were used. The seeds were germinated in the climate chamber as described above using a "sandwich" method arranging the seeds between filter paper sandwiched between sponges and PVC-plates on both sides. The "sandwiches" were placed into a box containing tap water. Seven days after germination the seedlings were cultured from 23 September to 3 November 2010 in the greenhouse in hydroponics as described above. The experiment was completely randomized with three to four biological replications.

Plant harvest and analysis

After 0, 3, 5, 7, 10 and 12 days of N starvation and after 7 and 12 DAT of optimal N nutrition plants were harvested. At harvest the plants were divided into root, shoot and three previously marked individual leaves, which were the youngest fully expanded leaf at the end of pre-culture and the two older leaves. In most cases the youngest fully expanded leaf was leaf 5 counted from the bottom to the top of the plant. During N starvation the senescence status of the three leaves was measured using non-destructive methods as describe above, but photosynthesis rate was measured at a photon flux density of 400 µmol m^{-2} s^{-1}. The harvest procedure, the sample preparation and the N analysis were performed as described above.

Xylem sap collection and analysis

At each harvest xylem exudates were collected. The nutrient solution was changed 1 h before starting xylem sap collection according to the N variants and additionally KCl (2.0 *mM*) was added, to enhance exudation. The plants were horizontally cut using a razor blade at the root collar and a well-fitting silicone tube was attached. After 5 min the exudates were discarded and then collected for 1 h. The collected exudates were kept on ice and protected from light. The exudates were stored until the analysis at -20°C. The exudates were gently defrozen on ice and protected from light.

Phytohormone analysis

Phytohormones were analyzed in the root, the xylem sap and two individual leaves per plant (the 2nd and 3rd oldest mature leaves at the end of pre-culture). For phytohormone extraction from leaves and roots 250 mg of frozen and ground tissue, for extraction from the xylem sap 100 µL were used.

Cytokinins (CKs), abscisic acid (ABA), jasmonic acid (JA) and salicylic acid (SA) were extracted and purified according to Großkinsky *et al.* (2014). One mL of 80% (v/v) methanol was added into each sample and vortexed. Then 4 µL of internal standard mix (5 µg mL^{-1}) composed of deuterium-labelled

hormones ([$^2H_5$]Z (zeatin), [$^2H_5$]ZR (zeatin riboside), [$^2H_5$]ZOG (zeatin-O-glucoside), [$^2H_5$]ZROG (zeatin-O-glucoside riboside), [$^2H_6$]iP (riboside 5'-diphosphate), [$^2H_5$]DHZ (dehydro-zeatin), [$^2H_5$]DHZR (dehydro-zeatin riboside), [$^2H_6$]ABA, and [$^2H_5$]JA, Olchemin Ltd, Olomouc, Czech Republic) was added, well mixed and incubated for 30 min at 4°C. Afterwards, the samples were centrifuged at 20,000 g and 4°C for 15 min. The supernatant was passed through pre-equilibrated Chromafix C18 columns (Macherey-Nagel, Düren, Germany) with 80% (v/v) methanol. Samples were collected in 5 mL tubes on ice, and 1 mL 80% (v/v) methanol was added and vortexed thoroughly. After centrifuging at 20,000 g and 4°C for 15 min the filtration step was repeated. The collected samples were concentrated to dryness using a Thermo ISS110 centrifugal vacuum evaporator (Thermo Savant, Holbrook, USA). The residue from each sample was re-dissolved in 500 µL 20% (v/v) methanol, sonicated for 8 min, filtrated through 0.22 µm syringe filters (Chromafil PES-20/25, Macherey-Nagel, Düren, Germany). The filtered samples were immediately frozen for phytohormone measurement. Analyses were carried out on a UPCL-MS/MS system consisting of a Thermo ACCELA UPLC (Thermo Scientific, Waltham, USA) coupled to a thermostated HTCPAL autosampler (CTC Analytics, Zwingen, Switzerland), and connected to a Thermo TSQ Quantum Acces Max Mass Spectrometer (Thermo Scientific, Waltham, USA) with a heated electrospray ionization interface. Ten µL of each standard (known concentrations of each phytohormone) and the internal standards or sample were injected into a Thermo Hypersil Gold column (1.9 µm, 50 x 2.1 mm, Thermo Scientific, Waltham, USA) eluted at a flow rate of 250 µL min^{-1}. Mobile phase A consisting of water/methanol/acetic acid (89.5/10/0.5, v/v/v) and mobile phase B consisting of methanol/acetic acid (99.5/0.5, v/v) were used for chromatographic separation. The elution consisted in 2 min of 95% A and a linear gradient from 5 to 100% of B in 8 min. 100% B was maintained 6 min and afterwards the column was equilibrated with the starting composition (95% A) for 8 min before each analytical run. The mass spectrometer was operated in the positive mode for all the hormones analyzed, except JA and SA that were measured in the negative mode. Capillary spray voltage was set to 4,000 V, the nebulizer gas (He) pressure to 40 psi with a flow rate of 8 L s^{-1} at a temperature of 250°C, and the scan cycle time was 0.5 s from 100 to 600 m z^{-1}. The chromatogram of each hormone from both standards and samples was extracted, and the peak area quantified using the Thermo XCalibur software version 2.1.0.

RNA isolation and cDNA synthesis

RNA was extracted from 100 mg of frozen and ground leaf material with TRIsure™ (Bioline, London, UK) reagent according to the instructions of the manufacturer. RNA integrity was tested on 1% agarose gel electrophoresis and photometrically quantified (NanoPhotometer™, Implen, München, Germany). Two µg of RNA were applied to synthesize cDNA with the RevertAid™ H Minus First Strand kit (Fermentas, Waltham, USA). For the reaction the supplied random hexamer primer were used to

synthesize the first strand cDNA of the *m*RNA according to the instructions of the manufacturer. Quality and quantity of cDNA was determined as for RNA.

Primer design and qRT-PCR

The relative expression of the gene *SAG12-1* encoding a senescence-specific cysteine protease and selected genes involved in CK synthesis (isopentenyltransferase - *IPT*), in the reversible and irreversible glycosylation (uridine diphosphate glucosyltransferase - *UGT*) converting biologically active CKs (aCKs) to biologically inactive but activatable CKs (iCK) or biologically inactive forms, in the release of highly aCK nucleobases from their ribosides with lower biological activity (cytokinin ribosid 5'-monophosphate phosphoribohydrolase - *LOG*), in the breakdown (cytokinins oxidase/dehydrogenase – *CKX*) of aCKs, and in the aCK perception and response (histidine kinase 3 – A*HK3;* response regulator 2 - A*RR2*) were analyzed using qRT-PCR. The gene *EF1-alpha* encoding an elongation factor was used as reference gene (Desclos *et al.,* 2008). The initial selection of the analyzed genes related to cytokinin homeostasis were based on the availability of sequence information in *A. thaliana* and *B. napus*. The final selection of the respective isogenes was based on the detectability in the leaf tissue. A gene was detected when the fluorescence signal of its amplicon exceeded the threshold within 50 PCR cycles. For the design of the primer pairs *B. napus* sequences were used. If no suitable primer pair could be designed on the *B. napus* sequence the primer pair was designed on the sequence of the *A. thaliana* homologues gene. The *B. napus* sequences were retrieved from the NCBI public database and The Gene Index Project at the Dana-Farber Cancer Institute (DFCI; http://compbio.dfci.harvard.edu/tgi/plant.html). The *A. thaliana* sequences were obtained from the Arabidopsis Information Resource Version 10 (TAIR; http://www.arabidopsis.org). Primer pairs were designed using PrimerQuest (Integrated DNA Technologies, Coralville, USA) for genes having NCBI accession numbers, or using QuantPrime (Arvidsson *et al.,* 2008) for genes having DFCI or TAIR accession numbers (Table III-S1). PCR reactions for qRT-PCR were performed in 96 well-plates in a thermo cycler (CFX96™ Real-time system, BioRad Laboratories, Hercules, USA) and consisted of an initial denaturation at 95°C (10 min), followed by 50 cycles at 95°C (15 s), 60°C (30 s), 72°C (30 s) and a final melting curve analysis from 60°C to 95°C with a 0.5°C 5 s^{-1} increasing temperature gradient. The 25 µl SYBR Green-based mix included 2.5 µL 10x Hot-Start PCR buffer, 3.6 µL of 1000-times diluted 1000x SYBR Green-I (Invitrogen GmbH, Darmstadt, Germany), 0.5 µL 10 mM dNTP mix, 0.63 µL of each 10 µM forward and reverse primer, 0.15 µL 5U μL^{-1} U DCS Hot Start DNA polymerase (DNA Cloning Service, Hamburg, Germany), 1 µL of 50 ng μL^{-1} cDNA template. The mean relative expression and the standard error of the qRT-PCR results and their standard errors were calculated based on the $2^{-\Delta\Delta Ct}$-method by Livak & Schmittgen (2001).

Statistical analysis

The statistical analysis was performed using the statistic software SAS version 9.2 (SAS Institute, Cary, USA). For the comparison of the two grafting experiments the data were ranked using the PROC RANK procedure followed by an analysis of variance (ANOVA) using the PROC GLM procedure. For analysis of the data of the shown grafting experiment and the experiment investigating the kinetics of the development of N starvation-induced leaf senescence the ANOVA was calculated using the PROC GLM procedure. For the ANOVA the Type III sum of squares was applied, if an unequal number of replicates occurred. Multiple comparisons of means were calculated by the MEANS statement of the PROC GLM procedure. For all tests of significance a p-value of 0.05 was used and the p-values were Bonferroni-Holm adjusted. In the tables and figures for the F-Test +, *, ** and *** indicate significance at the $p < 0.10$, < 0.05, < 0.01 and < 0.001 level, respectively. ns = non-significant. The same symbols were used to mark the significance for the correlations. Curves were fitted using the graphic software SIGMA PLOT version 11 (Systat software, San Jose, USA). The relative qRT-PCR data were analyzed using the %QPCR MIXED macro after Steibel *et al.* (2009) based on the PROC MIXED procedure.

Results

Grafting experiment

In order to investigate, if cultivar differences in N starvation-induced leaf senescence are due to leaf-inherent factors and/or governed by root-mediated signals a reciprocal grafting experiment was performed using the two pairs of cultivars differing in N efficiency and N starvation-induced senescence described under “Plant material” above. The experiment was repeated two times. Since both experiments did not differ in N starvation-induced leaf senescence (Table III-S2) the results of only one experiment are shown.

Chlorophyll content (SPAD) and photosynthesis rate in senescing leaves

At optimal N supply the SPAD values of all variants were high and did not differ (Figure III-2a). After 12 days of N starvation the SPAD values declined reflecting senescence induction. Highly significant differences existed between the variants. The non-grafted controls and the self-grafted plants showed the expected differences in senescence within the cultivar pairs: cvs. Apex and NPZ-1 remained greener (higher SPAD values) than the cvs. Capitol and NPZ-2 (although the controls of cvs. Apex and Capitol differed only in tendency). For the reciprocal grafts of cvs. Apex & Capitol and cvs. NPZ-1 & NPZ-2 the leaf SPAD value depended on the origin of the shoot: the cv. Apex shoot (significantly) and the cv. NPZ-1 shoot (in tendency) conferred delayed leaf senescence when grafted on the cv. Capitol and cv. NPZ-2 roots, respectively. As an additional indicator of the leaf senescence status photosynthesis was measured (Figure III-2b). Photosynthesis reacted more sensitive to N starvation than SPAD with a significant decline. No differences existed between the variants at high N supply. Under N starvation leaf photosynthesis of non-grafted and self-grafted plants of cv. Capitol (in tendency) and cv. NPZ-2 (significantly) was lower than of cv. Apex and cv. NPZ-1, respectively. As for SPAD, photosynthesis of the grafted plants was determined by the origin of the shoot: the cv. Apex shoot conferred less decline of photosynthesis than the cv. Capitol shoot when reciprocally grafted on the respective roots. For the cultivar pair NPZ-1 & NPZ-2 a comparative shoot effect was visible only in tendency.

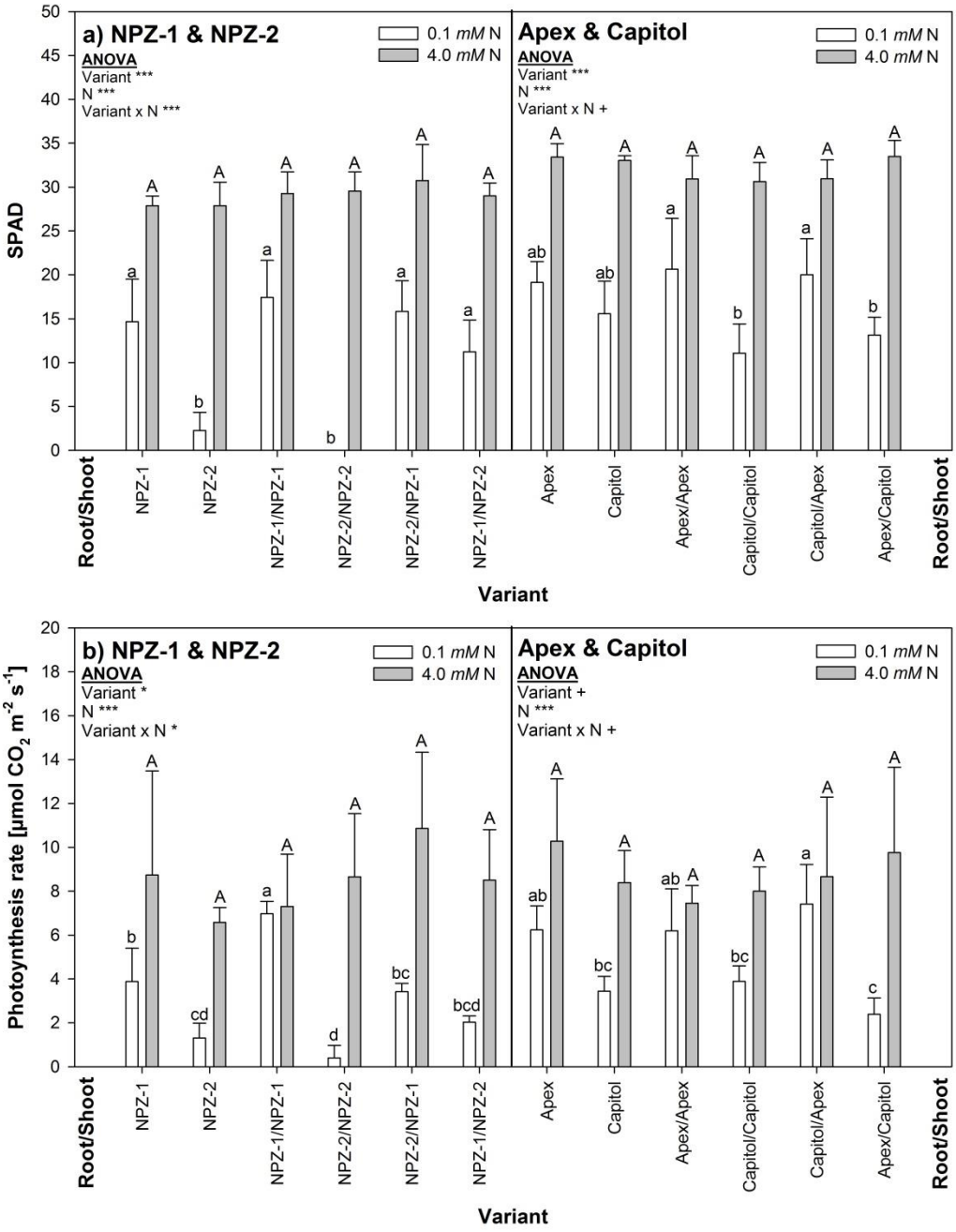

Figure III-2 SPAD values (a) and photosynthesis rate (b) of leaf four of non-grafted, self-grafted and reciprocally-grafted plants of the winter oilseed-rape cultivars NPZ-1 & NPZ-2 (left) and Apex & Capitol (right) grown in hydroponics after 12 days of N starvation (0.1 *mM* N) or optimal N supply (4.0 *mM* N). The plants were pre-cultured for 28 days at 2.0 *mM* N. Different letters on top of the columns indicate differences between the variants (p <0.05). For the ANOVA +, *, * indicate significant differences at p <0.10, <0.05, <0.001, respectively. The error bars represent the standard deviations of the means (n = 3 to 4).**

Expression of senescence-specific cysteine protease gene *SAG12-1* in senescing leaves

As a further senescence marker the relative expression of the gene *SAG12-1* coding for a senescence-specific cysteine protease was determined. *SAG12-1* expression proved to be a much more sensitive indicator than SPAD and photosynthesis (compare Figures III-2 and III-3). The lower up-regulation by

N starvation of *SAG12-1* in the non-grafted and self-grafted cvs. Apex and NPZ-1 compared to cvs. Capitol and NPZ-2 confirm a delayed leaf-senescence development in former cultivars. The dominant role of the shoot origin in N starvation-induced leaf senescence was well reflected by the *SAG12-1* expression in leaves of the grafted plants which was only greatly enhanced when cv. Capitol and cv. NPZ-2 were used as shoots.

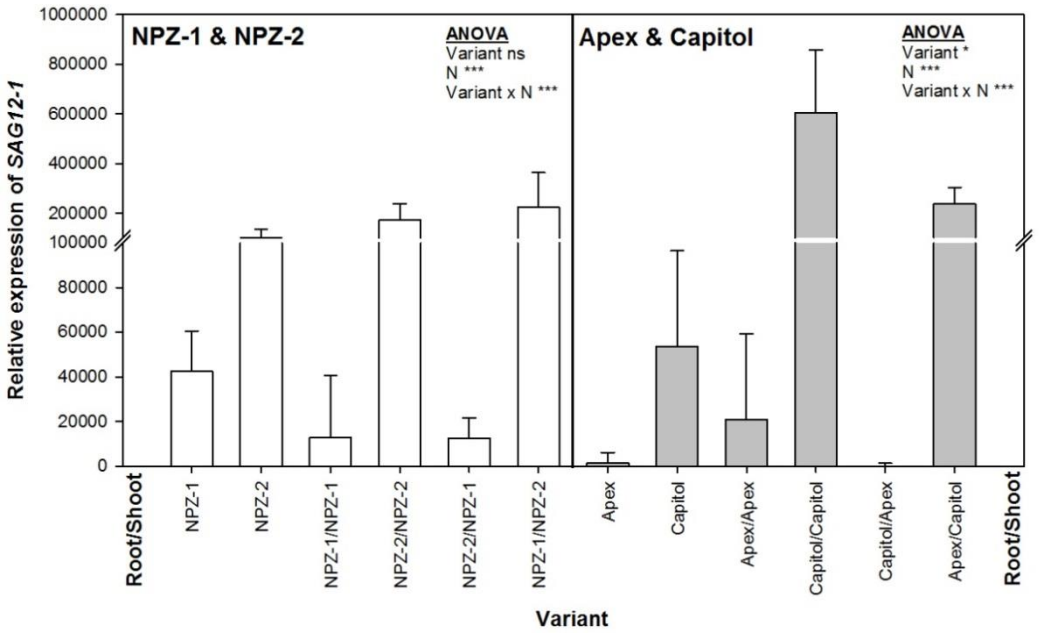

Figure III-3 Relative expression ($2^{-\Delta\Delta Ct}$) of *SAG12-1* of leaf four of non-grafted, self-grafted and reciprocally-grafted plants of the winter oilseed-rape cultivars. NPZ-1 & NPZ-2 (left) and Apex & Capitol (right) grown in hydroponics after 12 days of N starvation (0.1 *mM* N). The plants were pre-cultured for 28 days at 2.0 *mM* N. The data are shown relative to the control (4.0 *mM* N) harvested at the same day. For the ANOVA *, * indicate significant differences at p <0.05, <0.001, respectively. ns = non-significant. The error bars represent the standard errors of the means (n = 3 to 4).**

Specific leaf N content in senescing leaves

The cultivar differences in N starvation-induced leaf senescence could be due to differences in the depletion of the leaf N content. After 12 days of N starvation the specific leaf N content of leaf four significantly declined compared to continuous high N supply for all cultivars and variants (Figure III-4). The non-grafted (significantly) and the self-grafted (tendencially) functional stay-green cv. NPZ-1 showed a higher specific leaf N content compared to the early senescing counterpart cv. NPZ-2 under N starvation. However, between the cvs. Apex and Capitol no significant differences existed.

Under maintained high N supply the cvs. NPZ-1 & NPZ-2 did not differ between the variants in the specific leaf N contents. But for the cultivar pair Apex & Capitol the specific leaf N content of the non-grafted was generally higher than of the grafted plants, a difference which was even significant between the non- and the self-grafted plants of cv. Capitol.

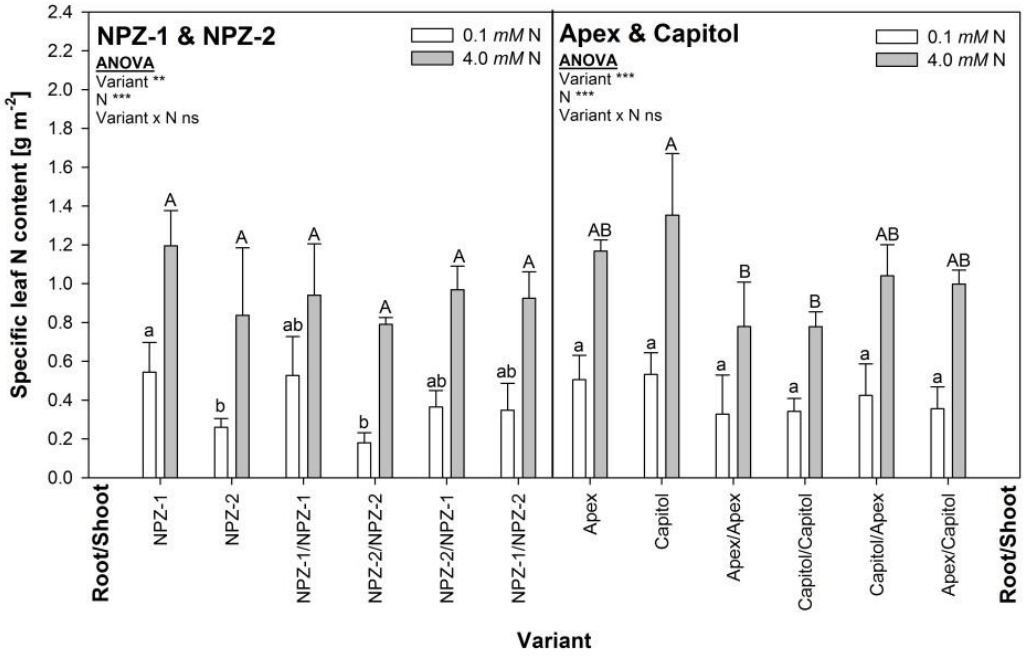

Figure III-4 Specific leaf N content of leaf four of non-grafted, self-grafted and reciprocally-grafted plants of the winter oilseed-rape cultivars NPZ-1 & NPZ-2 (left) and Apex & Capitol (right) grown in hydroponics after 12 days of N starvation (0.1 *mM* N) or optimal N supply (4.0 *mM* N). The plants were pre-cultured for 28 days at 2.0 *mM* N. Different letters on top of the columns indicate differences between the variants (p <0.05). For the ANOVA **, * indicate significant differences at p <0.01, <0.001, respectively. ns = non-significant. The error bars represent the standard deviations of the means (n = 3 to 4).**

Development of N deficiency-induced leaf senescence

To further clarify if root-to-shoot communication and which leaf-inherent factors are decisive for the cultivar differences in stay-green, phytohormones were analyzed in roots, xylem sap and individual leaves in a complementary time-course experiment with the same four cultivars as used for the grafting approach. Also in this experiment the cultivars showed the established cultivar-specific response to N starvation characterizing the cvs. NPZ-1 and Apex as functional stay-green and the cvs. NPZ-2 and Capitol as early senescing (Chapter II).

Plant phytohormone status

Since phytohormones play a major role in root-to-shoot communication and in the control of leaf senescence, the phytohormones SA, JA, ABA and CKs in roots, xylem exudates and leaves as affected by N starvation and cultivar were analyzed. Only the results of the second oldest leaf are presented since the statistical analysis did not reveal a consistent difference between the leaf positions (Tables III-S3, III-S4). To identify a possible relationship between the root pool and the specific content of mature leaves showing leaf senescence during the treatment period, the root content, the xylem transport rate and the specific leaf contents were determined. Despite significant differences

between cultivars for some phytohormones (Tables III-S3, III-S4), only the iCKs responded in a consistent way in relation to the cultivar-specific differences in N starvation-induced leaf senescence. Therefore, the following results showing the effects of treatment duration and N supply are means over the four cultivars.

The root SA content increased under both N supplies reflecting the gain and differences in root biomass during the N treatment period (Figure III-S5a). The SA xylem transport-rates did not differ neither between the N supplies nor the treatment times. The leaf specific content of SA increased during the treatment time from 7 until 12 DAT independent of the N supply (no significant N effect). Also the JA root content increased until 12 DAT under both N supplies (Figure III-S5b). But in contrast to SA the JA root content was higher under N starvation compared to sufficient N supply at 12 DAT. The JA xylem transport-rate did not show significant N-supply and treatment-time effects. Up to 7 DAT the specific JA leaf content was neither affected by treatment duration nor by N supply. But after 7 DAT the JA content significantly increased under N starvation while at sufficient N supply it decreased (significant N x DAT interaction). The ABA root contents increased with treatment duration apparently more under high N supply than under N starvation, but this difference was not significant (Figure III-S5c). The ABA transport-rate in the xylem increased significantly with treatment time under sufficient N supply but not under N starvation. In the leaf tissue the specific ABA content increased until 7 DAT for both N supplies. At 12 DAT the ABA content was significantly higher in N-starved leaves because it remained at the high level whereas it deceased under sufficient N.

Among the phytohormones CKs play a major role in both root-to-shoot communication and leaf senescence. The individually measured CKs were grouped according to their biological activity (Schmitz *et al.,* 1972; Schmülling, 2004) into biologically active (aCKs) and biologically inactive but activatable (iCKs) CKs. The aCKs (tZ, iP, DHZ, cZ, tZR) are of particular importance in relation to stay-green. In the following, for the root, xylem sap and leaf the aCKs were combined, since the overall statistical analysis (Table III-S4) revealed that in spite of significant differences between the individual aCKs neither the cultivar nor the N supply affected the aCKs. Moreover, no systematic pattern occurred between cultivar, treatment duration (DAT) and N supply (no significant cultivar x DAT x N x CKs interaction).

In the root and leaf tissues tZ was the most abundant aCK (51% and 42%, respectively; Figure III-5a). However, in the xylem sap iP was the most abundant aCK (47%). In the root the aCK content increased until 12 DAT under both N supplies, but significantly more under sufficient N supply primarily due to increasing root biomass. The xylem transport-rate of aCKs remained stable over the treatment time (no significant DAT effect), however, it was significantly enhanced under high N supply. The specific leaf content of the aCKs was neither affected by the duration of N starvation (DAT) nor by N supply and remained at a constant level.

The glycosylation of biologically active CKs to O-glycosides (iCKs) leads to their reversible inactivation. This inactivation of the aCKs in the leaf tissue might be of importance for cultivar differences in N starvation-induced leaf senescence. The iCKs quantitatively played the by far major role of the total CKs in root and leaf tissues (Figure III-5b). Among the iCKs, tZOG represented more than 99% of that fraction in root and leaf tissues independent of N supply and duration of N starvation (DAT, not shown). In the xylem, iCKs were also mostly transported as tZOG (76%). The highly significant influence of the duration of N starvation (DAT) on the root content of iCKs was due to root growth during the treatment period rather than root concentrations (not shown). The xylem transport rate of iCKs increased during the treatment period only at high N supply. The lack of a significant DAT effect (ANOVA) may be explained by the high variation of the mean at 7 DAT at high N supply. In the leaf tissue, the iCKs significantly increased over the treatment period. The increase was steeper under N starvation than at optimum N supply (significant N x DAT interaction).

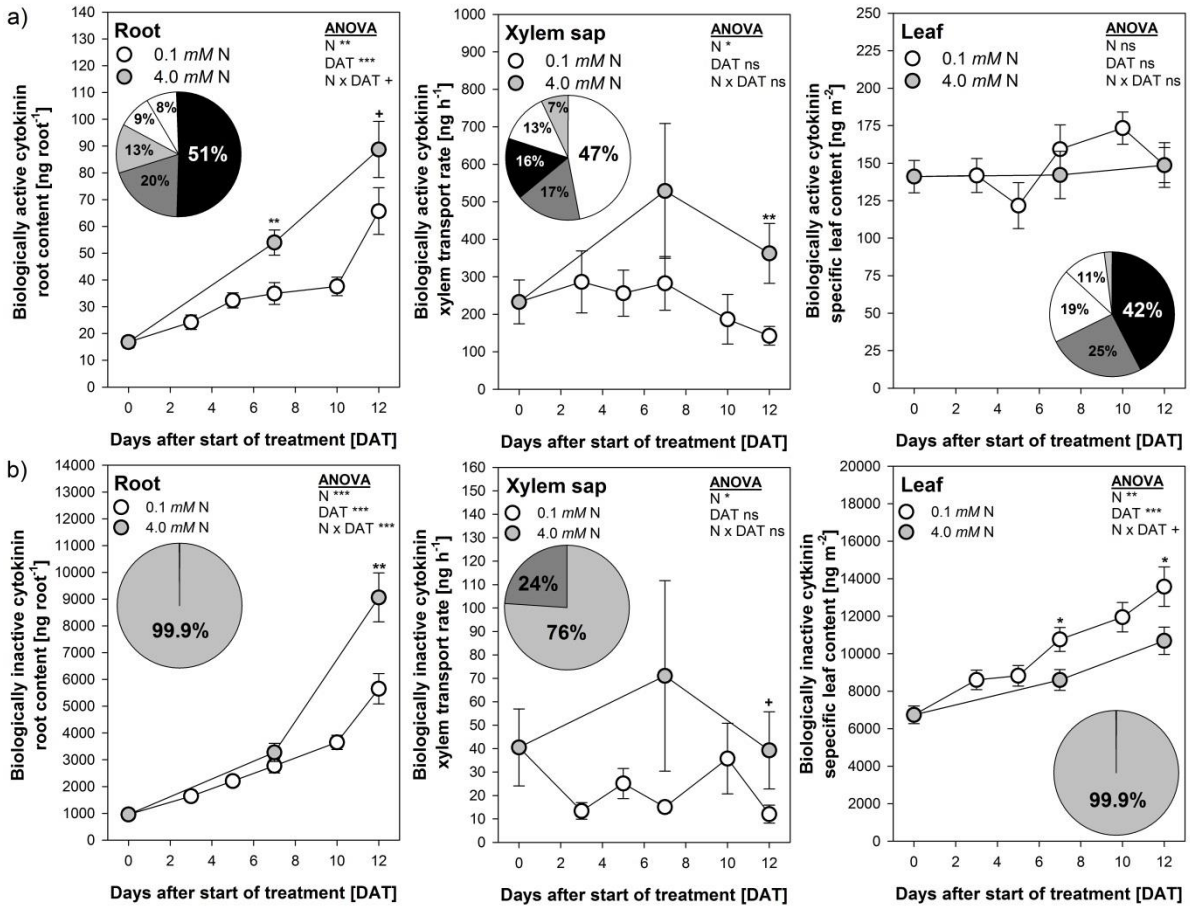

Figure III-5 Biologically active cytokinins (tZ, iP, DHZ, cZ, tZR) (a) and biologically inactive but activatable cytokinins (tZOR, tZORG) (b) in the root, the xylem sap and the second oldest mature leaf of four winter oilseed-rape cultivars grown in hydroponics during 12 days N starvation (0.1 *mM*) or optimal N supply (4.0 *mM*). The plants were pre-cultured for 28 days at 2.0 *mM* N. Pie chart in a: tZ (black), DHZ (dark grey), tZR (grey), cZ (white), iP (hatched). Pie chart in b: tZOG (grey), tZROG (dark grey). For the ANOVA +, *, **, * indicate significant differences at p <0.10, <0.05, <0.01, <0.001, respectively. ns = non-significant. At 7 and 12 DAT +, *, ** indicate differences between the N supplies at p <0.10, <0.05, <0.01, respectively. The error bars (visible only when greater than the symbols) represent the standard errors of the means across the cultivars (n = 3 to 4).**

The overall statistical evaluation revealed that the iCKs but not the aCKs showed a consistent difference between the cultivars and N supplies in the leaf tissue (significant cultivar x DAT x N interaction, Table III-S3). Therefore, the cultivar-specific specific leaf contents of the dominating individual aCKs (tZ) and iCKs (tZOG) are shown in Figure III-6. The specific leaf content of tZ was not affected by N supply and the duration of N starvation (ANOVA). Differences between cultivars were only significant in high-N leaves at 12 DAT. However, the tZOG specific leaf content highly significantly increased during treatment duration more in N-starved than in N-sufficient leaves (significant N x DAT interaction). There was a consistent trend that under N starvation, but also at high N supply and thus constitutively, the early senescing cvs. NPZ-2 and Capitol mostly showed higher tZOG contents than their functional stay-green counterparts NPZ-1 and Apex.

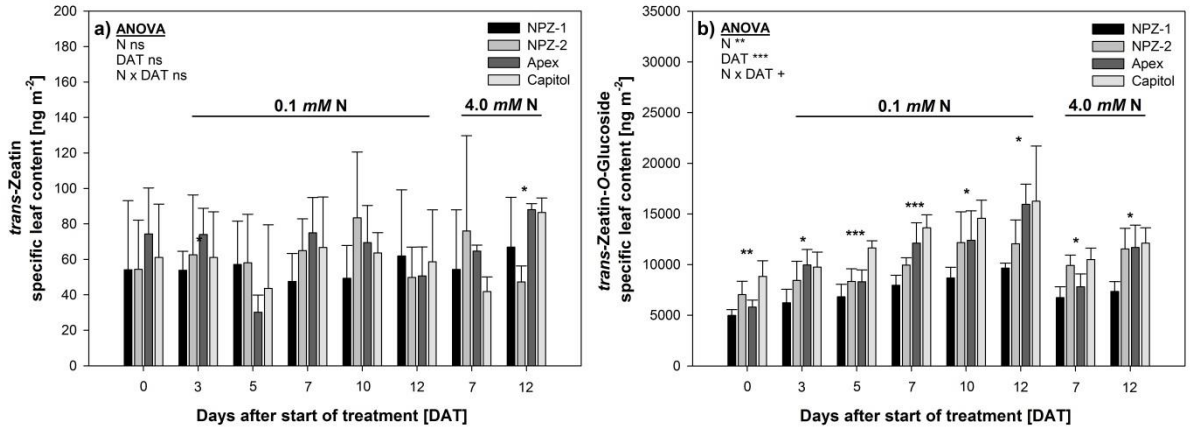

Figure III-6 *trans*-Zeatin (a) and *trans*-Zeatin-O-Glucoside (b) specific leaf content of the second oldest mature leaf of four winter oilseed-rape cultivars grown in hydroponics during 12 days N starvation (0.1 *mM*) or optimal N supply (4.0 *mM*). The plants were pre-cultured for 28 days at 2.0 *mM* N. For the ANOVA +, *, **, * indicate significant differences at p <0.10, <0.05, <0.01, <0.001, respectively. ns = non-significant. *, **, *** above the columns indicate significant differences between the cultivars at p <0.05, <0.01, <0.001, respectively. The error bars represent the standard deviations of the means (n = 3 to 4).**

Regulation of cytokinin homeostasis-related genes in senescing leaves

Cytokinin biosynthesis

The ATP/ADP isopentenyltransferases encoded by *IPTs* catalyze the first step of CK synthesis. Transcripts of the three isopentenyltransferase genes *IPT2, IPT5* and *IPT9* were detected in the leaf tissue under both N supplies (Figure III-7). *IPT2* expression did not change under sufficient N nutrition (Figure III-7a). However, in general N starvation enhanced *IPT2* up-regulation and at most of the harvest days, at least in tendency, cultivar-specific higher up-regulation occurred in the functional stay-green compared to the early senescing cultivars: over the twelve days N starvation period *IPT2* was two-fold up-regulated in cv. NPZ-1 compared to only 1.5-fold in cv. NPZ-2, and 1.5 to two-fold up-regulated in cv. Apex compared to hardly any regulation and even down-regulation in cv. Capitol.

IPT5 was expressed in the leaf tissue under low as well as high N supply during the treatment period (Figure III-7b). Only under N starvation the gene was clearly up-regulated exclusively in the cvs. Apex and Capitol at 12 DAT to a comparable extent. At shorter N starvation periods *IPT5* was only slightly up-regulated with no or no consistent differences between the cultivars. In comparison to *IPT2* and *IPT5*, *IPT9* was more responsive (up-regulation up to 5-fold) to longer (>5 DAT) N starvation (Figure III-7c). However, also under high N supply *IPT9* was up-regulated about two-fold after 7 and 12 DAT. Again, particularly under N starvation, but also under sufficient N supply, the regulation was stronger in the functional stay-green cvs. NPZ-1 and Apex compared to their respective early senescing counterparts cvs. NPZ-2 and Capitol.

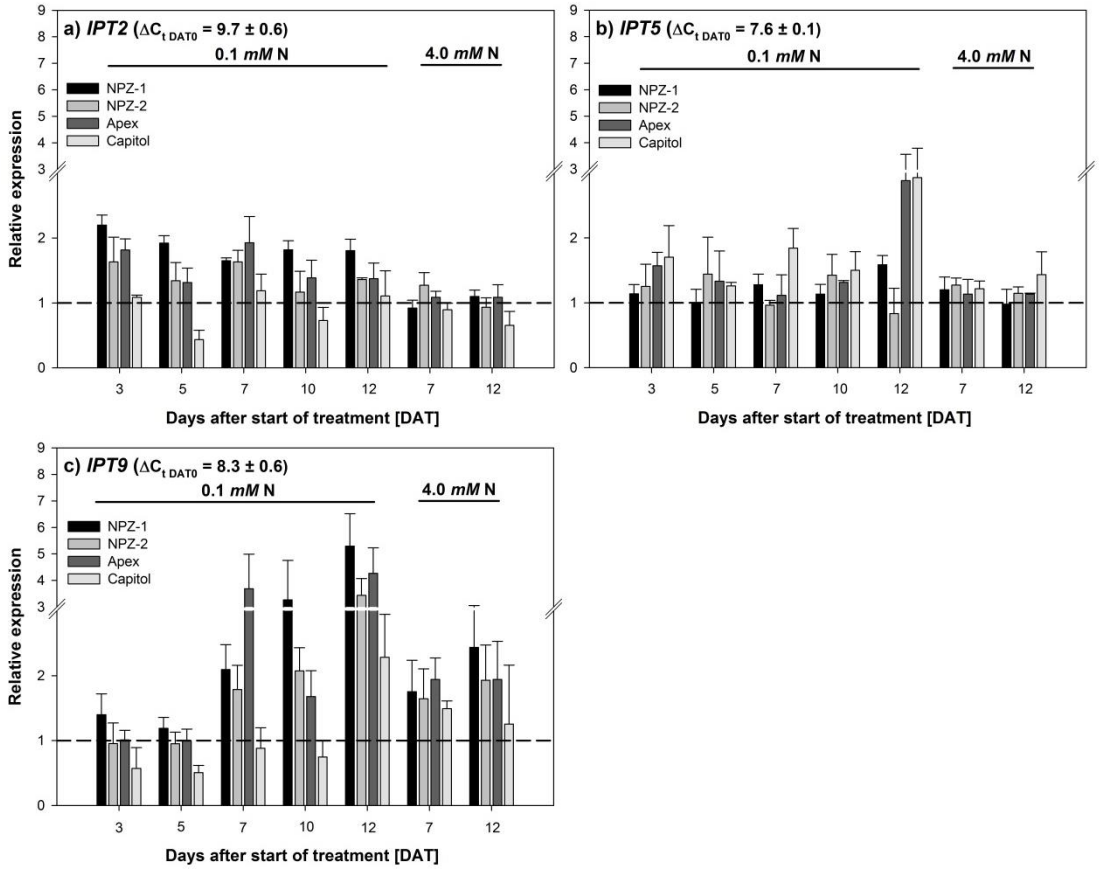

Figure III-7 Relative expression ($2^{-\Delta\Delta Ct}$) of the isopentenyltransferase (IPT) genes *IPT2* (a), *IPT5* (b) and *IPT9* (c) in the second oldest mature leaf of four winter oilseed-rape cultivars grown in hydroponics during 12 days N starvation (0.1 *mM*) or optimal N supply (4.0 *mM*). The plants were pre-cultured for 28 days at 2.0 *mM* N. The data are shown relative to the cultivar-specific control at DAT 0 (dashed line). The error bars represent the standard errors of the means. ± indicate the standard deviation of the mean for the ΔCt across the four cultivars (n = 3 to 4).

Cytokinin inactivation

The glycosylation of biologically active CKs leading to their inactivation is catalyzed by specific uridine diphosphate glycosyltransferases (UGTs). The cultivars generally showed a similar basal expression (DAT 0), but the basal expression level (ΔC_t) differed greatly between the five analyzed UGT genes, in ascending order: *UGT76C1* <= *UGT73C4* < *UGT73C5* <= *UGT73C1* < *UGT85A1* (Figure III-8). Among the

five UGT genes, *UGT73C1* and *UGT76C1* did not respond to N starvation by an enhanced transcription (Figures III-8a, d). Compared to the high N controls at 7 and 12 DAT the up-regulation of *UGT76C1* was even lower under limiting N supply. *UGT73C4* and *UGT73C5* were up-regulated already after three days of N starvation and the up-regulation increased steadily with treatment duration up to 12 DAT. *UGT85A1* with the highest basal expression level was only strongly up-regulated after 12 days of N starvation considering the slight up-regulation also at continuous high N supply. The three *UGT* genes clearly responding to N starvation (*UGT73C4*, *UGT73C5* and *UGT85A1*) showed a consistent cultivar-specific response pattern: the early senescing cvs. NPZ-2 and Capitol had higher transcript abundance than the functional stay-green cvs. NPZ-1 and Apex. For *UGT85A1* this difference between the cultivars was apparent even under high N supply at 7 and 12 DAT.

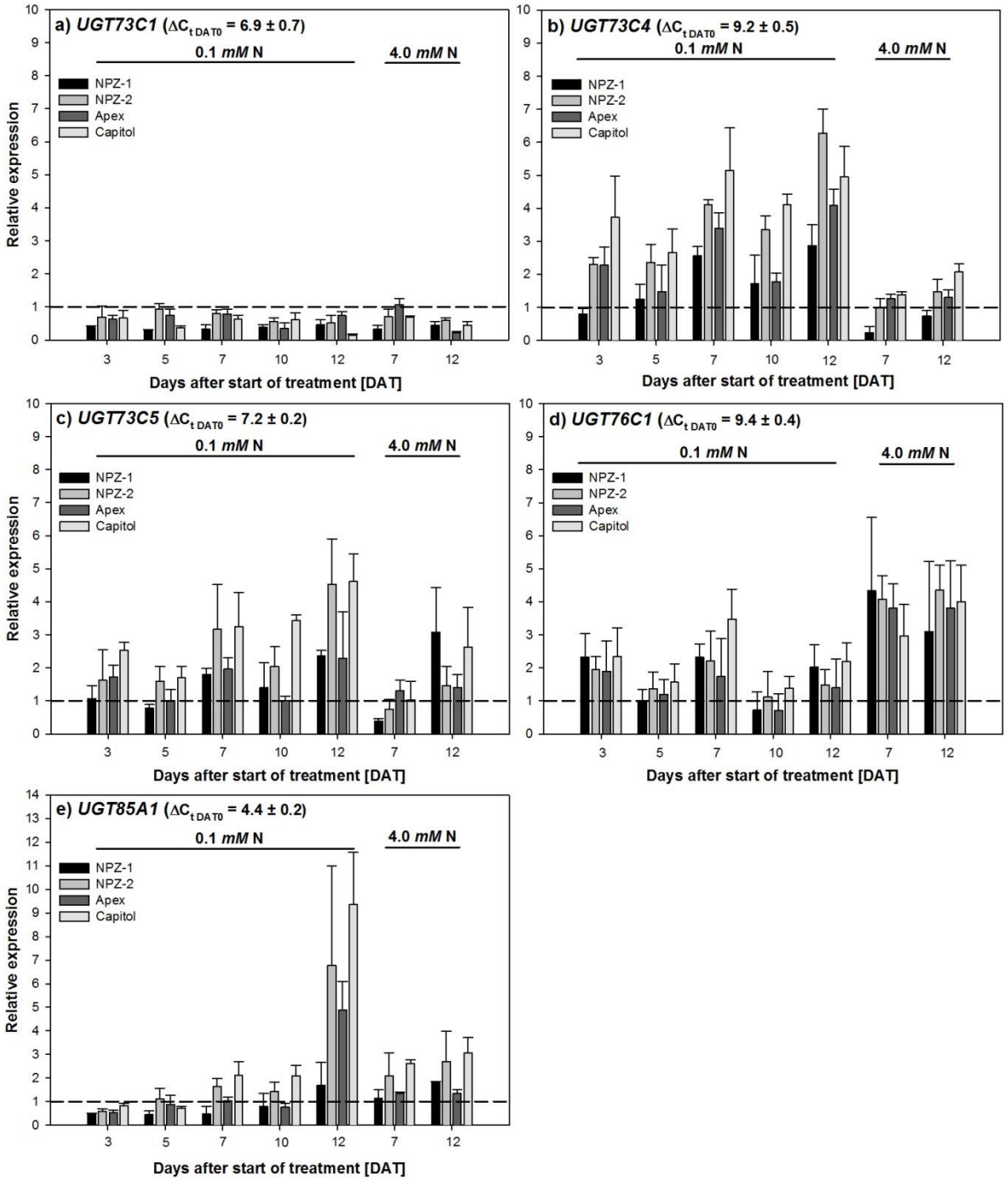

Figure III-8 Relative expression ($2^{-\Delta\Delta Ct}$) of the uridine diphosphate glycosyltransferases (UGT) genes *UGT73C1* (a), *UGT73C4* (b), *UGT73C5* (c), *UGT76C1* (d) and *UGT85A1* (e) in the second oldest mature leaf of four winter oilseed-rape cultivars grown in hydroponics during 12 days N starvation (0.1 *mM*) or optimal N supply (4.0 *mM*). The plants were pre-cultured for 28 days at 2.0 *mM* N. The data are shown relative to the cultivar-specific control at DAT 0 (dashed line). The error bars represent the standard errors of the means (n = 3 to 4). ± indicate the standard deviation of the mean for the ΔC_t across the four cultivars.

Cytokinin activation

The release of the bioactive CK nucleobases from their CK riboside 5' monophosphates is catalyzed in a single-step by the enzyme cytokinin ribosid 5'-monophosphate phosphoribohydrolase, which is encoded by *LONELY GUY* (*LOG*). The cultivars generally showed a similar basal expression (DAT 0),

but the basal expression level (ΔC_t) differed greatly depending on the gene, in decreasing order *LOG1* > *LOG7* > *LOG4* > *LOG5* (Figure III-9). Among the *LOG* genes *LOG1* with the highest basal expression level was not or down-regulated during the treatment time independent of the N supply and cultivar (Figure III-9a). *LOG4,* > *LOG7*, > *LOG5* were generally up-regulated by N starvation not only compared to the DAT 0 control but also to the DAT 7 and DAT 12 high N supply (Figures III-9b to d). *LOG5* with the lowest basal expression level showed the greatest up-regulation with increasing duration of N starvation (75-fold at DAT 12) (Figure III-9c). For *LOG4* and *LOG7* (but not *LOG5*) a mostly consistent cultivar-specific response to N starvation across the treatment duration was apparent: a higher up-regulation occurred for the functional stay-green cvs. NPZ-1 and Apex in comparison to their early senescing counterparts cvs. NPZ-2 and Capitol (Figures III-9b, d). Considering the high up-regulation of *LOG7* in cv. Capitol after 7 days of high N treatment the up-regulation by N starvation is even less than suggested by the $\Delta\Delta C_t$ values shown in Figure III-9, increasing the difference in comparison to cv. Apex.

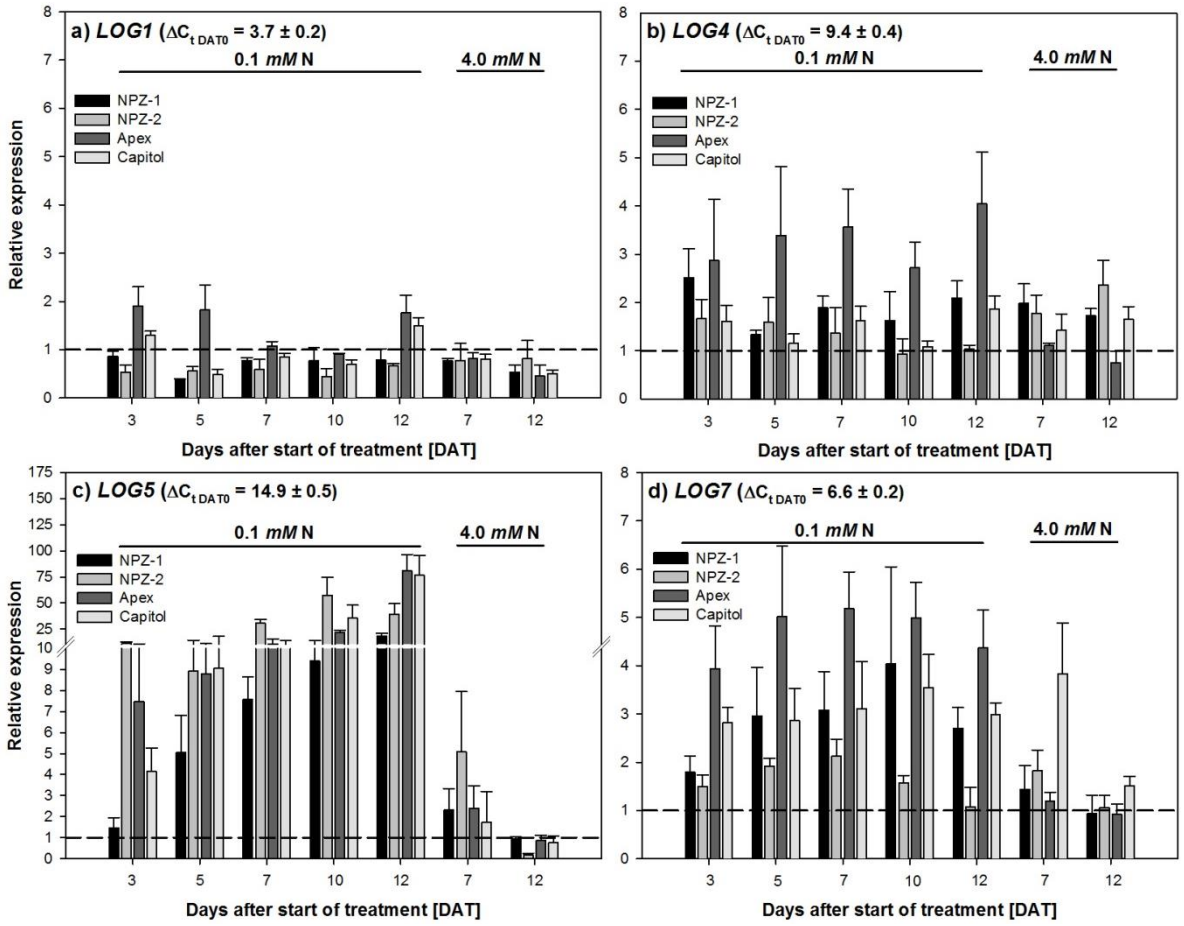

Figure III-9 Relative expression ($2^{-\Delta\Delta Ct}$) of the cytokinin ribosid 5' monophosphate phosphoribohydrolase genes *LOG1* (a), *LOG4* (b), *LOG5* (c) and *LOG7* (d) in the second oldest mature leaf of four winter oilseed-rape cultivars grown in hydroponics during 12 days N starvation (0.1 *mM*) or optimal N supply (4.0 *mM*). The plants were pre-cultured for 28 days at 2.0 *mM* N. The data are shown relative to the cultivar-specific control at DAT 0 (dashed line). The error bars represent the standard errors of the means (n = 3 to 4). ± indicate the standard deviation of the mean for the ΔC_t across the four cultivars.

Cytokinin degradation

The catabolism of biologically active CKs is tightly regulated by cytokinin oxidase/dehydrogenases (CKXs). The five analyzed *CKX* genes generally showed a similar basal expression (DAT 0; Figure III-10). But the basal expression level (ΔC_t) differed depending on the gene in decreasing order *CKX6* < *CKX7* < *CKX1* < *CKX*3 < *CKX*2. *CKX1*, *CKX2* and *CKX3* were generally up-regulated by N starvation (Figures III-10a to c), whereas *CKX6* and *CKX7* were not affected considering the DAT 0 control and the DAT 7 and DAT 12 high-N treatment durations (Figures III-10d, e). For *CKX1* the functional stay-green cv. NPZ-1 showed a consistently higher up-regulation than cv. NPZ-2. Such difference was only clear for the comparison of cvs. Apex and Capitol (Apex > Capitol) after twelve days of N starvation. Among all *CKX* genes, *CKX2* with the lowest basal expression level was most strongly expressed by N starvation in a highly cultivar-specific way (Figure III-10b). The early senescing cv. Capitol showed the highest up-regulation independent of the duration of N starvation, whereas the functional stay-green cv. Apex only little responded to N starvation. *CKX2* was down-regulated in the cvs. NPZ-1 and NPZ-2 until DAT 12 when the early senescing cv. NPZ-2 strongly up-regulated *CKX2* expression. For *CKX3* a comparable cultivar-specific response with the early senescing cultivars (more clearly for NPZ-2 than for Capitol) could be observed (Figure III-10c).

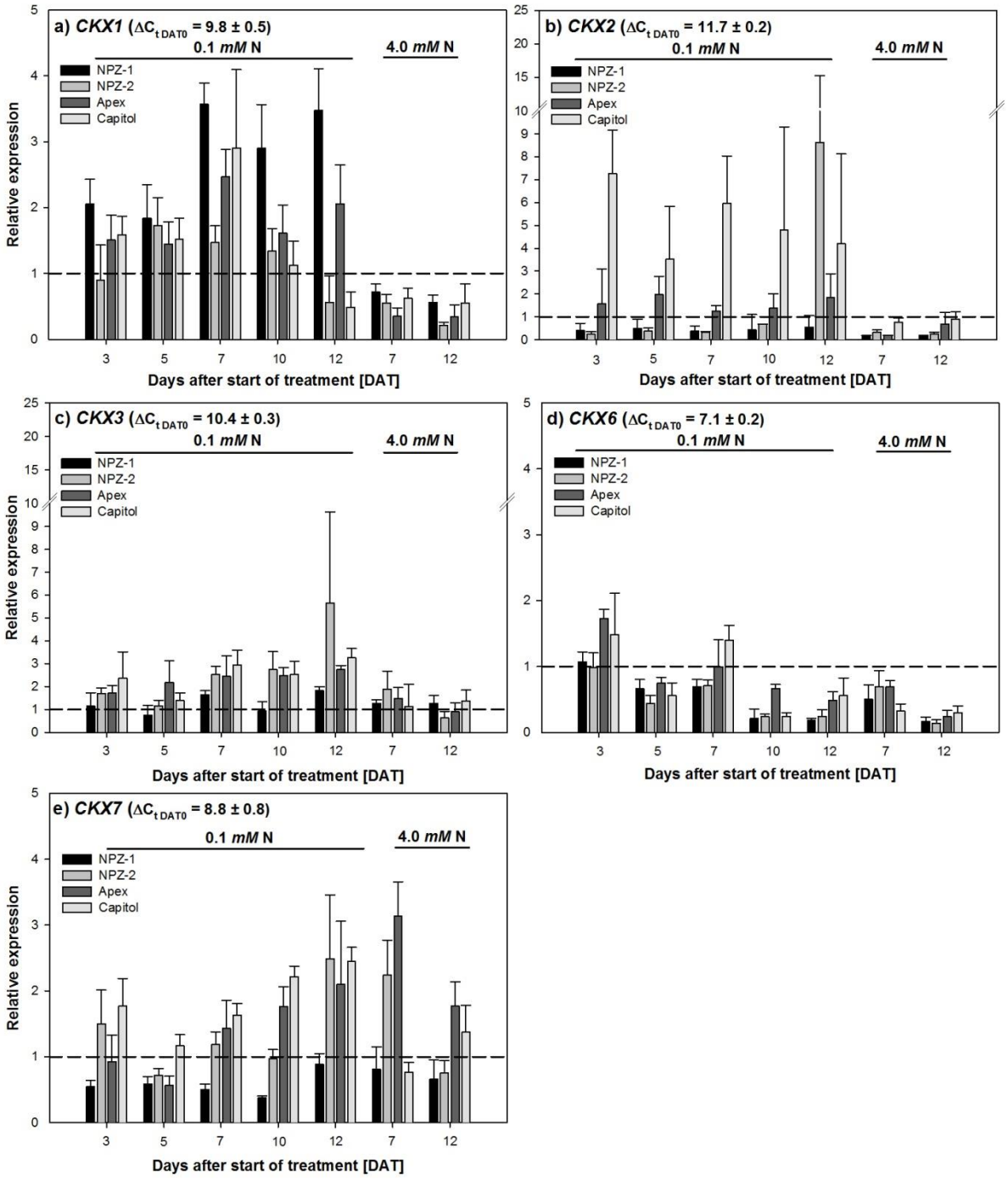

Figure III-10 Relative expression ($2^{-\Delta\Delta Ct}$) of the cytokinin oxidase (CKX) genes *CKX1* (a), *CKX2* (b), *CKX3* (c), *CKX6* (d) and *CKX7* (e) in the second oldest mature leaf of four winter oilseed-rape cultivars grown in hydroponics during 12 days N starvation (0.1 *mM*) or optimal N supply (4.0 *mM*). The plants were pre-cultured for 28 days at 2.0 *mM* N. The data are shown relative to the cultivar-specific control at DAT 0 (dashed line). The error bars represent the standard errors of the means (n = 3 to 4). ± indicated the standard deviation of the mean for the ΔC_t across the four cultivars.

Regulation of cytokinin perception- and signaling-related genes in senescing leaves

For the local perception of and response to biologically active CKs the binding to specific receptors and the activation of response regulators are necessary. The CK receptor encoded by the histidine

kinase receptor *AHK3* and the downstream response regulator encoded by *ARR2* are involved in the CK-regulated leaf longevity. Both genes did not show differences between the cultivars in the basal expression (DAT 0; Figure III-11). *AKH3* up-regulation increased with the duration of N starvation in a cultivar-specific way (Figure III-11a). Considering the down-regulation during the treatment period at high N supply, *AHK3* was most strongly up-regulated by N starvation in the functional stay-green cv. NPZ-1 particularly in comparison to its early senescing counterpart cv. NPZ-2. A comparable higher expression existed in the functional stay-green cv. Apex than in cv. Capitol which did not show any up-regulation. *ARR2* up-regulation generally increased with the duration of N starvation in all cultivars (Figure III-11b). However, there was mostly consistently higher up-regulation of *ARR2* under N starvation in the leaves of the functional stay-green cvs. NPZ-1 and Apex on the one and cvs. NPZ-2 and Capitol on the other hand side.

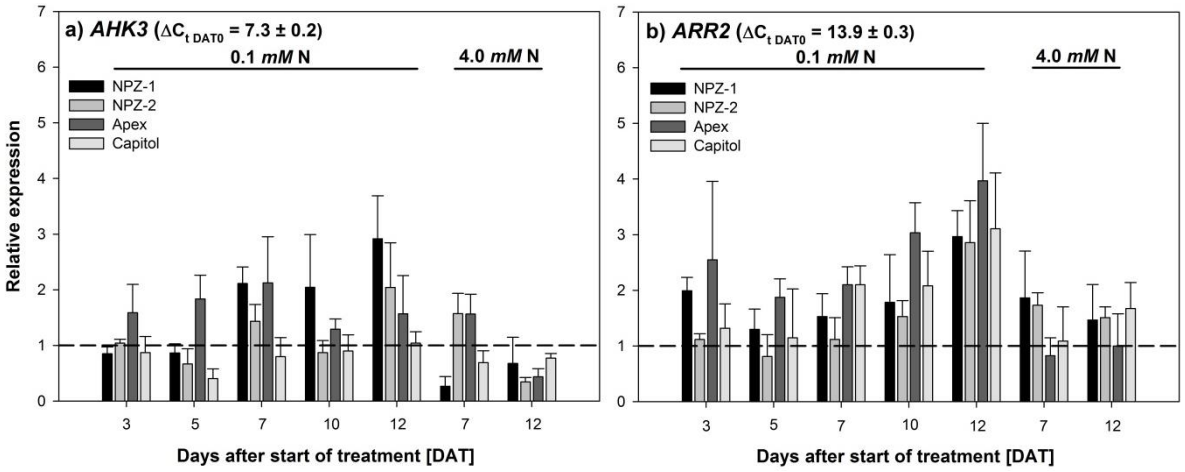

Figure III-11 Relative expression ($2^{-\Delta\Delta Ct}$) of the histidine kinase (HK) gene A*HK3* (a) and the response regulator (RR) gene *ARR2* (b) in the second oldest mature leaf of four winter oilseed-rape cultivars grown in hydroponics during 12 days N starvation (0.1 *mM*) or optimal N supply (4.0 *mM*). The plants were pre-cultured for 28 days at 2.0 *mM* N. The data are shown relative to the cultivar-specific control at DAT 0 (dashed line).The error bars represent the standard errors of the means (n = 3 to 4). ± indicate the standard deviation of the mean for the ΔC_t across the four cultivars.

Discussion

Nitrogen efficiency of line cultivars has been primarily attributed to maintained N uptake during reproductive growth (N uptake efficiency) in combination with delayed leaf senescence of the older leaves accompanied by maintained photosynthetic capacity (functional stay-green) (Schulte auf'm Erley *et al.,* 2007). But currently it is not clear whether higher root growth and N uptake during early reproductive growth of N-efficient cultivars are causally related, and when related, if delayed leaf senescence is the cause or the consequence of maintained root growth.

The experimental approaches were based on experimental evidence showing that the cvs. NPZ-1 and NPZ-2 reacted differently in leaf senescence to N starvation and leaf detaching, indicating root-derived factors, whereas the cvs. Apex and Capitol reacted in the same way, indicating leaf-inherent factors (Figure III-S1). In order to unequivocally clarify whether the cultivar differences in N starvation-induced leaf senescence are root-mediated and/or leaf-inherent a reciprocal grafting approach was applied.

The senescence status of older leaves of the reciprocal grafts after twelve days of N deprivation, assessed by SPAD (Figure III-2a), photosynthesis (Figure III-2b) and, most prominently, by *SAG12-1* expression (Figure III-3) clearly revealed that the cultivar differences between the functional stay-green cvs. NPZ-1 and Apex and their respective early senescing counterparts cvs. NPZ-2 and Capitol were based on leaf-inherent factors rather than on root-derived signals. Since no cultivar differences existed under N starvation at 12 DAT in shoot and root N uptake (Figures III-S2a, b) as well as N concentrations (Figures III-S3a, b) it appears rather unlikely that the genetic variation in functional stay-green was based on differences in N uptake or N utilization efficiency.

Since N content and photosynthetic activity of leaves are closely related (Evans, 1989), the specific leaf-N content might be an important leaf-inherent factor for genetic variation in functional stay-green. Particularly under N starvation, maintained photosynthetic activity could be related to the remaining specific leaf N content (Schulte auf'm Erley *et al.,* 2007; Koeslin-Findeklee *et al.,* 2014). But in the present study, cultivar differences in N starvation-induced leaf senescence at early stages with declined but still substantial photosynthesis rates were not reflected by the specific leaf-N content (Figure III-4). Solely the specific leaf-N contents of the severely senescent non- and self-grafted cv. NPZ-2 at 12 DAT were either significantly or by trend lower compared to the respective variants of cv. NPZ-1. This may explain the generally significant positive correlation between the specific leaf N content and photosynthesis rate (r^2 = 0.20**; Figure III-S4). But only 20% of the variation in photosynthesis rate could be attributed to the specific leaf N content. Consequently, the development of cultivar differences in functional stay-green under N starvation depended primarily on other leaf-inherent factors than the specific leaf-N content. This is in agreement with the results

of Schulte auf'm Erley *et al.* (2010) for genotypic differences in N starvation-induced leaf senescence in maize.

Phytohormones are master-regulators of the leaf senescence process, in which SA, JA and ABA promote senescence whereas CKs delay it (Lim *et al.,* 2007). Supporting the leaf-inherent control of N starvation-induced leaf senescence, the root contents of SA, JA ABA and aCKs and iCKs and their transport rates in the xylem in the complementary time-course experiment did not suggest a role of root-derived phytohormone signals for cultivar differences in stay-green (Figures III-5a, b; III-S5a to c). Under N starvation SA as well as JA accumulated in the leaf, but only at later stages of N starvation from 7 until 12 DAT (Figures III-S5a, b) suggesting that SA and JA were involved in the regulation of N starvation-induced leaf senescence only at advanced stages. Thus a major role of SA and JA as leaf-inherent factors for the development of genetic variation in stay-green under N starvation is unlikely.

Rapidly after exposure to N starvation photosynthetic activity of the leaves declined (not shown). Abscisic acid regulates the stomatal conductance which influences the photosynthesis rate (He *et al.,* 2005). Under N starvation accumulation of ABA in the leaf was accompanied with a decrease of the photosynthesis rate (not shown). Thus ABA accumulation in the leaf under N starvation might be an important leaf-inherent factor for the termination of photoassimilation and thus the final stage of the leaf senescence process. But the cultivar differences in functional stay-green could not be explained by differences in the specific ABA leaf content (Table III-S3).

With regard to functional stay-green CKs are of particular importance (Lara *et al.,* 2004, del Mar Rubi-Wilhelmi *et al.,* 2014). In the present study, the measured aCKs remained at a constant level independent of N supply and cultivar (Figure III-5a) in the complementary time-course experiment. Only the iCKs responded in a N starvation and cultivar-specific way: the functional stay-green cvs. NPZ-1 and Apex showed a lower accumulation of iCKs in senescing leaf tissue compared to their respective early senescing counterparts cvs. NPZ-2 and Capitol (Figure III-5b). This suggests that CK homeostasis is a decisive leaf-inherent factor for genetic variation in functional stay-green under N starvation. Hence the regulation of genes assigned to CK *de novo* synthesis, inter-conversion and breakdown were analyzed in the same experiment. The rate-limiting step of CK biosynthesis is catalyzed by the enzyme isopentenyltransferase (IPT) (Schmülling, 2004; Sakakibara, 2006). Among the detected *IPT* genes in the leaf, particularly the tRNA IPTs *IPT2* and *IPT9* were up-regulated by N starvation and in a cultivar-specific way (Figures III-7a, c). Both IPT isoforms catalyze the formation of cZ derived from tRNA degradation (Schmülling, 2004; Sakakibara, 2006). Although the cZ content in the leaf did not change, the *IPT* expression-patterns indicated a higher leaf-inherent cZ biosynthesis in the functional stay-green cvs. NPZ-1 and Apex compared to their respective early senescing counterpart cvs. NPZ-2 and Capitol under N starvation. Despite the fact,

that cZ is less biologically active (Schmitz *et al.,* 1972) and its biosynthesis requires a high tRNA turnover (Sakakibara, 2006), it might have significance for genetic variation in functional stay-green, because during senescence a high tRNA turnover occurs (Buchanan-Wollaston, 1997) and cZ is less susceptible to degradation (Sakakibara, 2006). Moreover, the results of Miyawaki *et al.* (2004) support the view that in senescing leaves tRNA may be an important source for the leaf-inherent synthesis of biologically active CKs.

However, in addition to the biosynthesis of biologically active CKs the spatial and temporal fine-regulated metabolic inter-conversion of CKs decisively affects the impact of CKs on plant processes (Schmülling, 2004; Sakakibara, 2006). The glycosylation of biologically active CKs lead to their inactivation. This is mediated by specific CK uridine diphosphate (UDP) glucosyltransferases (UGTs) forming either reversible *O*-glycosides or irreversible *N*-glycosides (Schmülling, 2004; Sakakibara, 2006). The UGTs encoded by *UGT73C1, UGT73C5, UGT85A* (Figure III-8) particularly catalyze the formation of tZOG and DHZOG, whereas *UGT76C1* is involved in the formation of irreversibly inactivated N-glycosides of tZ, DHZ, iP and cZ (Hou *et al.,* 2004; Wang *et al.,* 2013). Among the CK-specific UGTs UGT85A1 has been identified as the key enzyme for the formation of tZOG. The transcript amount correlated with the accumulation of tZOG in plant tissues (Hou *et al.*, 2004; Jin *et al.,* 2013). In the complementary time-course experiment the expression pattern of *UGT85A1* reflected the cultivar-specific tZOG accumulation in the leaf under both N supplies (Figure III-8e): *UGT85A1* was higher expressed in the leaf tissue of cv. NPZ-1 compared to cv. NPZ-2 as well as of cv. Apex compared to cv. Capitol under N starvation and optimal N supply (Figure III-8e). In addition to *UGT85A1* also the cultivar-specific higher up-regulation of *UGT73C4* and *UGT73C5* particularly under N starvation corresponded to the higher accumulation of iCKs in the leaf of the early senescing cvs. NPZ-2 and Capitol compared to their respective functional stay-green counterparts cvs. NPZ-1 and Apex (Figures III-8b, c). Contrastingly *UGT73C1* was generally down-regulated (Figure III-8a). Although no N-glycoside CKs were determined, the expression pattern of *UGT76C1* (Figure III-8d) suggests that N-glycosylation did not play a role for leaf-inherent CK inter-conversion under N starvation.

An alternative pathway for limiting the biological activity of CKs is the attachment of ribose or ribose-5´-monophosphate to CK bases (Schmülling, 2004). The release of CK nucleobases from their respective CK ribose 5'-monophosphate is catalyzed inter alia in a single-step by cytokinin specific riboside 5'-monophosphate phosphoribohydrolase encoded by *LONELY GUY* (*LOG*) (Kuroha *et al.,* 2009). Among the four *LOG*s detected in the leaf, particularly *LOG4* and *LOG7* were mostly higher expressed by N starvation in the functional stay-green cvs. NPZ-1 and Apex compared to their respective early senescing counterparts cvs. NPZ-2 and Capitol (Figures III-9b, d). Particularly LOG7 has been identified as the key enzyme on the whole plant level for the release of highly

biological active CKs from their corresponding ribosides (Tokunaga *et al.,* 2012). But despite the cultivar-specific enhanced *LOG7* (and *LOG4*) expression in the functional stay-green cultivars, the levels of the aCKs were not increased. In contrast to *LOG4* and *LOG7*, *LOG1* expression neither responded to the N supply nor the duration of the treatment (Figure III-9a). Although occasionally cultivar differences occurred, no systematic expression pattern existed. However, the generally low change of *LOG1* regulation is most likely the result of the comparable high basal transcript abundance (ΔCt = 3.7 ± 0.2). Although *LOG5* showed the highest relative induction with the progression of N starvation-induced leaf senescence (Figure III-9c) the initial (DAT0) and final (DAT12) expression level (ΔCt) under both N supplies was comparable low. Thus it is most likely that *LOG5* did not play a decisive role in leaf CK activation. This is in agreement with results in *A. thaliana* where the main sites of *LOG5* transcription were the inflorescences (Kuroha *et al.,* 2009).

The level of biologically active CKs is also determined by their rate of degradation (Schmülling, 2004; Sakakibara, 2006). The CK bases as well as their ribosides are irreversibly degraded by CK-specific oxidase/dehydrogenase (CKX) in a single-step by oxidative cleavage of the side chain (Schmülling *et al.,* 2003). CKX activity is regulated on the transcriptional level, in which significant differences exist between the seven known isoenzymes in the ability to target specific CKs (Schmülling *et al.,* 2003; Galuszka *et al.,* 2007; Kowalska *et al.,* 2010; Gajdošová *et al.,* 2011; Trifunović *et al.,* 2013; Köllmer *et al.,* 2014). The regulation patterns of *CKX1*, *CKX2*, *CKX3*, *CKX6* and *CKX7* during N starvation-induced leaf senescence (Figure III-10) reveals that CK degradation most likely did not play a major role for cultivar differences in functional stay-green.

For the CK-mediated leaf longevity not only the presence of biologically active CKs is important, but also their binding to the CK-specific receptor histidine kinase AHK3 as well as the subsequent activation of the response regulator ARR2 (Kim *et al.,* 2006). The response regulator ARR2 induces downstream CK-responsive genes and, directly or indirectly, induces or represses a set of target genes responsible for the regulation of leaf senescence (Kim *et al.,* 2006). According to the cultivar differences in N starvation-induced leaf senescence *AHK3* was at least in tendency higher up-regulated in the functional stay-green cvs. NPZ-1 and Apex compared to their respective early senescing counterparts cv. NPZ-2 and cv. Capitol (Figure III-11a). In accordance to the regulation of *AHK3*, also *ARR2* was at least in tendency higher up-regulated in the functional stay-green cvs. NPZ-1 and Apex compared to their respective early senescing counterparts cv. NPZ-2 and cv. Capitol, too (Figure III-11b). Thus the expression patterns suggest that the binding of and the response to biologically active CKs mediated by AHK3 and ARR2 are additional leaf-inherent factors responsible for cultivar differences in N starvation-induced leaf senescence.

In conclusion, the present study revealed that the cultivar differences in N starvation-induced leaf senescence were governed by leaf-inherent factors. The specific leaf contents of CKs differing in

biological activity and the expression of genes involved in CK homeostasis suggest that leaves of early senescing cultivars was characterized by inactivation of biologically active CKs, whereas in functional stay-green cultivars synthesis, activation, binding of and response to biologically active CKs were favored. Thus the homeostasis of biologically active CKs was the decisive leaf-inherent factor for cultivar differences in N starvation-induced leaf senescence.

IV Contribution of nitrogen uptake and retranslocation during reproductive growth to the nitrogen efficiency of winter oilseed-rape cultivars (*Brassica napus* L.) differing in leaf senescence

Fabian Köslin-Findeklee[1], Gerhard Baumgärtel[2] and Walter J. Horst[1]

[1]Institute of Plant Nutrition, Leibniz University of Hannover, Herrenhäuser Str. 2, D-30419 Hannover, Germany
[2]Landwirtschaftskammer Niedersachsen, Hans-Böckler-Allee 20, D-30173 Hannover, Germany

Abstract

The cultivation of winter oilseed-rape (*Brassica napus* L.) causes high nitrogen (N) balance surpluses. The breeding and cultivation of cultivars with high N efficiency, defined as high grain yield under limited N supply, might contribute to reduce the crop-specific N balance surpluses. Genetic variation in N efficiency of winter oilseed-rape line-cultivars has been predominantly attributed to N uptake efficiency (NUPT) through maintained N uptake during reproductive growth related to delayed leaf senescence accompanied by maintained photosynthetic capacity (functional stay-green).

For investigating the role of delayed leaf senescence, N retranslocation and N uptake during the reproductive phase for grain yield formation under N limitation two line-cultivar pairs differing in N starvation-induced leaf senescence were grown in a field experiment under two N fertilizer rates, without mineral N (N0) and with 160 kg N ha^{-1} (N160). Through frequent harvests from full flowering until maturity N uptake, N utilization and apparent N remobilization from vegetative plant parts to the pods could be calculated.

In the present field experiment NUPT was more important than N utilization efficiency (NUE) for grain yield formation under N-limiting (N0) as well as under sufficient N (N160) conditions. For cultivar differences in N efficiency, particularly N uptake during flowering (NUPT) and biomass allocation efficiency (HI) to the grains were decisive. Both crop traits were related to delayed senescence of the older leaves. Nevertheless, remobilization of N particularly from stems and leaves rather than form the tap root was more important for pod N accumulation than N uptake after full flowering. The main sources for the high N amounts remaining in the crop resides at maturity were the pod walls (high N concentrations) and the stems (high biomass). Decreasing the crop-inherent high N budget surplus of winter oilseed-rape requires increasing the low N remobilization efficiency of pod wall N to the grains.

Keywords: *Brassica napus*, line cultivars, genotypic differences, nitrogen efficiency, nitrogen uptake, nitrogen utilization, nitrogen retranslocation, functional stay-green

Introduction

Winter oilseed-rape (*Brassica napus* L.) is the most important oil crop in northern Europe. The oil is used for human consumption (edible oil) or industrial purposes (lubricant, biodiesel). (Booth & Gunstone, 2004).

In most cropping systems N availability is one of the major factors determining crop growth and thus yield formation. For optimum grain yield winter oilseed-rape requires about 200 kg N ha^{-1} (Rathke *et al.*, 2006). Under best agronomic practices a grain yield of 4.5 t ha^{-1} causes an N budget surplus of around 60 kg N ha^{-1} for which an incomplete depletion of plant available soil-N by the crop and an incomplete retranslocation of N from vegetative plans parts into the grains are responsible (Aufhammer *et al.*, 1994; Lickfett *et al.*, 2001). Thus a substantial part of the N required for optimal crop development is not removed from the field with the harvested grains. For economic and ecological reasons the high crop-specific N balance surplus has to be reduced, but without reducing the current yields. A promising approach is the breeding and cultivation of N-efficient (high yield under low N input) cultivars (Sylvester-Bradley & Kindred, 2009) allowing to decrease the N application necessary achieve optimum yields. N efficiency is a complex crop trait and is based on two pillars: I. the effectiveness of a cultivar in absorbing nutrients from the soil (N uptake efficiency/NUPT) and/or II. the efficiency with which the N is utilized to produce yield (N utilization efficiency/NUE) (Sattelmacher *et al.*, 1994). The relative contribution of either efficiency trait to N efficiency depends on the crop species (Moll *et al.*, 1982; Wiesler *et al.*, 2001) but also on the severity of the N deficiency stress as could be shown for winter oilseed-rape (Berry *et al.*, 2010; Schulte auf´m Erley *et al.*, 2011; Koeslin-Findeklee *et al.,* 2014). Genetic variation in N efficiency in winter oilseed-rape has been mainly attributed to NUPT particularly after transition from the vegetative to the reproductive developmental period during flowering (Berry *et al.*, 2010; Schulte auf'm Erley *et al.*, 2011; Ulas *et al.,* 2012).

Insufficient N supply induces and accelerates senescence (Mei & Thimann, 1984), which causes enhanced crop maturation and thus reduces yields (Gregersen *et al.*, 2013). A characteristic of N-efficient cultivars with prolonged N uptake into the reproductive growth phase under N-limiting conditions is a functional stay-green phenotype, expressed as delayed senescence of the older leaves, accompanied by maintenance of the photosynthetic capacity (Schulte auf'm Erley *et al.*, 2007). Despite the fact that it is currently not clear whether the functional stay-green phenotype of N-efficient cultivars is the cause or the consequence of maintained root growth (Kamh *et al.*, 2005), it is assumed that the prolonged assimilate supply to the roots enhances the N uptake into the reproductive phase because of extending the leaf-photosynthesis duration.

However, for yield formation and low amounts of N remaining in the crop residues plant senescence finally, is a prerequisite. A key function of senescence is the remobilization of particularly N from the

vegetative plant parts to reproductive organs (particularly the grains) (Masclaux-Daubresse *et al.*, 2008). In winter oilseed-rape more than 70% of pod N is derived from N remobilization (Malagoli *et al.*, 2005; Gombert *et al.*, 2010).

The aim of the study was to investigate under field conditions the role of functional stay-green and the importance of the amount and the timing of N retranslocation and N uptake during the reproductive phase for genetic variation in N efficiency of two winter oilseed-rape cultivar-pairs differing in N starvation-induced leaf senescence.

Material and Methods

Plant material and growing conditions

For investigating the role of delayed leaf senescence, N retranslocation and N uptake during the reproductive phase for grain yield formation under N limitation the two line-cultivar pairs cvs. NPZ-1 and NPZ-2 and cvs. Apex and Capitol were selected for the field experiment. The commercial cvs. Apex and Capitol were selected, since previous field and nutrient solution experiments classified cv. Apex as N-efficient and cv. Capitol as N-inefficient (Schulte auf'm Erley *et al.,* 2007). The cvs. NPZ-1 and NPZ-2 were selected based on their differential functional stay-green character (Koeslin-Findeklee *et al.,* 2014) and their classification by the breeder Norddeutsche Pflanzenzucht Hans-Georg Lembke KG (NPZ) as N-efficient and N-inefficient, respectively. The cvs. NPZ-1 and NPZ-2 are breeding lines with a similar genetic background. The seeds of all cultivars were received from NPZ. The field experiment was performed in the year 2011 at the experimental station Poppenburg of the Landwirtschaftskammer Niedersachsen on a loess soil in Nordstemmen, Germany. The cultivars were grown under two N fertilizer rates, without mineral N (N0) and 160 kg N ha^{-1} (N160) as calcium ammonium nitrate. The soil mineral N content (N_{min}) in autumn 2010 before N fertilizer application was N_{min} = 75 kg N ha^{-1} for a soil depth of 0.9 m. The experiment was laid out in a block design with the N fertilization levels as blocks. Within each block the cultivars were completely randomized in four replicates. The plot size was 12.0 m x 1.5 m (18 m^2). The seeds were sown on 6 September 2010 with a target plant density of 60 plants m^{-2}. The plant distance between the rows was 25 cm and within a row 12 cm. Due to the hard frosts in the winter 2010/2011 the actual plant density in spring was only 30 plants m^{-2}.

Plant harvest and analysis

The developmental stage of the plants was determined using the BBCH-code (Biologische **B**undesanstalt, **B**undessortenamt und **Ch**emische Industrie) (Lancashire *et al.,* 1991). From full flowering (BBCH65; 50% of the flowers on the main raceme open) until maturity (BBCH89) in weekly intervals 0.75 m^2 of each plot were harvested. At the head ends, the plots were shortened by one meter and the border plants (0.5 m) were discarded. The plants were separated into stems, leaves, pods, grains and pod walls. Furthermore the shed leaves were weekly collected and the taproots were dug out. The shoot represented the entire above-ground plant parts: stem, shaded leaves, intact leaves and pods. From BBCH79 on (all pods have reached the cultivar-specific size) pod walls and grains were separated. The straw represented the same above-ground plant organs as for the shoot excluding the grains. N concentrations of the dried and ground plant material were determined using an elemental analyzer (Vario EL, Elementar Analysensysteme, Hanau, Germany). At maturity

the oil concentration in the grain and the protein concentration in the grains and grain-meal were determined by near infrared reflectance spectroscopy (NIRS) according to the method of Tkachuk (1981). In addition to the destructive harvests the senescence status of three leaves of three previously marked plants were determined at eleven time points from 5 days after full flowering (DAFF) (BBCH65) until 52 DAFF, near maturity (BBCH89). The chlorophyll contents of the leaves 2, 4, and 6 on the main stem counted from the inflorescence to the bottom of plant was assessed using a portable chlorophyll meter (SPAD-502, Konica Minolta, Tokyo, Japan). Three readings per leaf were taken. The senescence status of the whole plant was assessed for three previously marked plants per plot by counting the number of remaining green leaves on the main stem at thirteen time points from full flowering (BBCH65) until 52 DAFF, near maturity (BBCH89). Further agronomic relevant traits and apparent N remobilization and uptake at maturity were calculated based on the following equations:

N uptake (NUPT) = N_{Straw} [kg N ha^{-1}] + N_{Grain} [kg N ha^{-1}]

N utilization (NUE) = Grain dry weight [kg ha^{-1}] / N_{Shoot} [kg ha^{-1}]

Nitrogen harvest index (NHI) = N_{Grain} [kg N ha^{-1}] / N_{Shoot} [kg N ha^{-1}]

Harvest index (HI) = Grain dry weight [t ha^{-1}] / Shoot dry weight [t ha^{-1}]

Apparent taproot N remobilization$_{BBCH89}$ = Taproot N_{BBCH89} [kg N ha^{-1}] – Taproot N_{BBCH65} [kg N ha^{-1}]

Apparent stem N remobilization = Stem N_{BBCH89} [kg N ha^{-1}] – Stem N_{BBCH65} [kg N ha^{-1}]

Apparent leaf N remobilization =
Intact leaf N_{BBCH89} [kg N ha^{-1}] – (Intact leaf N_{BBCH65} [kg N ha^{-1}] + (Shed leaf N_{BBCH89} [kg N ha^{-1}])

Apparent N remobilization to the pods =
Apparent taproot N remobilization [kg N ha^{-1}] + Apparent stem N remobilization [kg N ha^{-1}] + Apparent leaf N remobilization [kg N ha^{-1}]

Apparent N uptake of the pods = Pod N_{BBCH89} [kg N ha^{-1}] - Apparent N remobilization to the pods [kg N ha^{-1}]

Statistical analysis

The statistical analysis of the field experiment was performed using the statistic software SAS version 9.2 (SAS Institute, Cary, USA). For the field trials the analysis of variance (ANOVA) was calculated using the PROC MIXED procedure. For the ANOVA the Type III sum of squares was applied, if an unequal number of replicates occurred. For the overall analysis cultivar, N rate, DAF and their interactions were set as fixed factors. For the comparison of the cvs. NPZ-1 and NPZ-2, respectively Apex and Capitol within the N levels the LSMEANS statement was used. For each comparison the

linear combinations were defined for the cultivar and the cultivar x N rate interaction using the ESTIMATE statement. For all tests of significance a p-value of 0.05 was used and the p-values were Bonferroni-Holm adjusted. In the tables and figures for the F-Test +, *, ** and *** indicate significance at the $p < 0.10$, < 0.05, < 0.01 and < 0.001 level, respectively. ns = non-significant. The same symbols were used to mark the significance for the correlations. For the comparison of means different letters on top of the columns indicate differences between the columns at $p < 0.05$. Curves were fitted using the graphic software SIGMA PLOT version 11 (Systat software, San Jose, USA).

Results

The cultivars included into the field study had been selected on the basis of their differential response to N starvation in hydroponics (early senescence or functional stay-green). In order to verify if these differences also hold true under field conditions the number of green leaves remaining at the plant and the chlorophyll content (SPAD) of specific leaves on the main stem were counted/measured from flowering (BBCH65) until near maturity. For the SPAD measurement the leaves 2, 4 and 6 on the main stem counted basipetally from the inflorescence were selected. Leaf 2 was the leaf which could reliably be measured until near maturity whereas the older leaves 4 and 6 were shed earlier. Therefore, and since the older leaves showed the same differences between N supplies and cultivars (Figures IV-S1, IV-S2), results are shown only for leaf two. SPAD of leaf two decreased substantially during reproductive growth under both N fertilization rates, but the decline was faster without N fertilization (Figure IV-1). The slower decline of the SPAD values of cv. NPZ-1 compared to cv. NPZ-2 (Figure IV-1a) and cv. Apex compared to cv. Capitol (Figure IV-1b) particularly under N0 confirm the stay-green character of the cvs. NPZ-1 and Apex.

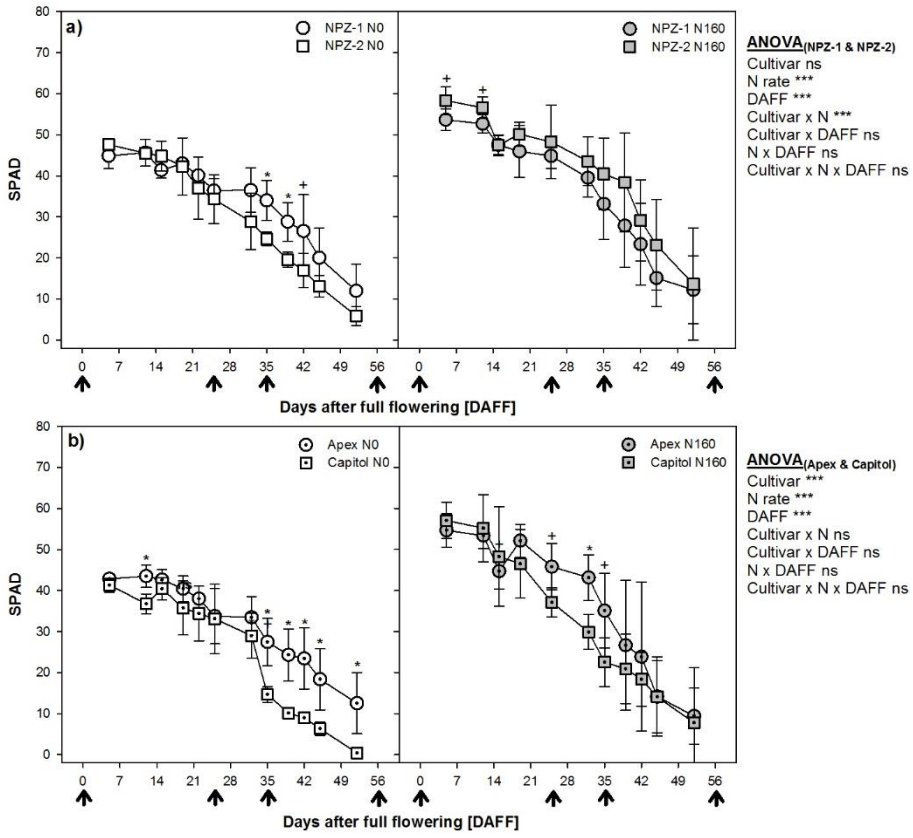

Figure IV-1 SPAD of leaf position two on the main stem of the winter oilseed-rape line-cultivars NPZ-1 and NPZ-2 (a) and Apex and Capitol (b) from 5 days after full flowering (BBCH65) until near maturity (BBCH89) as affected by the N fertilization rate (N0, N160). The arrows indicate the developmental stages BBCH65, BBCH69, BBCH79, BBCH89, respectively. For the ANOVA * indicate significant differences at p <0.001. ns = non-significant. At the individual DAFF +, * indicate significant differences between the cultivars within the N fertilization rates at p <0.10, <0.05, respectively. The error bars (visible only when greater than the symbols) represent the standard deviations of the means (n = 3 to 4).**

Additionally and as a comprehensive parameter of leaf senescence the number of green leaves remaining on the main stem was continuously counted from full flowering (BBCH65) until near maturity (BBCH89). During reproductive growth the percentage of green leaves remaining on the main stem decreased substantially for all cultivars and N supplies (Figure IV-2). For the cvs. Apex and Capitol the decline was significantly faster at N0 than at high N supply (signficant N x DAFF interaction). In agreement with the SPAD values of leaf two, without N fertilization the number of green leaves was consistently higher for cv. NPZ-1 than for NPZ-2 from DAFF 10 on, although the difference was not significant at individual DAFF (Figure IV-2a). Also cv. Apex maintained a higher number of green leaves than cv. Capitol at N0 but not at N160, a difference which was significant between DAFF 25 and 45 (Figure IV-2b). Thus the stay-green phenotype of cvs. NPZ-1 and Apex could be confirmed under field conditions.

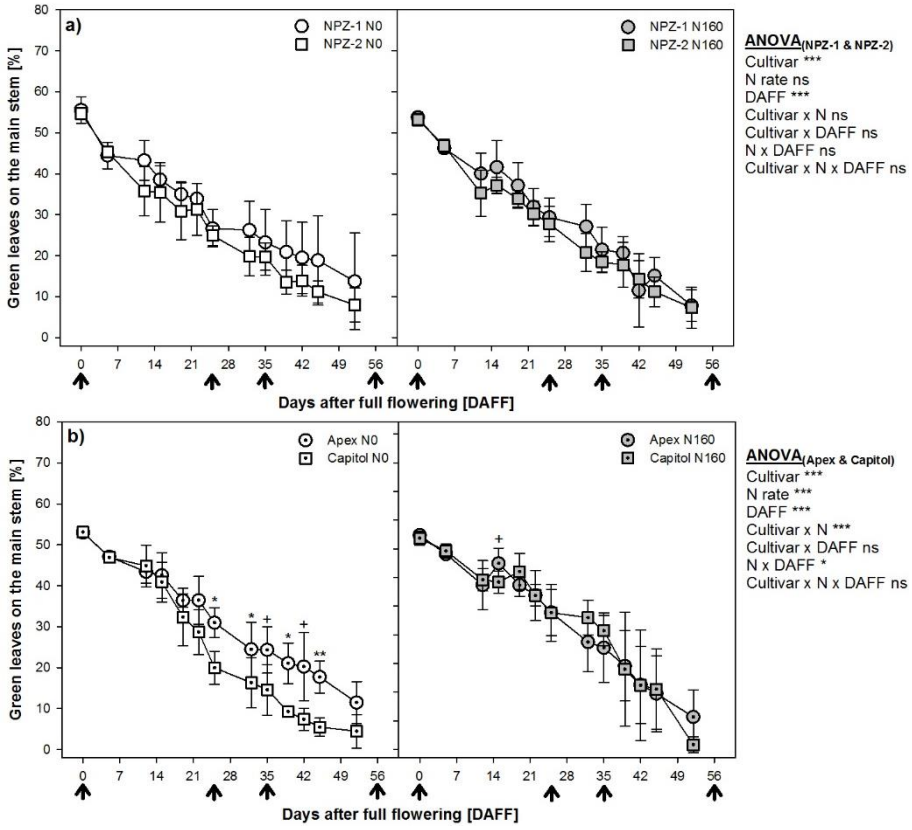

Figure IV-2 Remaining green leaves on the main stem of the winter oilseed-rape line-cultivars NPZ-1 and NPZ-2 (a) and Apex and Capitol (b) from full flowering (BBCH65) until near maturity (BBCH89) as affected by the N fertilization rate (N0, N160). The arrows indicate the developmental stages BBCH65, BBCH69, BBCH79, BBCH89, respectively. For the ANOVA * indicate significant differences at p <0.001. ns = non-significant. At the individual DAFF +, *, ** indicate significant differences between the cultivars within the N fertilization rates at p <0.10, <0.05, <0.01, respectively. The error bars (visible only when greater than the symbols) represent the standard deviations of the means (n = 3 to 4).**

Grain yield and straw dry matter

At maturity (BBCH89) grain yields of the cultivar pairs cvs. NPZ-1 and NPZ-2, and Apex and Capitol were significantly affected by the N fertilization rate (Figure IV-3a). Under high N fertilization all four

cultivars reached a similar grain yield (2.5 to 2.9 t ha^{-1}) and no significant differences occurred within the cultivar pairs (Figure IV-3a). Without N fertilization grain yields were substantially lower. But cv. NPZ-1 (1.3 t ha^{-1}) showed at least in tendency and cv. Apex (1.1 t ha^{-1}) significantly a higher grain yield compared to their respective counterparts cv. NPZ-2 (1.1 t ha^{-1}) and cv. Capitol (0.6 t ha^{-1}) (Figure IV-3a). The significant cultivar x N interaction for cvs. Apex and Capitol reflects the significantly higher but in tendency lower grain yield of cv. Apex under limited and sufficient N supply, respectively. Generally, the grain yields were low. This was mainly due to the low plant density, because the grain yields per plant under unlimited N supply were 8 to 10 g per plant for all cultivars which could have allowed grain yields of 5 to 6 t ha^{-1} at the target plant density of 60 plants m^{-2}. In conclusion, the previously reported or expected higher N-efficiency of cv. Apex and NPZ-1, respectively, compared to cvs. Capitol and NPZ-2 could be confirmed (in tendency for cvs. NPZ-1 and NPZ-2). For both cultivar pairs straw dry matter production (shoot + pod walls) at maturity (BBCH89) was significantly increased by N fertilization (Figure IV-3b). Under high N fertilization all four cultivars reached a similar straw dry weight (7.9 to 8.1 t ha^{-1}) and no significant differences occurred within the cultivar pairs. Also under N limitation the cvs. NPZ-1 and NPZ-2 did not differ in straw yield. However, the N-efficient cv. Apex (5.3 t ha^{-1}) reached a significantly higher straw dry weight compared to the N-inefficient cv. Capitol (4.4 t ha^{-1}) explaining the significant cultivar x N interaction.

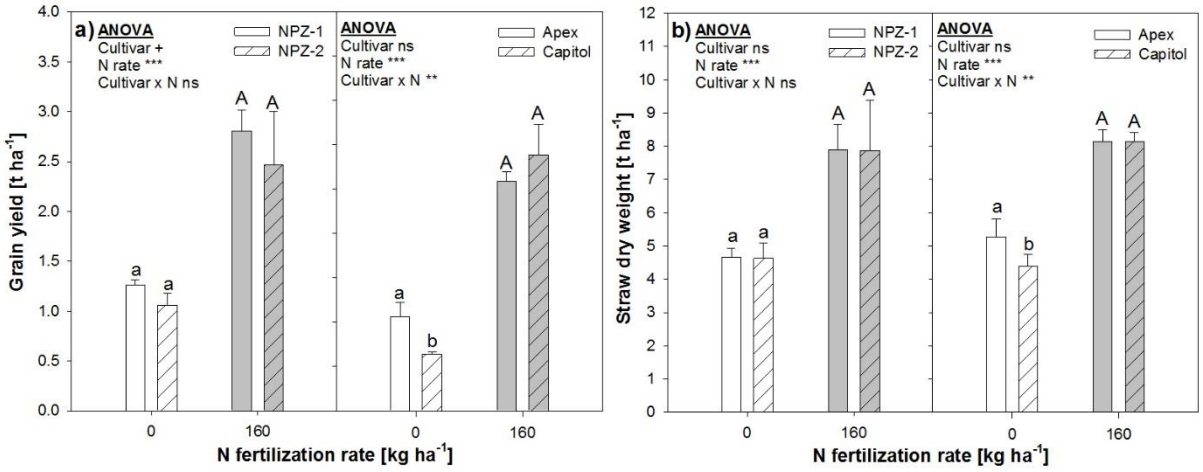

Figure IV-3 Grain yield (a) and straw dry weight (b) at maturity (BBCH89) of the winter oilseed-rape line-cultivars NPZ-1 and NPZ-2 (left) and Apex and Capitol (right) as affected by the N fertilization rate (N0, N160). Different lower case and upper case letters on the top of the columns indicate differences between the cultivars within the N fertilizer rates at p <0.05. For the ANOVA +, **, * indicate significant differences at p <0.10, 0.01, 0.001, respectively. ns = non-significant. The error bars represent the standard deviations of the means (n = 3 to 4).**

Harvest Index

The separate determination of straw and grain dry weights allowed the calculation of the biomass-distribution efficiency for grain-yield formation, for which the harvest index (HI) is a measure. In general N fertilization significantly increased the HI at maturity (BBCH89) (Figure IV-4). Under high N

fertilization the HI of the four cultivars was similar and did not differ between cultivars (Figure IV-4). Under N limitation the HI of cv. NPZ-1 was at least in tendency and the HI of cv. Apex was significantly higher compared to their respective counterparts cv. NPZ-2 and cv. Capitol. The significant cultivar x N interaction for cvs. Apex and Capitol is based on the higher HI of cv. Apex under N limitation.

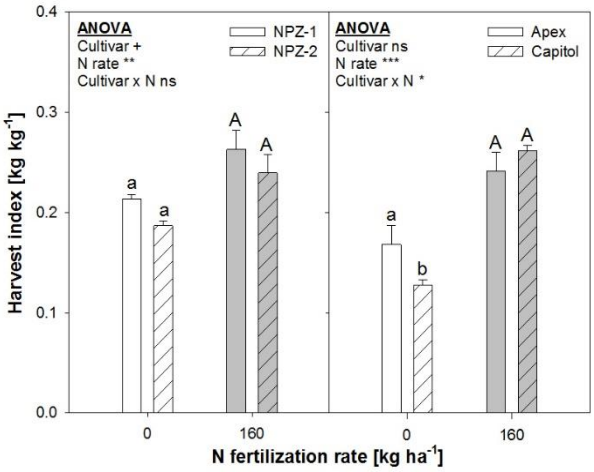

Figure IV-4 Harvest index at maturity (BBCH89) of the winter oilseed-rape line-cultivars NPZ-1 and NPZ-2 (left) and Apex and Capitol (right) as affected by the N fertilization rate (N0 and N160). Different lower case and upper case letters on top of the columns indicate differences between the cultivars within the N fertilizer rates at p <0.05. For the ANOVA +, *, **, * indicate significant differences at p <0.10, <0.05, <0.01, <0.001, respectively. ns = non-significant. The error bars represent the standard deviations of the means (n = 3 to 4).**

Shoot nitrogen uptake

At high N fertilization rate (N160) N uptake by shoots reached 96 to 148 kg N ha^{-1} at full flowering (BBCH65) and increased up to DAFF 42 to 131 to 177 kg N ha^{-1} (Figure IV-5). At limiting N supply (N0) the N uptake until full flowering was about two times lower (42 to 51 kg N ha^{-1}) and increased only until DAFF 28 to 58 to 79 kg N ha^{-1}. The cvs. NPZ-1 and NPZ-2 did not differ in their N uptake pattern neither at high nor at limiting N supply. However, at N0 cv. Capitol showed a consistent and mostly significantly lower N uptake from DAFF 14 until maturity than cv. Apex. Whereas the magnitude of post-full-flowering N uptake at N0 did not differ between cvs. NPZ-1 (21 kg N ha^{-1}) and NPZ-2 (26 kg N ha^{-1}), the N-efficient cv. Apex (31 kg N ha^{-1}) showed significantly higher post-full-flowering N uptake than the N-inefficient cv. Capitol (10 kg N ha^{-1}).

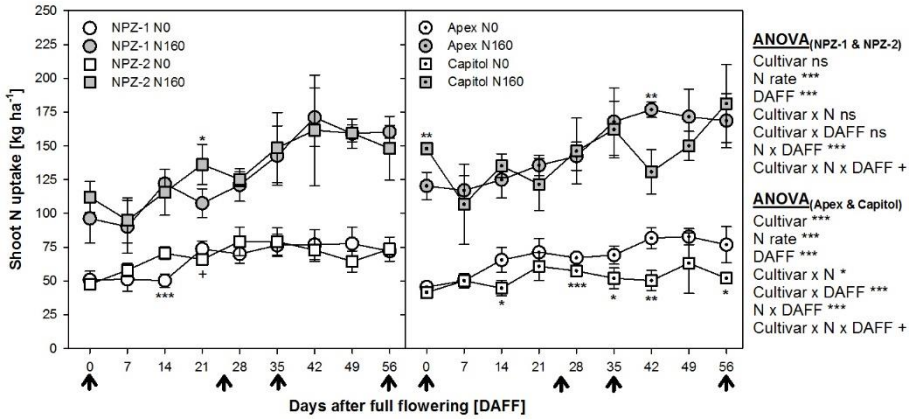

Figure IV-5 Shoot N uptake from full flowering (BBCH65) until maturity (BBCH89) of the winter oilseed-rape line-cultivars NPZ-1 and NPZ-2 (left) and Apex and Capitol (right) as affected by N fertilization rate (N0, N160). The arrows indicate the developmental stages BBCH65, BBCH69, BBCH79, BBCH89, respectively. For the ANOVA +, *, * indicate significant differences at p <0.10, 0.05, 0.001, respectively. ns = non-significant. At the individual DAFF +, *, **, *** indicate significant differences between the cultivars within the N fertilization rates at p <0.10, 0.05, 0.01, 0.001, respectively. The error bars (visible only when greater than the symbols) represent the standard deviations of the means (n = 3 to 4).**

Nitrogen accumulation in pods from flowering until maturity

After transition to the reproductive phase the developing pods are the main accumulation sites for N. From full flowering (BCCH65) until maturity (BBCH89) N contents in the pods increased under both N supplies with a significantly higher increase under high N fertilization rate (Figure IV-6). Under high N fertilization the accumulation generally continued up to about DAFF 42. Without N fertilization N accumulation continued only up to about DAFF 28, with the exception of cv. Apex. The pod N content of cv. Apex increased until about DAFF 42 and thus significantly longer compared to cv. Capitol (highly significant Cultivar x N x DAFF interaction). The cvs. NPZ-1 and NPZ-2 did not significantly differ at neither of the N fertilization rates. However, the N accumulation in the pods was significantly higher in the N-efficient cv. Apex compared to its N-inefficient counterpart cv. Capitol at limiting but not at high N supply (significant Cultivar x N x DAFF interaction).

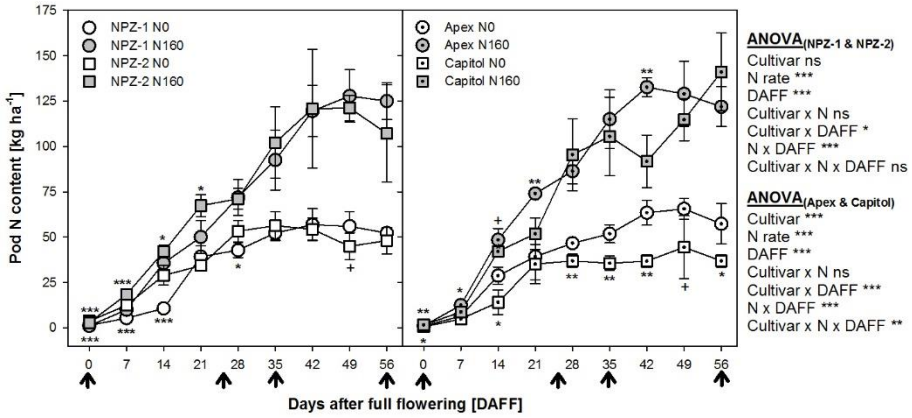

Figure IV-6 Nitrogen accumulation in the pods from flowering (BBCH65) until maturity (BBCH89) of the winter oilseed-rape line-cultivars NPZ-1 and NPZ-2 (left) and Apex and Capitol (right) as affected by the N fertilization rate (N0, N160). The arrows indicate the developmental stages BBCH65, BBCH69, BBCH79, BBCH89, respectively. For the ANOVA *, **, * indicate significant differences at p <0.05, <0.01, <0.001, respectively. ns = non-significant. At the individual DAFF +, *, **, *** indicate significant differences between the cultivars within the N fertilization rates at p <0.10, <0.05, <0.01, <0.001, respectively. The error bars (visible only when greater than the symbols) indicate the standard deviations of the means (n = 3 to 4).**

The separation of the pods into pod walls and grains from BBCH79, when all pods had reached the cultivar-specific size, until maturity (BBCH89) revealed that N accumulation in the grains continued up to DAFF 49 generally independently of cultivar and N fertilization rate, but at a much higher rate at high compared to limited N supply (Figure IV-7a). Only cv. Capitol continued to accumulate N in the grains until maturity at N160. In agreement with the lower grain yield at N0 (Figure IV-3a) the N-inefficient cv. Capitol accumulated significantly less N in the grains than the N-efficient cv. Apex. The increase in N contents of the grains during reproductive growth were exclusively due to the increase in grain mass since the grain-N concentrations did not change (Figure IV-7b). Only for the cvs. NPZ-2 and particularly NPZ-1 the high N supply lead to higher grain-N concentrations (highly significant N rate effect and significant cultivar x N interaction). The cvs. Apex and Capitol did not respond to the N fertilization rate and did not differ in grain-N concentrations.

During the same period (DAFF 35 to 49) in which the N contents in the grains increased the N contents of the pod walls decreased, except for cvs. Apex and Capitol at N0 (compare Figure IV-7a and IV-7c) for which the pod N contents did not markedly change. Only in cvs. NPZ-1 and NPZ-2 at high N supply the pod-wall N-content increased up to 42 DAFF. The increase in N accumulation in the grains and the decrease of the N content of the pod walls was particularly marked at high N fertilization rate. However, at high N supply the amount of N remaining in the pod walls at maturity (DAFF 56) was significantly higher (29 to 44 kg N ha^{-1}) compared to N0 (14 to 24 kg N ha^{-1}) with no significant differences between the cultivar pairs. The N concentration of the pod wall was generally about two times lower than in the grains (compare Figures IV-7b and IV-7d). They were significantly higher at the high N fertilization rate for all cultivars except cv. NPZ-2 which had lower pod-wall N-concentrations than cv. NPZ-1 at high but not at low N supply (significant cultivar x N interaction).

The decline in pod-wall N-contents generally and particularly at N160 and of cvs. NPZ-1 and NPZ-2 at N0 was based on decreased pod-wall N-concentrations. Although the N concentrations of the pod wall of the cvs. Apex and Capitol as well decreased from DAFF 35 until maturity (DAFF 56) at N0, pod-wall N-contents did not markedly change.

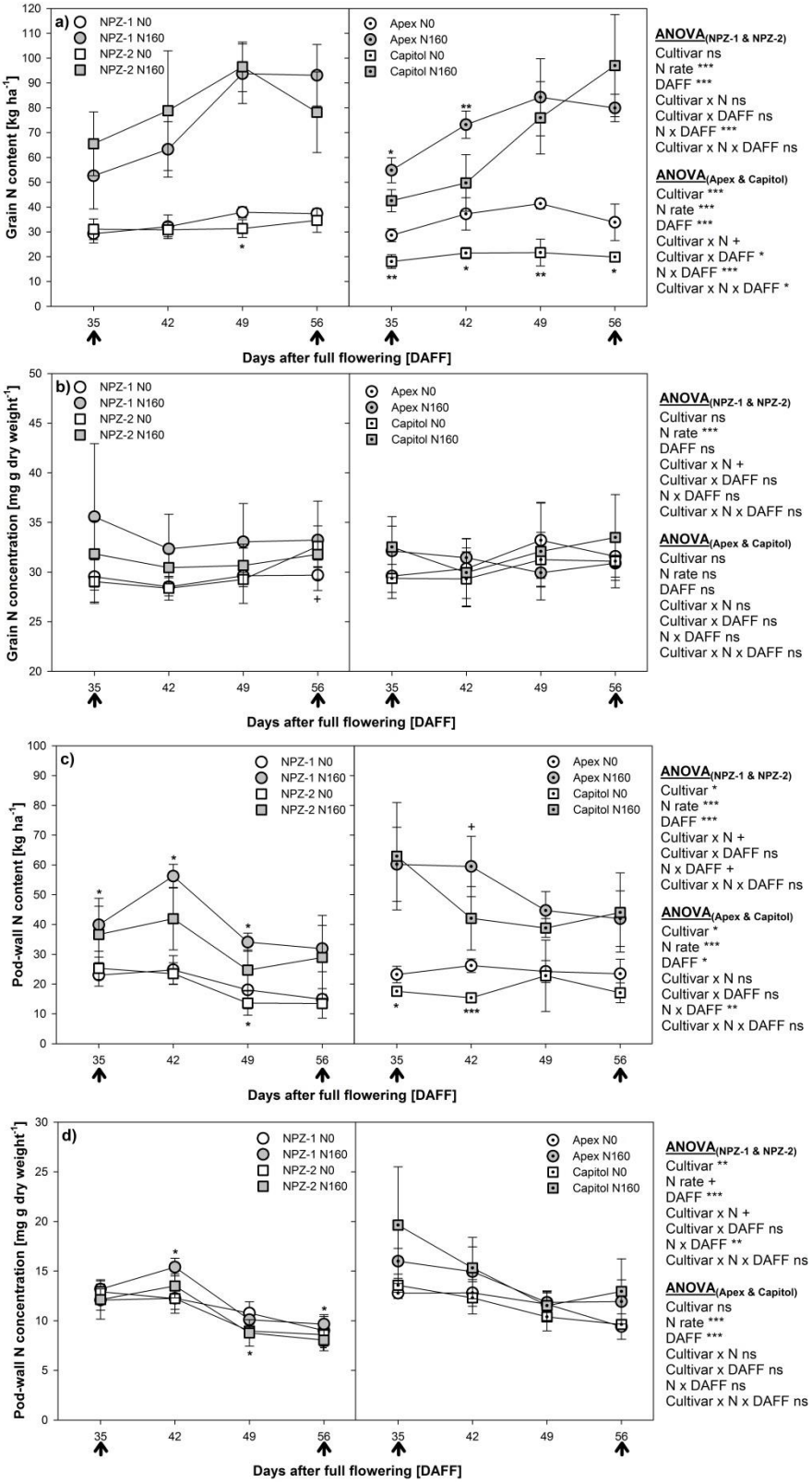

Figure IV-7 Nitrogen contents and concentrations of the grain (a, b) and pod wall (c, d) from BBCH79 (all pods have reached the cultivar-specific size) until maturity (BBCH89) of the winter oilseed-rape line-cultivars NPZ-1 and NPZ-2 (left) and Apex and Capitol (right) as affected by the N fertilization rate (N0, N160). The arrows indicate the developmental stages BBCH79 and BBCH89. For the ANOVA +, *, * indicate significant differences at p <0.10, <0.05, <0.001, respectively. ns = non-significant. At the individual DAFF +, *, ** indicate significant differences between the cultivars within the N fertilization rates at p <0.10, <0.05, <0.01, respectively. The error bars (visible only when greater than the symbols) indicate the standard deviations of the means (n = 3 to 4).**

Apparent N uptake and retranslocation to the pods

The increase in pod N content is based on two processes: N uptake during reproductive growth and direct transport to the pods, and retranslocation from vegetative plant organs of N taken up during vegetative growth. Remobilization of N in vegetative plant organs (roots, stems, leaves) for transport to the pods can be quantified through the decrease in N contents of these organs. In the taproot the N contents were significantly affected by the level of N fertilization and higher at N160 compared to N0 (Figure IV-8a). The taproot-N content decreased only slightly but significantly from full flowering until maturity mainly at high N fertilization rate for cvs. Apex and Capitol (significant N x DAFF interaction). At high N supply the late senescing cvs. NPZ-1 and Apex generally had higher taproot N contents particularly at N160. The decrease in N contents after full flowering of the taproots and the differences between the N fertilization rates can be mostly explained by the differences in taproot-N concentrations (Figure IV-8b). However, the mostly higher N contents of the taproots of the late senescing cvs. NPZ-1 and Apex are not related to higher N concentrations but rather to a high taproot biomass.

In contrast to the taproot, the stem proved to be a major intermediate storage organ for N at high N fertilization rates (Figure IV-8c). After full flowering, this N pool was gradually depleted more rapidly at N0 compared to N160 (significant N x DAFF interaction). At maturity the amount of N remaining in the stems was clearly higher at high N supply. The decrease in N contents of the stems after full flowering and the differences between the N fertilization rates can be fully explained by the stem N concentrations (FigureIV-8d). Differences between the cultivars were negligible.

The amount of N in intact leaves at full flowering was lower than in stems (compare Figures IV-9a and IV-8a). As for stems the N contents of the intact leaves decreased more rapidly under high compared to limiting N supply for all cultivars (Figure IV-9a). However, the decline was less rapid and less complete in cv. Apex particularly at high N supply. The N amounts remaining in intact leaves reached much lower levels than in the stems. This can be attributed to the shedding of nearly all leaves until maturity which is supported by an increasing N content of shed leaves (Figure IV-9c). The higher N content of intact leaves at high N supply in cv. Apex can be explained by a delayed leaf shedding reflected by a slower increase in N content of shed leaves. At low N supply the cultivars did not or only slightly differ in N contents in stems and leaves. Among all vegetative plant organs the intact leaves had the highest N concentrations (Figure IV-9b) clearly higher at N160 compared to N0. With development the N concentrations decreased, but less than the N contents supporting the major role of leaf shedding for the decline in leaf N contents. Close to maturity the differences between the N fertilization rates disappeared and the N concentrations of the intact leaves even increased again which can be explained by the decreasing leaf age of the final remaining leaves on the inflorescences. Only the cvs. Apex and Capitol differed with generally slightly higher leaf-N concentrations of

cv. Capitol clearly suggesting that the higher N contents of cv. Apex were due to delayed leaf shedding. The N concentrations in the shed leaves decreased up to maturity to very low values in N-deficient but less in N-sufficient plants (highly significant N x DAFF interaction). Only the cvs. Apex and Capitol differed significantly but quantitatively insignificantly.

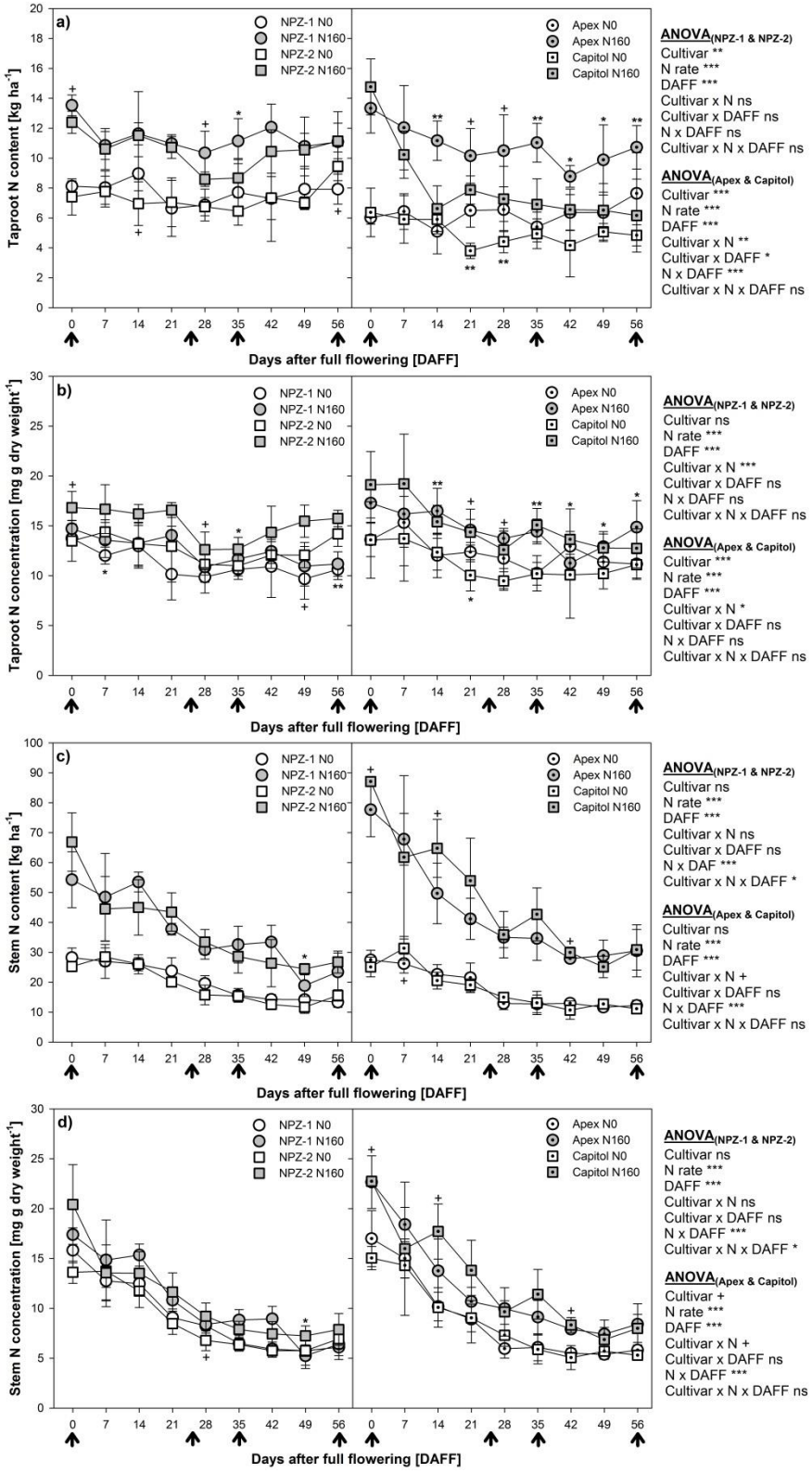

Figure IV-8 Nitrogen contents and concentrations of the taproot (a, b) and the stem (c, d) from full flowering (BBCH65) until maturity (BBCH89) of the winter oilseed-rape line-cultivars NPZ-1 and NPZ-2 (left) and Apex and Capitol (right) as affected by the N fertilization rate (N0, N160). The arrows indicate the developmental stages BBCH65, BBCH69, BBCH79, BBCH89, respectively. For the ANOVA +, *, **, * indicate significant differences at p <0.10, <0.05, <0.01, <0.001, respectively. ns = non-significant. At the individual DAFF +, *, ** indicate significant differences between the cultivars within the N fertilization rates at p <0.10, <0.05, <0.01, respectively. The error bars (visible only when greater than the symbols) indicate the standard deviations of the means (n = 3 to 4).**

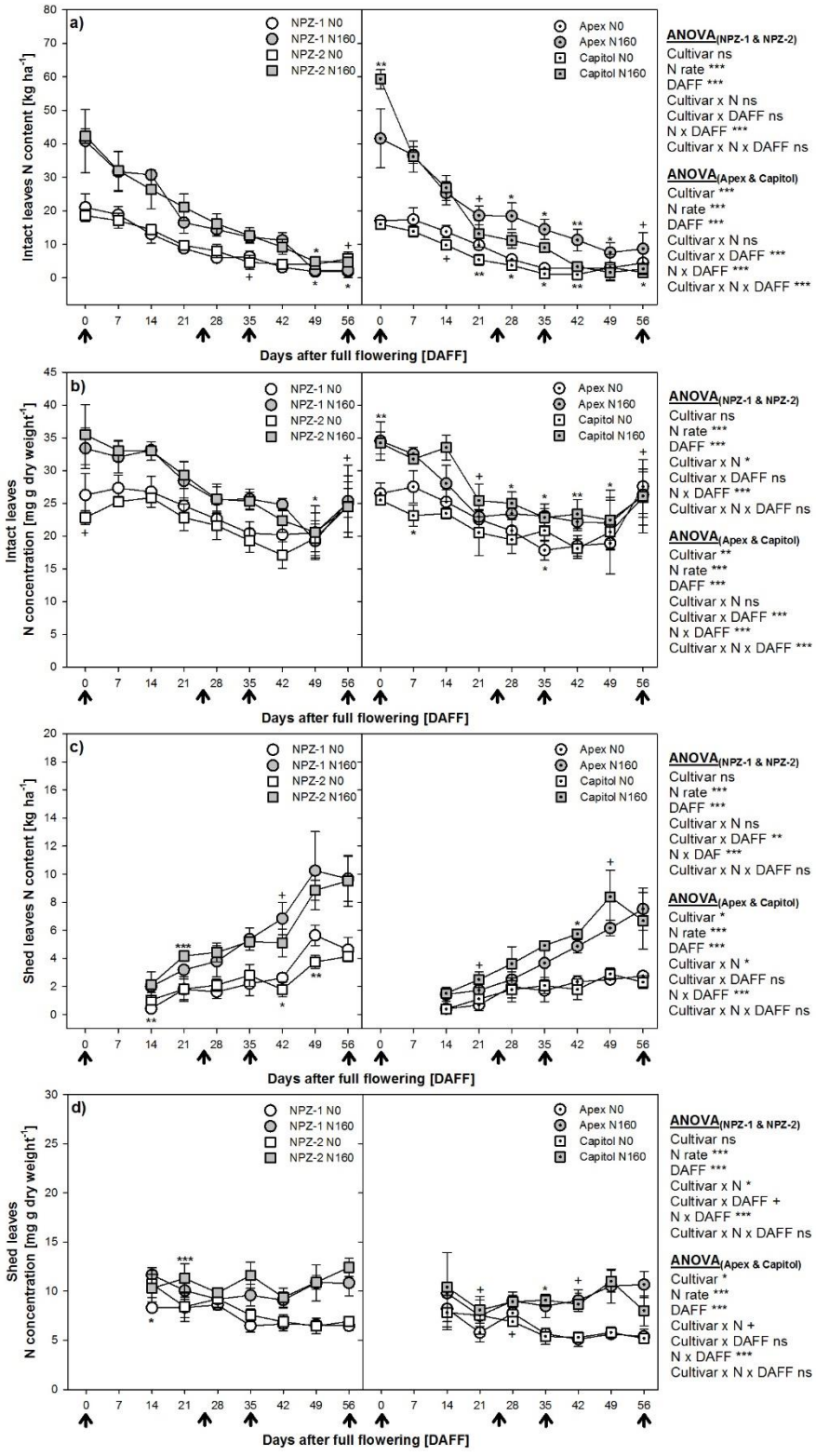

Figure IV-9 Nitrogen contents and concentrations of the intact (a, b) and the shed leaves (c, d) from full flowering (BBCH65) until maturity (BBCH89) of the oilseed-rape line-cultivars NPZ-1 and NPZ-2 (left) and Apex and Capitol (right) as affected by the N fertilization rate (N0, N160). The arrows indicate the developmental stages BBCH65, BBCH69, BBCH79, BBCH89, respectively. For the ANOVA *, **, * indicate significant differences at p <0.05, <0.01, <0.001, respectively. ns = non-significant. At the individual DAFF +, *, **, *** indicate significant differences between the cultivars within the N fertilization rates at p <0.10, <0.05, <0.01, <0.001, respectively. The error bars (visible only when greater than the symbols) indicate the standard deviations of the means (n = 3 to 4).**

The apparent direct N uptake by the pods was compared with the N retranslocation from vegetative plant organs to the pods from full flowering (BBCH65) to maturity (BBCH89) (Table IV-1). Under N-limiting conditions (N0) the apparent N retranslocation to the pods of the N-efficient cv. NPZ-1 (30 kg N ha^{-1}) compared to its N-inefficient counterpart cv. NPZ-2 (16 kg N ha^{-1}) was around two times higher, but this difference was not significant owing to the high variation. The cvs. Apex and Capitol showed a similar apparent N retranslocation to the pods. N fertilization (N 160) significantly increased the apparent N retranslocation to the pods in all four cultivars and ranged between 62 to 115 kg N ha^{-1}. The apparent N retranslocation to the pods of cv. Capitol (115 kg N ha^{-1}) was significantly higher than of cv. Apex (75 kg N ha^{-1}).

The apparent direct N uptake by the pods was calculated as the difference between the pod N content and the apparent N retranslocation. The overall statistical analysis revealed that apparent N uptake was not or only little ($p < 0.10$) affected by the level of N fertilization. At maturity at N0 the N-efficient cv. Apex (34 kg N ha^{-1}) showed a nearly four-times higher apparent N uptake compared to its N-inefficient counterpart cv. Capitol (9 kg N ha^{-1}). But due to the high variation the difference in apparent N uptake between the cvs. Apex and Capitol was only significant at $p < 0.10$. The cvs. NPZ-1 and NPZ-2 did not differ in apparent N uptake at N0 as well as at N160, but without N fertilization the contribution of apparent N uptake to pod N was in tendency higher for cv. NPZ-2.

Table IV-1 Apparent N retranslocation and apparent N uptake directly allocated to the pods from full flowering (BBCH 65) to maturity (BBCH89) of the winter oilseed-rape line-cultivars NPZ-1 and NPZ-2 and Apex and Capitol as affected by the N fertilization rate (N0, N160). For the ANOVA +, *, **, * indicate significant differences at p <0.10, <0.05, <0.01, <0.001, respectively. ns = non-significant. Different lower case and upper case letters indicate significant cultivar differences within the cultivar pair at N0 and N160 at p <0.05. SD = Standard deviations of the means (n = 3 to 4).**

Cultivar	Apparent N retranslocation Mean	SD		Apparent N uptake Mean	SD	
	[kg ha^{-1}]			[kg ha^{-1}]		
N0						
NPZ-1	30	± 8	a	23	± 10	a
NPZ-2	16	± 2	a	32	± 9	a
N160						
NPZ-1	62	± 22	A	63	± 24	A
NPZ-2	69	± 11	A	38	± 33	A
ANOVA						
Cultivar	ns			ns		
N rate	***			+		
Cultivar x N	ns			ns		

Cultivar	Apparent N retranslocation Mean	SD		Apparent N uptake Mean	SD	
	[kg ha^{-1}]			[kg ha^{-1}]		
N0						
Apex	23.0	± 8	a	34	± 19	a
Capitol	28.0	± 1	a	9	± 3	a
N160						
Apex	75.0	± 20	B	47	± 25	A
Capitol	115.0	± 9	A	26	± 29	A
ANOVA						
Cultivar	**			+		
N rate	***			ns		
Cultivar x N	*			ns		

Nitrogen utilization efficiency and N harvest index

The N utilization efficiency (NUE) reflects the efficiency with which N is utilized to produce yield. For the four cultivars the NUE ranged from 30 to 34 kg kg^{-1} without significant cultivar and N application effects (Figure IV-10a).

The nitrogen harvest index (NHI) is a measure for the efficiency of the allocation of N to the grains (uptake and retranslocation). The high N fertilization rate (N160) generally increased NHI in all four cultivars (Figure IV-10b). Whereas cv. NPZ-1 had a higher NHI than cv. NPZ-2 at both N fertilizer levels, cv. Apex showed a higher NHI than cv. Capitol at N0 but a lower NHI at N160 (significant cultivar x N interaction).

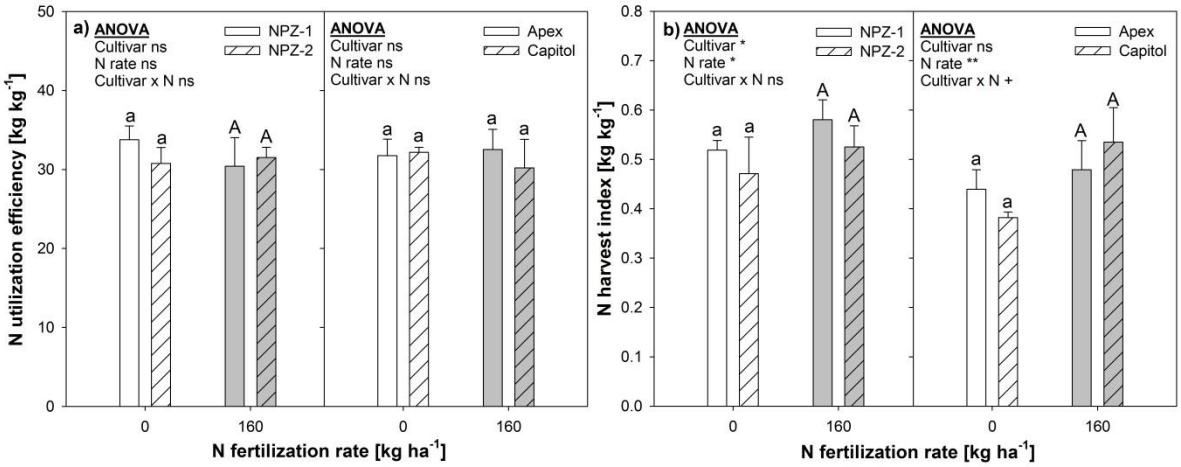

Figure IV-10 Nitrogen utilization efficiency (a) and N harvest index (b) at maturity (BBCH89) of the winter oilseed-rape line-cultivars NPZ-1 and NPZ-1 (right) and Apex and Capitol (left) as affected by the N fertilization rate (N0, N160). Different lower case and upper case letters on the top of the columns indicate differences between the cultivars within the N fertilizer rates at p <0.05. For the ANOVA +, *, ** indicate significant differences at p <0.10, <0.05, <0.01, respectively. ns = non-significant. The error bars represent the standard deviations of the means (n = 3 to 4).

Nitrogen remaining in crop residues

At maturity (BBCH89) under both N supplies only approximately 50% of the total N in the above-ground plant-parts was removed from the field with the grains (Table IV-2). The remaining N in the crop residues of the four cultivars ranged between 37 to 52 kg N ha^{-1} without N fertilization and was about two times higher at high N fertilization rate (78 to 101 kg N ha^{-1}). The main sources for the remaining N in the crop residues were the pod walls and the stems independent of the N fertilization rate and accounted for 60 to 70% (N0) and 69 to 80% (N160) of the crop-residue N. The N remaining in the taproot was the next important crop-residue N source particularly under N deficiency (N0). The quantitative contribution of N in intact and shed leaves was low.

Table IV-2 Amount of N removed from the field and remaining in the crop residues at maturity (BBCH89) of the winter oilseed-rape line-cultivars NPZ-1 and NPZ-2 and Apex and Capitol as affected by the N fertilization rate (N0, N160).

	N0				N160			
	[kg ha^{-1}]							
	NPZ-1	NPZ-2	Apex	Capitol	NPZ-1	NPZ-2	Apex	Capitol
N removal								
Grain	37	35	34	20	93	78	80	97
N in crop residues								
Pod wall	15	14	24	17	32	29	42	44
Stem	13	16	12	11	23	27	31	31
Taproot	8	10	8	5	11	11	11	6
Intact leaves	2	6	5	2	2	5	9	3
Shed leaves	5	4	3	2	10	10	8	7
Total	43	50	52	37	78	82	101	91

Grain quality

The thousand grain weight (TGW) at maturity (BBCH89) of cvs. NPZ-1 and NPZ-2 was generally higher than of the cvs. Apex and Capitol (Figure IV-11). High N supply significantly reduced the TGW in all cultivars. Whereas cvs. NPZ-1 and NPZ-2 did not differ much in TGW independent of the N fertilization level, cv. Capitol had a significantly higher TGW compared to cv. Apex at both N fertilizer rates.

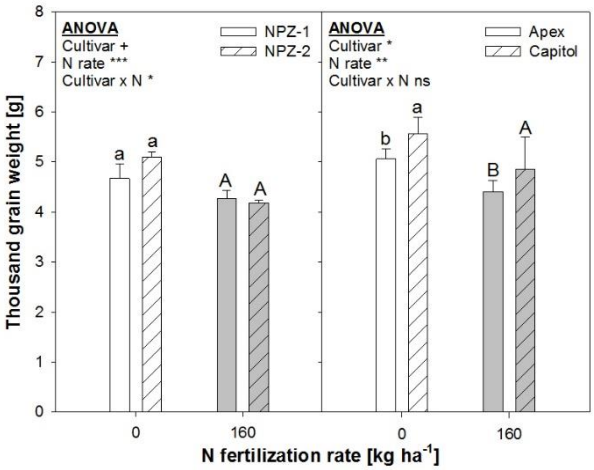

Figure IV-11 Thousand grain weight at maturity (BBCH89) of the winter oilseed-rape line-cultivars NPZ-1 and NPZ-2 (left) and Apex and Capitol (right) as affected by N the fertilization rate (N0, N160). Different lower case and upper case letters on the top of the columns indicate differences between the cultivars within the N fertilizer rates at p <0.05. For the ANOVA +, *, **, * indicate significant differences at p <0.10, <0.05, <0.01, <0.001, respectively. ns = non-significant. The error bars represent the standard deviations of the means (n = 3 to 4).**

Winter oilseed-rape grains are mainly harvested for oil production; hence the oil concentration is not only the most important quality criterion but also the most important economic factor. At maturity (BBCH89) the oil concentrations in the grains (44.5 to 47.2% dry weight) were not affected by the N fertilization rate in none of the cultivars (Figure IV-12). Significant cultivar differences occurred only under optimal N conditions between cvs. Apex and Capitol.

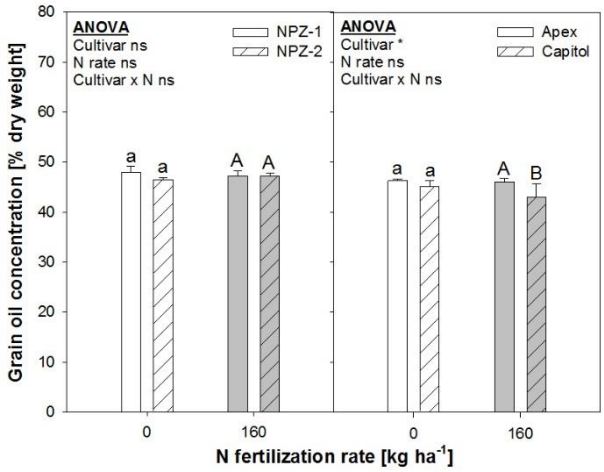

Figure IV-12 Grain oil concentration at maturity (BBCH89) of the winter oilseed-rape line-cultivars NPZ-1 and NPZ-2 (left) and Apex and Capitol (right) as affected by the N fertilization rate (N0, N160). Different lower case and upper case letters on the top of the columns indicate differences between the cultivars within the N fertilizer rates at p <0.05. For the ANOVA * indicate significant differences at p <0.05. ns = non-significant. The error bars represent the standard deviations of the means (n = 3 to 4).

The remaining rapeseed-cake is a valuable animal feed. Thus the protein concentration is an important quality criterion, too. At maturity (BBCH89) the protein concentration of the grains ranged from 19.0 to 23.2% dry weight (Figure IV-13a) and was approximately two times lower than the grain-meal protein concentration (35.9 to 40.8% dry weight; Figure IV-13b). Both grain and grain-meal protein-concentrations were not affected by the N fertilization rate in none of the cultivars. But grain and grain-meal protein concentrations were consistently higher in cv. Capitol than in cv. Apex, whereas no cultivar differences existed between cvs. NPZ-1 and NPZ-2.

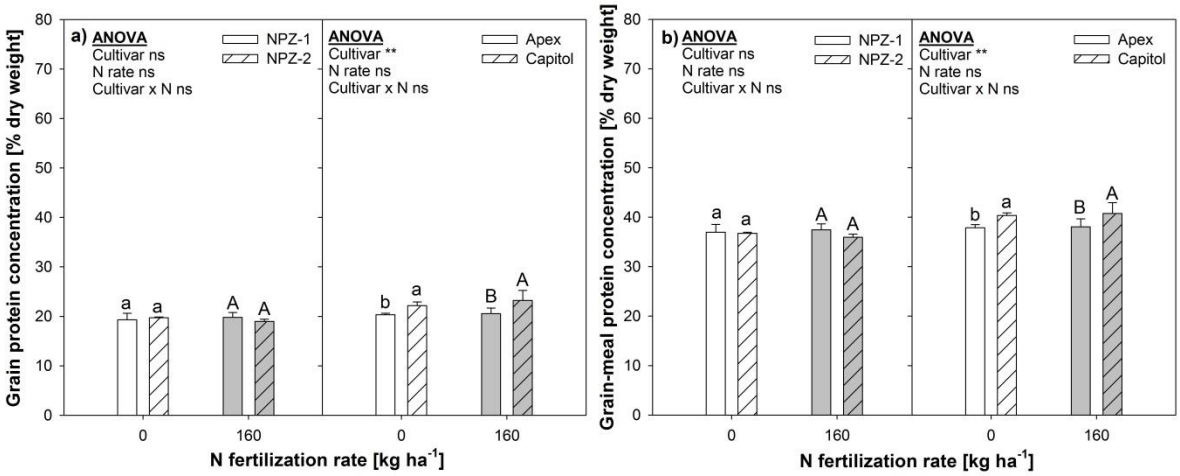

Figure IV-13 Grain protein concentration (a) and grain-meal protein concentration (b) at maturity (BBCH89) of the winter oilseed-rape line-cultivars NPZ-1 and NPZ-2 (left) and Apex and Capitol (right) as affected by the N fertilization rate (N0, N160). Different lower case and upper case letters on the top of the columns indicate differences between the cultivars within the N fertilizer rates at p <0.05. For the ANOVA ** indicate significant differences at p <0.01. ns = non-significant. The error bars represent the standard deviations of the means (n = 3 to 4).

Discussion

Under favorable environmental conditions winter oilseed-rape line-cultivars usually achieve a grain yield between 4 and 5 t ha^{-1} (Ulas *et al.,* 2013; Koeslin-Findeklee *et al.,* 2014). In the present field experiment N fertilization significantly increased grain yield formation. (Figure IV-3a). But even under sufficient N supply (N160) a grain yield of 2.7 t ha^{-1} on average was still low (Figure IV-3a). For grain yield formation the most important yield component in winter oilseed-rape is the number of pods per area, which is a combination of number of plants per area and number of pods per plant (Diepenbrock & Grosse, 1995). The canopy density in spring was reduced by about 50% to about 30 plants per m^{-2}. This was most likely due to the hard frosts during winter (not shown). But winter oilseed-rape canopies with 20 to 30 plants m^{-2} can achieve comparable grain yields to canopies with 70 to 80 plants m^{-2} (Mendham *et al.,* 1981b). In winter oilseed-rape for yield stability the high compensation capacity for lower plant density by branching is of major importance (Leach *et al.,* 1999). But for the exploitation of the yield potential the plant development before winter is decisive (Sierts *et al.,* 1987; Boelcke *et al.,* 1991). The yield potential and winter hardiness of an individual plant depends on biomass formation during autumn. Both are decisively affected by the time of sowing (Mendham & Scott, 1975; Stoy, 1982). Late sowing in September often results in lower and more variable grain yields (Scott *et al.,* 1973; Mendham *et al.,* 1981a, b; Bolecke *et al.,* 1991). Thus the late sowing date in September most likely led to an inferior plant growth before winter, which resulted in low grain yields, because of the high plant losses occurred during winter in combination with the low yield potential of the remaining plants.

Without N fertilization (N0) the N deficiency stress was severe with 60% yield reduction across the four cultivars (Figure IV-3a). Under N-limiting conditions (N0) cultivar differences in grain yield formation and thus N efficiency occurred (Figure IV-3a). Nitrogen efficiency was defined according to Graham (1984) and Sattelmacher *et al.* (1994) as the ability of a cultivar/genotype to produce a high grain yield under conditions of limited N supply. Without N fertilization (N0) the cvs. NPZ-1 and Apex either tendencially or significantly produced a higher grain yield compared to the respective counterparts cv. NPZ-2 and cv. Capitol (Figure IV-3a). Thus, the expected cultivar differences in N efficiency for the cvs. NPZ-1 (N-efficient) and NPZ-2 (N-inefficient) and the reported cultivar differences in N efficiency for the cvs. Apex (N-efficient) and Capitol (N-inefficient) (Kamh *et al.,* 2005; Schulte auf'm Erley *et al.,* 2007) could be confirmed. The either tendencially or significantly higher harvest index (HI) of the N-efficient cultivars compared to the respective N-inefficient counterparts revealed that genetic variation in N efficiency was at least partially based on a higher biomass allocation efficiency to the grains (Figure IV-4). However, N efficiency of winter oilseed-rape line-cultivars has been primarily attributed to high N uptake efficiency (NUPT), which mainly results from maintained N uptake during reproductive growth (Berry *et al.,* 2010;

Schulte auf'm Erley *et al.*, 2011; Ulas *et al.,* 2012). Under N-limiting conditions (N0) the N-efficient cultivars showed a tendencially or significantly higher NUPT than the respective N-inefficient counterparts (Figure IV-5). The significantly higher NUPT of cv. Apex was based on a prolonged post-full-flowering N uptake until the early phase of grain maturation (DAFF 42) (Figure IV-5). Nitrogen uptake after entering the reproductive phase is regulated by the sink size (Mi *et al.,* 2000) and maintenance of assimilate allocation to the roots (Imsande & Touraine, 1994). In winter oilseed-rape a characteristic of N-efficient line cultivars with high NUPT during reproductive growth is a functional stay-green phenotype, expressed as delayed senescence of the older leaves and accompanied by maintenance of the photosynthetic capacity (Schulte auf'm Erley *et al.,* 2007). Thus it is assumed that maintained photosynthetic capacity particularly of lower leaves through delayed leaf senescence will not only result in a better assimilate supply to the pods but also to the root and consequently enhanced N uptake (Osaki, 1995; Mi *et al.,* 2003). In the present field experiment N limitation (N0) prematurely induced senescence of individual leaves on the main stem (Figures IV-1, IV-S1, IV-S2) as well as on the whole plant level (Figure IV-2). But, particularly under N-limiting conditions (N0) the N-efficient cvs. NPZ-1 and Apex showed a delayed senescence-course of the older leaves compared to their respective N-inefficient counterparts cvs. NPZ-2 and Capitol. The functional stay-green phenotype may also be an explanation for the higher HI of the N-efficient cultivars (Figure IV-4).

The second pillar of N efficiency is N utilization efficiency (NUE) (Sattelmacher *et al.,* 1994). Berry *et al.* (2010) and Schulte auf'm Erley *et al.* (2011) reported that under severe N limitation NUE played a minor role for N efficiency. Under N-limiting conditions (N0) no significant cultivar differences in NUE occurred between the N-efficient cultivars and the respective N-inefficient counterparts. Nevertheless NUE of cv. NPZ-1 was in tendency higher compared to cv. NPZ-2 without N fertilization (N0). Thus NUE may have contributed to the higher N efficiency of cv. NPZ-1 (Figure IV-10a). However, with increasing N supply NUE became equally or even more important for grain yield formation than NUPT (Schulte auf'm Erley *et al.,* 2011; Koeslin-Findeklee *et al.,* 2014). But in the present study, most likely owing to the low yield potential, NUE was similar for both N supplies (N0, N160) for both cultivar pairs (Figure IV-10a). Physiological traits which may contribute to NUE are a low grain N concentration and an efficient allocation of N to the grains. Under N-limiting conditions (N0) the grain N concentration of cv. NPZ-1 was lower compared to the respective counterpart cv. NPZ-2. But the difference was of low significance ($p < 0.10$) (Figure IV-7a). The grain protein and grain-meal protein concentrations of the N-efficient cv. Apex were significantly lower than of the respective N-inefficient counterpart cv. Capitol independent of the N supply (N0, N160). Lower protein concentrations of grains contributing to N efficiency, however, is equivocal from the grain quality and crop N-balance point of view. Although winter oilseed-rape is an oil crop and the oil yield is the most important economic parameter (Funk & Mohr, 2010), the remaining oilseed meal is

a valuable animal feedstuff and protein source (Wittkop *et al.,* 2009). Also, a lower grain N concentration might leave higher N amounts in crop residues contributing to high N balance-surpluses. Therefore, a high N retranslocation for which the N harvest index (NHI) is an overall indicator is of greater importance as component of NUE. The NHI was 0.45 and 0.53 for limited (N0) and sufficient N supply (N160), respectively (Figure IV-10b) and thus in the range as reported by Aufhammer *et al.* (1994). But depending on environment and agronomic practices the allocation to the grains can be highly efficient and reach a NHI of up to 0.83 (Ulas *et al.,* 2013). Thus, although under N limitation (N0) the N-efficient cultivars showed at least in tendency a higher NHI compared to the respective N-inefficient counterparts higher N allocation efficiency did not contribute to the higher N utilization efficiency. But the shoot N uptake at maturity was either in tendency or significantly higher in the N-efficient cultivars compared to the respective counterparts (Figure IV-5). Thus a similar NHI led to an either by trend or significantly higher grain N content (Figure IV-7a) in the N-efficient cultivars than in the respective N-inefficient counterparts.

Particularly under N-limiting conditions (N0) high pod N contents were related to high grain yields (compare Figures IV-3a and IV-6). The final pod N content is primarily based on the duration of N accumulation. Nitrogen uptake during reproductive growth directly contributes to pod N accumulation (Malagoli *et al.,* 2005). The continued N accumulation of N-efficient cv. Apex led to a significantly higher pod N content compared to the respective N-inefficient counterpart cv. Capitol (Figure IV-6). Accordingly, the pod-N increase closely coincided with the duration of shoot N uptake during reproductive growth (compare Figures IV-6 and IV-5). The calculation of the apparent N uptake for pod N accumulation across the four cultivars revealed that the pod N apparently originating from N uptake after full flowering was greater under N limitation (N0, 48%) than at high N fertilization (N160, 36%) (Table IV-1). Under N limiting conditions (N0) post-full-flowering N uptake contributing to pod N content was greater, at least in tendency, for the N-efficient cv. Apex compared to the respective N-inefficient counterpart cv. Capitol (Table IV-1).

In general the N uptake after full flowering is not sufficient to meet the N demand of the pods. In winter oilseed-rape around 70% of pod N derives from N remobilization primarily from leaves and stems (Malagoli *et al.,* 2005; Gombert *et al.,* 2010). In the present study, 52% and 64% of pod N apparently originated from N remobilization from full flowering until maturity under low (N0) and high N fertilization (N160), respectively (Table IV-1). At full flowering the stems and the leaves represented the largest N pools under both N supplies (Figures IV-8c, IV-9a). Owing to the high amount of N apparently remobilized from the stem (Figure IV-8c), the stem was a major source for apparent N remobilization to the pods. But the N remobilization efficiency from the stems with 51% and 61% for limited (N0) and sufficient N supply (N160), respectively, was comparatively low. Ulas *et al.* (2013) reported that the apparent N remobilization from the stem during reproductive

growth can reach up 88% particularly under N-limiting conditions. Since leaf N losses with shed leaves were rather low, the leaves were the second major source for N remobilization to the pods (Figure IV-9c). The apparent N remobilization from the leaves was about 10% higher compared to the stems, with 62% and 72% for limited (N0) and sufficient N supply (N160), respectively, and thus also substantially lower as reported by Ulas *et al.* (2013). Within the N fertilization levels (N0, N160) no cultivar differences in the N concentrations of stem and shed leaves occurred at maturity (Figures IV-8d, IV-9d). Thus the cultivar differences in the amount of N remobilized from stems and leaves were based on differences in N accumulation during vegetative biomass formation rather than N remobilization efficiency.

The N remobilization efficiencies of the leaves and the stem did not differ much, particularly under N-limiting conditions (compare Figures IV-8d and IV-9d). But the amount of N remaining in the stem was about twice higher under both N supplies (Table IV-2) owing to the higher dry matter of the stems (not shown). Less than 10% of the N taken up by the shoot remained in the leaves and did not exceed more than 16 kg N ha^{-1}. Thus the leaves did not contribute much to the amount of N in crop residues, confirming the results reported by Ulas *et al.* (2013).

In agreement with the reported small contribution of N remobilization from the taproot to the pods (Malagoli *et al.,* 2005; Gombert *et al.,* 2010) the N pool in the taproot was low compared to the shoot and amounted only to 15% and 11% of the shoot N pool at N0 and N160, respectively (Figure IV-8a). The taproot was not an important intermediate storage organ for N remobilization, since the N pool during reproductive growth remained generally on a constant level even under severe N limitation (N0) (Figure IV-8a). Only under sufficient N supply (N160) the taproot N content slightly but significantly decreased for the cvs. Apex and Capitol.

The generally higher N concentrations remaining in the taproots (Figure IV-8b), stems (Figure IV-8d) and shed leaves (Figure IV-9d) at maturity under high (N160) compared to low N supply (N0) indicate a sink-limitation of grain yield formation. This was in agreement with the above mentioned lower N remobilization efficiency from vegetative plant parts to the grains compared to previous studies (Ulas *et al.,* 2013). The sink limitation may be explained by the unfavorable climatic conditions during the main growing period in combination with the delayed development before winter, since improved growing conditions in the spring could not compensate an inferior development in the autumn (Stoy, 1982; Diepenbrock & Geisler, 1985b).

The residual N in stems and particularly pod walls contributed mainly to the N amounts remaining in the crop residues independent of the N supply (Table IV-2). Based on the change in the N content of the pod walls during grain filling a remobilization efficiency 23% and 27% could be calculated for N0 and N160 across the cultivars (Figure IV-7c). The lower N remobilization efficiency of pod walls compared to stems and leaves might be due to a limited N requirement and storage capacity for N in

the grains which primarily store oil rather than proteins. However, enhancing N remobilization from pod walls to the grains with the objective to reduce the N content in crop residues and thus decreasing the N budget surplus of the winter oilseed-rape crop is possible without compromising the oil yield, since for both quality criteria independent QTLs could be identified (Zhao *et al.,* 2006).

In conclusion, for grain yield formation under N-limiting conditions (N0) as well as sufficient N supply (N160) NUPT was more important than NUE in the present experiment. For genetic variation in N efficiency NUPT, particularly N uptake during flowering and biomass allocation efficiency to the grains (HI) were decisive. Both were related to delayed senescence of the older leaves (stay-green). For pod N accumulation N remobilization from the vegetative plant parts was more important than N uptake after full flowering. The main sources for the high N amounts remaining in the crop residues at maturity were the pod walls (high N concentrations) and the stems (high biomass). Decreasing the crop-inherent high N budget surplus of winter oilseed-rape requires increasing the N remobilization efficiency of pod wall N to the grains.

General Discussion

Environmental pollution through high N balance surpluses is a widely spread problem in high-intensity agriculture cropping-systems. The surplus N is environmentally harmful, because of enhanced nitrate transport into ground and surface waters and enhanced nitrous oxide emission into the atmosphere, which contributes to global warming (Good & Beatty, 2011).

Winter oilseed-rape is the most important oil crop in the countries of northern Europe as well as the cold temperate climate zone worldwide. But it is one of the crops with the highest N balance surpluses even under best agronomic practices. The crop-specific balance surpluses are resulting from a low N uptake during the reproductive phase in combination with high N amounts remaining in the crop residues, due to an incomplete N retranslocation into the grains (Aufhammer *et al.,* 1994; Lickfett *et al.,* 2001). Thus, for the reduction of the crop-specific N balance surplus the reduction of the high fertilizer rates and the high N amounts remaining in the crop residues is a perquisite. But the current grain yield level should not be compromised. A promising approach to achieve this is the breeding and cultivation of N-efficient cultivars (Sylvester-Bradley & Kindred 2009), which have the ability to produce high grain yields under reduced N input (Graham, 1984; Sattelmacher *et al.,* 1994).

The potential of the cultivar type to enhance the N efficiency of winter oilseed-rape crops and reduce the high crop-specific N balance surpluses

In the present study dwarf, hybrid and line cultivars were compared to determine the potential to enhance the N efficiency of winter oilseed-rape crops by the cultivation of different cultivar types (Chapter I). Particular the cultivation of dwarf cultivars seems to be promising to enhance the N efficiency and reduce the high crop-specific N balance surpluses in winter oilseed-rape crops, since they are characterized by an increased biomass distribution efficiency and allocation efficiency of N to the grains through a lower vegetative above-ground biomass formation and thus a lower N uptake for maximum grain-yield formation. This would reduce the N amount remaining in the crop residues, primarily because of the lower straw biomass left on the field (Sieling & Kage, 2008). In contrast, high yielding hybrid cultivars are often considered to be not sustainable in relation to the utilization of resources such as water and nutrients, particularly N, and thus it is a widespread assumption that their cultivation conflicts with a sustainable agriculture.

Between the cultivar types considerable differences in the yield capacity and N efficiency were found (Chapter I). Independent of the N supply the hybrids were superior in grain yield formation and thus were more N-efficient than the line and dwarf cultivars. Although in the two years field experiment the N deficiency stress was mild with only 16% yield reduction across all cultivars (Chapter I), hybrid cultivars proved to be superior in N efficiency to other cultivars also at more severe N deficiency

stress (Gehringer *et al.,* 2007; Kessel *et al.,* 2012). Particularly under suboptimal environmental conditions the higher tolerance against environmental stresses such as N limitation of the hybrids leads to higher yield stability (Brandle & McVetty, 1989; Tollenaar & Wu, 1999).

From the crop N-balance point of view the N amounts remaining in the crops residues did not differ between the cultivar types, thus at first sight despite the superior N efficiency the cultivation of hybrid cultivars seems not be promising for the reduction of the crop-specific N balance surpluses. But the more vigorous growth at the rosette stage of the hybrids in hydroponics compared to the lines at high N supply particularly also under N limitation, which may be representative for the growth in the field at this growth stage, suggests a high N uptake before winter in the field, which will contribute to reduce the N losses through leaching during winter. Particularly the N accumulated before winter is protected from N leaching (Sieling & Kage, 2006) and contributes to growth and yield formation in spring.

The dwarfs generally met the expectations of a lower biomass formation and N uptake until maturity, but without increasing N efficiency and reducing the residual N in the straw. Thus, in agreement with the results of Sieling & Kage (2008) the cultivation of dwarf cultivars neither enhanced the N efficiency of winter oilseed-rape nor contributed to a reduction of the residual N in the crop residues (Chapter I).

However, the present study revealed that the high N-balance surplus of winter oilseed-rape is not due to inherent low N uptake efficiency, but is mainly based on the high amounts of N remaining in the crop residues (Chapter I, IV). Among these the stems and the pod walls were quantitatively the most important plant parts (Chapter IV). Thus an important future trait of N-efficient cultivars should be improved N allocation efficiency from stems and particularly pod walls to the grains. But this will be difficult, since winter oilseed-rape is an oil crop and oil and protein content in the grain are negatively correlated (Zhao *et al.,* 2006; Würschum *et al.,* 2012).

The contribution of N uptake efficiency and N utilization efficiency to the superior N efficiency of hybrid cultivars

The superior N efficiency of winter oilseed-rape hybrid-cultivars could be based on two components (I) the effectiveness of a cultivar in absorbing N from the soil (N uptake efficiency; NUPT) and/or (II) the efficiency with which the N taken up is utilized to produce yield (N utilization efficiency; NUE). Cultivar variation in N efficiency of winter oilseed-rape line-cultivars has been primarily attributed to high NUPT until maturity, particularly during reproductive growth (Wiesler *et al.,* 2001; Behrens, 2002; Kamh *et al.,* 2005; Schulte auf'm Erley *et al.,* 2007; Ulas, 2010; Schulte auf'm Erley *et al.,* 2011). Also the greater N efficiency of the hybrids was related to a high

NUPT until maturity. The N uptake during reproductive growth was unfortunately not quantified in this study (Chapter I). But the conducted hydroponic experiment suggests a superior N accumulation capacity of hybrids already during early vegetative growth, which primarily based on the vigor growth (Chapter I). For high NUPT of line cultivars particularly at later developmental stages such as flowering the acquisition of subsoil nitrate appeared decisive, for which a higher root length in deeper soil layers is important (Kamh *et al.,* 2005). Although in the present field experiments root growth was not studied, however, the potential root growth of the cultivars has been evaluated in the hydroponic experiment. In agreement with the shoot growth the hybrids showed also a more vigorous root growth on a dry weight basis than the line cultivars at limiting and non-limiting N supply. Moreover, the specific root length which is a measure of the root fineness differed significantly between the two cultivar types with hybrids showing coarser roots (Chapter I). In particular thicker roots might be beneficial for nitrate acquisition from the subsoil, because thicker roots have a higher soil penetration capability (Clark *et al.,* 2003).

The second pillar of N efficiency is N utilization efficiency (NUE) (Sattelmacher *et al.,* 1994). Among the cultivars the hybrids and dwarfs showed a higher NUE compared to the lines (Chapter I). Physiological traits which may contribute to NUE are a low grain N concentration and an efficient allocation of N to the grains. The hybrids were characterized by a lower grain protein (except grain protein at N0) and grain-meal protein concentrations. Lower protein concentration of grains as contributing to N efficiency, however, is equivocal from the grain quality and crop N-balance point of view. Although winter oilseed-rape is an oil crop and the oil yield is the most important economic parameter (Funk & Mohr, 2010), the remaining rapeseed-meal is a valuable animal feedstuff and protein source (Wittkop *et al.,* 2009). Also, a lower N concentration in the grain might leave higher N amounts in crop residues contributing to an increasing negative crop N balance. Therefore, a high retranslocation of N from vegetative plant organs to the grains, for which the N harvest index (NHI) is an overall indicator, is of greater importance as component of NUE. But the cultivar types did not significantly differ in NHI suggesting that N retranslocation efficiency did not contribute to the higher N utilization efficiency of the hybrids. In conclusion, the present study revealed that under mild N limitation both, N uptake and N utilization efficiency were decisive for the superior N efficiency of the hybrids.

The importance of functional stay-green for the N efficiency of winter oilseed-rape cultivars

Insufficient N supply induces and accelerates senescence (Mei & Thimann, 1984), which leads to premature crop maturation and thus compromises yield formation (Gregersen *et al.,* 2013). Thus in

many crop species stay-green phenotypes are superior in yield formation particularly under abiotic stress conditions such as drought or N limitation (Gregersen *et al.,* 2013). A characteristic of N-efficient line cultivars is a functional stay-green phenotype expressed through delayed senescence of the older leaves accompanied with maintained photosynthetic capacity (Schulte auf'm Erley *et al.,* 2007). Particularly during flowering the availability of assimilates from leaf-photosynthesis is the most source-limiting factor for exploiting the yield capacity in winter oilseed-rape (Pechan & Morgan, 1985; Keiller & Morgan, 1988). But under N-limiting conditions it is still not clear, whether the maintained photoassimilation enhances N efficiency mainly through maintained assimilate allocation to the grains or to the roots and thus mainly through prolonged N uptake. Particularly N uptake during flowering appeared decisive for cultivar variation in N efficiency of line cultivars (Behrens, 2002; Kamh *et al.,* 2005; Schulte auf'm Erley *et al.,* 2011; Ulas *et al.,* 2012). However, the superior N efficiency of the hybrid cultivars under mild N limitation in the field was clearly not related to a functional stay-green phenotype. This was in agreement with a hydroponic experiment in which the hybrids were particularly responsive in N starvation-induced leaf senescence of older leaves also under severe N starvation (Chapter I). It appears that in hybrids the high N accumulation through high biomass formation during vegetative growth is sufficient to meet the N requirement for the formation of a high number of pod-bearing side shoots through N remobilization rather than post-flowering N uptake. The high capacity of leaf N remobilization during N starvation-induced leaf senescence was clearly demonstrated in the hydroponic experiment, where the hybrids showed the lowest specific leaf N contents after 10 days of N starvation (Chapter I). Nevertheless, it remains the question whether the stay-green trait becomes more important for N efficiency of the hybrids under field conditions under more severe N limitation, since the present study clearly showed for the line cultivars that the importance of the functional stay-green trait with regard to N efficiency depended on the strength of N limitation (compare Chapters I and IV). Particularly under severe N-limiting conditions the higher N-efficiency of the line-cultivars cv. NPZ-1 and cv. Apex was accompanied with a delayed senescence of the older leaves compared to their respective N-inefficient counterparts cv. NPZ-2 and cv. Capitol. Both, N uptake during flowering and biomass allocation efficiency to the grains were enhanced in the N-efficient, functional stay-green cultivars (Chapter IV).

The importance of leaf-inherent factors and root-derived signals for cultivar variation in functional stay-green under N starvation

The senescence phenotype expressing in the field under limited N supply during reproductive growth was reproducible at the rosette stage in the established hydroponic system (Chapters I, II, III, IV). The

positive correlation between field conditions and hydroponics encouraged the investigation of important leaf and root traits of N-efficient cultivars in short-term hydroponic experiments under controlled conditions (Schulte auf'm Erley *et al.,* 2007).

The reciprocal grafts of the N-efficient and functional stay-green cvs. NPZ-1 and Apex with the respective N-inefficient and early senescing counterpart cv. NPZ-2 and cv. Capitol, respectively, revealed that genetic variation in functional stay-green under N limitation was governed by leaf-inherent factors rather than root-derived signals (Chapter III). For the identification of important leaf-inherent factors which are responsible for genetic variation in N-starvation induced leaf senescence, the same four cultivars were submitted to twelve days of N starvation in a complementary time-course experiment. The specific leaf contents of biologically active and inactive cytokinins (CKs) and the expression of genes involved in CK homeostasis revealed that under N starvation leaves of early senescing cvs. NPZ-2 and Capitol were characterized by inactivation of biologically active CKs, whereas in stay-green cvs. NPZ-1 and Apex synthesis, activation, binding of and response to biologically active CKs were favored. These results suggest that the homeostasis of biologically active CKs is the decisive leaf-inherent factor for cultivar differences in N starvation-induced leaf senescence. However, despite the clear leaf-inherent control of functional stay-green it has to be considered that a possible delaying effect of a prolonged N uptake by the roots on the development of leaf senescence under field conditions cannot be investigated in the used hydroponic system. In the field, for high N uptake capacity during flowering particularly the acquisition of sub-soil nitrate is of major importance (Kamh *et al.,* 2005). But root morphological and physiological parameters which are decisive for N uptake in the soil are not important in the used hydroponic system. It is considered that a prolonged N uptake delays the onset of leaf senescence, since the N demand of the sink can be longer met without massive N remobilization particularly from the leaves and related leaf senescence. This is particularly the case when the N demand of the plant is especially high for branching and pod formation.

Using functional stay-green as a selection parameter for the breeding of N-efficient cultivars

Functional stay-green is an inheritable, mostly polygene-regulated quantitative trait (Wang *et al.,* 2012). But using functional stay-green as a selection parameter for the breeding of N-efficient cultivars is difficult owing to additional senescence inducers under field conditions interacting with N limitation, particularly shading of lower by upper leaves, inflorescences and pods and developmental senescence typically induced by the transition from the vegetative to the reproductive stage. Also dry spells during the growing period can lead to premature leaf senescence and may mask genetic variation in N starvation-induced leaf senescence (Gregersen *et al.,* 2013).

However, in the hydroponic system where N starvation could be isolated as the only factor inducing senescence the relative expression of the senescence-specific cysteine protease gene *SAG12-1* proved to be a suitable and sensitive marker for the detection of genetic variation in N starvation-induced leaf senescence compared to leaf chlorophyll concentration (SPAD) and photosynthesis rate (Chapters I, II, II). But *SAG12-1* was also very responsive to senescence induced by leaf shading or detaching and was thus not N starvation-specific (Chapter II). Thus, there is a need for more sensitive and N starvation-specific leaf senescence marker genes capable of identifying cultivar differences in functional stay-green. Therefore, the transcriptomes of leaves of the cvs. Apex and Capitol differing in N efficiency and N-starvation-induced leaf senescence were analyzed using a 60k *B. napus* custom-made microarray four days after the induction of senescence by N starvation, leaf shading and detaching. The global analysis of gene expression revealed an N starvation-specific program different from that of leaf shading and detaching in leaves four days after the treatment began. This is in agreement with Buchanan-Wollaston *et al.* (2005) and van der Graaf *et al.* (2006) who observed distinctive differences between senescence inducers on the transcriptional level in *A. thaliana*.

In addition to N metabolism genes, N starvation rapidly mostly (and specifically) repressed genes related to photosynthesis, photorespiration and cell-wall structure, while genes related to mitochondrial electron transport and flavonoid biosynthesis were rapidly predominately up-regulated (Chapter II). Moreover, a cultivar-specific response at the transcriptinal level was particularly pronounced for N starvation (Chapter II). Among the N starvation specifically regulated genes applying qRT-PCR, in a kinetic study over 12 days of N starvation with the N-efficient and stay-green cvs. NPZ-1 and Apex and the respective N-inefficient and early senescing counterparts cvs. NPZ-2 and Capitol six genes could be identified as highly sensitive molecular leaf-senescence markers suitable for revealing cultivar differences in N starvation-induced leaf senescence in *B. napus*: the senescence regulator *ANAC029*, the anthocyanin synthesis-related gene *ANS* and possibly anthocyanin synthesis-related gene *DFR-like1*, the ammonium transporter *AMT1;4*, the ureide transporter *UPS5*, and *SPS1* involved in sucrose biosynthesis. But the general suitability of these marker genes for the identification of cultivar differences in functional stay-green cultivars and their role in N efficiency need to be validated using a larger and more diverse set of cultivars in the future.

Outlook

Nitrogen starvation-induced leaf senescence

The present as well as previous studies revealed that delayed leaf senescence of the older leaves accompanied by maintenance of photosynthetic capacity (functional stay-green) is an important trait of N-efficient winter oilseed-rape line-cultivars (Chapter IV, Schulte auf'm Erley *et al.,* 2007). Particularly during flowering the availability of assimilates from leaf-photosynthesis is the most source-limiting factor for exploiting the yield capacity in winter oilseed-rape (Pechan & Morgan, 1985; Keiller & Morgan, 1988). But under N-limiting conditions it is still not clear, whether the maintained photoassimilation enhances N efficiency mainly through maintained assimilate allocation to the grains or to the roots and thus mainly through prolonged N uptake. Particularly N uptake during flowering appeared decisive for cultivar differences in N efficiency of line cultivars (Behrens, 2002; Kamh *et al.,* 2005; Schulte auf'm Erley et al., 2011; Ulas *et al.,* 2012). The relation between functional stay-green and post-flowering N uptake could be clarified by partially defoliation of the main stem at the beginning of flowering or the periodical application of cytokinins to the leaves during flowering. The artificially reduction of the green leaf area by leaf cutting or a cytokinin mediated maintenance will contribute to reveal the effect of assimilate availability on yield formation and N uptake capacity during the reproductive phase.

The senescence phenotype under N-limiting conditions in the field after beginning of flowering was reproducible under N starvation in hydroponics already at the rosette stage (Chapters I, II, III, IV; Schulte auf'm Erley *et al.,* 2007). The positive correlation between field conditions and hydroponics encouraged the investigation of important leaf and root traits of N-efficient cultivars in short-term hydroponic experiments under controlled conditions (Schulte auf'm Erley *et al.,* 2007). The reciprocal grafting approach in hydroponics of two pairs of cultivars differing in N starvation-induced leaf senescence in the field (Chapter IV) clearly showed that cultivar variation in N starvation-induced leaf senescence was governed by leaf-inherent factors (Chapter III). A complementary time-course experiment revealed that particularly during the progression of N starvation-induced leaf senescence genes involved in synthesis, activation, binding of and response to biologically active CKs coincided with the respective senescence phenotype (Chapter III). For these genes single as well as multiple mutants for *B. napus* should be created overexpressing these genes in order to clarify whether the overexpression leads to a prolonged functional stay-green phenotype and whether this phenotype leads finally to enhanced N efficiency.

In agreement with the leaf-inherent control of functional stay-green the global transcriptomic analysis revealed a cultivar-specific shift in gene regulation in the leaf tissues shortly after exposure to N starvation (Chapter II). The comparison to the senescence inducer shading and leaf detaching

allowed the identification of N starvation-specific leaf-senescence marker-genes capable of identifying cultivar differences in functional stay-green (Chapter II). Surprisingly, the CK-related genes which appeared decisive for cultivar variation in functional stay-green under N starvation were not among the selected marker genes. This apparent discrepancy may be explained by three reasons: (i) oligonucleotides of several of the CK-related genes were not represented on the 60k *B. napus* custom-made microarray; (ii) the present oligonucleotides on the microarray lacked specificity for the respective isogenes, and (iii) the regulation of the CK genes were not N starvation-specific compared to shading and leaf detaching. To circumvent the technical limitations of microarrays the leaf transcriptome could be analysis using a next generation sequence technique such as the massive analysis of cDNA ends (MACE).

For the final verification of the selected marker genes they need to be analyzed in a more divers set of cultivars and tested under field conditions. Under field conditions senescence is often induced by drought, too. Drought as senescence inducer was not included in the hydroponic experiment, and N specificity is solely valid in comparison to shading and detaching. Also, the marker genes were selected at the rosette stage; thus their suitability for detecting cultivar differences in functional stay-green has to be confirmed at the transition from the vegetative into the reproductive phase when the stay-green phenotype becomes particularly important for N efficiency. At this developmental stage leaf senescence is also developmentally triggered, which might mask the regulation of the marker genes by N limitation.

Among the criteria for the selection of the marker genes has been their putative function. But the functions attributed to the respective *B. napus* sequences were solely based on sequence homology to *A. thaliana*. Thus, the functional characterization of these marker genes in *B. napus* is necessary, which require reverse genetic approaches. The respective gene could be knocked out or overexpressed by the use of mutants like T-DNA insertion lines or knocked out by virus-induced gene silencing. Particularly the use of overexpression mutants seems promising, since knockout of genes often leads either to lethal phenotypes or substitution of the knockout gene by redundant genes. Particularly the creation of mutants overexpressing single or several of the selected marker genes which were higher up-regulated in the functional stay-green cultivars appears promising aiming at enhancing the functional stay-green trait in *B. napus* and finally N efficiency.

However, despite the clear leaf-inherent control of functional stay-green it has to be considered that a possible delaying effect of a prolonged N uptake on the development of leaf senescence cannot be investigated in hydroponic systems. In the soil, for high N uptake capacity during flowering particularly the acquisition of sub-soil nitrate is of major importance (Kamh *et al.,* 2005). But root morphological and physiological parameters which are decisive for N uptake in the soil are not important in hydroponic systems. It is considered that a prolonged N uptake delays the onset of leaf

senescence, since the N demand of the sink can be longer met without massive N remobilization particularly from the leaves. This is particularly the case during flowering when a high N demand is required for branching. Thus for the investigation of the effect of a maintained N uptake on leaf senescence, plants should be cultivated in rhizotrons where a local placement of N is possible and root morphological parameters are decisive for N uptake efficiency, particularly with regard to the acquisition of subsoil N.

Nitrogen efficiency of winter oilseed-rape hybrid-cultivars

An unexpected result of the present work was that the superior N efficiency of the hybrid cultivars was clearly not related to delayed leaf senescence (Chapter I). But, it has to be considered that in the two years field experiment the N deficiency stress was only mild, and thus the question remains whether the stay-green trait becomes more important under more severe N limitation. The conducted field experiments revealed that both, N uptake and N utilization efficiency were decisive for the superior N efficiency of the hybrids (Chapter I). But the physiological reasons are not yet well understood. Based on the present results, a main objective of future experimental approaches should be the clarification whether the overall high N efficiency of hybrids results from a high NUPT and N accumulation during vegetative growth rather than from maintained N uptake during flowering. This NUPT needs to be combined with high NUE by efficient retranslocation of N from the vegetative plant parts (for which senescence is a prerequisite) and utilization for pod and particularly grain formation.

In terms of the high NUPT of the hybrids the identification of the decisive root traits is a key task of future experimental approaches. For high NUPT particularly the acquisition of sub-soil nitrate appears decisive (Kamh *et al.,* 2005). The hydroponic experiment revealed that the hybrids have thicker roots (Chapter I). This might be important particularly under field conditions, since thicker roots have a higher soil-penetration ability allowing better exploiting deeper soil layers (Clark *et al.,* 2003). Thus the root systems of contrasting hybrids should be characterized by using established techniques (Kamh *et al.,* 2005; Ulas *et al.,* 2012). Moreover, the nitrate depletion of soil layers should be determined in order to clarify whether a relationship between root traits and nitrate uptake exists. With regard to NUE the transformation of early senescing hybrids with the identified “stay-green” genes appears very attractive to clarify whether and under which conditions delayed leaf senescence and thus retranslocation of N from leaves to reproductive organs is beneficial or detrimental for N efficiency of hybrids.

Reducing the N balance surplus of winter oilseed-rape crops

The present study revealed that the high N-balance surplus of winter oilseed-rape is not due to inherent low N uptake efficiency, but is mainly based on the high amounts of N remaining in the crop residues (Chapters I, IV). Among these the stems and the pod walls were quantitatively the most important plant parts (Chapter IV). Thus an important future trait of N-efficient cultivars should be improved N allocation efficiency from stems and pod walls to the grains. The low remobilization efficiency particularly from the pod walls clearly reflects the rather low sink capacity of the oilseed-raps grains for N. This is not surprising, since oilseed rape is primarily an oil crop storing fatty acids in the grains. Enhancing the N sink capacity of the grains would require an increase of the protein content of the grains. This is not only a desirable trait from the crop N-balance point of view, but also important for the nutritional value of the remaining rapeseed-cake after the extraction of the oil, which is commonly used in livestock feeding (Wittkop *et al.,* 2009). However, the well-established negative genetic and phenotypic correlations between oil and protein content seem to make the breeding of cultivars with higher grain protein contents without compromising the grain oil content difficult (Zhao *et al.,* 2006; Würschum *et al.,* 2012). But, the identification of independent QTLs for both quality criteria (Zhao *et al.,* 2006) suggests breeding of cultivars with high grain-oil and protein-contents could be possible in future. This should be a key priority for reducing the inherent high N-balance surpluses of winter oilseed-rape crops.

Literature

Albacete, A., Cantero-Navarro, E., Großkinsky, D. K., Arias C. L., Balibrea M. E., Bru R., Franger, L., Ghanem, M. E., de la Cruz González, M., Hernández, J. A., Martínez-Andújar, C., van der Graaff, E., Weckwerth, W., Zellnig, G., Pérez-Alfocea, F. and Roitsch, T. (2014): Ectopic overexpression of the cell wall invertase gene *CIN1* increases water use efficiency in tomato (*Solanum lycopersicum* L.) and confers extreme drought tolerance. J. Exp. Bot. doi: 10.1093/jxb/eru448.

Allen, E. J. and Morgan, D. G. (1972): A quantitative analysis of the effects of nitrogen on the growth, development and yield of oilseed rape. J. Agric. Sci. 78, 315-324.

Arvidsson, S., Kwasniewski, M., Riaño-Pachón, D. M. and Mueller-Roeber, B. (2008): QuantPrime – a flexible tool for reliable high-throughput primer design for quantitative PCR. BMC Bioinformatics 9, 465.

Asare, E. and Scarisbrick, D. H. (1995): Rate of nitrogen and sulphur fertilizers on yield, yield components and seed quality of oilseed rape (*Brassica napus* L.). Field Crops Res. 44, 41-46.

Aufhammer, W., Kübler, E. and Bury, M. (1994): Nitrogen uptake and nitrogen residuals of winter oil-seed rape and fallout rape. J. Agron. Crop. Sci. 172, 255-264.

Ay, N., Raum, U., Balazadeh, S., Seidensticker, T., Fischer, A., Reuter, G. and Humbeck, K. (2013): Regulatory factors of leaf senescence are affected in *Arabidopsis* plants overexpressing the histone methyltransferase SUVH2. J. Plant Growth Regul. 33, 119-136.

Balazadeh, S., Parlitz, S., Mueller-Roeber B. and Meyer, R. C. (2008a): Natural developmental variations in leaf and plant senescence in *Arabidopsis thaliana***.** Plant Biol. 10, 136-147.

Balazadeh, S., Riaño-Pachón, D. M. and Mueller-Roeber, B. (2008b): Transcription factors regulating leaf senescence in *Arabidopsis thaliana*. Plant Biol. 10, 63-75.

Balazadeh, S., Siddiqui, H., Allu, A. D., Matallana-Ramirez, L. P., Caldana, C., Mehrnia, M., Zanor, M.-I., Köhler, B. and Mueller-Roeber, B. (2010): A gene regulatory network controlled by the NAC transcription factor ANAC092/AtNAC2/ORE1 during salt-promoted senescence. Plant J. 62, 250-264.

Balazadeh, S., Schildhauer, J., Araújo, W. L., Munnè-Bosch, S., Fernie, A. R., Proost, S., Humbeck, K. and Mueller-Roeber, B. (2014): Reversal of senescence by N resupply to N-starved Arabidopsis thaliana: transcriptomic and metobolomic consequences. J. Exp. Bot. doi: 10.1093/jxb/eru119.

Barlow, P. W. (1982): Cell death – an integral part of plant development. In Jackson, M. B., Grout, B., Mackenzie, I. A. (ed.): In Growth Regulators in Plant Senescence. British Plant Growth Regulator Group, pp. 27-45.

Barth, C. A. (2009): Nutritional value of rapeseed oil and its high oleic/low linolenic variety – A call for differentiation. Eur. J. Lipid Sci. Technol. 111, 953-956.

Bänzinger, M., Betrán, F. J. and Lafitte, H. R. (1997): Efficiency of High-Nitrogen Selection Environments for Improving Growth Regulators in Plant Senescence Maize for Low-Nitrogen Target Environments. Crop Sci. 37, 1103-1109.

Becker, H. C. (1987): Quantitative Zuchtmethodik bei Raps – Der Versuch einer Literaturübersicht. Bericht über die Arbeitstagung der Saatzuchtleiter in Gumpenstein. Verlag der Bundesanstalt für alpenländische Landwirtschaft. Gumpenstein, pp. 67-82.

Behrens, T. (2002): Stickstoffeffizienz von Winterraps (*Brassica napus* L.) in Abhängigkeit von Sorte sowie einer Menge, Zeit und Form variierte Stickstoffmenge. Ph.D. Thesis. University of Hannover, Germany.

Belícuas, P. R., Aguiar, A. M., Bento, D. A. V., Câmara, T. M. M. and de Souza Junior, C. L. (2014): Inheritance of the stay-green trait in tropical maize. Euphytica 198, 163-173.

Berry, P. M. and Spink, J. H. (2006): A physiological analysis of oilseed rape yields past and future. J. Agric. Sci. 144, 381-392.

Berry, P. M., Spink, J., Foulkes, M. J. and White, P. J. (2010): The physiological basis of genotypic differences in nitrogen use efficiency in oilseed rape (*Brassica napus* L.). Field Crops Res. 119, 365-373.

Bertin, P. and Gallais, A. (2000): Genetic variation for nitrogen use efficiency in a set of recombinant maize inbred lines. I Agrophysical results. Maydica 45, 53-66.

Besseau, S., Li, J. and Palava, E. T. (2012): *WRKY54* and *WRKY70* co-operate as negative regulators of leaf senescence in *Arabidopsis thaliana*. J. Exp. Bot. 63, 2667-2679.

Bi, Y.-M., Wang, R.-L., Zhu, T. and Rothstein, S. J. (2007): Global transcription profiling reveals differential responses to chronic nitrogen stress and putative nitrogen regulatory components in *Arabidopsis*. BMC Genomics 8, 281.

Blair, G. (1993): Nutrient efficiency – what do we really mean? In Randall, P. J., Delhaize, E., Richards, R. A. and Munns, R. (ed): Genetic aspects of plant mineral nutrition. Kluwer Academic Publishers, Dordrecht, pp. 205-213.

Boelcke, B., Léon, J., Schulz, R. R., Schröder, G. and Diepenbrock, W. (1991): Yield stability of winter oil-seed rape (*Brassica napus* L.) as affected by stand establishment and nitrogen fertilization. J. Agron. Crop Sci. 167, 241-248.

Bolstad, B. M., Irizarry, R. A., Astrand, M. and Speed, T.P. (2003): A comparison of normalization methods for high density oligonucleotide array data based on variance and bias. Bioinformatics 19, 185-193.

Borlaug, N. E. and Dowswell, C. R. (1994): Feeding a human population that increasingly crowds a fragile planet 15th Word congress of soil science, 10th to 16th July 1994, Acapulco, Mexico.

Booth, E. J. and Gunstone, F. D. (2004): Rapeseeds and rapeseed oil: agronomy, production, and trade. In Gunstone, F.D. (ed.): Rapeseed and Canola Oil. Blackwell Publishing, Oxford, pp. 1-15.

Brandle, J. E. and McVetty, P. B. E. (1989): Heterosis and combining ability in hybrids derived from oilseed rape cultivars and inbred lines. Crop Sci. 29, 1191-1195.

Breeze, E., Harrison, E., McHattle, S., Hughes, L., Hickman, L., Hill, C., Kiddle, S., Kim, Y.-S., Penfold, C. A., Jenkins, D., Zhang, C., Morris, K., Jenner, C., Jackson, S., Thomas, B., Tabrett, A., Legale, R., Moore, J. D., Wild, D. L., Ott, S., Rand, D., Beynon, J., Denby, K., Mead, A. and Buchanan-Wollaston, V. (2011): High-resolution temporal profiling of transcripts during Arabidopsis leaf senescence reveals a distinct chronology of processes and regulation. Plant Cell 23, 873-894.

Brunel-Muguet, S., Beauclair, P., Bataillé, M.-P., Avice, J.C., Trouverie, J., Etienne, P. and Ourry, A. (2013): Light restriction delays leaf senescence in winter oilseed rape (*Brassica napus* L.). J. Plant Growth Regul. doi: 10.1007/s00344-013-9317-9.

Buchanan-Wollaston, V. (1997): The molecular biology of leaf senescence. J. Exp. Bot. 48, 181-199.

Buchanan-Wollaston, V. and Ainsworth, C. (1997): Leaf senescence in *Brassica napus*: cloning of senescence related genes by subtractive hybridisation. Plant Mol. Biol. 33, 821-834.

Buchanan-Wollaston, V., Page, T., Harrison, E., Breeze, E., Lim, P. O., Nam, H. G., Lin, J.F., Wu, S.H., Swidzinski, J., Ishizaki, K. and Leaver, C. J. (2005): Comparative transcriptome analysis reveals significant differences in gene expression and signalling pathways between developmental and dark/starvation-induced senescence in *Arabidopsis*. Plant J. 42, 567-585.

Chay, P. and Thurling, N. (1989a): Variation in pod length in spring rape (*Brassica napus*) and its effect on seed yield and yield components. J. Agric. Sci. 113, 139-147.

Chay, P. and Thurling, N. (1989b): Identification of genes controlling pod length in spring rapeseed, Brassica napus L., and their utilization for yield improvement. Plant Breeding. 103, 54-62.

Christ, B. and Hörtensteiner, S. (2014): Mechanism and significance of chlorophyll breakdown. J. Plant Growth Regul. 33, 4-20.

Christianson, J. A., Wilson, I. W., Llewellyn, D. J., and Dennis, E. S. (2009): The low-oxygen-induced NAC domain transcription factor ANAC102 affects viability of Arabidopsis seeds following low-oxygen treatment. Plant Physiol. 149, 1724-1738.

Chung, Y and Choe, S. (2013): The regulation of brassinosteroid biosynthesis in *Arabidopsis*. Crit. Rev. Plant Sci. 32, 396-410.

Clark, L. J., Whalley, W. R. and Barraclough, P. B. (2003): How do roots penetrate strong soil? Plant Soil 255, 93-104.

Craswell, E. T. and Godwin, D. C. (1984): The efficiency of nitrogen fertilizers applied to cereals in different climates. In Tinkler, P. B. and Läuchli, A. (ed.): Advances in Plant Nutrition 1. Praeger Publishers, New York, pp. 1-55.

del Mar Rubio-Wilhelmi, M., Reguera, M., Sanchez-Rodriguez, E., Romero, L., Blumwald, E. and Ruiz, J. M. (2014): PSARK::IPT expression causes protection of photosynthesis in tobacco plants during N deficiency. Environ. Exp. Bot. 98, 40-46.

Desclos, M., Dubousset, L., Etienne, P., Le Caherec, F., Satoh, H., Bonnefoy, J., Ourry, A. and Avice, J.-C. (2008): A proteomic approach to reveal a noval role of *Brassica napus* drought 22 kD/water-soluble chlorophyll-binding protein in young leaves during nitrogen remobilization induced by stressful conditions. Plant Physiol. 147, 1830-1844.

Desimone, M., Catoni, E., Ludewig, U., Hilpert, M., Schneider, A., Kunze, R., Tegeder, M., Frommer, W. B. and Schumacher, K. (2002): A novel superfamily of transporters for allantoin and other oxo derivates of nitrogen heterocyclic compounds in Arabidopsis. Plant Cell 14, 847-856.

Diaz, C., Saliba-Colombani, V., Loudet, O., Belluomo, P., Moreau, L., Daniel-Vedele, F., Morot-Gaudry, J.-F. and Masclaux-Daubresse, C. (2006): Leaf yellowing and anthocyanin accumulation are two genetically independent strategies in response to nitrogen limitation in *Arabidopsis thaliana*. Plant Cell Physiol. 47, 74–83.

Diepenbrock, W. and Geisler, G. (1985a): Die Ertragsstruktur von Raps I. Ertragsbildungsprozesse. Kali-Briefe (Büntehof) 17, 585-603.

Diepenbrock, W. and Geisler, G. (1985b): Die Ertragsstruktur von Raps II. Ertragskomponenten. Kali-Briefe (Büntehof) 17, 605-618.

Diepenbrock, W. and Grosse, F. (1995): Rapeseed (*Brassica napus* L.) physiology. In Diepenbrock, W. and Becker H. C. (ed.): Physiological Potentials for Yield Improvement of Annual Oil and Protein Crops. Adv. Plant Breeding 17, 21-53.

Diepenbrock, W. (2000): Yield analysis of winter oilseed rape (Brassica napus L.): a review. Field Crops Res. 67, 35-49.

Dodd, I. C. (2005): Root-to-shoot signaling: Assessing the roles of 'up' in the up and down world of long-distance signaling in *planta***.** Plant Soil 274, 251-270.

Dong, H., Niu, Y., Li, W. and Zhang, D. (2008): Effects of cotton rootstock on endogenous cytokinins and abscisic acid in xylem sap and leaves in relation to leaf senescence. J. Exp. Bot. 59, 1295-1304.

Downey, R. K. and Rimmer, S. R. (1993): Agronomic improvement in oilseed brassicas. Adv. Agron. 50, 1-66.

Etienne, P., Desclos, M., Le Gou, L., Gombert, J., Bonnefoy, J., Maurel, K., Le Dily, F., Ourry, A. and Avice, J.-C. (2007): N-protein mobilization associated with leaf senescence process in oilseed rape is concomitant with the disappearance of trypsin inhibitor activity. Funct. Plant Biol. 34, 895-906.

Evans, E. J. (1984): Pre-anthesis growth and its influence on seed yield in winter oilseed rape. Aspects Appl. Biol. 6, 81-90.

Evans, J. R. (1989): Photosynthesis and nitrogen relationships in leaves of C3 plants. Oecologia 78, 9-19.

Fageria, N. K., Baligar, V. C. and Li, Y. C. (2008): The role of nutrient efficient plants in improving crop yields in the twenty first century. J. Plant Nutr. 31, 1121-1157.

Fischer, A. M. (2007): Nutrient remobilization during leaf senescence. In Gan, S. (ed.): Senescence Processes in Plants, Blackwell Publishing, Ames, Oxford, Carlton, pp. 87-107.

Funk, H. and Mohr, R. (2010): Die Rapsabrechnung. UFOP-Praxisinformation.

Friedt, W., Lühs, W., Müller, M. and Ordon, F. (2003): Utility of winter oilseed rape (*Brassica napus* L.) cultivars and new breeding lines for low-input cropping systems. Pflanzenbauwissenschaften 7, 49-55.

Gajdošová, S., Spíchal, L. and Kamínek, M. (2011): Distribution, biological activities, metabolism, and the conceivable function of cis-zeatin-type cytokinins in plants. J. Exp. Bot. 62, 2827-2840.

Galtier, N., Foyer, C.H., Murchie, E., Alred, R., Quick, P., Voelker, T. A., Thépenier, C., Lascéve, G. and Betsche, T. (1995): Effects of light and atmospheric carbon dioxide enrichment on photosynthesis and carbon partitioning in the leaves of tomato (*Lycopersicon esculentum* L.) plants over-expressing sucrose phosphate synthase. J. Exp. Bot. 46, 1335-1344.

Galuszka, P., Popelková, H., Werner, T., Frébortová, J., Pospísilová, H., Mik, V., Köllmer, I., Schmülling, T. and Frébort, I. (2007): Biochemical characterization of cytokinins oxidases/dehydrogenases from *Arabidopsis thaliana* expressed in Nicotiana tabacum L.. J. Plant Growth Regul. 26, 255-267.

Gan, S. and Amasino, R. M. (1995): Inhibition of leaf senescence by autoregulated production of cytokinins. Science 270, 1986-1988.

Gazzarrini, S., Lejay, L., Gojon, A., Ninnemann, O., Frommer, W.-B. and von Wirén, N. (1999): Three functional transporters for constitutive, diurnally regulated, and starvation-induced uptake of ammonium into *Arabidopsis* roots. Plant Cell 11, 937-947.

Gehringer, A., Snowdon, R., Spiller, T., Basunanda, P. and Friedt, W. (2007): New oilseed rape (*Brassica napus*) hybrids with high levels of heterosis for seed yield under nutrient-poor conditions. Breeding Sci. 57, 315-320.

Geisler, G. and Henning, K. (1981a): Untersuchungen zur Ertragsstruktur von Raps (*Brassica napus* L. var. *napus*) I. Die vegetative Entwicklung der Rapspflanze in Abhängigkeit von der Bestandesdichte. Bayer. Landw. Jahrb. 58, 203-211.

Geisler, G. and Henning, K. (1981b): Untersuchungen zur Ertragsstruktur von Raps (*Brassica napus* L. var. *napus*) II. Die generative Entwicklung der Rapspflanze in Abhängigkeit von der Bestandesdichte. Bayer. Landw. Jahrb. 58, 322-332.

Gombert, J., Etienne, P., Ourry, A. and Le Dily, F. (2006): The expression patterns of SAG12/Cab genes reveal the spatial and temporal progression of leaf senescence in (*Brassica napus* L.) with sensitivity to the environment. J. Exp. Bot. 57, 1949-1956.

Gombert, J., Le Dily, F., Lothier, J., Etienne, P., Rossato, L., Allirand, J.-M., Jullien, A., Savin, A. and Ourry, A. (2010): Effect of nitrogen fertilization on nitrogen dynamics in oilseed rape using 15N-labeling field experiment. J. Plant Nutr. Soil Sci. 173, 875-884.

Good, A. G. and Beatty, P. H. (2011): Fertilizing nature: a tragedy of excess in the commons. PLoS Biol. 9, e1001124 doi: 10.1371/journal.pbio.1001124.

Graham, R. D. (1984): Breeding for nutritional characteristics in cereals. In Tinkler, P. B. and Läuchli, A. (ed.): Advances in Plant Nutrition 1. Praeger Publishers, New York, pp. 57-102.

Grebic, V. (2003): SAG2 and SAG12 protein expression in senescing Arabidopsis plants. Physiol. Plant. 119, 263-269.

Gregersen, P. L., Culetic, A., Boschian, L. and Krupinska, K. (2013): Plant senescence and crop productivity. Plant Mol. Biol. 82, 603-622.

Grosse, F., Léon, J. and Diepenbrock, W. (1992): Ertragsbildung und Ertragsstruktur bei Winterraps (*Brassica napus* L.) I. Genotypische Variabilität. J. Agron. Crop. Sci. 169, 70-93.

Großkinsky, D. K., Albacete, A., Jammer, A., Krbez, P., van der Graaff, E., Pfeifhofer, H. and Roitsch, T. (2014): A rapid phytohormone and phytoalexin screening method for physiological phenotyping. Mol. Plant 7, 1053-1056.

Guo, Y., Cai, Z. and Gan, S. (2004): Transcriptome of *Arabidopsis* leaf senescence. Plant Cell Environ. 27, 521-549.

Guo, Y. and Gan, S. (2006): AtNAP, a NAC family transcription factor, has an important role in leaf senescence. Plant J. 46, 601-612.

Habekotté, B. (1993): Quantitative analysis of pod formation, seed set and seed filling in winter oilseed rape (*Brassica napus* L.) under field conditions. Field Crops Res. 35, 21-33.

Haussmann, B. I. G., Mahalakshmi, V., Reddy, B. V. S., Seetharama, N., Hash, C. T. and Geiger, H. H. (2002): QTL mapping of stay-green in two sorghum recombinant inbred populations. Theor. Appl. Genet. 106, 133-142.

He, P., Osaki, M., Takebe, M., Shinano, T and Wasaki, J. (2005): Endogenous hormones and expression of senescence-related genes in different senescent types of maize. J. Exp. Bot. 56, 1117-1128.

Hesse, H., Sonnewald, U. and Wilmitzer, L. (1995): Cloning and expression analysis of sucrose-phosphate synthase from sugar beet (*Beta vulgaris*). Mol. Genet. Genomics 247, 515-520.

Hocking, P. J., Randall, P. J. and DeMarco, D. (1997): The response of dryland canola to nitrogen fertilizer: partitioning and mobilization of dry matter and nitrogen, and nitrogen effects on yield components. Field Crops Res. 54, 201-220.

Hoffer, G. N. (1926): Some differences in the functioning of selfed lines of corn under varying nutritional conditions. J. Am. Soc. Agron. 18, 322-334.

Holton, A. T. and Cornish, C. E. (1995): Genetics and biochemistry of anthocyanin biosynthesis. Plant Cell 7, 1071-1083.

Hou, B, Lim, E.-K., Higgins, G. S. and Bowles, D. J. (2004): N-glucosylation of cytokinins by glycosyltransferases of *Arabidopsis thaliana*. J. Biol. Chem. 279, 47822-47832.

Housley, T. L. and Pollock, C. J. (1985): Photosynthesis and carbohydrate metabolism in detached leaves of *Lolium temulentum* L. New Phytol. 99, 499-507.

Hörtensteiner, S. and Feller, U. (2002): Nitrogen metabolism and remobilization during senescence. J. Exp. Bot. 53, 927-937.

Huber, S. C. and Huber, J. L. (1996): Role and regulation of sucrose-phosphate synthase in higher plants. Annu. Rev. Plant Physiol. Plant Mol. Biol. 47, 431-444.

Huber, D. M. and Thomson, I. A. (2007): Nitrogen and plant disease. In Datnoff, L. E., Elmer, W. H. and Huber, D. M. (ed.): Mineral nutrition and plant disease. APS Press, St. Paul, pp. 31-44.

Husted, S. and Schjoerring, J. K. (1996): Ammonia flux between oilseed rape plants and the atmosphere in response to changes in leaf temperature, light intensity, and air humidity. Plant Physiol. 112, 67-74.

Hühn, M. and Schuster, W. (1975): Untersuchungen zur quantitativen Einschätzung von Konkurrenzeffekten in Winterrapsbeständen. Z. Pflanzenzüchtg. 75, 217-236.

Hühn, M. and Schuster, W. (1982): Einige experimentelle Ergebnisse über den Einfluß unterschiedlicher Konkurrenzsituationen auf die Korrelationen zwischen Einzelpflanzenmerkmalen (Ertragskomponenten) bei Winterraps. Z. Pflanzenzüchtg. 89, 60-73.

Imsande, J. and Touraine, B. (1994): N demand and regulation of nitrate uptake. Plant Physiol. 105, 3-7.

Jiang, G. H., He, Y. Q. Xu, C. G., Li, X. H. and Zhang, Q. (2004): The genetic basis of stay-green in rice analyzed in a population of doubled haploid lines derived from an *indica* by *japonica* cross. Theor. Appl. Genet. 108, 688-698.

Jin, S.H., Ma, X.-M., Kojima, M., Sakakibara, H., Wang, Y.-W. and Hou, B.-K. (2013): Overexpression of glucosyltransferase UGT85A1 influences trans-Zeatin homeostasis and trans-zeatin responses likely through O-glucosylation. Planta 237, 991-999.

Kaiser, H. F. (1960): The application of electronic computers to factor analysis. Educ. Psychol. Meas. 20, 141-151.

Kamh, M., Wiesler, F., Ulas, A. and Horst, W. J. (2005): Root growth and N-uptake of oilseed rape (*Brassica napus* L.) cultivars differing in nitrogen efficiency. J. Plant Nutr. Soil Sci. 168, 130-137.

Keech, O., Pesquet, E., Ahad, A., Askne, A., Nordvall, D., Vodnala, S. M., Tuominen, H., Hurry, V., Dizengremel, P. and Gardeström, P. (2007): The different fates of mitochondria and chloroplasts during dark-induced senescence in *Arabidopsis* leaves. Plant Cell Environ. 30, 1523-1534.

Keiller, D. R. and Morgan, D. G. (1988): Distribution of ^{14}carbon labelled assimilates in flowering plant of oilseed rape (*Brassica napus* L.). J. Agric. Sci. 111, 347-355.

Kessel, B., Schierholt, A. and Becker, H. C. (2012): Nitrogen use efficiency in a genetically diverse set of winter oilseed rape (*Brassica napus* L.). Crop Sci. 52, 2546-2554.

Kim, H. J., Hojin, R., Hong, S. H., Woo, H. R., Lim, P. O., Lee, I. C., Sheen, J., Nam, H. G. and Hwang, I. (2006): Cytokinin-mediated control of leaf longevity by AHK3 through phosphorylation of ARR2 in *Arabidopsis*. Proc. Natl. Acad. Sci. U.S.A. 103, 814-819.

Kim, J. H., Woo, H. R., Lim PO, Kim, J., Lim, P. O., Lee, I. C., Choi, S. H., Hwang, D. and Nam, H. G. (2009): Trifurcate feed-forward regulation of age-dependent cell death involving miR164 in *Arabidopsis*. Science 323, 1053-1057.

Koeslin-Findeklee, F., Meyer, A., Girke, A., Beckmann, K. and Horst, W. J. (2014): The superior nitrogen efficiency of winter oilseed rape (*Brassica napus* L.) hybrids is not related to delayed nitrogen starvation-induced leaf senescence. Plant Soil 384, 347-362.

Kowalska, M., Galuszka, P., Frébortová, J., Ŝebela, M., Béres, T., Hluska, T., Ŝmehilová, M., Bilyeu, K. D. and Frébort, I. (2010): Vacuolar and cytosolic cytokinin dehydrogenases of *Arabidopsis thaliana*. Phytochem. 71, 1970-1978.

Köllmer, I., Novák, O., Strnad, M., Schmülling, T. and Werner, T. (2014): Overexpression of the cytosolic cytokinin oxidase/dehydrogenase (CKX7) from *Arabidopsis* causes specific changes in root growth and xylem differentiation. Plant J. doi: 10.1111/tpj. 12477.

Kusaba, M., Tanaka, A. and Tanaka, R. (2013): Stay-green plants: what do they tell us about the molecular mechanism of leaf senescence. Photosynt. Res. 117, 221-234.

Krapp, A., Berthomé, R., Orsel, M., Mercey-Boutet, S., Yu, A., Castaings, L., Elftieh, S., Major, H., Renou, J.-P. and Daniel-Vedele, F. (2011): *Arabidopsis* roots and shoots show distinct temporal adaption patterns toward nitrogen starvation. Plant Physiol. 157, 1255-1282.

Kuroha, T., Tokungaga, H., Kojima, M., Ueda, N., Ishida, T., Nagawa, S., Fukuda, H., Sugimoto, K. and Sakakibara, H. (2009): Functional analyses of LONELY GUY cytokinin-activating enzymes reveal the importance of the direct activation pathway in *Arabidopsis*. Plant Cell 21, 3152-3169.

Lamesch, P., Berardini, T. Z., Swarbreck, D., Wilks, C., Sasidharan, R., Muller, R., Dreher, K., Alexander, D. L., Garcia-Hernandez, M., Karthikeyan A. S., Lee, C. H., Nelson, W. D., Ploetz, L., Singh, S., Wensel, A. and Huala, E. (2012): The *Arabidopsis* Information Resource (TAIR): improved gene annotation and new tools. Nucleic Acids Res. 40, (Database issue) D1202-10.

Lancashire, P. D., Bleiholder, H., Boom, T. V. D., Langelüddeke, P., Strauss, R., Weber, E. and Witzenberger, A. (1991): A uniform decimal code for growth stages of crops and weeds. Ann. Appl. Biol. 119, 561-601.

Lara, M. E. B., Gonzalez, M.-C. G., Fatima, T., Ehneß, T., Lee, T. K., Roels, R., Tanner, W. and Roitsch, T. (2004): Extracellular invertase is an essential component of cytokinin mediated delay of senescence. Plant Cell 16, 1276-1287.

Leach, J. E., Stevenson, H. J., Rainbow, A. J. and Mullen, L. A. (1999): Effects of high plant populations on the growth and yield of winter oilseed rape (*Brassica napus*). J. Agr. Sci. 132, 173-180.

Lee, Y.-H., Kim, K.-S., Jang, Y.-S., Hwang, J.-H., Lee, D.-H. and Choi, I.-H. (2014): Global gene expression responses to waterlogging in leaves of rape seedlings. Plant Cell Rep. 33, 289-299.

Léon, J. (1991): Heterosis and mixing effects in winter oilseed rape. Crop Sci. 31, 281-284.

Lickfett, T., Behrens, T., Ulas, A., Horst, W. J. and Wiesler, F. (2001): Lösen N-effizientere Genotypen kurzfristig das Nitratproblem nach Raps? VDLUFA Schriftenreihe 57, 1-4.

Lim, P. O., Kim H. J. and Nam, H. G. (2007): Leaf senescence. Annu. Rev. Plant Biol. 58, 115-136.

Livak, K. J. and Schmittgen, T. D. (2001): Analysis of relative gene expression data using real-time quantification PCR and the 2-ΔΔCT Method. Methods 25, 402-408.

Malagoli, P., Laine, P., Rossato, L. and Ourry, A. (2005): Dynamics of nitrogen uptake and mobilization in field-grown winter oilseed rape (*Brassica napus*) from stem extension to harvest. II. An ^{15}N-labelling-based simulation model of N partitioning between vegetative and reproductive tissues. Ann. Bot. 95, 1187-1198.

Masclaux, C., Valadier M.-H., Brugiére, N., Morot-Gaudry J.-F. and Hirel, B. (2000): Characterization of the sink/source transition in tobacco (*Nicotiana tabacum* L.) shoots in relation to nitrogen management and leaf senescence. Planta 211, 510-518.

Masclaux-Daubresse, C., Reisdorf-Cren, M. and Orsel, M. (2008): Leaf nitrogen remobilization for plant development and grain filling. Plant Biol. 10, 23-36.

Mattsson, M. and Schjoerring, J. K. (2003): Senescence-induced changes in apoplastic and bulk tissue ammonia concentrations of ryegrass leaves. New Phytol. 160, 489-499.

Mei H.-S. and Thimann, K. V. (1984): The relation between nitrogen deficiency and leaf senescence. Physiol. Plant. 62, 157-161.

Mendham, N. J. and Scott, R. K. (1975): The limiting effect of plant size at inflorescence initiation on subsequent growth and yield of oilseed rape (*Brassica napus*). J. Agr. Sci. 84, 487-502.

Mendham, N. J., Shipway, P. A. and Scott, R. K. (1981a): The effects of delayed sowing and weather on growth, development and yield of winter oil-seed rape (*Brassica napus*). J. Agr. Sci. 96, 389-416.

Mendham, N. J., Shipway, P. A. and Scott, R. K. (1981b): The effects of seed size, autumn nitrogen and plant population density on the response to delayed sowing in winter oil-seed rape (*Brassica napus*). J. Agr. Sci. 96, 417-428.

Mi, G., Tang, L., Zhang, F. and Zhang, J. (2000): Is nitrogen after anthesis in wheat regulated by sink size? Field Crop Res. 68, 183-190.

Mi, G. H., Liu, J. A., Chen, F. J., Zhang, F. S., Cui, Z. L. and Liu, X. S. (2003): Nitrogen uptake and remobilization in maize hybrids differing in leaf senescence. J. Plant Nutr. 26, 237–247.

Misyura, M., Colasanti, J. and Rothstein, S. J. (2013): Physiological and genetic analysis of *Arabidopsis thaliana* anthocyanin biosynthesis mutants under chronic adverse environmental conditions. J. Exp. Bot. 64, 229-240.

Miyawaki, K., Matsumoto-Kitano, M. and Kakimoto, T. (2004): Expression of cytokinin biosynthetic isopentenyltransferaes genes in *Arabidopsis*: tissue specificity and regulation by auxin, cytokinin, and nitrate. Plant J. 37, 128-138.

Moll, R. H., Kamprath, E. J. and Jackson, W. A. (1982): Analysis and interpretation of factors which contribute to efficiency of nitrogen utilization. Agron. J. 74, 562-564.

Moroni, J. S. (1997): Studies on the efficiency of rapeseed (*Brassica napus* L.) germplasm for the acquisition and the utilization of inorganic nitrogen. Ph.D. Thesis. University of Alberta, Canada.

Nemie-Feyissa, D., Olafsdottir, S. M., Heidari, B. and Lillo, C. (2014): Nitrogen depletion and small R3-MYB transcription factors affecting anthocyanin accumulation in *Arabidopsis* leaves. Phytochem. 98, 34-40.

Newmann, E. I. (1966): A method of estimating the total length of root in a sample. J. Appl. Ecol. 3, 139-145.

Osaki, M. (1995): Comparison of productivity between tropical and temperate maize. I. Leaf senescence and productivity in relation to nitrogen nutrition. Soil Sci. Plant Nutr. 41, 439–450.

Parlitz, S., Kunze, R., Mueller-Roeber, B. and Balazadeh, S. (2011): Regulation of photosynthesis and transcription factor expression by leaf shading and re-illumination in *Arabidopsis* leaves. J. Plant Physiol. 168, 1311-1319.

Pechan, P. A. and Morgan, D. G. (1985): Defoliation and its effect on pod and seed development in oil seed rape (*Brassica napus* L.). J. Exp. Bot. 36, 458-468.

Peng, M., Hudson, D., Schofield, A., Tsao, R., Yang, R., Gu, H., Bi, Y.-M. and Rothstein, S. J. (2008): Adaption of *Arabidopsis* to nitrogen limitation involves induction of anthocyanin synthesis which is controlled by the NLA gene. J. Exp. Bot. 59, 2933-2944.

Pommel, B., Gallais, A., Coque, M., Quilleré, I., Hirel, B., Prioul, J. L., Adrieu, B. and Floriot, M. (2006): carbon and nitrogen allocation and grain filling in three maize hybrids differing in leaf senescence. Europ. J. Agronomy 24, 203-211.

Presterl, T., Seitz, G., Landbeck, M., Thiemt, E. M., Schmidt, W. and Geiger, H. H. (2003): Improving nitrogen-use efficiency in European maize: Estimation of quantitative genetic parameters. Crop Sci. 43, 1259-1265.

Quirino, B. F., Noh, Y.-S., Himelblau, E. and Amasino, R. M. (2000): Molecular aspects of leaf senescence. Trends Plant Sci. 5, 278-282.

Rakow, G. (1978): Zur Formulierung von Zuchtzielen für Körnerraps. Fat. Sci. Technol. 80, 93-99.

Rathke, G.-W., Behrens, T. and Diepenbrock, W. (2006): Integrated nitrogen management strategies to improve seed yield, oil content and nitrogen efficiency of winter oilseed rape (Brassica napus L.): A review. Agric. Ecosyst. Environ. 117, 80-108.

Rauf, M., Arif, M., Dortay, H., Matallana-Ramírez, L. P., Waters, M. T., Nam, H.G., Lim, P.-O., Mueller-Roeber, B. and Balazadeh, S. (2013): *ORE1* balances leaf senescence against maintenance by antagonizing G2-like-mediated transcription. EMBO Reports 14, 382-388.

Raun, W. R. and Johnson, G. V. (1999): Improving nitrogen use efficiency for cereal production. Agron. J. 91, 357-363.

Richards, R. A. and Thurling, N. (1979): Genetic analysis of drought stress response in rapeseed (Brassica campestris and B. napus). II. Yield improvement and the application of selection indices. Euphytica 28, 169-177.

Saeed, A.I., Sharov, V., White, J., Li, J., Liang, W., Bhagabati, N., Braisted, J., Klapa, M., Currier, T., Thiagarajan, M., Sturn, A., Snuffin, M., Rezantsev, A., Popov, D., Ryltov, A., Konstukovich, E., Borisovsky, I., Liu, Z., Vinsavich, A., Trush, V. and Quackenbush, J. (2003): TM4: a free, open-source system for microarray data management and analysis. Biotechniques 34, 374-378.

Sakakibara, H. (2006): Cytokinins: activity, biosynthesis, and translocation. Annu. Rev. Plant. Biol. 57, 431-449.

Sakuraba, Y., Balazadeh, S., Tanaka, R., Mueller-Roeber, B. and Tanaka, A. (2012a): Overproduction of chl B retards senescence through transcriptional reprogramming in *Arabidopsis*. Plant Cell Physiol. 53, 505-517.

Sakuraba, Y., Schelbert, S., Park, S.-Y., Han, S.-H., Lee, B.-D., Andrès, C. B., Kessler, F., Hörtensteiner, S. and Paeck, N.-C. (2012b): Stay-green and chlorophyll catabolic enzymes interact at light-harvesting complex II for chlorophyll detoxification during leaf senescence in *Arabidopsis*. Plant Cell 24, 507-518.

Sattelmacher, B., Horst, W. J. and Becker, H. C. (1994): Factors contribute to genetic variation for nutrient efficiency of crop plants. Z. Pflanzenernähr. Bodenk. 157, 215-224.

Scheible, W.-R., Morcuende, R., Czechowski, T., Fritz, C., Osuna, D., Palacios-Rojas, N., Schindelasch O., Udvardi, M. K. and Stitt, M. (2004): Genome-wide reprogramming of primary and secondary metabolism, protein synthesis, cellular growth processes, and the regulatory infrastructure of *Arabidopsis* in response to nitrogen. Plant Physiol. 136, 2483–2499.

Schmidt, A., Baumann, N., Schwarzkopf, A., Frommer, W. B. and Desimone, M. (2006): Comparative studies on ureide permeases in *Arabidopsis thaliana* and analysis of two alternative splice variants of *AtUPS5*. Planta 224, 1329-1340.

Schmitz, R. Y., Skoog, F., Playtis, A. J. and Leonard, N. J. (1972): Cytokinins: synthesis and biological activity of geometric and position isomers of zeatin. Plant Physiol. 50, 702-705.

Schmülling, T., Werner, T., Riefler, M., Krupková, E. and Bartina y Manns, B. (2003): Structure and function of cytokinin oxidase/dehydrogenase genes of maize, rice, *Arabidopsis* and other species. J. Plant. Res. 116, 241-252.

Schmülling, T. (2004): Cytokinin. In Lennarz, W. and Lane, M. D. (ed.): Encyclopedia of Biological Chemistry. Academic Press / Elsevier Science.

Schull, G. H. (1922): Über die Heterozygotie mit Rücksicht auf den praktischen Züchtungserfolg. Beiträge zur Pflanzenzucht 5, pp. 134-158.

Schulte auf'm Erley, G., Wijaya, K.-A., Ulas, A. Becker, H, Wiesler, F. and Horst, W. J. (2007): Leaf senescence and N uptake parameters as selection traits for nitrogen efficiency of oilseed rape cultivars. Physiol. Plant. 130, 519-531.

Schulte auf'm Erley, G., Ambebe, T. F., Worku, M., Bänzinger, M. and Horst, W. J. (2010): Photosynthesis and leaf-nitrogen dynamics during leaf senescence of tropical maize cultivars in hydroponics in relation to N efficiency in the field. Plant Soil 330, 313-328.

Schulte auf'm Erley, G., Behrens, T., Ulas, A., Wiesler, F. and Horst W. J. (2011): Agronomic traits contributing to nitrogen efficiency of winter oilseed rape cultivars. Field Crops Res. 124, 114-123.

Scott, R. K., Ogunremi, E. A., Irvins, J. D. and Mendham, N. J. (1973): The effect of fertilizers and harvest date by growth and yield of oilseed rape sown in autumn and spring. J. Agric. Sci. 81, 287-293.

Sieling, K., Stahl, C., Winkelmann, C. and Christen, O. (2005): Growth and yield of winter wheat in the first 3 years of a monoculture under varying N fertilization in NW Germany. Europ. J. Agron. 22, 71-84.

Sieling, K. and Kage, H. (2006): N balance as an indicator of N leaching in an oilseed rape – winter wheat – winter barley rotation. Agric. Ecosyst. Environ. 115, 261-269.

Sieling, K. and Kage, H. (2008): The potential of semi-dwarf oilseed rape genotypes to reduce the risk of N leaching. J .Agr. Sci. 146, 77-84.

Sierts, H.-P., Geisler, G., Leon, J. and Diepenbrock, W. (1987): Stability of yield components from winter oil-seed rape (*Brassica napus* L.). J. Agron. Crop Sci. 158, 107-113.

Smart, C. M. (1994): Gene expression during leaf senescence. New. Phytol. 126, 419-448.

Smith, F. (1934): Response of inbred lines and crosses in maize to variations of nitrogen and phosphorous supplied as nutrients. J. Am. Soc. Agron. 26, 785-804.

Solfanelli, C., Poggi, A., Loreti, E., Alpi, A. and Perata, P. (2006): Sucrose-specific induction of the anthocyanin biosynthetic pathway in *Arabidopsis.* Plant Physiol. 140, 637-646.

Steibel, J. P., Poletto, R., Coussens, P. M. and Rosa, G. J. M. (2009): A powerful and flexible linear mixed model framework for the analysis of relative quantification RT-PCR data. Genomics 94, 146–152.

Stitt, M., Writz, W. and Heldt, H. W. (1983): Regulation of sucrose synthesis by cytoplasmic fructosebisphosphatase and sucrose phosphate synthase during photosynthesis in varying light and carbon dioxide. Plant Physiol. 72, 767-774.

Stitt, M., Wilke, I., Feil, R. and Heldt, H. W. (1988): Coarse control of sucrose-phosphate synthase in leaves: Alternations of the kinetic properties in response to the rate of photosynthesis and the accumulation of sucrose. Planta 174, 217-230.

Stoy, A. (1982): Die Herbstentwicklungen bestimmen den Rapsertrag, Bestandesdichte und Regenerationsvermögen bei Raps. DLG.-Mitt. 97, 791-792.

Sun, J., Zhang, J., Larue, C. T. and Huber, S. C. (2011): Decrease in leaf sucrose synthesis leads to increased leaf starch turnover and decreased RuBP regeneration-limited photosynthesis but not Rubisco-limited photosynthesis in *Arabidopsis* null mutants of SPSA1. Plant Cell Environ. 34, 592-604.

Sylvester-Bradley, R. and Kindred, D. R. (2009): Analyzing nitrogen responses of cereals to prioritize routes to the improvement of nitrogen use efficiency. J. Exp. Bot. 60, 1939–1951.

Szal, B. and Podgórska, A. (2012): The role of mitochondria in leaf nitrogen metabolism. Plant Cell Environ. 35, 1756-1768.

Tao, Y. Z., Henzell, R. G., Jordan, D. R., Butler, D. G., Kelly, A. M. and McIntyre, C. L. (2000): Identification of genomic regions associated with stay green in sorghum by testing RILs in multiple environments. Theor. Appl. Genet. 100, 12225-1235.

Tayo, T. O. and Morgan, D. G. (1975): Quantitative analysis of the growth, development and distribution of flowers and pods in oil seed rape (*Brassica napus* L.). J. Agric. Sci. 85, 103-110.

Teng, S., Keurentjes, J., Bentsink, L., Koornneef, M. and Smeekens, S. (2005): Sucrose-specific induction of anthocyanin biosynthesis in *Arabidopsis r*equires the *MYB75/PAP1* gene. Plant Physiol. 139, 1840-1852.

Thimm, O., Bläsing, O., Gibon, Y., Nagel, A., Meyer, S., Krüger, P., Selbig, J., Müller, L. A., Rhee, S. Y. and Stitt, M. (2004): MAPMAN: a user-driven tool to display genomics data sets onto diagrams of metabolic pathways and other biological processes. Plant J. 37, 914-939.

Thomas, H. and Howarth, C. J. (2000): Five ways to stay green. J. Exp. Bot. 51, 329-337.

Thomas, H. and Ougham, H. (2014): The stay-green trait. J. Exp. Bot. 65, 3889-3900.

Tilman, D. (1999): Global environmental impacts of agricultural expansion: The need for sustainable and efficient practices. Proc. Natl. Acad. Sci. 96, 5995-6000.

Tkachuk, R. (1981): Oil and protein analysis of whole rapeseed kernels by near infrared reflectance spectroscopy. J. Am. Oil Chem. Soc. 58, 819-822.

Tokunaga, H., Kojima, M., Kuroha, T., Ishida, T., Sugimoto, K., Kiba, T. and Sakakibara, H. (2012): *Arabidopsis* lonely guy (LOG) multiple mutants reveal a central role of the LOG-dependent pathway in cytokinin activation. Plant J. 69, 355-365.

Tollenaar, M. and Wu, J. (1999): Yield improvement in temperate maize is attributable to greater stress tolerance. Crop Sci. 39, 1597–1604.

Trifunović, M., Cingel, A., Simonović, A., Jevremović, S., Petrić, M., Dragićević, I. C., Motyka, V., Bobrev, P. I., Zahajská, L. and Subotić, A. (2013): Overexpression of Arabidopsis cytokinin oxidase/dehydrogenase genes *AtCKX1* and *AtCKX2* in transgenic *Centaurium erythraea* Rafn.. Plant Cell Tiss. Organ. Cult. 115, 139-150.

Ulas, A. (2010): Agronomic and physiological parameters of genetic nitrogen efficiency in oilseed rape (*Brassica napus* L.). Ph.D. Thesis. Leibniz University Hannover, Germany.

Ulas, A., Schulte auf'm Erley, G., Kamh, M., Wiesler, F. and Horst, W. J. (2012): Root-growth characteristics contributing to genetic variation in nitrogen efficiency of oilseed rape. J. Plant Nutr. Soil Sci. 175, 489-498.

Ulas, A., Behrens, T., Wiesler, F., Horst, W. J. and Schulte auf'm Erley, G. (2013): Does genotypic variation in nitrogen remobilization efficiency contribute to nitrogen efficiency of winter oilseed-rape cultivars (*Brassica napus* L.)? Plant Soil 371, 463-471.

van der Graaff, E., Schwacke, R., Scheider, A., Desimone, M., Flügge, U.-F. and Kunze, R. (2006): Transcription analysis of *Arabidopsis* membrane transporters and hormone pathways during developmental and induced leaf senescence. Plant Physiol. 141, 776-792.

Verwoerd, T. C., Dekker, B. M. M. and Hoekema, A. (1989): A small-scale procedure for rapid isolation of plant RNAs. Nucleic Acids Res. 17, 2362.

von Wirén, N. and Merrick, M. (2004): Regulation and function of ammonium carriers in bacteria, fungi, and plants. Top. Curr. Genet. 9, 95-120.

Wang, A., Li, Y. and Zhang, C. (2012): QTL mapping for stay-green in maize (*Zea mays*). Can. J. Plant Sci. 92, 249-256.

Wang, J., Ma, X.-M., Kojima, M., Sakakibara, H. and Hou, B.-K. (2013): Glucosyltransgerase *UGT76C1* finely modulates cytokinin responses via cytokinin *N*-glucosylation in *Arabidopsis thaliana*. Plant Physiol. Biochem. 65, 9-16.

Ward, J. T., Basford, W. D., Hawkins, J. H. and Holliday, J. M. (1985): Species and varieties of oilseed rape. In Ward, J. T., Basford, W. D., Hawkins, J. H. and Holliday, J. M.: Oilseed rape. Farming Press, pp. 42-58.

Weltmeier, F., Mäser, A., Menze, A., Henning, S., Schad, M., Breuer, F., Schulz, B., Holtschulte, B., Nehls, R. and Stahl, D. J. (2011): Transcript profiles in sugar beet genotypes uncover timing and strength of defense reactions to Cercospora beticola infection. Mol. Plant Microbe Int. 24, 758-772.

Wiesler, F., Behrens, T. and Horst, W. J. (2001): The role of nitrogen-efficient cultivars in sustainable agriculture. In Optimizing Nitrogen Management in Food and Energy Production and Environmental Protection: Proceedings of the 2nd International Nitrogen Conference on Science and Policy. TheScientificWorld 1(S2), 61-69.

Wingler, A., Purdy, S., MacLean, J. A. and Pourtau, N. (2006): The role of sugars in integrating environmental signals during the regulation of leaf senescence. J. Exp. Bot. 57, 391-399.

Wittkop, B. Snowdown, R. J. and Friedt, W. (2009): Status and perspectives of breeding for enhanced yield and quality of oilseed crops for Europe. Euphytika 170, 131-140.

Wolfe, D. W., Henderson, D. W., Hsiao, T. C. and Alvino, A. (**1988):** Interactive water and nitrogen effects on senescence of maize. I. leaf area duration, nitrogen distribution, and yield. Agron. J. 80, 859-864.

Worku, M., Bänzinger M., Schulte auf'm Erley, G., Friesen, D., Diallo, A. O. and Horst, W. J. (2007): Nitrogen uptake and utilization in contrasting nitrogen efficient tropical maize hybrids. Crop. Sci. 47, 519-528.

Worrell, A. C., Bruneau J. M., Summerfelt, K., Boersig, M. and Voelker, T. A. (1991): Expression of a maize sucrose phosphate synthase in tomato alters leaf carbohydrate partitioning. Plant Cell 3, 1121-1130.

Wu, A., Allu, A. D., Garapati, P., Siddiqui, H., Dortay, H., Zanor, M.-I., Asensi-Fabado, M. A., Munné-Bosch, S., Antonio, C., Tohge, T., Fernie, A. R., Kaufmann, K., Xue, G.-P., Mueller-Roeber, B. and Balazadeh, S. (2012): JUNGBRUNNEN1, a Reactive Oxygen Species–Responsive NAC Transcription Factor, Regulates Longevity in *Arabidopsis*. Plant Cell 24, 482-506.

Würschum, T., Liu, W., Maurer, H. P., Abel, S. and Reif, J. C. (2012): Dissecting the genetic architecture of agronomic traits in multiple segregating populations in rapeseed (*Brasscia naups* L.). Theor. Appl. Genet. 124, 153-161.

Xu, W., Subudhi, P. K., Crasta, O. R., Rosenow, D. T., Mullet, J. E. and Nguyen, H. T. (2000): Molecular mapping of QTLs conferring stay-green in grain sorghum (*Sorghum bicolor* L. Moench). Genome 43, 461-469.

Yoshiharu, W., Kunio, M. and Kazuyuki, W. (1993): Effects of source-to-sink ratio on carbohydrate production and senescence of rice flag leaves during the ripening period. Jpn. J. Crop Sci. 62, 547-553.

Yuan, T., Fujioka, S., Takatsuto, S., Matsumoto, S., Gou, X., He, K., Russell, S. D. and Li, J. (2007): *BEN1*, a gene encoding a dihydroflavonol 4-reductase (DFR)-like protein, regulates the levels of brassinosteroids in *Arabidopsis thaliana*. Plant J. 51, 220-233.

Zhao, J., Becker, H. C., Zhang, D., Zhang, Y. and Ecke, W. (2006): Conditional QTL mapping of oil content in rapessed with respect to protein content and traits related to plant development and grain yield. Theor. Appl. Genet. 113, 33-38.

Zrenner, R., Stitt, M., Sonnewald, U. and Boldt, R. (2006): Pyrimidine and purine biosynthesis and degradation in plants. Annu. Rev. of Plant Biol. 57, 805-836.

Zwack, P. J. and Rashotte, A. M. (2013): Cytokinin inhibition on leaf senescence. Plant Signal. Behav. 8, e24737; http://dx.doi.org/10.4161/psb.24737.

Supplementary Material

Supplementary Material for Chapter I

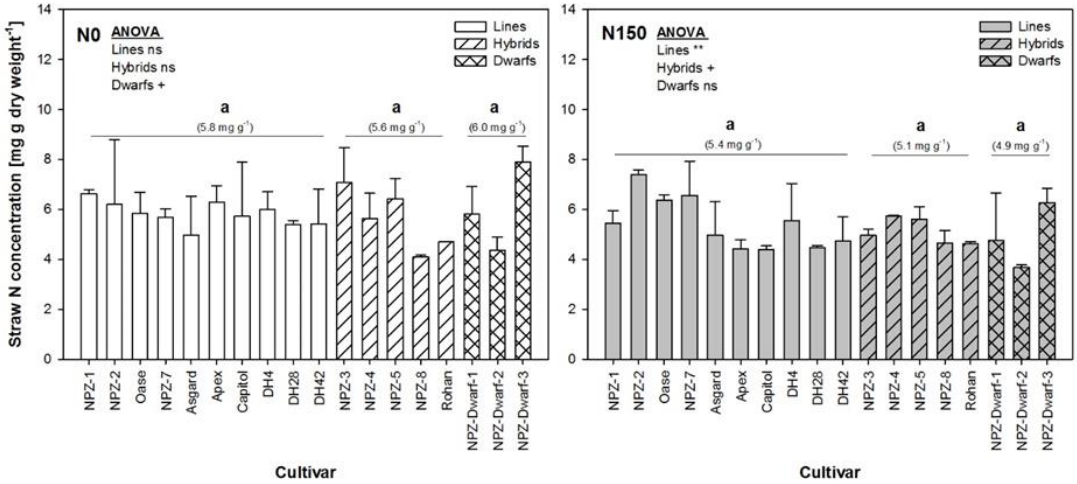

Figure SI-1 Straw (shoot + pod walls) N concentration of winter oilseed-rape lines (*n* = 10), hybrids (*n* = 5) and dwarfs (*n* = 3) as affected by N fertilization rate in 2009. () mean N concentrations. Different letters on top of the columns indicate differences between the types of cultivars at p <0.05. For the ANOVA +, ** indicate significant differences at p <0.10, <0.01, respectively. ns = non-significant. The error bars represent the standard deviations of the means (n = 2).

Table SI-1 F-test for straw dry weight in 2009 and 2010 as affected by cultivar, N fertilization rate and year and their interactions for all cultivars, and separately for lines, hybrids and dwarfs (n = 2). For the F-test +, **, * indicate significant differences at p <0.10, <0.01, <0.001, respectively. ns = non-significant.**

	Straw dry weight			
	All (*n* = 18)	**Lines (*n* = 10)**	**Hybrids (*n* = 5)**	**Dwarfs (*n* = 3)**
Cultivar	***	**	**	ns
N rate	ns	ns	ns	ns
Year	ns	ns	ns	ns
Cultivar x N	ns	ns	ns	ns
Cultivar x Year	ns	ns	ns	ns
Cultivar x N x Year	ns	ns	ns	ns

Table SI-2 F-test for the grain yield in 2009 and 2010 as affected by cultivar, N fertilization rate and year and their interactions for all cultivars, and separately for lines, hybrids and dwarfs (n = 2). For the F-test +, *, **, * indicate significant differences at p <0.10, <0.05, <0.01, <0.001, respectively. ns = non-significant.**

	All (*n* = 18)	**Lines (*n* = 10)**	**Hybrids (*n* = 5)**	**Dwarfs (*n* = 3)**
Cultivar	***	***	+	**
N rate	*	+	ns	+
Year	ns	ns	ns	ns
Cultivar x N	ns	ns	ns	ns
Cultivar x Year	*	*	ns	ns
Cultivar x N x Year	ns	ns	ns	ns

Table SI-3 F-test for the thousand grain weight in 2009 as affected by cultivar and N fertilization rate and their interaction for all cultivars, and separately for lines, hybrids and dwarfs (n = 2). For the F-test *, * indicate significant differences at p <0.05, <0.001, respectively. ns = non-significant.**

	All (*n* = 18)	Lines (*n* = 10)	Hybrids (*n* = 5)	Dwarfs (*n* = 3)
Cultivar	***	***	ns	*
N rate	ns	ns	ns	ns
Cultivar x N	ns	ns	ns	ns

Table SI-4 F-test for the grain N concentration in 2009 as affected by cultivar and N fertilization rate and their interaction for all cultivars, and separately for lines, hybrids and dwarfs (n = 2). For the F-test +, *, ** indicate significant differences at p <0.10, <0.05, <0.01, respectively. ns = non-significant.

	All (*n* = 18)	Lines (*n* = 10)	Hybrids (*n* = 5)	Dwarfs (*n* = 3)
Cultivar	**	ns	+	*
N rate	+	**	ns	ns
Cultivar x N	ns	ns	ns	ns

Table SI-5 F-test for the oil concentration in the grain in 2009 and 2010 as affected by cultivar, N fertilization rate and year and their interactions for all cultivars, and separately for lines, hybrids and dwarfs (n = 2). For the F-test +, * indicate significant differences at p <0.10, <0.001, respectively. ns = non-significant.**

	All (*n* = 18)	Lines (*n* = 10)	Hybrids (*n* = 5)	Dwarfs (*n* = 3)
Cultivar	***	***	***	***
N rate	ns	ns	ns	ns
Year	ns	ns	ns	ns
Cultivar x N	ns	+	ns	ns
Cultivar x Year	ns	ns	ns	ns
Cultivar x N x Year	***	***	***	***

Table SI-6 F-test for the protein concentration in the grain and in the grain-meal in 2009 and 2010 as affected by cultivar, N fertilization rate and year and their interactions for all cultivars, and separately for lines, hybrids and dwarfs (n = 2). For the F-test *, * indicate significant differences at p <0.05, <0.001, respectively. ns = non-significant.**

	Grain				Rapeseed meal			
	All (*n* = 18)	Lines (*n* = 10)	Hybrids (*n* = 5)	Dwarfs (*n* = 3)	All (*n* = 18)	Lines (*n* = 10)	Hybrids (*n* = 5)	Dwarfs (*n* = 3)
Cultivar	***	***	*	***	***	***	*	***
N rate	ns	ns	ns	ns	ns	ns	ns	ns
Year	ns	ns	ns	ns	ns	ns	ns	ns
Cultivar x N	ns	ns	ns	ns	ns	ns	ns	ns
Cultivar x Year	ns	ns	ns	ns	ns	ns	ns	ns
Cultivar x N x Year	***	***	ns	ns	***	***	ns	ns

Table SI-7 F-test for the N content in the grain and straw at maturity in 2009 as affected by cultivar, N fertilization rate and their interaction for all cultivars, and separately for lines, hybrids and dwarfs (n = 2). For the F-test +, *, **, * indicate significant differences at p <0.10, <0.05, <0.01, <0.001, respectively. ns = non-significant.**

	Grain				Straw			
	All (*n* = 18)	**Lines** (*n* = 10)	**Hybrids** (*n* = 5)	**Dwarfs** (*n* = 3)	**All** (*n* = 18)	**Lines** (*n* = 10)	**Hybrids** (*n* = 5)	**Dwarfs** (*n* = 3)
Cultivar	***	***	ns	ns	***	***	**	**
N rate	+	*	ns	ns	ns	ns	ns	ns
Cultivar x N	ns	ns	ns	ns	**	*	*	ns

Table SI-8 F-test for the N utilization efficiency (NUE), N harvest index (NHI) and harvest index (HI) at maturity in 2009 as affected by cultivar, N fertilization rate and their interaction for all cultivars, and separately for lines, hybrids and dwarfs (n = 2). For the F-test +, *, **, * indicate significant differences at p <0.10, <0.05, <0.01, <0.001, respectively. ns = non-significant.**

	NUE				NHI				HI			
	All (*n* = 18)	**Lines** (*n* = 10)	**Hybrids** (*n* = 5)	**Dwarfs** (*n* = 3)	**All** (*n* = 18)	**Lines** (*n* = 10)	**Hybrids** (*n* = 5)	**Dwarfs** (*n* = 3)	**All** (*n* = 18)	**Lines** (*n* = 10)	**Hybrids** (*n* = 5)	**Dwarfs** (*n* = 3)
Cultivar	***	**	***	**	***	+	*	**	***	***	*	**
N	ns	ns	ns	ns	ns	ns	ns	**	ns	ns	ns	ns
Cultivar x N	+	ns	**	ns	+	+	ns	ns	ns	ns	+	ns

Table SI-9 F-test for SPAD affected by cultivar, N fertilization rate, leaf position, BBCH and year and their interactions for all and separately for lines, hybrids and dwarfs (n = 2). For the F-test +, *, **, * indicate significant differences at p <0.10, <0.05, <0.01, <0.001, respectively. ns = non-significant.**

	All (*n* = 18)	Lines (*n* = 10)	Hybrids (*n* = 5)	Dwarfs (*n* = 3)
Cultivar	***	***	ns	***
N rate	+	+	ns	+
Leaf	***	***	***	***
BBCH	***	***	***	***
Year	ns	ns	ns	ns
Cultivar x N	***	**	***	*
Cultivar x Leaf	***	**	*	***
Cultivar x BBCH	***	***	**	***
Cultivar x Year	***	**	**	***
N x leaf	ns	ns	ns	ns
N x BBCH	ns	ns	ns	+
N x Year	ns	ns	ns	ns
Leaf x BBCH	***	***	***	***
Leaf x Year	***	***	+	ns
Cultivar x N x Leaf	ns	ns	ns	ns
Cultivar x N x BBCH	*	+	ns	ns
Cultivar x N x Year	*	*	ns	ns
N x Leaf x BBCH	ns	ns	ns	ns
N x Leaf x Year	***	**	ns	*
Cultivar x N x Leaf x BBCH	ns	ns	ns	ns
Cultivar x N x Leaf x Year	ns	ns	ns	ns
N x Leaf x BBCH x Year	***	***	*	***
Cultivar x N x Leaf x BBCH x Year	***	ns	+	***

Table SI-10 F-test for SPAD of leaf 6 on the main stem affected by cultivar, N fertilization rate, BBCH and year and their interactions for all and separately for lines, hybrids and dwarfs (n = 2). For the F-test +, *, **, * indicate significant differences at p <0.10, <0.05, <0.01, <0.001, respectively. ns = non-significant.**

	All (*n* = 18)	Lines (*n* = 10)	Hybrids (*n* = 5)	Dwarfs (*n* = 3)
Cultivar	***	***	*	***
N rate	ns	ns	ns	ns
BBCH	***	***	**	***
Year	ns	ns	ns	ns
Cultivar x N	*	*	ns	ns
Cultivar x BBCH	***	***	*	***
Cultivar x Year	***	ns	**	**
N x BBCH	ns	ns	ns	*
N x Year	ns	ns	ns	ns
Cultivar x N x BBCH	*	*	ns	ns
Cultivar x N x Year	*	+	ns	ns
N x BBCH x Year	***	***	+	***
Cultivar x N x BBCH x Year	***	*	*	*

Table SI-11 F-test for percentage of green leaves during the reproductive phase on the main stem affected by cultivar, N fertilization rate, DAF and year and their interactions for all and separately for lines, hybrids and dwarfs (n = 2). For the F-test +, **, * indicate significant differences at p <0.10, <0.01, <0.001, respectively. ns = non-significant.**

	All (*n* = 18)	Lines (*n* = 10)	Hybrids (*n* = 5)	Dwarfs (*n* = 3)
Cultivar	***	***	***	***
N rate	ns	ns	ns	ns
DAF	***	***	***	***
Year	ns	ns	ns	ns
Cultivar x N	***	***	***	***
Cultivar x DAF	***	***	***	***
Cultivar x Year	***	***	***	***
N x DAF	***	***	***	***
N x Year	ns	ns	ns	ns
Cultivar x N x DAF	**	+	**	ns
Cultivar x N x Year	***	***	**	**
N x DAF x Year	***	***	**	***
Cultivar x N x DAF x Year	**	**	ns	ns

Table SI-12 F-test for the shoot and root dry matter and the root to shoot ratio as affected by the cultivar and N supply and their interaction separately for lines and hybrids grown in hydroponics 12 days after treatment started (n = 4). For the F-test +, *, **, * indicate significant differences at p <0.10, <0.05, <0.01, <0.001, respectively. ns = non-significant.**

	Shoot dry matter [g shoot^{-1}]	Root dry matter [g root^{-1}]	Root:Shoot [g g^{-1}]
Lines (*n* = 9)			
Cultivar	**	ns	**
N rate	***	***	***
Cultivar x N	ns	*	**
Hybrids (*n* = 3)			
Cultivar	+	ns	ns
N rate	***	ns	***
Cultivar x N	ns	*	ns

Table SI-13 F-test for the shoot and root N concentration and Nuptake as affected by the cultivar and N supply and their interaction separately for lines and hybrids grown in hydroponics 12 days after treatment started (n = 4). For the F-test *, **, * indicate significant differences at p <0.05, <0.01, <0.001, respectively. ns = non-significant.**

	Shoot		Root	
	N conc. [%]	N uptake [mg plant^{-1}]	N conc. [%]	N uptake [mg root^{-1}]
Lines (*n* = 9)				
Cultivar	**	*	**	*
N rate	***	***	***	***
Cultivar x N	ns	ns	ns	ns
Hybrids (*n* = 3)				
Cultivar	ns	*	***	ns
N rate	***	***	***	***
Cultivar x N	ns	*	ns	ns

Table SI-14 F-test for root length, length to weight ratio and N uptake per unit root length as affected by the cultivar and N supply and their interaction separately for lines and hybrids grown in hydroponics 12 days after treatment started (n = 4). For the F-test +, *, **, * indicate significant differences at p <0.10, <0.05, <0.01, <0.001, respectively. ns = non-significant.**

	Root length [m]	Root length:weight [m g^{-1}]	N uptake:length [mg m^{-1}]
Lines (*n* = 9)			
Cultivar	+	ns	ns
N rate	+	**	***
Cultivar x N	ns	*	ns
Hybrids (*n* = 3)			
Cultivar	*	ns	ns
N rate	ns	ns	***
Cultivar x N	ns	ns	ns

Supplementary Material for Chapter II

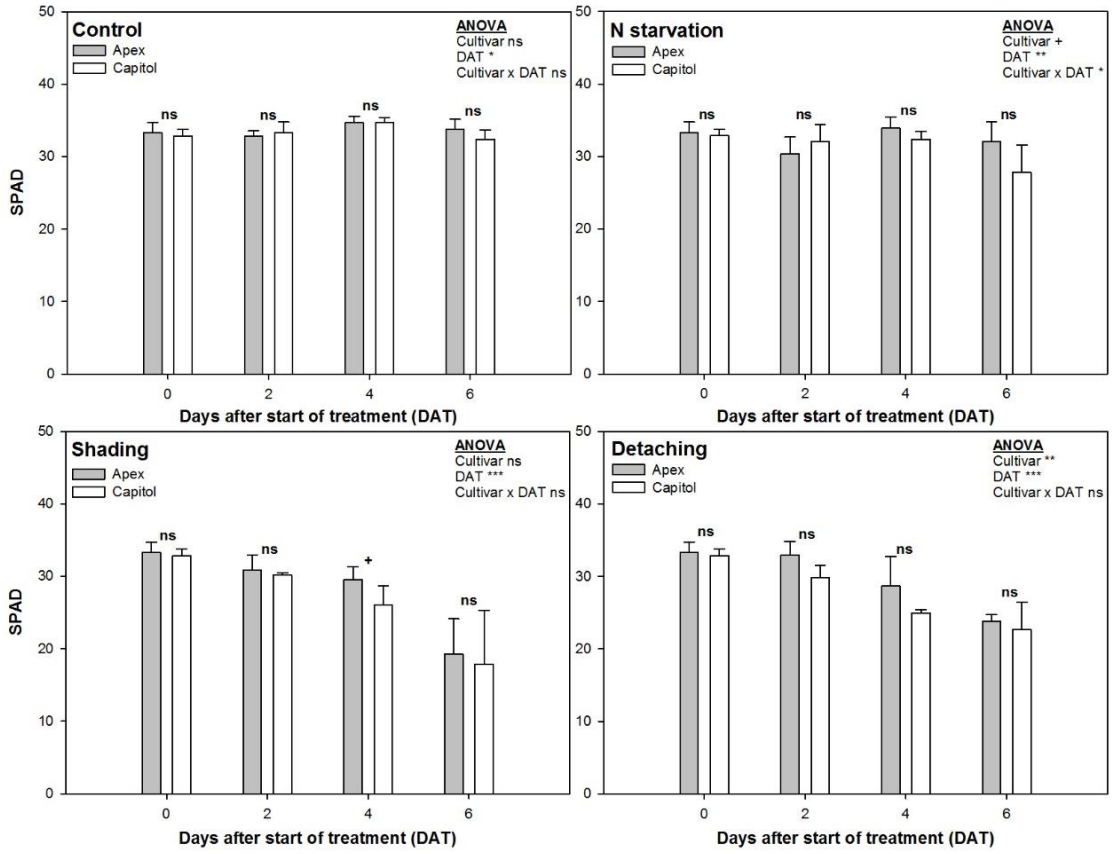

Figure SII-1 SPAD of leaf three of the winter oilseed-rape cultivars Apex and Capitol as affected by three leaf-senescence inducers (0.1 mM N, shading, detaching) and the 2.0 *mM* N control. The plants were grown in hydroponics for 28 days at 2.0 mM N and were then treated for up to six days. Detached leaves were cultured in Erlenmeyer flasks containing deionized water. For the ANOVA +, *, **, * indicate significant differences at p <0.10, <0.05, <0.01, <0.001, respectively. ns = non-significant. The error bars represent the standard deviations of the means (n = 3 to 5).**

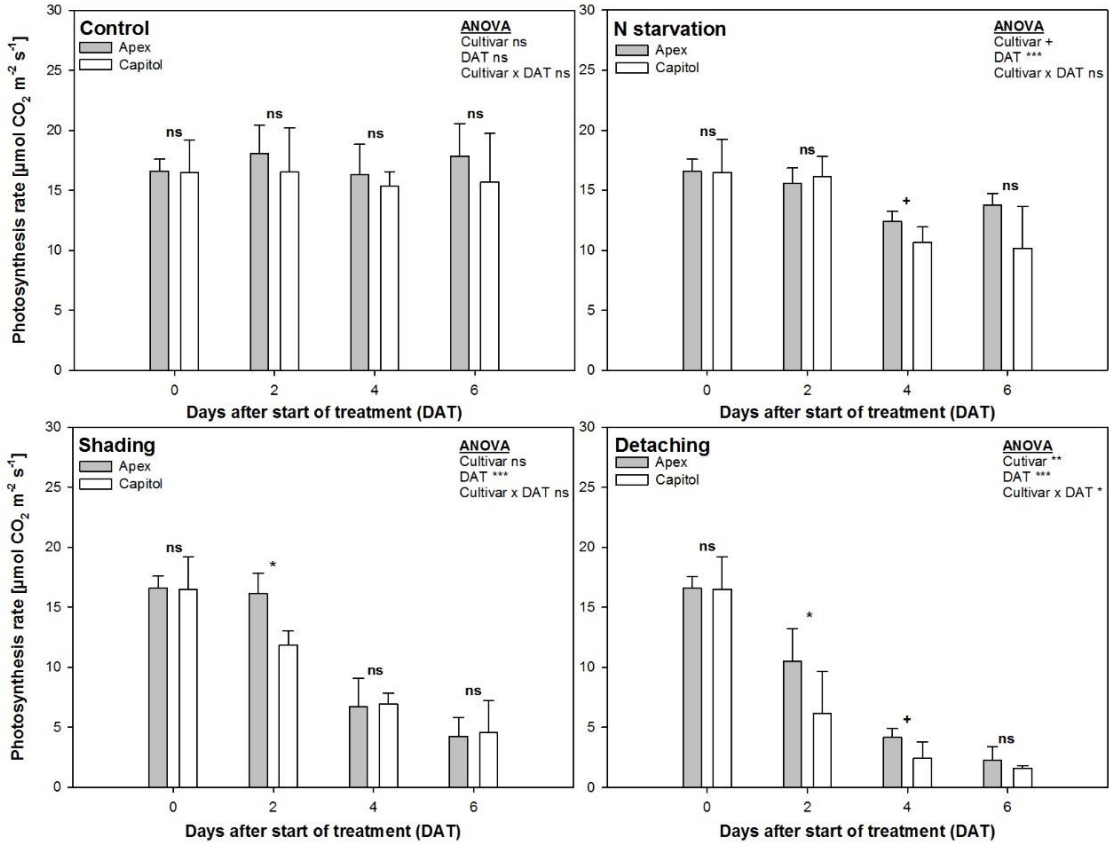

Figure SII-2 Photosynthesis rate of leaf three of the winter oilseed-rape cultivars Apex and Capitol as affected by three different leaf senescence inducers (0.1 *mM* N, shading, detaching) and the 2.0 *mM* N control. The plants were grown in hydroponics for 28 days at 2.0 *mM* N and were then treated for up to six days. Detached leaves were cultured in Erlenmeyer flasks containing deionized water. For the ANOVA +, *, **, * indicate significant differences at p <0.10, <0.05, <0.01, <0.001, respectively. ns = non-significant. The error bars represent the standard diviations of the means (n = 3 to 5).**

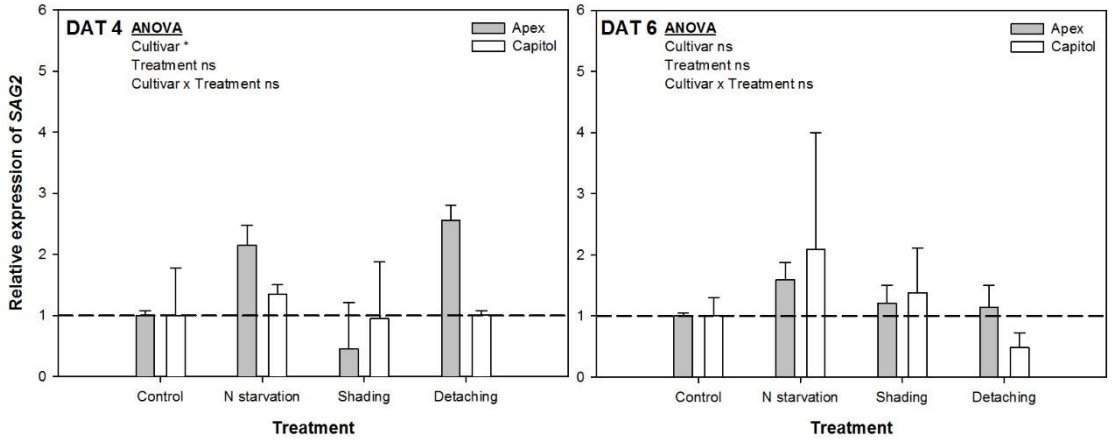

Figure SII-3 Relative expression ($2^{-\Delta\Delta Ct}$) of the senescence-specific cysteine protease *SAG2* of leaf three of the winter oilseed-rape cultivars Apex and Capitol as affected by three different leaf senescence inducers (0.1 *mM* N, shading, detaching) and the 2.0 *mM* N control. The plants were grown in hydroponics for 28 days at 2.0 *mM* N and were then treated for up to six days. The data are shown relative to the control. For the ANOVA * indicates significant differences at p <0.05. ns = non-significant. The error bars represent the standard errors of the means (n = 3).

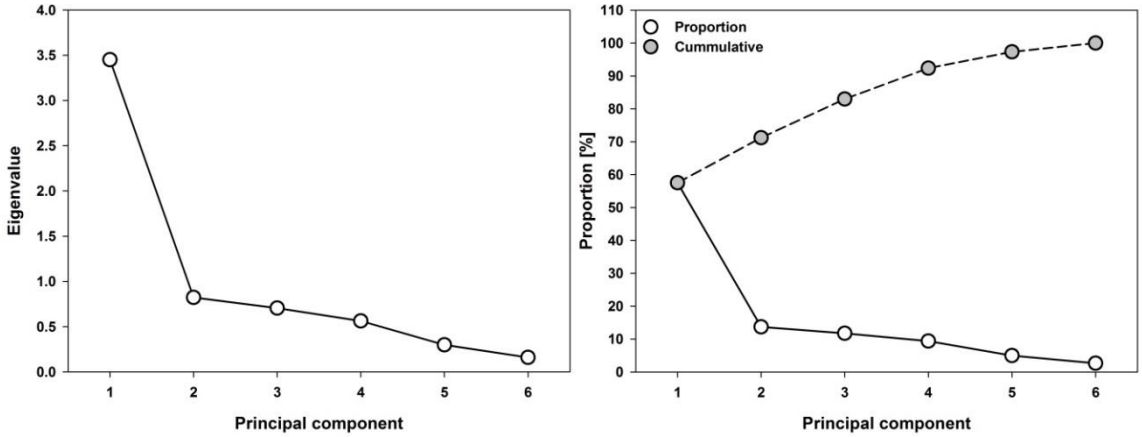

Figure SII-4 Eigenvalues of the six principal factors and their proportion to the overall eigenvalue of the six experimental variants. The different leaf senescence inducers (0.1 *mM* N, shading, detaching) were compared to the 2.0 *mM* N control (n = 3). The plants were grown in hydroponics for 28 days at 2.0 mM N and were then treated for four days.

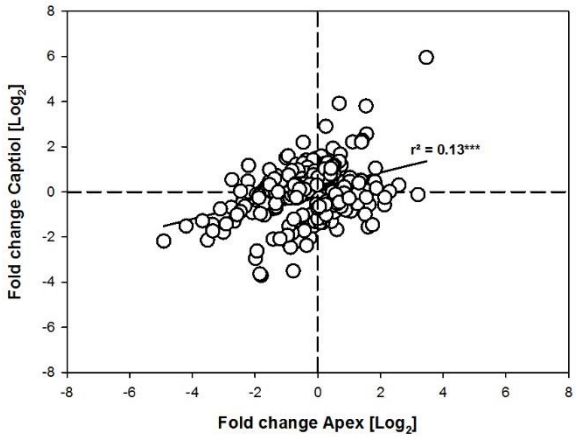

Figure SII-5 Correlation of the log_2-fold changes of the 407 N starvation-specifically regulated and a significant cultivar x inductor interaction showing targets on the custom microarray of the winter oilseed-rape cultivars Apex and Capitol. The log_2-fold changes of the 407 targets for each cultivar were calculated between N starvation (0.1 *mM* N) and the 2.0 *mM* N (n = 3).

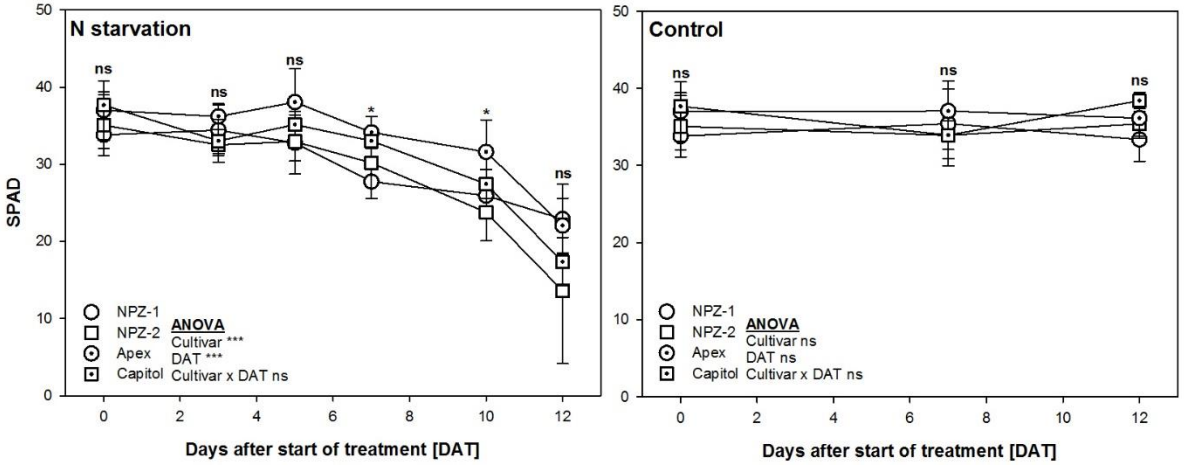

Figure SII-6 SPAD of the second oldest harvested leaf of four winter oilseed-rape cultivars grown in hydroponics during 12 days of N starvation (0.1 *mM*) or optimal N supply (4.0 *mM*). The plants were pre-cultured for 28 days at 2.0 *mM* N. For the ANOVA *, * indicate significant differences at p <0.05, <0.001, respectively. ns = non-significant. The error bars represent the standard deviations of the means (n = 3 to 4).**

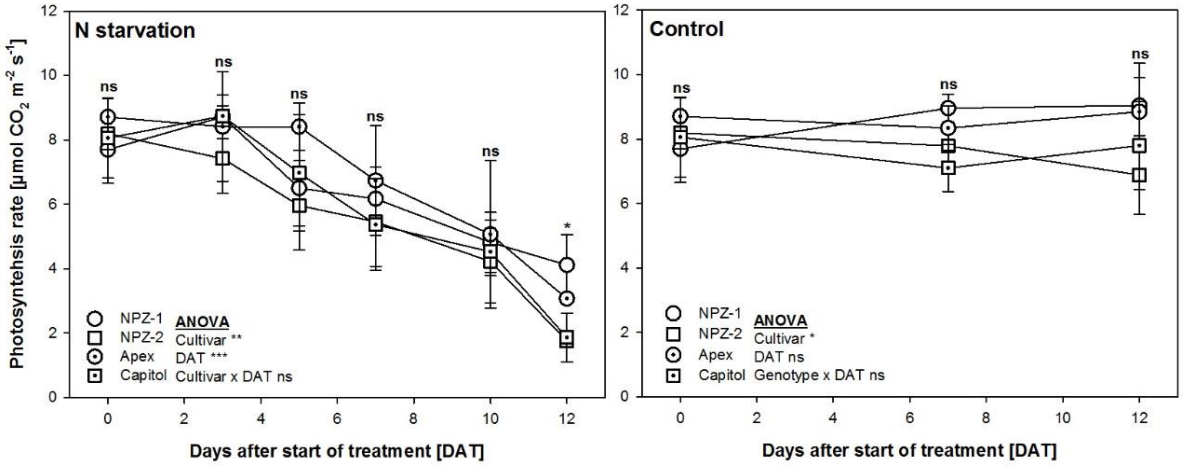

Figure SII-7 Photosynthesis rate of the second oldest harvested leaf of four winter oilseed-rape cultivars grown in hydroponics during 12 days of N starvation (0.1 *mM*) or optimal N supply (4.0 *mM*). The plants were pre-cultured for 28 days at 2.0 *mM* N. For the ANOVA *, **, * indicate significant differences at p <0.05, <0.01, <0.001, respectively. ns = non-significant. The error bars represent the standard deviations of the means (n = 3 to 4).**

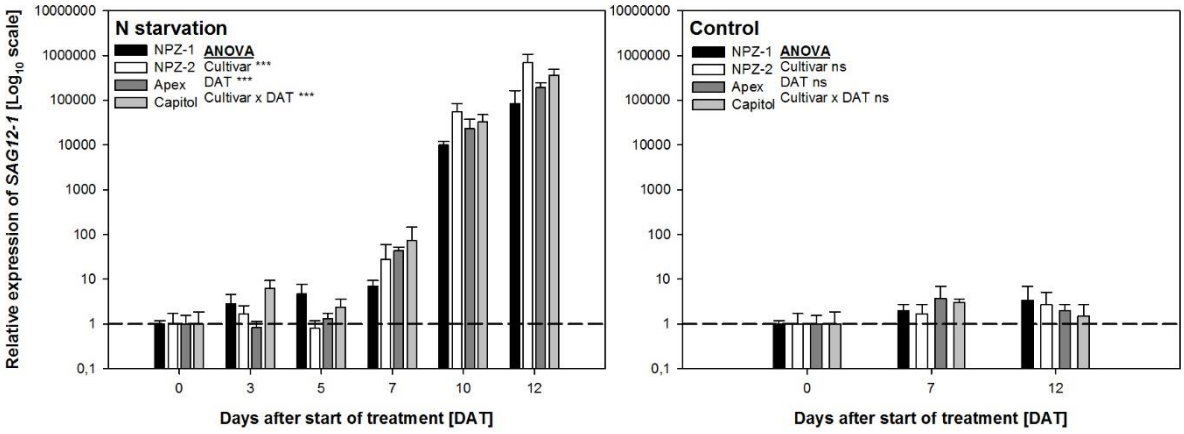

Figure SII-8 Relative expression ($2^{-\Delta\Delta Ct}$) of *SAG12-1* of the second oldest harvested leaf of four winter oilseed-rape cultivars grown in hydroponics during 12 days of N starvation (0.1 *mM*) or optimal N supply (4.0 *mM*). The plants were pre-cultured for 28 days at 2.0 *mM* N. For the ANOVA *, **, * indicate significant differences at p <0.05, <0.01, <0.001, respectively. ns = non-significant. The error bars represent the standard error of the means (n = 3 to 4).**

Table SII-1 Primer sequences of the genes of interest and the reference genes (underlined).

DFCI (NCBI) accession number	Forward primer sequence (5' → 3')	Reverse primer sequence (5' → 3')
(DQ312264)	AGGTCCACCAACCTTGACTG	CCGTTCCAATACCACCAATC
(DQ209288)	GAGCAACAGCTTGTGGATTGTGCT	GGCCGCCGTTGGATTTGATGTATT
(AF089848)	TACGTGTAGGATGTTGTTGGGCGT	TGGCCATTATGTGCTCAAACGCAG
TC111660	GTGTTCTTGGCCGGTACAAACC	ACCGTCGCAACTTGTGTCATGG
TC111745	GAGGGAACATAGCGCATAACGTC	CCAACACACCAATCCCTGACTC
TC194033	AGCCTGAGGAGATATTAGCAGGAA	ATCTCACTGCAGCTCCACCAT
CD832369	CACTGGAAGAGGAGTGATGTTGGG	TGACCAAACGTTGCCCTGAGATG
cluster000639.a1.2	AGGTCGAAGGTGCAGACTCATC	TGAAATCCTGACCGTCTGATTGAC
cluster001239.a1.1	AGGCCAGTCTTTGGTGGTTTGG	TGTCCACCTGAGATGCAGCTTG
cluster001790.a1.1	TGAACAGGGTTAGGAACGGTGAG	TACAACGCAGGCTGCACAAAGG
cluster003131.a1.1	GCTTCAACCATGAGACGCAACG	AGGCATGATGACACGGTCGTAG
cluster003131.a1.2	ACACTGGCCAAAGAAGGAGAAAG	GTTGCGAATACGGCCAAGACAG
cluster003288.a1.490	AGTCCCTTTGATGGTGGTCGAAG	GAACGTCTTGTTCTCGGCTTGC
cluster004849.a1.1	CACGAAGCTAGGTCCTTGGAAGTG	AGGACGAATCGTTGAAGCTTCTGG
cluster005374.a1.1	ACGAGAGCTTTCTTGACGCCTAC	TTGGAAAGCGACCGGTACAGAC
cluster005426.a1.1	TCAGTTCAAGGGACAAGAGTTCGC	TAACCCTGTGGGTGCTAAGTGG
cluster006216.a1.1	ACCAAACCCGTAGCTTCCCTTC	TCATCGGACTCCACAGCTTTCTTG
cluster006594.a1.1	AGCAGAGACAGCGATCTTGAAGC	GCAAAGCTACAGCCTTCACAGC
cluster006605.a1.686	ACATAGCCCATCTCGCGTGAATC	TGGCAAGAAGCCTGAGAACTTCG
cluster009061.a1.1	GCTGCTAACCATCCAACTGATCCC	TGTCTGGGAGAATGACCACACC
cluster010637.a1.1	GTCGAGTCCGACGTTTGTGTTG	TTCCTTCTGTCGCCTGAGTTCC
cluster011761.a1.1	TCCACACGTTACCCATCAGTCC	AGTCGTAATGCAGCCTGTTAAGC
cluster012345.a1.1	CAAACGCACCCTTGCTTCAACC	TAGAGGCAGGGTTTCCCAGAAG
cluster012772.a1.1	TGCGTTGATTGCGGAACACTCC	TTGCACAGCGACTTAGGACCAG
cluster013228.a1.1	AACACCGACATGGGAGTCATCC	AGTTGAGCGCATGAGACGAACG
cluster013301.a1.1	TAGTCCTGCGACTCCTCTAGCATC	AGACAACGCAGTGCTTCTTCGC
cluster016928.a1.1	CAACCACTTTAGCTGGCTGCAC	TAACGTTCCAGTGTCCCGAGAG
cluster018029.a1.1	AGAAACGCTCCTTGGAATGTCCTC	AAACTCTGCTCCTGCAGTTTGGC
cluster019568.a1.1	ACTTGGCTCACAAGGGAAGTGC	AGCACTCTGGTTACGGTTCAGC
cluster020567.a1.1	TGGCAGAGCTTGGAGACGAATC	AGCATGGCTTCGAATCTGAACCG
cluster022584.a1.1	TGCCTTGGGAACTCTTGAGCAC	ATCGGACCCACCGGTTACATTC
cluster024535.a1.1	TAGGCACTTTCGACACTCCCGAAG	TTTGATGCCACGGAGGAAACGG
cluster025990.a1.1	AGCAGAGAAGGAGATGGTCACAGG	AGGCTGTGAAGAGCATCAACGAAC
cluster026106.a1.1	AGGCGACACGAAGAAGACATGC	ACCACGCCAAAGTGGAGTCTTG
cluster032894.a1.1	ACTCCCGAGGAAGATCAGAAGC	AGAGTTCGCCATCCACCTTCAC
cluster034340.a1.1	GAGCTGTGCTTGTTGCTGTTGC	CAGCTCCTGCAATAGTTGCGTTG
cluster034847.a1.1	AAGGCGTTCGTGTCTGGTTAGG	AAAGCAGCCCTGTCGTAACCTC
cluster038644.a1.1	ACAGTCATCAGGTTCGGTTCACG	TGACCAACCCATGTTGCTGTCTG
CN727103	TAGCGAAAGACTTGGGCAGCAC	AGCGCACACAAAGACCACAACC
DY000543	TCAGCGAAACGATTTGCGACAATG	TTGTTGTTGCGGAGAGCTTGGC
DY023720	TGCATGAGAGGCAGGAAATACAAG	TCCAGAAACCTGAACCGGTGAC
EE436585	TTTACCAGTCAGAGATGGCCAAGG	GAAGAAACTGCTTTCCCAATCTGC
EE447860	CGTGGCATTCGCCAATTCCTTAC	AGCAAAGGCGATGAGTCCAATC
EE478159	CGCAGAAGTCATGTGGCAAGAAC	TCGGAATGACTTCGCTCATTGGC
EE545548	ACTGTCGGAGCCTTGTCACTTG	ACCTGTTCCAAATACAACCGCAAC

DFCI (NCBI) accession number	Forward primer sequence (5' → 3')	Reverse primer sequence (5' → 3')
EE558066	TGATATAAGCGACGAGCATTCGG	ACGTCGACGGGATAAAGAGAGG
EG020899	TTCAAGGCCACGAGATGACCAC	AATCCGACCCGTGTTGAGAGAG
EL623648	TAGGGCTTACGATGCTGCTCTC	AGTGCTTGGGAAGTTGAGATTGGC
ES265746	CGAAACCGTCTCCGGCAAATTC	AGAGGAGGTACGTGTTGTCGATG
ES901674	AGACCCGACATTAAGAGAGGAGAG	ATTGCGGCCCACTTGTTACC
ES910034	ACTGTTGCTTGTACAGTTCCTCTG	AAACCAAGTTTGGGCCCTACAG
ES913305	ACCAACCAGCGGAGAAACGTAG	CGATCAAGATCCTCCCACATAGCC
ES952533	TCTTCCGTGGAGCTAGACCCTAAC	AGAGAACCGAAGGGTCAAACGG
EV018246	CGGAGGCCATGAACATTCTGTCAC	GATCCGGTTGCTTGCATTGTGG
EV049455	AGGAACGGGATTAGGGTTTGGC	GCTTGGTCGTAAGCAAGAGCTG
EV098418	CGCTTCTCTCCTGTCATCCAAC	TTTCGGTGATGAAACCCTAAGCC
EV121581	AGTCAACGGAAGATGCGTGTGG	AGACTCTTCGACTGTATCCTGCTG
EV121815	AGGCCAAGTGGGACTTATTGGG	TCGCAACGGCAATTACCTCGTC
EV165209	AGAGTATATCCCGCCGATTCACC	GCCGGAGCTGAAATTGTCTGAG
EV191123	ACTCGAACCAAGTGGTTGTGGTG	TAACCGTCTTGACCGTGGAGTG
EV194778	ACCTAATCGCCGCTCTGGAATG	CTGCTGCTGTTGTTGTTGTTGTTG
EV194888	ATGCCAAATGCTGTTGGTGCTG	AGCTCGAGACAAACGGTCTAAGG
EV221705	CGATGGGTTCGTTAGGAGATGAGC	TGTTGTCGGCATCGAACAGTGTC
EV223094	TGGTTACAACCCACAGGACTGC	CTTCGTACCTGGACCATTCAGC
FG567004	TCCAAAGCTCCTCGTGATTCGC	GAAACTACACAAGCGAGTCCTCTG
R95K-contig3.403	TGTCGAGGAGATGCTGAGCAATG	TGTTTGGTCTGCCTCCTCTTGC
r95K-EX127401	TCGGTAGCGTTTCAGAGCGTTG	ACTGTGGTCATCCCTTGGAGAG
r95K-EX128395	TTGCGGCGCTGAGTATCAAAGG	TCGTGGCAGAGAGTTAGTGAGC
r95K-JCVI_3710	GTTTCTTGTGCCGCAAGCTAGG	AAGGCAACCACGGAACCAAAGG
TC113371	AGCGGGATCATAGGACCATGAAG	AGTTGACCGACCATGGCGTAAG
TC114800	ACCGACTCTTAAACCGGGCAAG	CGATTGCAACCGCGATTTGATCC
TC117386	TCCAATCTCAGATCCACCACAACC	CTTCGCCAGGAAACAAGATCCG
TC117453	CTTCACTTGATGGTCACAGGACTC	ACCGGTGGGAAACAACAACTAC
TC118206	ATCCAAAGAGTCGCCGCACAAG	TGTTCTTGATCCGACGGTGACG
TC118536	ATGAGCACGGCAAGAGCATTTC	CATGAGCCCACATTCCCAAACC
TC119093	TGTTCCTACTGGCGACTCACTG	TGTTCCCTTCGGGTTTGGCATC
TC119753	TGAAGCTGCTCAACGAACTGCTC	TCCCAGTCAACGCTTTCGATCTTC
TC120961	AACTACCCGACCCGGAAACATC	TGGAGGTGCATGTTAGCAACCC
TC124845	CCGGAGAAACTCATTAGCCGGTTC	ACGGCCGGTTTGGTTTGAGAAG
TC125322	GGTGGCTGTCATTGGCAACATC	TGGCTTCTTCATCAGCGGGTTC
TC125623	TTGGGAACCGTCTTCGTCATCC	TCTTCGCCGGAACAGAATCCAC
TC127023	CAGCAGCAGGCATGAAACTTG	ACGAGGACTGAGCAAGAAGATAGC
TC127081	TCGATCTCAATCGCGTCTCTGTG	TCATCGCTCGCAGCCATTGAAC
TC128235	TCTGGACAATGGTCTCCTTGTGG	ACAAGCTTGAGAAGAGCTTCGG
TC128844	TCTGGTGTCGCATGCTTCTTGG	AGCAGAGTTTGAAGAGTGGACAGC
TC134068	GATCGCACACGTTTCGGTTCATC	TTTCCTTGTCGCCCGTTGTTAC
TC135331	CGGTTGCATGGTGGCAACTAAAC	TCCATGGACTGTTGGGTGGTAG
TC136004	TGTGGTTGCTGTGGCTATACCTTG	AACAGAACTGGCGCGTAGAACG
TC136039	TGAGCCACCCAAGGATAAGATCG	GCACCAACTCCTCTTGTTCGTTTC
TC136070	CAACGGCGAGACACAATTCAGC	AAGCATTGCCGGTGACATGAGC
TC138274	AAGCTCTCGCAGCATCTTCAGC	ATCAAAGGCGTTCGAGTTTGGC

DFCI (NCBI) accession number	Forward primer sequence (5' → 3')	Reverse primer sequence (5' → 3')
TC138605	ATGACGACCAATGGGTGAAGAGG	TGCATCATGGATGCGCAGAGAC
TC145738	ACCACCATGGCCAACTTGCTTAG	TACACAGAGCTGGGATCAAGCC
TC150950	GTTGTGGAGTGAGGAAGCAAGTAG	GTTGGGACGTCGTGATTGTGTC
TC151604	TCTCAGGGCTCATGTACAACCC	ACGCTCAAGCGGAGATGTTCAG
TC154033	TGTGTCCGAGGATGCTAAACCTG	AGTGGTTGAAGAGCCTGAGCAC
TC154441	AGCCCTTGCTCTAGGACAACAAC	TGGAAGTGCAGCTGATGAGGAAG
TC155464	TGCCACCAGCATCCTAACCATC	CCCATCCATATCCCAACAACTGAG
TC156928	TGCTTGGCCCATTAAGGAGTGG	TCCGCCTCTAACGGAGAAAGAAAG
TC158708	AATACGCGACTGGGCTGAGAAC	TCCCTGTGGCTTTCCAATATCCG
TC158818	AGCTCAATGTCTACACCGCCTTC	TCAGAGCAAGCACAAATGCAGAG

Table SII-2 Nienty-five microarray selected N starvation-specifically regulated potential marker genes four days after stress induction. [a]Internal code microarray, [b]putative function suggested by TAIR; [c]manual categorization based on putative function, [d]Log_2-fold change. The log_2-fold changes for each cultivar were calculated between N starvation and the 2.0 *mM* N control (n = 3).

UID[a]	DFCI accession number	TAIR accession number	Putative function[b]	Category[c]	FC[d] Apex	FC[d] Capitol
46613	TC136039	AT4G22880	Anthocyanidin synthase	Anthocyanidin	3.5	6.0
7856	cluster011761.a1.1	AT4G35420	Dihydroflavonol 4-reductase-like1	Anthocyanidin	0.5	3.0
42980	TC128235	AT5G20280	Sucrose-phosphate synthase 1	C metabolism	1.8	1.3
20255	EE545548	AT1G50460	Hexokinase-3	C metabolism	-0.3	-0.9
2163	cluster001790.a1.1	AT5G20830	Sucrose synthase 1	C metabolism	-1.0	-1.0
13374	cluster034340.a1.1	AT4G35300	Sugar transporter MSSP2	C transporter	1.1	1.0
46600	TC136004	AT1G34580	Sugar transporter	C transporter	-0.5	1.3
14630	CN727103	AT3G05960	Hexose transporter 6	C transporter	0.9	1.0
2770	cluster003131.a1.2	AT1G21460	Sugar transporter SWEET1	C transporter	-2.0	-1.0
3269	cluster003288.a1.490	AT5G16570	Glutamine synthetase 1-4	N metaboilsm	2.2	1.9
1884	cluster001239.a1.1	AT5G53460	Glutamate synthase 1	N metaboilsm	-1.2	-0.9
980	CD832369	AT5G18170	Glutamate dehydrogenase 1	N metaboilsm	-1.3	-0.6
6753	cluster009061.a1.1	AT5G18170	Glutamate dehydrogenase 1	N metaboilsm	-1.3	-0.7
38774	TC118536	AT5G18170	Glutamate dehydrogenase 1	N metaboilsm	-1.7	-1.1
58156	TC158818	AT2G03590	Ureide permease 1	N transporter	2.8	1.5
43232	TC128844	AT1G26440	Ureide permease 5	N transporter	2.7	2.5
23776	ES265746	AT4G28700	Ammonium transporter 1;4	N transporter	2.2	0.9
35852	r95K-JCVI_3710	AT4G21120	Amino acid transporter 1	N transporter	1.9	1.7
8439	cluster013228.a1.1	AT1G69870	Nitrate transporter 1.7	N transporter	1.2	0.6
11433	cluster022584.a1.1	AT3G54140	Peptide transporter 1	N transporter	1.0	1.1
9767	cluster016928.a1.1	AT4G13510	Ammonium transporter 1;1	N transporter	1.0	0.5
35534	r95K-EX127401	AT2G34960	Amino acid transporter 5	N transporter	0.9	1.4
32571	EV223094	AT2G01170	Bidirectional amino acid transporter 1	N transporter	0.9	1.1
46275	TC135331	AT5G64410	Oligopeptide transporter 4	N transporter	0.9	-0.4
51347	TC145738	AT5G65990	Amino acid transporter	N transporter	-0.9	-1.1
36854	TC113371	AT5G50200	Nitrate transporter 3.1	N transporter	-1.1	-1.0
56426	TC155464	AT4G26590	Oligopeptide transporter 5	N transporter	-1.3	-0.8

UID[a]	DFCI accession number	TAIR accession number	Putative function[b]	Category[c]	FC[d] Apex	FC[d] Capitol
5068	cluster006594.a1.1	AT5G57685	Glutamine dumper 3	N transporter	-1.3	-0.3
2769	cluster003131.a1.1	AT2G26690	Nitrate transporter 1.1	N transporter	-1.7	-1.0
18348	EE447860	AT4G31730	Glutamine dumper 1	N transporter	-2.1	-2.4
39023	TC119093	AT4G25760	Glutamine dumper 2	N transporter	-2.8	-1.4
31591	EV191123	AT4G21680	Nitrate transporter 1.8	N transporter	-3.2	-1.7
25087	ES913305	AT2G40080	Early flowering 4	Other	2.2	1.4
55676	TC154033	AT4G29140	ADS1	Other	0.6	0.1
30216	EV121581	AT5G67310	Cytchrome P450	Other	-0.5	-1.1
31149	EV165209	AT2G27080	Harpin-induced protein	Other	-1.9	-3.6
4541	cluster005426.a1.1	AT4G29340	Profilin 4	Other	-2.1	-3.0
1624	cluster000639.a1.2	AT3G22840	Early light-inducible 1	Photosynthesis	2.1	2.7
38357	TC117453	AT4G22920	Non-yellowing protein 1	Photosynthesis	1.8	1.2
45661	TC134068	AT3G27690	LHCB2	Photosynthesis	1.4	0.7
5710	cluster006605.a1.686	AT4G10340	LHCB5	Photosynthesis	-0.8	-2.0
42466	TC127081	AT3G05120	Gibberellin receptor GID1A	Phytohormone	1.2	1.8
39323	TC119753	AT1G77330	1-aminocyclopropane-1-carboxylate oxidase	Phytohormone	0.5	1.1
57175	TC156928	AT2G19500	Cytokinin dehydrogenase 2 CKX2	Phytohormone	-0.7	-1.0
37364	TC114800	AT4G11280	1-aminocyclopropane-1-carboxylate oxidase 6	Phytohormone	-0.7	-1.8
27288	EV018246	AT5G07200	Gibberellin 20 oxidase 3	Phytohormone	-2.2	-2.8
17805	EE436585	AT2G19590	1-aminocyclopropane-1-carboxylate oxidase 1	Phytohormone	-2.6	-0.7
25492	ES952533	AT5G65510	AIL7	Transcription factor	0.9	1.3
31776	EV194888	AT1G12260	ANAC007	Transcription factor	-1.2	-1.3
58094	TC158708	AT1G56010	ANAC021 /ANAC022	Transcription factor	1.4	1.1
4517	cluster005374.a1.1	AT1G69490	ANAC029	Transcription factor	1.0	1.8
16572	DY023720	AT2G43000	ANAC042	Transcription factor	1.9	1.4
13843	cluster038644.a1.1	AT3G10500	ANAC053	Transcription factor	1.1	0.9
41684	TC125322	AT4G01550	ANAC069	Transcription factor	1.4	1.1
34401	R95K-contig3.403	AT5G22380	ANAC090	Transcription factor	-1.0	-1.7
24823	ES910034	AT5G63790	ANAC102	Transcription factor	2.1	1.9

UID[a]	DFCI accession number	TAIR accession number	Putative function[b]	Category[c]	FC[d] Apex	FC[d] Capitol
47837	TC138605	AT2G23340	DEAR3	Transcription factor	1.1	1.3
19412	EE478159	AT3G60490	DREB4A	Transcription factor	0.9	1.8
22121	EL623648	AT1G77640	DREB	Transcription factor	-1.4	-0.9
38653	TC118206	AT1G21910	DREB26	Transcription factor	-1.3	-1.1
13424	cluster034847.a1.1	AT5G51190	ERF	Transcription factor	-1.2	-0.6
41823	TC125623	AT4G17500	ERF001	Transcription factor	-1.0	-1.2
11944	cluster024535.a1.1	AT1G28360	ERF012	Transcription factor	1.2	0.8
28288	EV049455	AT2G31230	ERF015	Transcription factor	0.3	0.8
8463	cluster013301.a1.1	AT3G16770	ERF072	Transcription factor	2.4	2.7
47687	TC138274	AT1G72360	ERF073	Transcription factor	1.5	0.5
35539	r95K-EX128395	AT2G25820	ESE2	Transcription factor	2.7	2.9
12357	cluster026106.a1.1	AT4G16141	GATA	Transcription factor	-1.1	-1.0
7380	cluster010637.a1.1	AT3G60530	GATA004	Transcription factor	-1.2	-1.3
8258	cluster012772.a1.1	AT3G16870	GATA017	Transcription factor	-1.2	-1.0
8103	cluster012345.a1.1	AT4G01280	MYB	Transcription factor	1.0	1.0
10114	cluster018029.a1.1	AT2G38090	MYB	Transcription factor	0.7	1.1
10893	cluster020567.a1.1	AT5G37260	MYB	Transcription factor	-0.7	-1.0
29692	EV098418	AT1G58220	MYB	Transcription factor	-1.0	-0.7
32545	EV221705	AT1G49560	MYB	Transcription factor	-2.3	-2.3
12334	cluster025990.a1.1	AT4G37180	MYB	Transcription factor	-3.6	-3.0
15947	DY000543	AT1G06180	MYB013	Transcription factor	-1.4	-0.5
55891	TC154441	AT3G61250	MYB017	Transcription factor	0.9	0.5
33243	FG567004	AT4G34990	MYB032	Transcription factor	1.1	0.6
24210	ES901674	AT5G60890	MYB034	Transcription factor	-2.6	-1.8
20695	EE558066	AT1G18710	MYB047	Transcription factor	-0.6	-1.1
13258	cluster032894.a1.1	AT1G18570	MYB051	Transcription factor	-0.2	-1.0
54389	TC151604	AT3G50060	MYB077	Transcription factor	0.3	-0.4
39838	TC120961	AT4G36900	RAP2.10	Transcription factor	-1.1	0.1
4900	cluster006216.a1.1	AT3G16770	RAP2.3	Transcription factor	0.1	1.1

UID[a]	DFCI accession number	TAIR accession number	Putative function[b]	Category[c]	FC[d] Apex	FC[d] Capitol
38328	TC117386	AT1G78080	RAP2.4	Transcription factor	0.2	-0.9
10600	cluster019568.a1.1	AT1G74950	TIFY10B	Transcription factor	1.4	1.0
4273	cluster004849.a1.1	AT5G20900	TIFY3B	Transcription factor	1.0	0.8
42437	TC127023	AT1G70700	TIFY7	Transcription factor	-0.8	-1.2
31768	EV194778	AT5G56270	WRKY002	Transcription factor	1.2	0.7
46625	TC136070	AT4G26640	WRKY020	Transcription factor	0.9	0.2
54025	TC150950	AT2G30250	WRKY025	Transcription factor	1.1	0.7
41493	TC124845	AT4G23550	WRKY029	Transcription factor	-1.1	-1.0
30230	EV121815	AT2G34830	WRKY035	Transcription factor	-1.2	-1.0
21584	EG020899	AT3G56400	WRKY070	Transcription factor	-1.8	-1.4

Table SII-3 *Arabidopsis thaliana* homologues genes to the 407 *Brassica napus* sequences on the custom microarray specifically regulated by N starvation and showing a significant cultivar x treatment interaction in leaf three of winter oilsee-rape cultivars Apex and Capitol four days after induction of N starvation (n = 3). [a]Internal code microarray, [b]putative function suggested by TAIR; [c]Log_2-fold change. The log_2-fold changes for each cultivar were calculated between N starvation and the 2.0 *mM* N control. The sorting is in descending order of the absolute fold change difference between Apex and Capitol. --- not applicable.

UID[a]	DFCI accession number	TAIR accession number	Putative function[b]	FC[c] Apex	FC[c] Capitol	Absolute FC[c] difference
36145	TC111344	AT4G11320	Cysteine protease 2	-2.2	1.2	3.4
39370	TC119870	AT1G32583	microRNA MIR400	3.2	-0.1	3.3
14661	CN727308	AT3G21330	Basic helix-loop-helix (bHLH) DNA-binding superfamily protein	-2.7	0.5	3.3
11304	cluster022067,a1,1	AT3G19550	Unknown protein	0.7	3.9	3.2
44886	TC132386	AT1G32710	Cytochrome C oxidase	1.7	-1.5	3.2
18808	EE460618	AT4G00460	ROP (Rho Of Plants) guanine nucleotide exchange factor 3	1.6	-1.6	3.2
15810	DQ023593	AT3G16530	Lectin like protein	-4.9	-2.2	2.7
56961	TC156487	AT5G24910	Cytochrome P450	-0.8	-3.5	2.7
13831	cluster038549,a1,1	AT3G24450	Heavy metal transport/detoxification superfamily protein	-2.2	0.5	2.7
45954	TC134657	AT5G22110	DNA polymerase epsilon subunit B2	2.1	-0.6	2.7
15830	DV643310	AT3G16530	Lectin like protein	-4.2	-1.5	2.7
54297	TC151429	AT4G15396	Cytochrome P450	-0.5	2.2	2.7
27768	EV033128	AT2G17470	Aluminium activated malate transporter 6	0.3	2.9	2.6
7346	cluster010542,a1,1	AT5G03795	Exostosin family protein	-1.0	1.6	2.5
46485	TC135774	AT2G42610	Light sensitive hypocotyls 10	-1.5	1.0	2.5
5157	cluster006605,a1,176	AT1G12080	Vacuolar calcium-binding protein-related	-1.0	1.5	2.5
42275	TC126663	AT4G29770	Heat-induced TAS1 target 1	1.5	-1.0	2.5
57417	TC157384	AT1G20500	AMP-dependent synthetase and ligase family protein	-2.5	0.0	2.5
46613	TC136039	AT4G22880	Anthocyanidin synthase	3.5	6.0	2.5
31740	EV194355	AT1G28290	Arabinogalactan protein 31	-3.7	-1.3	2.4
56193	TC155026	AT5G28627	Unknown protein	2.1	-0.3	2.4
52646	TC148317	AT3G59480	PfkB-like carbohydrate kinase family protein	-3.1	-0.8	2.3
14717	CN728019	AT1G30050	Unknown protein	2.6	0.3	2.3
17013	EE412594	AT4G36600	Late embryogenesis abundant (LEA) protein	2.3	0.0	2.3
12237	cluster025613,a1,1	AT3G05930	Germin-like protein	0.6	-1.7	2.3
29304	EV084776	AT1G02930	Glutathione S-transferase 1	1.5	3.8	2.3
4027	cluster004324,a1,1	AT4G23680	Polyketide cyclase/dehydrase and lipid transport superfamily protein	-2.4	-0.1	2.2
26633	ES993759	AT3G60120	Beta glucosidase 27	1.6	-0.6	2.2
30039	EV116336	AT4G21680	Nitrate transporter 1.8	-2.2	0.0	2.2
23567	EL630126	AT2G32210	Unknown protein	-2.2	-0.1	2.1

UID[a]	DFCI accession number	TAIR accession number	Putative function[b]	FC[c] Apex	FC[c] Capitol	Absolute FC[c] difference
7286	cluster010375,a1,1	AT5G01210	HXXXD-type acyl-transferase family protein	-2.8	-0.7	2.1
41214	TC124226	AT2G26450	Plant invertase/pectin methylesterase inhibitor superfamily	-1.3	0.7	2.0
54925	TC152587	AT3G57260	Beta-1,3-glucanase 2	-0.4	-2.4	2.0
35721	r95K-JCVI_26277	AT3G08680	Leucine-rich repeat protein kinase family protein	-1.5	0.4	2.0
52337	TC147706	AT5G20810	SAUR70	-1.4	0.6	2.0
2059	cluster001584,a1,1	AT1G28290	Arabinogalactan protein 31	-3.4	-1.4	1.9
16422	DY020747	AT2G03720	Morphogenesis of root hair 6	1.1	-0.9	1.9
35380	r95K-EX086808	AT1G61760	Late embryogenesis abundant hydroxyproline-rich glycoprotein family	-0.7	1.2	1.9
5380	cluster006605,a1,383	AT4G25780	Cysteine-rich secretory proteins	-2.4	-0.5	1.9
25681	ES958034	AT1G76790	Indole glucosinolate O-methyltransferase 5	-1.8	-3.7	1.9
8329	cluster012976,a1,1	AT1G80760	Protein with boron transporter activity	-1.6	0.3	1.9
53733	TC150407	AT3G01220	Homeobox protein 20	-1.5	0.3	1.9
34756	r95K-EE529470	AT1G53250	Unknown protein	-2.0	-0.1	1.8
2245	cluster001942,a1,1	AT5G64080	Xylogen protein 1	-1.7	0.1	1.8
28020	EV042039	AT1G56220	Dormancy/auxin associated family protein	-1.9	-0.1	1.8
12563	cluster027126,a1,1	AT3G44840	S-adenosyl-L-methionine-dependent methyltransferases superfamily protein	-0.2	-2.0	1.8
40803	TC123311	AT2G31880	Supressor of BIR1 1	1.3	-0.5	1.8
31149	EV165209	AT2G27080	Late embryogenesis abundant (LEA) hydroxyproline-rich glycoprotein	-1.8	-3.6	1.8
48436	TC139815	AT1G12805	Nucleotide binding	1.5	-0.2	1.8
36041	TC111094	AT4G21380	Receptor kinase 3	-0.4	1.4	1.8
51699	TC146441	AT3G20260	Unknown protein	-0.8	0.9	1.8
26017	ES967211	AT1G24145	Unknown protein	0.4	-1.3	1.8
46600	TC136004	AT1G34580	Major facilitator superfamily protein	-0.5	1.3	1.7
30521	EV136716	AT5G20250	Raffinose synthase 6	1.5	-0.2	1.7
33633	FG577010	AT1G80760	NOD26-like intrinsic protein 6;1	-1.6	0.1	1.7
42858	TC127953	AT5G37478	TPX2 protein family	-1.9	-0.2	1.7
16579	DY023795	AT4G09530	SAUR17	-1.6	0.2	1.7
55626	TC153937	AT4G27160	Seed storage albumin 3	1.9	0.2	1.7
52245	TC147529	AT1G27110	Tetratricopeptide repeat (TPR)-like superfamily protein	0.9	-0.8	1.7
20292	EE548560	AT5G14230	Unknown protein	-0.7	1.0	1.7
25701	ES958754	AT1G67190	F-box/RNI-like protein	-0.9	0.7	1.7
33428	FG571615	AT1G49320	Unknown seed protein like 1	-2.3	-0.6	1.7
53423	TC149823	AT1G11185	Unknown gene	-0.9	0.7	1.7

UID[a]	DFCI accession number	TAIR accession number	Putative function[b]	FC[c] Apex	FC[c] Capitol	Absolute FC[c] difference
42811	TC127855	AT1G04120	Multidrug resistance-associated protein 5	-1.3	0.4	1.6
52121	TC147289	AT3G13520	Arabinogalactan protein 12	-1.2	0.4	1.6
59551	TC161473	AT4G17220	Microtubule-associated proteins 70-5	-1.9	-0.3	1.6
49652	TC142314	AT3G07320	O-Glycosyl hydrolases family 17 protein	-3.3	-1.7	1.6
49247	TC141465	AT3G16690	SWEET16	-0.6	1.0	1.6
36130	TC111292	AT3G16240	Delta tonoplast integral protein	-2.5	-0.9	1.6
8163	cluster012484,a1,1	AT5G11640	Thioredoxin superfamily protein	-1.3	0.3	1.6
42014	TC126052	AT5G47900	Unknown protein	-0.9	-2.5	1.6
46800	TC136397	AT1G72660	P-loop containing nucleoside triphosphate hydrolases superfamily protein	-0.1	1.4	1.6
32848	FG557701	AT3G50840	Phototropic-responsive NPH3 family protein	1.6	0.1	1.6
43100	TC128532	AT1G74370	RING/U-box superfamily protein	-2.6	-1.0	1.6
38504	TC117818	AT4G11280	1-Aminocyclopropane-1-carboxylic acid synthase 6	-0.6	-2.2	1.5
9490	cluster016162,a1,1	AT3G28750	Unknown protein	-0.1	1.5	1.5
7758	cluster011519,a1,1	AT1G02520	ATP-Binding cassette B11	-1.6	-0.1	1.5
26988	EV007110	AT4G21710	Embryo defective 1989	0.2	-1.4	1.5
35738	r95K-JCVI_28419	AT5G02250	Ribonucleotide reductase 1	0.8	-0.7	1.5
28228	EV048172	AT1G65470	Nucleosome/chromation assembly factor group B	-1.2	0.3	1.5
23367	EL628586	AT4G11920	Cell cycle switch protein 52 A2	-2.9	-1.4	1.5
29860	EV106632	AT2G47050	Plant invertase/pectin methylesterase inhibitor superfamily protein	-1.8	-0.3	1.5
16811	EE404089	AT2G44520	Cytochrome C oxidase 10	-1.4	0.1	1.5
24650	ES907317	AT3G09400	POL-like 3	0.1	1.6	1.5
41624	TC125184	AT1G63310	Unknown protein	-1.0	0.5	1.5
3193	cluster003288,a1,420	AT2G02100	Low-molecular-weight cysteine-rich 69	-1.5	0.0	1.5
16642	DY025105	AT5G23970	HXXXD-type acyl-transferase protein	0.5	1.9	1.4
30366	EV127093	AT2G45750	S-adenosyl-L-methionine-dependent methyltransferases protein	-1.2	0.2	1.4
35141	r95K-EX023581	AT5G24010	Protein kinase protein	0.1	-1.4	1.4
14203	cluster043420,a1,1	AT1G60995	Unknown protein	-0.6	0.8	1.4
13344	cluster033958,a1,1	AT1G07090	Light sensitive hypocotyls 6	-1.1	0.3	1.4
31977	EV201070	AT3G05360	Receptor like protein 30	0.5	-0.9	1.4
47039	TC136921	AT1G14790	RNA-dependent RNA polymerase 1	-0.3	1.1	1.4
30248	EV122380	AT2G26480	UDP-glucosyl transferase 76D1	-0.9	-2.3	1.4
56919	TC156408	AT3G04080	ApyraseE 1	0.7	-0.7	1.4
30932	EV157902	AT1G11790	Arogenate dehydratase 1	-0.1	-1.5	1.4

UID[a]	DFCI accession number	TAIR accession number	Putative function[b]	FC[c] Apex	FC[c] Capitol	Absolute FC[c] difference
32391	EV217496	AT4G37610	BTB and TAZ domain protein 5	-3.5	-2.1	1.4
42246	TC126597	AT2G38940	Phosphate transporter 2	1.8	0.5	1.4
1640	cluster000679,a1,1	AT4G37610	BTB and TAZ Domain protein 5	-2.7	-1.3	1.4
28604	EV059562	AT1G72300	PSY1 receptor	0.1	-1.3	1.4
25946	ES965944	AT5G49390	Unknown protein	0.2	-1.2	1.4
11882	cluster024306,a1,1	AT5G08020	Replication protein A 1B	-0.8	0.6	1.3
46275	TC135331	AT5G64410	Oligopeptide transporter 4	0.9	-0.4	1.3
6595	cluster008628,a1,1	AT2G34790	Maternal effect embryo arrest 23	-1.7	-0.4	1.3
45504	TC133718	AT1G74310	Heat shock protein 101	1.3	0.0	1.3
31932	EV199463	AT3G01670	Sieve element occlusion-related 2	-1.3	0.0	1.3
46013	TC134790	AT4G11280	1-Aminocyclopropane-1-carboxylic acid synthase 6	-0.4	-1.7	1.3
23848	ES267836	AT3G51070	S-adenosyl-L-methionine-dependent methyltransferases	0.5	-0.8	1.3
46305	TC135401	AT3G01680	Sieve-element-occlusion-related 1	-1.3	-0.1	1.3
46867	TC136534	AT2G29310	NAD(P)-binding Rossmann-fold superfamily protein	0.1	-1.1	1.3
28828	EV067923	AT5G28593	Gypsy-like retrotransposon family (Athila),	0.1	-1.1	1.3
53207	TC149404	AT2G16500	Arginine decarboxylase 1	0.3	-1.0	1.3
59327	TC161059	AT4G23180	Receptor-like protein kinase 10	1.0	-0.3	1.3
14154	cluster042516,a1,1	AT1G02920	Glutathione S-Transferase 11	0.3	1.6	1.3
58179	TC158856	AT5G49320	Unknown protein	-1.3	0.0	1.3
5309	cluster006605,a1,315	AT4G24110	Unknown protein	-1.4	-0.1	1.3
30707	EV147982	AT2G02100	Low-molecular-weight cysteine-rich 69	-1.1	0.2	1.3
2780	cluster003160,a1,1	AT4G34970	Actin depolymerizing factor 9	-1.3	-0.1	1.2
35358	r95K-EX083584	AT1G54400	HSP20-like chaperones superfamily protein	-0.8	0.5	1.2
31214	EV168691	AT2G32860	Beta glucosidase 33	-0.6	0.6	1.2
39838	TC120961	AT4G36900	RAP2.10	-1.1	0.1	1.2
32914	FG559243	AT4G02060	Prolifera	-0.1	-1.3	1.2
17912	EE438940	AT4G07810	Copia-like retrotransposon family	-3.0	-1.8	1.2
23589	EL630252	AT1G63310	Unknown protein	-1.2	0.0	1.2
4238	cluster004778,a1,1	AT2G26570	Weak chloroplast movement under blue light 1	-1.0	0.2	1.2
53544	TC150056	AT5G07322	Other RNA	-1.7	-0.5	1.2
22514	EL625139	AT5G02380	Metallothionein 2B	-0.5	0.7	1.2
2840	cluster003281,a1,1	AT5G19090	Heavy metal transport/detoxification superfamily protein	-0.6	0.5	1.2
15023	CX187940	AT3G18190	TCP-1/cpn60 chaperonin family protein	-0.4	0.8	1.2

UID[a]	DFCI accession number	TAIR accession number	Putative function[b]	FC[c] Apex	FC[c] Capitol	Absolute FC[c] difference
52461	TC147951	AT1G30370	DAD1-like acylhydrolase	0.0	-1.2	1.2
24974	ES911858	AT4G19680	Iron regulated transporter 2	1.3	0.1	1.2
48102	TC139160	AT1G14790	RNA-dependent RNA polymerase 1	-0.3	0.8	1.2
47959	TC138844	AT5G04890	Restricted TEV movement 2	-0.9	0.3	1.2
27080	EV010020	AT2G42690	Alpha/beta-Hydrolases superfamily protein	-2.1	-0.9	1.2
12980	cluster029483,a1,1	AT3G62360	Carbohydrate-binding-like fold	0.1	1.3	1.2
34638	r95K-DY019880	AT2G20180	Phytochrome interactinc factor 3-like 5	0.6	-0.6	1.2
59259	TC160931	AT5G08630	DDT domain-containing protein	0.7	-0.5	1.1
31473	EV184272	AT5G56720	Cytosolic-NAD-defendent malate dehydrogenase 3	-1.4	-0.3	1.1
1541	cluster000439,a1,1	AT3G03710	Chloroplast polynucleotide phosphorylase	-0.2	0.9	1.1
56960	TC156486	AT4G23150	Receptor-like protein kinase 7	0.6	-0.5	1.1
581	CD824694	AT3G01690	Alpha/beta-Hydrolases superfamily protein	-1.1	0.0	1.1
37721	TC115805	AT3G16180	Nitrate transporter 1.12	-1.1	0.1	1.1
37364	TC114800	AT4G11280	1-Aminocyclopropane-1-carboxylic acid synthase 6	-0.7	-1.8	1.1
23832	ES267324	AT4G00460	ROP (Rho Of Plants) guanine nucleotide exchange factor 3	-0.2	0.9	1.1
38210	TC117115	AT3G10610	Ribosomal S17 family protein	0.1	-1.0	1.1
38328	TC117386	AT1G78080	RAP2.4	0.2	-0.9	1.1
10096	cluster017996,a1,1	AT1G19570	Dehydroascorbate reductase 5	-0.9	0.2	1.1
40568	TC122723	AT5G02380	Metallothionein 2B	-0.5	0.6	1.1
6816	cluster009230,a1,1	AT4G38580	Farnesylated protein 6	1.1	2.2	1.1
51667	TC146371	AT2G32860	Beta glucosidase 33	-0.5	0.6	1.1
31548	EV189724	AT1G18420	Aluminium activated malate transporter family protein	0.0	1.0	1.1
35301	r95K-EX065040	AT3G11430	Glycerol-3-phosphate SN-2-acyltransferase 5	0.1	-1.0	1.1
56194	TC155028	AT5G20810	SAUR70	-0.7	0.4	1.1
1535	cluster000425,a1,1	AT3G22890	ATP Sulfurylase 1	0.6	-0.5	1.1
19291	EE474824	AT3G13650	Disease resistance-responsive protein	-1.4	-0.3	1.1
12192	cluster025472,a1,1	AT2G46250	Myosin heavy chain-related	0.0	-1.1	1.1
50323	TC143780	AT5G02380	Metallothionein 2B	-0.7	0.4	1.1
29245	EV081232	AT1G31940	Unknown protein	0.2	1.2	1.1
5823	cluster006743,a1,1	AT5G63530	Farnesylated protein 3	-1.7	-0.7	1.1
57395	TC157340	AT1G75720	Unknown protein	-0.7	0.3	1.0
49163	TC141290	AT3G52140	Friendly mitochondria	-0.1	0.9	1.0
43876	TC130207	AT3G25590	Unknown protein	-0.1	1.0	1.0

UID[a]	DFCI accession number	TAIR accession number	Putative function[b]	FC[c] Apex	FC[c] Capitol	Absolute FC[c] difference
50818	TC144727	AT2G24810	Pathogenesis-related thaumatin superfamily protein	-0.8	-1.8	1.0
12929	cluster029205,a1,1	AT4G37640	Calcium ATPase 2	0.3	-0.7	1.0
25655	ES957350	AT4G31270	Sequence-specific DNA binding transcription factor	-0.5	0.5	1.0
13638	cluster036541,a1,1	AT5G23955	Non-LTR retrotransposon family	1.6	2.6	1.0
31341	EV177449	AT5G28010	Polyketide cyclase/dehydrase and lipid transport superfamily protein	0.1	1.1	1.0
1835	cluster001137,a1,1	AT3G06050	Peroxiredoxin IIF	-0.3	0.7	1.0
3003	cluster003288,a1,246	AT1G78380	Glutathione S-transferase TAU 19	-0.4	0.6	1.0
38047	TC116725	AT4G22390	F-box associated ubiquitination effector family protein	-0.2	0.8	1.0
4900	cluster006216,a1,1	AT3G14230	RAP2.2	0.1	1.1	1.0
2700	cluster002989,a1,1	AT1G68220	Protein of unknown function	0.3	1.3	1.0
51194	TC145447	AT2G40200	Basic helix-loop-helix (bHLH) DNA-binding superfamily protein	0.3	1.3	1.0
46856	TC136518	AT3G51290	Unknown protein	-0.2	0.8	1.0
16719	EE392282	AT4G30270	Xyloglucan endotransglucosylase/hydrolase 24	-1.8	-0.8	1.0
30776	EV152793	AT4G21530	Anaphase promoting complex 4	0.7	-0.3	1.0
36515	TC112360	AT3G61460	Brassinosteroid-responsive ring-H2	-0.7	0.3	1.0
24314	ES902849	AT5G64870	SPFH/Band 7/PHB domain-containing membrane-associated protein	-2.0	-3.0	1.0
34335	r95K-AT000720	AT4G18540	Unknown protein	0.8	-0.1	1.0
21945	EL622851	AT3G23590	REF4-related 1	-0.6	0.4	1.0
52944	TC148872	AT3G10050	L-O-methylthreonine resistant 1	-1.0	-1.9	1.0
35238	r95K-EX055054	AT1G68130	Indeterminate(id)-domain 14	-0.1	0.8	1.0
22950	EL626932	AT5G38210	Protein kinase	0.2	-0.8	1.0
33480	FG573125	AT1G61610	S-locus lectin protein kinase family protein	0.7	1.7	0.9
25954	ES966108	AT1G58520	RXW8	0.7	-0.2	0.9
38460	TC117691	AT4G31200	SWAP	-0.4	0.5	0.9
37459	TC115048	AT1G29670	GDSL-like Lipase/Acylhydrolase superfamily protein	-0.8	-1.8	0.9
26538	ES990590	AT4G18540	Unknown protein	0.8	-0.2	0.9
55416	TC153539	AT3G09830	Protein kinase superfamily protein	1.3	0.4	0.9
22846	EL626433	AT1G29520	AWPM-19-like family protein	-0.9	0.0	0.9
31291	EV174150	AT3G15720	Pectin lyase-like protein	-0.5	0.4	0.9
14779	CN729470	AT3G06590	Basic helix-loop-helix (bHLH) DNA-binding superfamily protein	0.0	0.9	0.9
37965	TC116468	AT3G13660	Disease resistance-responsive (dirigent-like protein) family protein	-1.2	-0.3	0.9
11807	cluster023999,a1,1	AT4G38460	Geranylgeranyl reductase	0.4	-0.5	0.9
53555	TC150085	AT1G21560	Unknown protein	-0.1	0.8	0.9

UID[a]	DFCI accession number	TAIR accession number	Putative function[b]	FC[c] Apex	FC[c] Capitol	Absolute FC[c] difference
53147	TC149296	AT2G35590	Serine protease inhibitor	0.8	-0.1	0.9
52992	TC148953	AT4G16265	NRPD9B	-0.5	0.3	0.9
41273	TC124361	AT2G37530	Unknown protein	-0.9	0.0	0.9
58690	TC159857	AT5G47550	Cystatin/monellin superfamily protein	-1.2	-2.1	0.9
48419	TC139781	AT3G09390	Metallthionein 2A	-0.4	0.4	0.9
57985	TC158500	AT4G35690	Unknown protein	-1.8	-1.0	0.9
16466	DY021540	AT5G02380	Metallothionein 2B	-0.3	0.5	0.9
15397	CX193140	AT4G38580	Farnesylated protein 6	1.4	2.3	0.9
20170	EE542734	AT3G06890	Unknown protein	-0.1	-1.0	0.9
14296	cluster044988,a1,1	AT5G17410	Spc97 / Spc98 family of spindle pole body component	0.3	-0.5	0.9
55089	TC152922	AT5G29100	Gypsy-like retrotransposon family	-0.5	0.4	0.9
9069	cluster014942,a1,1	AT2G40880	Protein with cysteine proteinase inhibitor activity	1.4	0.5	0.9
54695	TC152151	AT4G24380	Unknown protein	0.5	-0.4	0.9
19201	EE472612	AT3G10450	Serine carboxypeptidase-like 7	-1.6	-0.8	0.9
44023	TC130534	AT2G02160	CCCH-type zinc finger family protein	0.1	-0.8	0.8
16503	DY022411	AT5G03050	Unknown protein	-0.1	0.7	0.8
57157	TC156896	AT2G01420	Pin-formed 4	-1.3	-0.5	0.8
20693	EE558038	---	---	-0.7	0.1	0.8
31647	EV192633	AT5G14120	Major facilitator superfamily protein	-0.5	0.3	0.8
32722	FG554829	AT1G72280	Endoplasmic reticulum oxidoreductins 1	0.0	-0.8	0.8
10834	cluster020341,a1,1	ATCG00190	Chloroplast DNA-dependent RNA polymerase B subunit	0.3	-0.5	0.8
30865	EV156296	AT1G52570	Phospholipase D alpha 2	0.2	-0.6	0.8
57090	TC156756	AT5G10560	Glycosyl hydrolase family protein	0.2	-0.6	0.8
49291	TC141550	AT4G38580	Farnesylated protein 6	1.4	2.2	0.8
52017	TC147065	AT3G09830	Protein kinase protein	0.6	-0.2	0.8
5711	cluster006605,a1,687	ATCG00900	Chloroplast ribosomal protein S7	0.1	-0.7	0.8
52752	TC148509	AT1G22510	RING/U-box protein	-0.2	0.6	0.8
31775	EV194886	AT5G10770	Eukaryotic aspartyl protease family protein	0.1	0.9	0.8
13258	cluster032894,a1,1	AT1G18570	MYB51	-0.2	-1.0	0.8
55455	TC153611	AT3G50070	Cyclin D3;3	0.2	1.0	0.8
260	CD814818	AT1G73700	MATE efflux family protein	0.6	-0.2	0.8
9503	cluster016209,a1,1	AT3G02555	Unknown protein	-1.1	-0.3	0.8
24976	ES911865	AT3G57680	Peptidase S41	1.8	1.0	0.8

UID[a]	DFCI accession number	TAIR accession number	Putative function[b]	FC[c] Apex	FC[c] Capitol	Absolute FC[c] difference
29759	EV100509	AT1G51830	Leucine-rich repeat protein kinase family protein	-0.2	-1.0	0.8
28042	EV042648	AT5G54590	Calcium/calmodulin-regulated receptor-like kinase 1	-0.5	0.3	0.8
15410	CX193346	AT3G06050	Peroxiredoxin IIF	-0.3	0.5	0.8
16393	DY020473	AT2G16800	High-affinity nickel-transport protein	-0.4	0.4	0.8
4302	cluster004919,a1,1	AT2G01320	ATP-Binding cassette G7	0.1	-0.7	0.8
1691	cluster000805,a1,2	AT1G56700	Peptidase C15	-0.5	0.3	0.8
9709	cluster016779,a1,1	AT4G24275	Identified as a screen for stress-responsive genes	-0.7	0.1	0.8
23606	EL630421	AT1G35830	VQ motif-containing protein	0.0	0.7	0.8
29088	EV076567	AT4G16690	Methyl esterase 16	-0.6	0.1	0.8
25995	ES966797	AT5G58170	Glycerophosphodiester phosphodiesterase like 7	-0.5	0.2	0.8
28249	EV048637	AT1G22660	Polynucleotide adenylyltransferase family protein	0.6	-0.1	0.8
32964	FG560090	AT5G44030	Cellulose synthase A4	-0.8	0.0	0.7
11525	cluster022978,a1,1	AT4G26750	Hydroxyproline-rich glycoprotein family protein	0.0	0.7	0.7
27500	EV024858	AT5G09250	Putative transcriptional co-activator (KIWI) mRNA	-0.4	0.4	0.7
41524	TC124916	AT1G06240	Unknown protein	0.4	-0.4	0.7
20444	EE552088	AT4G19440	Tetratricopeptide repeat (TPR)-like superfamily protein	-0.5	0.2	0.7
32970	FG560272	AT5G57350	H(+)-ATPase 3	0.4	1.1	0.7
55262	TC153244	AT1G27120	Galactosyltransferase family protein	0.0	-0.7	0.7
44983	TC132593	AT4G21720	Unknown protein	-0.8	-0.1	0.7
18339	EE447606	AT4G16690	Methyl esterase 16	-0.8	-0.1	0.7
7462	cluster010805,a1,1	AT4G33000	Calcineurin b-like protein 10	-1.5	-0.8	0.7
13065	cluster030098,a1,1	AT1G55340	Unknown protein	-1.4	-0.7	0.7
54389	TC151604	AT3G50060	MYB77	0.3	-0.4	0.7
57178	TC156932	AT2G39770	GDP-mannose pyrophosphorylase 1	0.1	-0.6	0.7
25863	ES963535	AT3G42860	Zinc knuckle (CCHC-type) family protein	0.1	0.8	0.7
57810	TC158172	AT2G02790	IQ-domain 29	-0.6	0.1	0.7
42143	TC126365	AT1G16790	Ribosomal protein-related	-0.3	0.4	0.7
13737	cluster037473,a1,1	AT3G05970	Long-chain acyl-CoA synthetase 6	-0.2	0.4	0.7
51285	TC145623	AT5G41685	Mitochondrial outer membrane translocase complex	0.2	0.9	0.7
30135	EV118944	AT1G61360	S-locus lectin protein kinase family protein	0.6	0.0	0.7
50856	TC144810	AT3G14420	Glycolate oxidase 1	-0.6	0.1	0.7
16463	DY021450	AT5G05080	Ubiquitin-conjugating enzyme 22	-0.2	0.5	0.7
54420	TC151652	AT1G67630	DANN polymerase alpha 2	-1.3	-0.7	0.7

UID[a]	DFCI accession number	TAIR accession number	Putative function[b]	FC[c] Apex	FC[c] Capitol	Absolute FC[c] difference
26778	ES999534	AT2G32370	Homeodomain glabrous 3	-1.9	-2.6	0.7
55555	TC153794	AT3G53830	Regulator of chromosome condensation family protein	0.6	-0.1	0.7
24978	ES911882	AT1G56700	Peptidase C15	-0.4	0.3	0.7
37463	TC115055	AT2G35190	Novel plant SNARE 11	-1.7	-1.0	0.7
48416	TC139773	AT1G05410	Unknown protein	0.7	1.4	0.7
16677	DY028617	AT5G09680	Reduced lateral root formation	-0.1	0.5	0.7
4094	cluster004460,a1,1	AT4G34710	Arginine decarboxlase 2	0.1	-0.5	0.7
3781	cluster003788,a1,1	AT2G37660	NAD(P)-binding Rossmann-fold superfamily protein	-1.4	-2.1	0.7
55005	TC152745	AT2G02170	Remorin family protein	0.5	1.1	0.7
49182	TC141322	AT4G30080	Auxin response factor 16	0.3	0.9	0.7
11535	cluster023005,a1,1	AT3G62700	Multidrug resistance-associated protein 10	0.2	-0.5	0.7
20663	EE557559	AT5G27440	Unknown protein	-0.8	-0.1	0.7
52316	TC147662	AT1G09794	Cox19 family protein	-0.7	-0.1	0.7
9176	cluster015228,a1,1	AT2G26110	Protein of unknown function	-0.5	0.2	0.6
50340	TC143810	AT4G28060	Cytochrome C oxidase	0.5	1.2	0.6
31344	EV177613	AT3G62700	Multidrug resistance-associated protein 10	0.3	-0.4	0.6
7652	cluster011294,a1,1	AT1G18840	IQ-domain 30	-0.8	-0.2	0.6
19127	EE471006	AT5G51140	Pseudouridine synthase	0.0	0.6	0.6
13366	cluster034164,a1,1	AT2G43770	Transducin/WD40 repeat-like superfamily protein	1.0	0.4	0.6
54429	TC151667	AT1G14820	Sec14p-like phosphatidylinositol transfer family protein	0.0	0.6	0.6
10054	cluster017847,a1,1	AT3G32930	Unknown protein	0.4	1.0	0.6
6540	cluster008490,a1,1	AT1G23040	Hydroxyproline-rich glycoprotein family protein	0.5	1.1	0.6
21003	EE563354	AT1G26470	SNRK2-substrate 1	-0.3	0.4	0.6
33562	FG574992	AT2G34310	Unknown protein	-1.3	-0.7	0.6
59273	TC160960	AT4G37000	Accelerated cell death 2	0.4	1.0	0.6
38772	TC118533	AT1G72340	NagB/RpiA/CoA transferase-like superfamily protein	-0.5	0.2	0.6
51992	TC147025	AT1G49910	Budding uninhibited by benzymidazol 3.2	0.1	0.7	0.6
43234	TC128851	AT4G22310	Unknown protein	0.2	0.8	0.6
44605	TC131822	AT5G63380	Peroxisomal protein	0.8	0.2	0.6
39394	TC119935	AT4G39470	Tetratricopeptide repeat (TPR)-like superfamily protein	-0.7	0.0	0.6
45599	TC133908	AT5G51020	Crumpled leaf	0.1	0.8	0.6
9409	cluster015920,a1,1	AT2G39900	LIM protein	-0.8	-0.2	0.6
18258	EE445589	AT3G11670	Digalactosyl diacylglycerol deficient 1	0.9	0.2	0.6

UID[a]	DFCI accession number	TAIR accession number	Putative function[b]	FC[c] Apex	FC[c] Capitol	Absolute FC[c] difference
48567	TC140086	AT3G07568	Unknown protein	-0.7	-0.1	0.6
44317	TC131190	AT1G76405	Unknown protein	-0.9	-0.3	0.6
47792	TC138512	AT1G55320	Acyl-activating enzyme 18	0.0	0.7	0.6
26249	ES981059	AT4G22390	F-box associated ubiquitination effector family protein	0.2	0.8	0.6
30216	EV121581	AT5G67310	Cytochrome P450	-0.5	-1.1	0.6
21768	EL590288	AT5G07960	Unknown protein	0.0	0.6	0.6
52379	TC147782	AT3G10050	L-O-methyltheronine resistant 1	-0.9	-1.5	0.6
34101	H74651	AT5G55940	Embryo defective 2731	-0.5	0.1	0.6
15863	DW997874	AT4G29735	Unknown protein	-0.4	0.2	0.6
4409	cluster005155,a1,1	AT3G53580	Diaminopimelate epimerase family protein	-0.4	0.2	0.6
28297	EV049709	AT4G35260	Isocitrate dehydrogenase I	0.3	0.9	0.6
7827	cluster011687,a1,1	AT2G27330	RNA-binding family protein	-0.2	0.3	0.6
11465	cluster022695,a1,1	AT3G57800	Basic helix-loop-helix (bHLH) DNA-binding superfamily protein	0.0	0.6	0.6
20316	EE549009	AT1G71950	Proteinase inhibitor	0.2	0.8	0.6
55406	TC153520	AT2G15530	RING/U-box protein	-0.2	0.3	0.6
6346	cluster008038,a1,1	AT5G51020	Crumpled leaf	-0.1	0.5	0.6
10703	cluster019908,a1,1	AT2G47630	Alpha/beta-hydrolases superfamily protein	0.5	-0.1	0.6
6312	cluster007953,a1,1	AT1G12350	Phosphopantothenoylcysteine synthetase	-0.2	0.4	0.6
1247	CD838816	AT3G62050	Putative endonuclease or glycosyl hydrolase	0.2	0.8	0.6
44376	TC131329	AT4G28400	Protein phosphatase 2C family protein	1.0	0.5	0.6
4583	cluster005514,a1,1	AT3G05070	mRNA splicing factor	-0.5	0.0	0.6
1771	cluster000988,a1,1	AT1G26110	Decapping 5	0.6	0.0	0.6
46725	TC136249	AT4G21660	Proline-rich spliceosome-associated family protein	0.0	-0.6	0.6
46684	TC136180	AT5G12150	Protein with similarity to REN1	-0.5	0.0	0.6
5361	cluster006605,a1,366	AT2G30410	Tubulin folding factor A	-0.4	0.2	0.5
37793	TC116004	AT4G30950	Fatty acid desaturase 6	-0.5	-1.0	0.5
2075	cluster001610,a1,1	AT4G25740	RNA binding Plectin/S10 domain-containing protein	-0.7	-0.1	0.5
46397	TC135591	AT1G03330	Sm-like 2	0.1	0.6	0.5
56130	TC154893	AT4G26710	ATPase	-0.4	0.1	0.5
52948	TC148879	AT3G05710	Syntaxin of plants 43	-0.1	0.4	0.5
42713	TC127646	AT4G32760	ENTH/VHS/GAT family protein	0.6	0.1	0.5
44073	TC130632	AT1G06500	Unknown protein	0.0	0.5	0.5
40018	TC121404	AT4G34430	Switch/sucrose nonfermenting 3D	0.0	0.5	0.5

UID[a]	DFCI accession number	TAIR accession number	Putative function[b]	FC[c] Apex	FC[c] Capitol	Absolute FC[c] difference
26163	ES978336	AT3G54910	RNI-like superfamily protein	0.1	0.6	0.5
20085	EE538110	AT4G32930	Unknown protein	-0.2	0.3	0.5
13242	cluster032739,a1,1	AT2G37975	Yos1-like protein	0.4	0.9	0.5
50692	TC144487	AT2G16370	Thymidylate synthase 1	0.0	-0.5	0.5
18215	EE444299	AT4G16710	Glycosyltransferase 28	-0.2	0.3	0.5
11035	cluster021129,a1,1	AT2G27960	Cyclin-dependent kinase-subunit 1	0.1	0.6	0.5
45334	TC133349	AT2G22480	Phosphofructokinase 5	-0.1	0.4	0.5
18846	EE462492	AT1G08530	Unknown protein	-0.4	0.1	0.5
53246	TC149470	AT3G14230	RAP2.2	0.0	0.5	0.5
11231	cluster021848,a1,3	AT3G43810	Calmodulin 7	0.2	0.6	0.5
36428	TC112082	AT5G06360	Ribosomal protein S8e family protein	-0.3	0.2	0.5
46791	TC136381	AT4G30000	Dihydropterin pyrophosphokinase	0.0	0.5	0.5
23557	EL630023	AT1G15910	Factor of DNA methylation 1	0.5	1.0	0.5
10364	cluster018779,a1,1	AT5G63520	Unknown protein	0.0	0.5	0.5
10650	cluster019744,a1,3	AT1G67250	Proteasome maturation factor	0.3	0.8	0.5
42515	TC127192	AT4G24760	Alpha/beta-hydrolases superfamily protein	0.4	0.9	0.5
8572	cluster013626,a1,1	AT4G21110	G10 family protein	-0.1	0.4	0.5
47825	TC138584	AT5G08590	SNF1-related protein kinase 2.1	0.5	0.0	0.5
9867	cluster017242,a1,1	AT1G71950	Proteinase inhibitor	0.3	0.7	0.5
37008	TC113784	AT3G13882	Ribosomal protein L34	-0.1	0.4	0.5
46854	TC136514	AT1G03330	Sm-like 2	0.0	0.5	0.5
28070	EV043274	AT1G10130	Endoplasmic reticulum-type-calcium-transporting ATPase 3	0.2	-0.2	0.5
27006	EV007619	AT1G71410	ARM repeat superfamily protein	0.0	-0.4	0.4
56495	TC155596	AT5G55230	Microtubule-associated proteins 65-1	-0.8	-1.2	0.4
51021	TC145136	AT1G29820	Magnesium transporter CorA-like family protein	0.1	0.6	0.4
27847	EV035724	AT4G30390	Unknown protein	0.1	0.6	0.4
50964	TC145005	AT3G02280	TAH18	0.3	0.8	0.4
11177	cluster021647,a1,1	AT1G54390	Inhibitor of growth 2	0.1	0.5	0.4
2721	cluster003038,a1,1	AT1G05720	Selenoprotein family protein	-0.1	0.3	0.4
15920	DW999861	AT5G42690	Unknown protein	0.7	1.2	0.4
12397	cluster026355,a1,1	AT3G10490	ANAC051, ANAC052	0.4	0.8	0.4
44969	TC132564	AT1G21720	Proteasome beta subunit C1	0.2	0.6	0.4
58954	TC160376	AT3G14420	Glycolate oxidase 1	-0.7	-0.3	0.4

UID[a]	DFCI accession number	TAIR accession number	Putative function[b]	FC[c] Apex	FC[c] Capitol	Absolute FC[c] difference
9134	cluster015107,a1,1	AT4G38220	Peptidase M20/M25/M40 family protein	0.1	-0.3	0.4
45031	TC132698	AT4G24820	26S proteasome, regulatory subunit Rpn7	0.0	0.4	0.4
4882	cluster006183,a1,1	AT3G14420	Glycolate oxidase 1	-0.6	-0.2	0.4
38977	TC118997	AT5G58920	Unknown protein	0.2	0.6	0.4
11048	cluster021183,a1,1	AT2G43310	Ribosomal L18p/L5e family protein	0.1	0.5	0.4
54288	TC151411	AT3G22630	20S proteasome beta subunit D1	0.2	0.6	0.4
52764	TC148528	AT3G51850	Calcium-dependent protein kinase 13	0.0	0.4	0.4
42790	TC127815	AT4G21110	G10 family protein	0.1	0.5	0.4
10906	cluster020609,a1,1	AT4G21110	G10 family protein	0.1	0.5	0.4
40079	TC121568	AT4G37020	Unknown protein	-0.1	0.3	0.4
26779	ES999577	AT2G39400	Alpha/beta-Hydrolases superfamily protein	-0.7	-0.3	0.4
33706	FG579085	AT3G27670	Resureection 1	0.1	0.5	0.4
44323	TC131209	AT3G18165	Modifier of SNC1,4	0.2	0.5	0.4
725	CD826628	AT5G41410	Homeodomain protein required for ovule identity	0.8	0.4	0.4
24145	ES900874	AT5G56630	Phosphofructokinase 7	1.0	0.6	0.4
53294	TC149570	AT1G72020	Unknown protein	0.1	0.5	0.4
50514	TC144138	AT1G61780	Unknown protein	0.0	0.4	0.4
30572	EV142643	AT2G20440	Ypt/Rab-GAP domain of gyp1p superfamily protein	0.1	0.5	0.4
58305	TC159113	AT3G28140	RNA ligase/cyclic nucleotide phosphodiesterase family protein	0.4	0.8	0.4
44448	TC131495	AT5G16260	Early flowering 9	-0.5	-0.1	0.4
40482	TC122529	AT5G13470	Unknown protein	0.2	0.6	0.4
51908	TC146855	AT2G32980	Unknown protein	-0.6	-0.2	0.4
5036	cluster006533,a1,1	AT4G16380	Heavy metal transport/detoxification superfamily protein	0.1	0.4	0.4
19476	EE480725	AT4G21110	G10 family protein	0.1	0.5	0.3
15892	DW998696	AT5G59613	Unknown protein	-0.1	0.2	0.3
4585	cluster005516,a1,1	AT1G52740	Histone H2A protein 9	-0.5	-0.1	0.3
4034	cluster004332,a1,1	AT4G10920	Transcriptional co-activator	0.2	0.5	0.3
47813	TC138560	AT2G18710	SECY homolog 1	-0.3	0.0	0.3
57907	TC158367	AT5G12190	RNA-binding (RRM/RBD/RNP motifs) family protein	0.0	0.3	0.3
37807	TC116044	AT5G13450	Delta subunit of MT ATP synthase	0.1	0.5	0.3
2458	cluster002405,a1,1	AT4G20330	Transcription initiation factor TFIIE	0.3	0.6	0.3
52867	TC148724	AT4G38910	Basic pentacysteine 5	0.3	0.6	0.3
16871	EE407113	AT2G25950	Unknown protein	0.0	0.3	0.3

UID[a]	DFCI accession number	TAIR accession number	Putative function[b]	FC[c] Apex	FC[c] Capitol	Absolute FC[c] difference
50367	TC143872	AT5G42480	Accumulation and replication of chloroplasts 6	0.0	-0.3	0.3
28535	EV057414	AT5G06480	Immunoglobulin E-set superfamily protein	0.5	0.8	0.3
37607	TC115479	AT3G20060	Ubiquitin-conjugating enzyme19	0.2	0.5	0.3
31773	EV194851	AT1G15860	Unknown protein	-0.4	-0.1	0.3
40063	TC121523	AT4G38910	Basic pentacysteine 5	0.4	0.7	0.3
18848	EE462502	AT5G23080	TOUGH	0.1	0.4	0.3
36500	TC112312	AT5G38470	Radiation sensitive23D	0.4	0.7	0.3
23915	ES269450	AT1G15810	S15/NS1, RNA-binding protein	0.2	0.5	0.3
5335	cluster006605,a1,340	AT3G41768	18S rRNA	0.1	0.4	0.3
7632	cluster011242,a1,1	AT3G12260	LYR family of Fe/S cluster biogenesis protein	0.3	0.5	0.3
17600	EE430689	AT3G54130	Josephin family protein	0.1	-0.2	0.3
5723	cluster006605,a1,74	AT5G58060	YKT6	0.3	0.6	0.2
36822	TC113291	AT1G15860	Unknown protein	-0.3	0.0	0.2
21400	EE569309	AT2G02760	Ubiquitin-conjugating enzyme 22	0.3	0.5	0.2

Supplementary Material for Chapter III

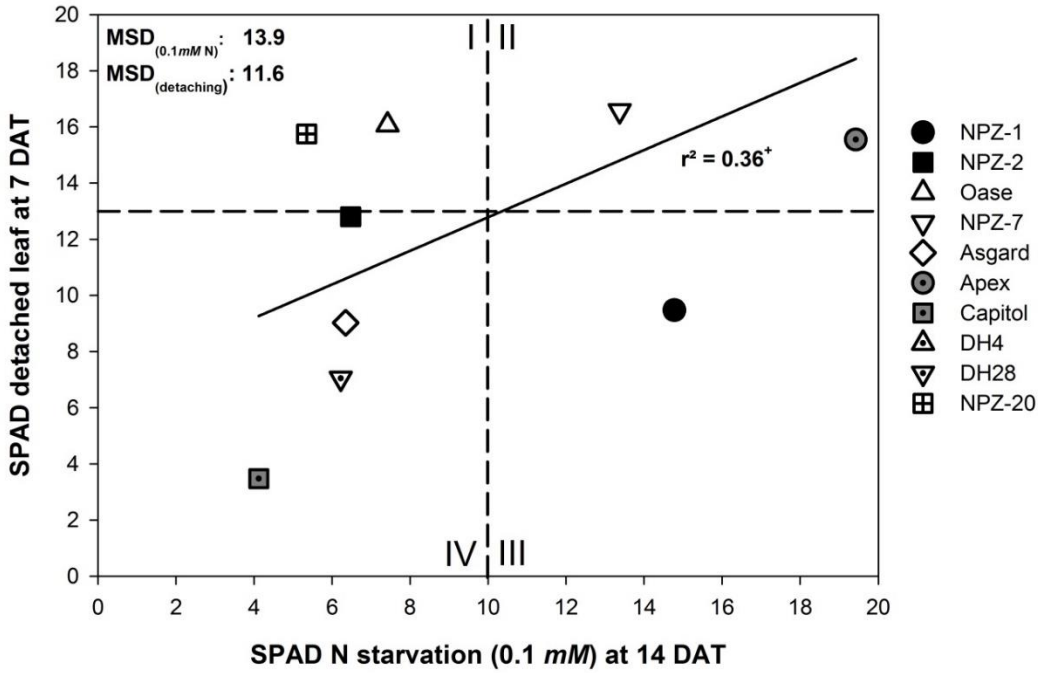

Figure SIII-1 Correlation between SPAD of detached leaves 7 DAT and SPAD of intact N-starved leaves 14 DAT of 10 winter oilseed-rape line-cultivars. The plants were pre-cultured for 28 days at 2.0 *mM* N. Detached leaves were cultured in Erlenmeyer flasks containing deionized water (for experimental details see Chapter II). The dashed lines show the average SPAD values across the ten line cultivars. Cultivars in quadrants I and III differ in SPAD whereas cultivars in the quadrants II and IV correspond with their responses in SPAD to detaching and N starvation. MSD = Minimum significant difference ($p < 0.05$). For the correlation + indicate significance at $p < 0.10$. Four biological replicates.

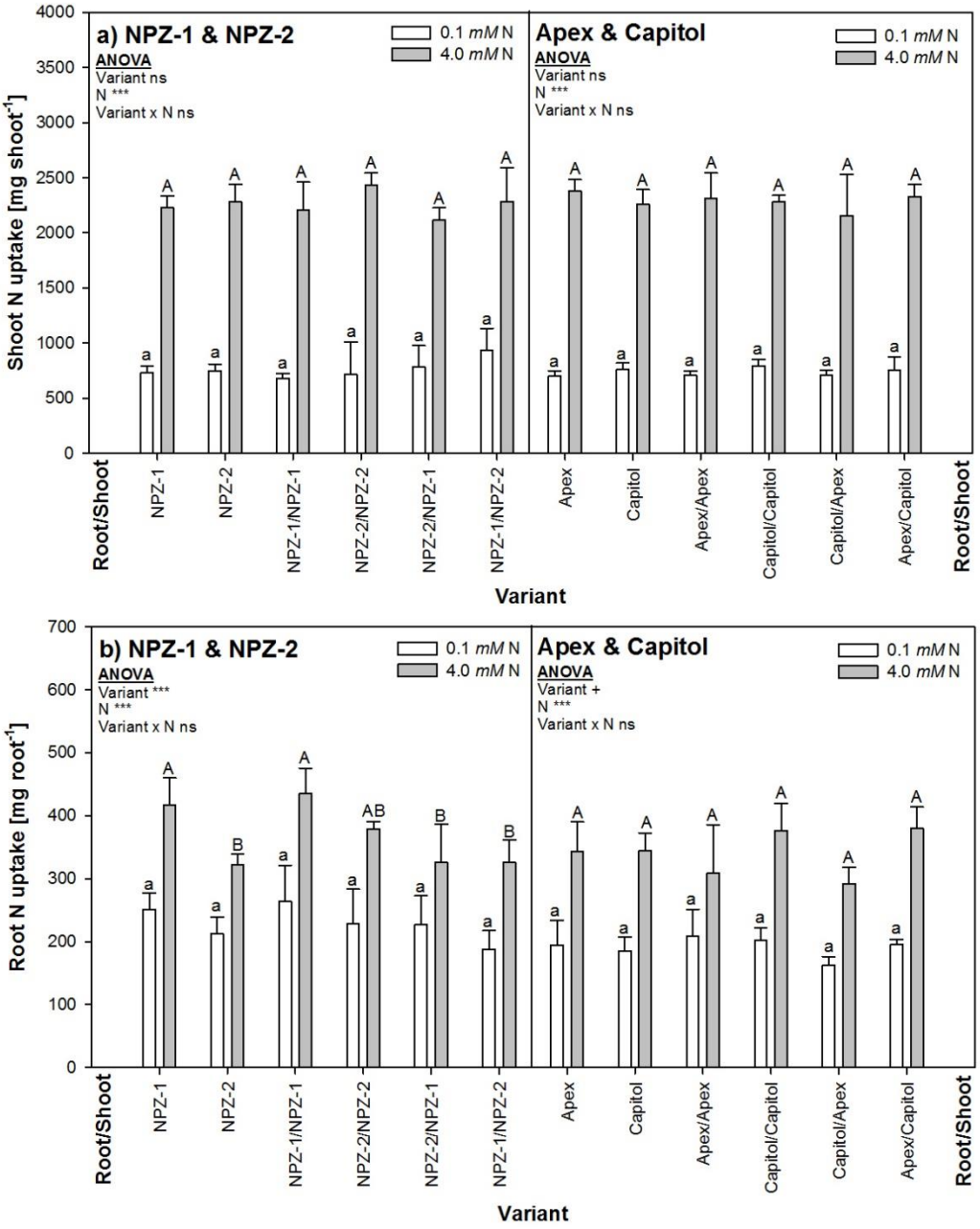

Figure SIII-2 Shoot (a) and root (b) N uptake of non-grafted, self-grafted and reciprocally-grafted plants of the winter oilseed-rape cultivars NPZ-1 & NPZ-2 (left) and Apex & Capitol (right) grown in hydroponics after 12 days of N starvation (0.1 *mM* N) or optimal N supply (4.0 *mM* N). The plants were pre-cultured for 28 days at 2.0 *mM* N. Different letters on top of the columns indicate differences between the variants (p <0.05). For the ANOVA +, * indicate significant differences at p <0.10, <0.001, respectively. ns = non-significant. The error bars represent the standard deviations of the means (n = 3 to 4).**

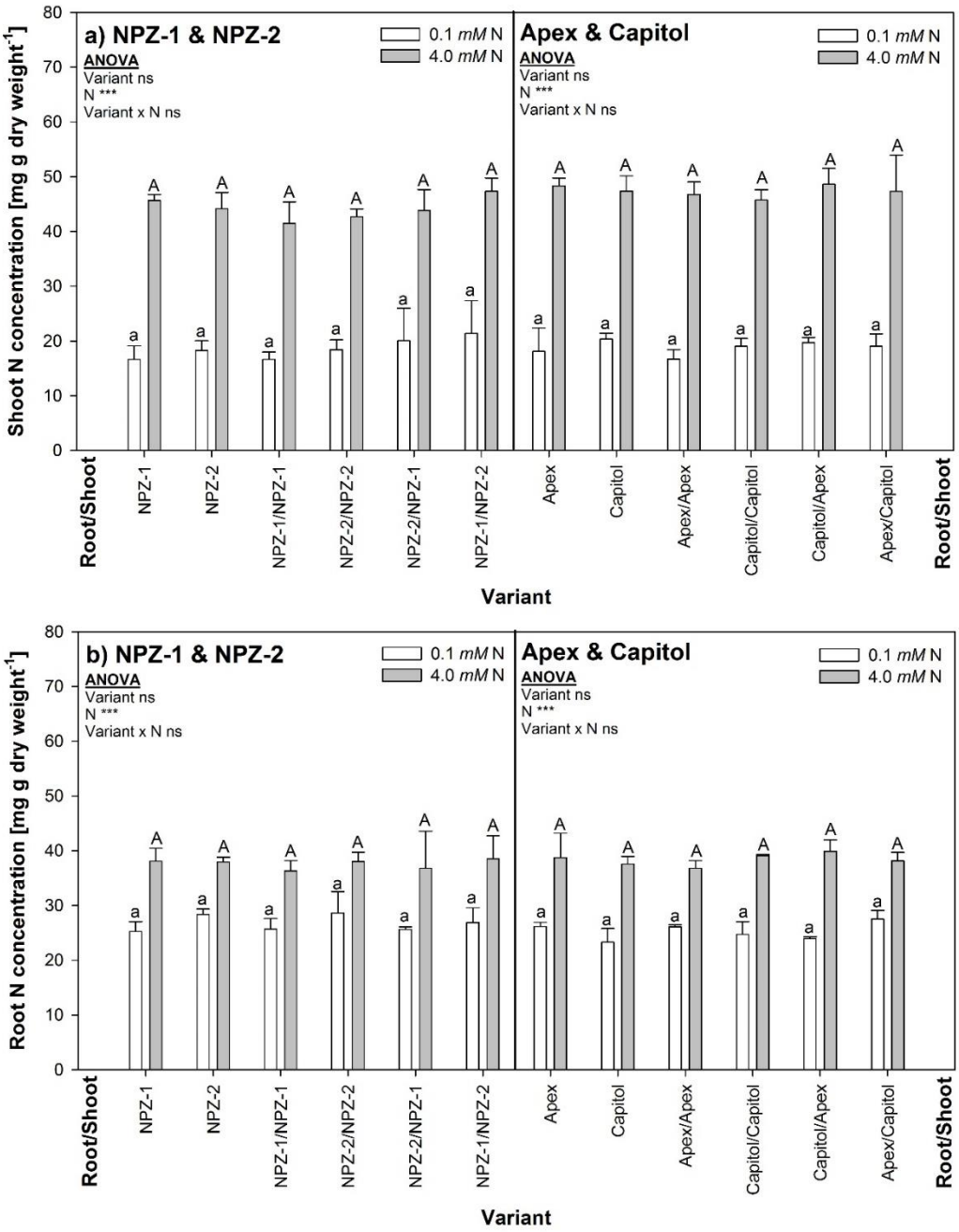

Figure SIII-3 Shoot (a) and root (b) N concentration of non-grafted, self-grafted and reciprocally-grafted plants of the winter oilseed-rape cultivars NPZ-1 & NPZ-2 (left) and Apex & Capitol (right) grown in hydroponics after 12 days of N starvation (0.1 *mM* N) or optimal N supply (4.0 *mM* N). The plants were pre-cultured for 28 days at 2.0 *mM* N. Different letters on top of the columns indicate differences between the variants (p <0.05). For the ANOVA * indicate significant differences at p <0.001. ns = non-significant. The error bars represent the standard deviations of the means (n = 3 to 4).**

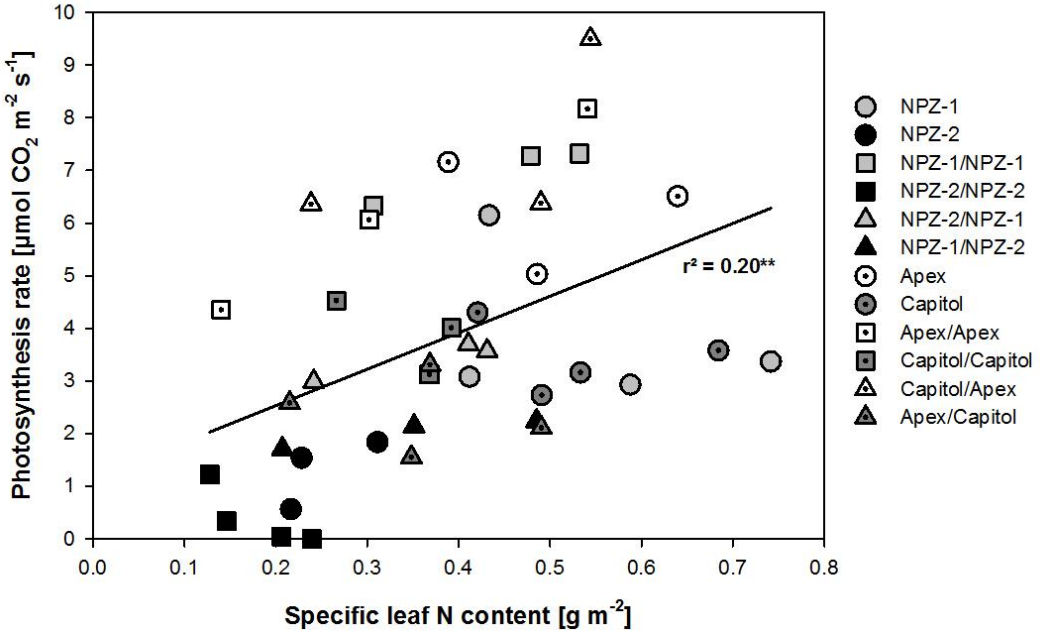

Figure SIII-4 Correlation between specific leaf N content and photosynthesis rate of non-grafted (circles), self-grafted (squares) and reciprocally-grafted (triangles) plants of the winter oilseed-rape cultivars NPZ-1 & NPZ-2 and Apex & Capitol grown in hydroponics after 12 days of N starvation (0.1 *mM* N). The plants were pre-cultured for 28 days at 2.0 *mM* N. For the correlation ** indicate significant differences at p <0.01.

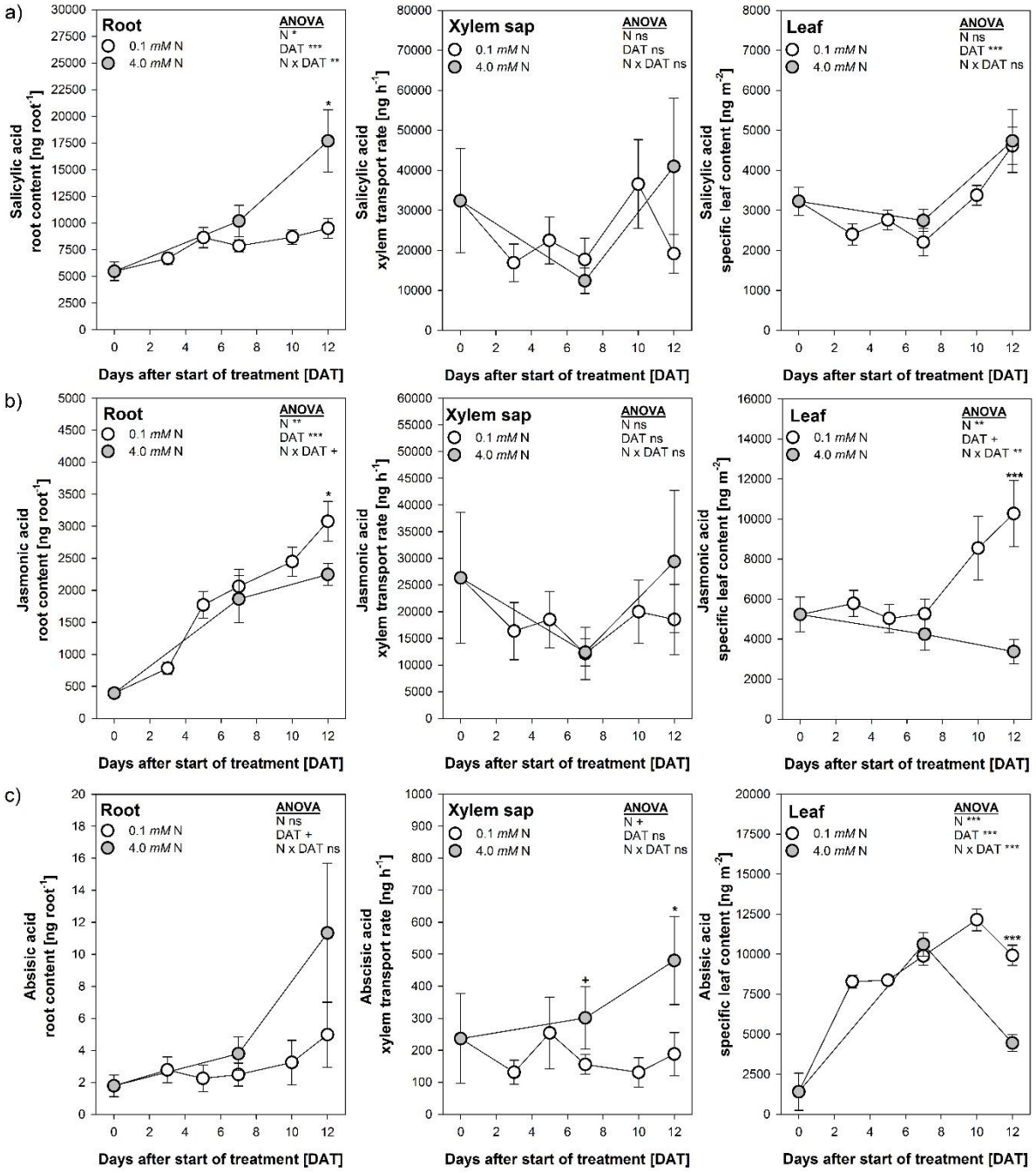

Figure SIII-5 Salicylic acid (a), jasmonic acid (b) and abscisic acid (c) in the root, the xylem sap and the second oldest mature leaf of four winter oilseed-rape cultivars (NPZ-1, NPZ-2, Apex and Capitol; n = 3 to 4) grown in hydroponics during 12 days N starvation (0.1 *mM*) or optimal N supply (4.0 *mM*). The plants were pre-cultured for 28 days at 2.0 *mM* N. For the ANOVA +, *, **, * indicate significant differences at p <0.10, <0.05, <0.01, <0.001, respectively. ns = non-significant. At 7 and 12 DAT +, *, *** indicate significant differences between the N supplies at p <0.10, <0.05 <0.001, respectively. The error bars (visible only when greater than the symbols) represent the standard errors of the means across the four cultivars.**

Table SIII-1 Primer sequences of the genes of interest and the reference gene.

Organism	Gene name	Putitative function	Database	Accession number		Oiligo sequence 5' → 3'
B. napus	*EF1-alpha*	Cell elongation	NCBI	DQ312264	+	AGGTCCACCAACCTTGACTG
					-	CCGTTCCAATACCACCAATC
B. napus	*SAG12-1*	Cysteine protease	NCBI	AF089848	+	TACGTGTAGGATGTTGTTGGGCGT
					-	TGGCCATTATGTGCTCAAACGCAG
B. napus	*IPT2*	Cytokinin synthesis	DFCI	TC151192	+	ACGGGATCAGGGAAATCGAAGC
					-	TTATCTCCACCGGGAAGTGAGACG
B. napus	*IPT5*	Cytokinin synthesis	DFCI	EE560823	+	TTCTTTCGAGATGGATGCAAGTGG
					-	AAGAGGGAGGGTTTGGTTACACG
B. napus	*IPT9*	Cytokinin synthesis	DFCI	TC151289	+	TTCCTGTCGAGTCCACGGATTG
					-	AACTCCATTGGCACCTGAGAGC
A. thaliana	*LOG1*	Cytokinin activation	TAIR	AT2G28305	+	ACTCGGAACCGAACTGGTATC
					-	CATTAAACCAATGCTCCCTCCAC
A. thaliana	*LOG4*	Cytokinin activation	TAIR	AT3G53450	+	GTGGTCGCCATGTTATTGGAG
					-	TGCAACTGCTCTTACTTCTCCTAC
A. thaliana	*LOG5*	Cytokinin activation	TAIR	AT4G35190	+	TAATAGCATGGGCACAACTTGG
					-	ATCCACATTTAACAAACCCACAGG
A. thaliana	*LOG7*	Cytokinin activation	TAIR	AT5G06300	+	TCAATTGGGTAACGAGTTGGTG
					-	TTGAGAGACGAGACCCATAAGC
B. napus	*UGT73C1*	Cytokinin inactivation (reversible)	DFCI	TC139808	+	TATGGAGCATCGGACCGGTTTC
					-	ACCTATGGCCGCCTTATTTCCC
A. thaliana	*UGT73C4*	Cytokinin inactivation? (reversible?)	TAIR	AT2G36770	+	GCGTTCTTGGACGAAATGGTAG
					-	ATAAGCAGGCTCCAACTCCTG
B. napus	*UGT73C5*	Cytokinin inactivation (reversible)	DFCI	TC140686	+	GAAGGTGGTTCTGTGCTCTACG
					-	CTGAGACAGAGGAAGATTGCAGAC
B. napus	*UGT76C1*	Cytokinin inactivation (irreversible)	DFCI	DY007790	+	AACAACTGCGAGAACCCGCTAC
					-	TCTCACCACCTTCCTCTGTTTCTG
B. napus	*UGT85A1*	Cytokinin inactivation (reversible)	DFCI	TC139953	+	GTTTGCTGGTCGGCAAAGAACG
					-	TCGACGTTGGAGAGTCTCTGTG
B. napus	*CKX1*	Cytokinin degradation	DFCI	EV217277	+	TGATGTCCACAACGCGTCCAAG
					-	TGGATGGAGAATTGCCAGAGGTG
B. napus	*CKX2*	Cytokinin degradation	DFCI	TC153766	+	TGTCGACGATGCCGTTTGAC
					-	ACAATGACACTGGAGTTGACTACG
A. thaliana	*CKX3*	Cytokinin degradation	TAIR	AT5G56970	+	CATCGTGTCATCTACTGCCTTG
					-	CGCTTAACTCCTCCATTTCCTC
A. thaliana	*CKX6*	Cytokinin degradation	TAIR	AT1G75450	+	CTGTCCAATGCTGGAATAAGCG
					-	TCCTGTGACAATCTCCAGTTGATG
B. napus	*CKX7*	Cytokinin degradation	DFCI	TC140449	+	ATATCGCCGGGAAGGACTTTGG
					-	ATATCTTCCGGTCCTAGCGGTCTC
A. thaliana	*AHK3*	Cytokinin receptor	TAIR	AT1G27320	+	GCAGATGTTGCAAAGTCACAGTTC
					-	TGCCTGTGCGGTCCTAACATAATC
A. thaliana	*ARR2*	Cytokinin response regulator	TAIR	AT4G16110	+	AAAGAGTGGCGGAGACAGTGAC
					-	GGATGGGATGCCTTCCTGTTTG

Table SIII-2 Statistical comparison of the two grafting experiments for the factors variant, experiment and their interaction for SPAD 12 days after exposure to N starvation. The ANOVA (p <0.05) is based on the ranked values of the replicates (n = 3 to 4).

	Apex & Capitol		NPZ-1 & NPZ-2	
	N [*mM*]			
	0.1	4.0	0.1	4.0
Variant	***	+	***	ns
Experiment	ns	ns	ns	ns
Variant*Experiment	ns	ns	*	ns

Table SIII-3 F-Test for cultivar, N supply, DAT and their interaction on the contents or concentrations of salicylic acid, jasmonic acid and abscisic acid in the root, xylem sap and leaf tissue of the second and third oldest leaves (n = 3 to 4). For the ANOVA: +, *, **, * indicate significant differences at p <0.10, <0.05, <0.01, <0.001, respectively. ns = non-significant. --- not applicable.**

	Salicylic acid			Jasmonic acid			Abscisic acid		
	Root content [ng root^{-1}]	Xylem transport [ng h^{-1}]	Leaf content [ng m^{-2}]	Root content [ng root^{-1}]	Xylem transport [ng h^{-1}]	Leaf content [ng m^{-2}]	Root content [ng root^{-1}]	Xylem transport [ng h^{-1}]	Leaf content [ng m^{-2}]
Cultivar	***	ns	***	***	ns	ns	+	ns	+
N	**	ns	ns	**	ns	**	+	+	***
DAT	***	ns	***	***	ns	*	***	ns	***
Leaf	---	---	***	---	---	---	---	---	ns
Cultivar x N	ns	ns	ns	ns	ns	ns	ns	ns	***
Cultivar x DAT	+	ns	***	ns	ns	ns	**	ns	***
Cultivar x Leaf	---	---	***	---	---	---	---	---	ns
N x DAT	***	ns	*	ns	ns	**	ns	ns	***
N x Leaf	---	---	*	---	---	---	---	---	*
Leaf x DAT	---	---	***	---	---	ns	---	---	***
Cultivar x N x DAT	*	ns	*	ns	ns	+	ns	ns	***
Cultivar x N x Leaf	---	---	ns	---	---	ns	---	---	**
Cultivar x N x DAT x Leaf	---	---	***	---	---	ns	---	---	***
N x DAT x Leaf	---	---	+	---	---	*	---	---	ns

Table SIII-4 S4 F-test for cultivar, N supply and duration of N starvation (DAT) on the contents or concentrations of cytokinins in root, xylem sap and leaf tissue of the second and third oldest leaves (n = 3 to 4). For the ANOVA +, *, **, * indicate significant differences at p <0.10, <0.05, <0.01, <0.001, respectively. ns = non-significant. --- not applicable.**

	Cytokinins					
	Root content [ng root^{-1}]		Xylem transport [ng h^{-1}]		Leaf content [ng m^{-2}]	
	Active	Activatable	Active	Activatable	Active	Activatable
Cultivar	ns	*	ns	*	ns	***
DAT	***	***	ns	ns	+	***
N	ns	**	ns	*	ns	***
Leaf	---	---	---	---	ns	ns
Compound	***	***	***	***	***	***
Cultivar x DAT	ns	ns	ns	***	ns	*
Cultivar x N	ns	ns	ns	+	ns	*
Cultivar x Leaf	---	---	---	---	ns	ns
Cultivar x Compound	ns	*	ns	ns	ns	***
Cultivar x DAT x N	ns	ns	+	**	ns	ns
Cultivar x DAT x Leaf	---	---	---	---	ns	ns
Cultivar x DAT x Compound	ns	ns	ns	**	ns	*
Cultivar x DAT x N x Leaf	---	---	---	---	ns	ns
Cultivar x DAT x N x Compound	ns	ns	ns	**	ns	ns
Cultivar x DAT x N x Leaf x Compound	---	---	---	---	ns	ns
DAT x N	ns	***	ns	ns	ns	**
DAT x Leaf	---	---	---	---	ns	ns
DAT x Compound	***	***	ns	ns	ns	***
DAT x N x Leaf	---	---	---	---	ns	ns
DAT x N Compound	ns	***	ns	ns	ns	**
DAT x N x Leaf x Compound	---	---	---	---	ns	ns
N x Leaf	---	---	---	---	ns	ns
N x Compound	*	**	ns	+	*	***
N x Leaf x Compound	---	---	---	---	ns	ns
Leaf x Compound	---	---	---	---	ns	ns

Supplementary Material for Chapter IV

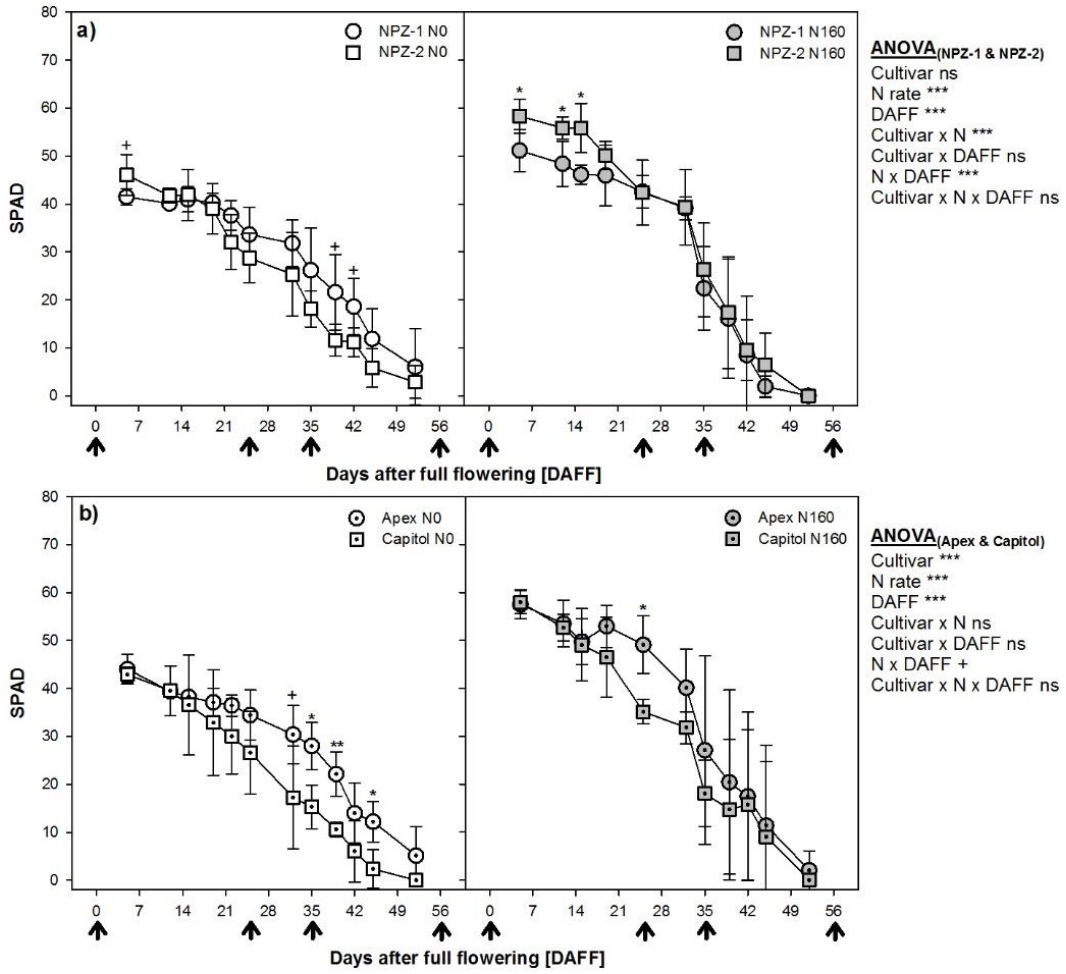

Figure IV-S1 SPAD of leaf position four on the main stem of the oilseed-rape line-cultivars NPZ-1 and NPZ-2 (a) and Apex and Capitol (b) from 5 days after full flowering (BBCH65) until near maturity (BBCH89) as affected by the N fertilization rate (N0, N160). The arrows indicate the developmental stages BBCH65, BBCH69, BBCH79, BBCH89, respectively. For the ANOVA +, * indicate significant differences at p <0.10, 0.001, respectively. ns = non-significant. At the individual DAFF +, *, *** indicate significant differences between the cultivars within the N fertilization rates at p <0.10, 0.05, 0.01, respectively. The error bars (visible only when greater than the symbols) represent the standard deviations of the means (n = 3 to 4).**

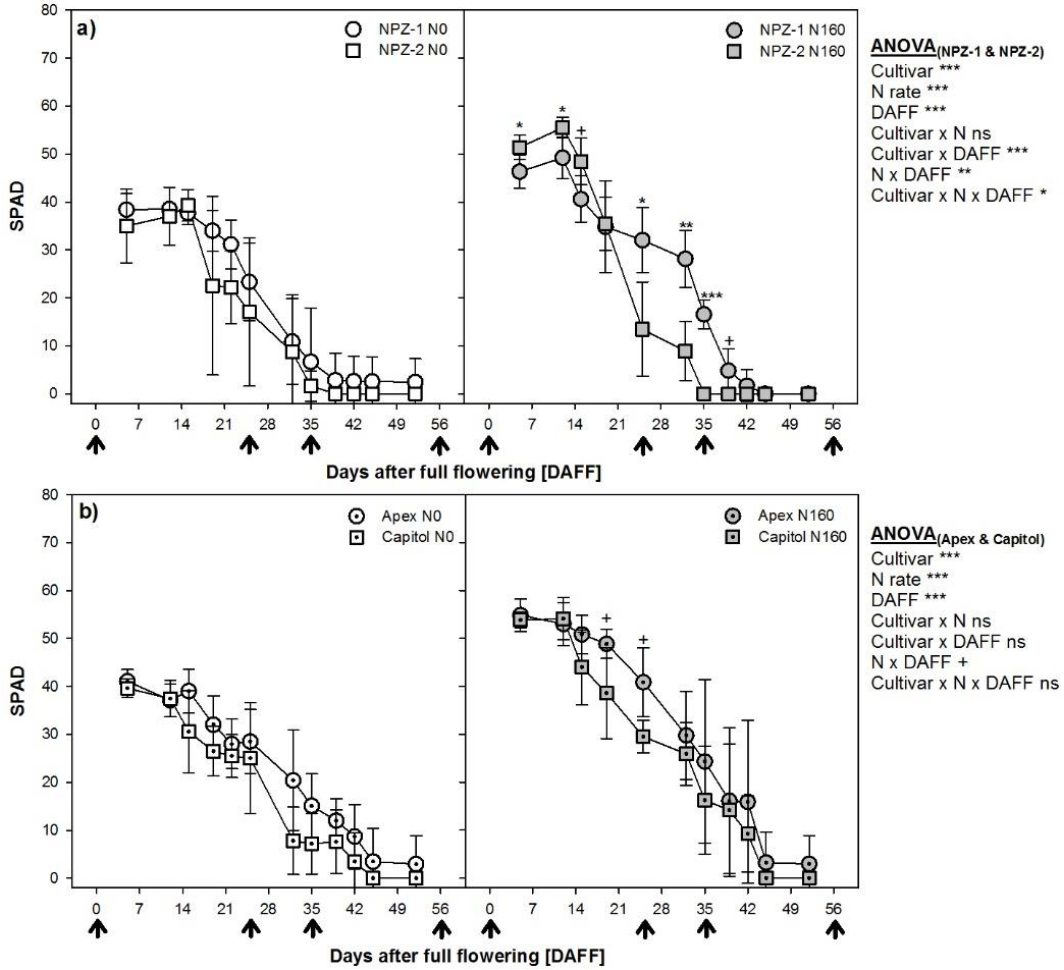

Figure IV-S2 SPAD of leaf position six on the main stem of the oilseed-rape line-cultivars NPZ-1 and NPZ-2 (a) and Apex and Capitol (b) from 5 days after full flowering (BBCH65) until near maturity (BBCH89) as affected by the N fertilization rate (N0, N160). The arrows indicate the developmental stages BBCH65, BBCH69, BBCH79, BBCH89, respectively. For the ANOVA +, *, * indicate significant differences at p <0.10, 0.05, 0.001, respectively. ns = non-significant. At the individual DAFF +, *, **, *** indicate significant differences between the cultivars within the N fertilization rates at p <0.10, 0.05, 0.01, 0.001, respectively. The error bars (visible only when greater than the symbols) represent the standard deviations of the means (n = 3 to 4).**

Curriculum Vitae

Personal data

Name:	Fabian Köslin-Findeklee
Date of Birth:	November 8, 1984
Place of birth:	Hamburg, Germany
Marital Status:	Married
Nationality:	German

Education

2009 - 2014	PhD. Gottfried Wilhelm Leibniz University of Hannover, Faculty of Natural Science, Institute of Plant Nutrition, Hannover, Germany.
2007 - 2009	Master of Science, Horticulture science, Gottfried Wilhelm Leibniz University of Hannover, Hannover, Germany.
2004 - 2007	Bachelor of Science, Horticulture science, Gottfried Wilhelm Leibniz University of Hannover, Hannover, Germany.
1995 - 2004	Gymnasium Marienthal, Hamburg, Germany.
1991 - 1995	Grundschule Sterntalerstraße, Hamburg, Germany.

List of Publications

Publications in peer-reviewed journals

2015 Koeslin-Findeklee, F., Safavi Rizi, V., Becker, M. A., Parra-Londono, S., Arif, M., Balazadeh, S., Mueller-Roeber, B., Kunze, R. and Horst, W. J. (2015): Transcriptomic analysis of nitrogen starvation- and cultivar-specific leaf senescence in winter oilseed rape (*Brassica napus* L.). Plant Science doi: 10.1016/j.plantsci.2014.11.018.

2014 Koeslin-Findeklee, F., Meyer, A., Girke, A., Beckmann, K. and Horst, W. J. (2014): The superior nitrogen efficiency of winter oilseed rape (*Brassica napus* L.) hybrids is not related to delayed nitrogen starvation-induced leaf senescence. Plant and Soil 384, 347-362.

Scientific presentations

2014 Doctoral Researcher's Conference of GRK1798 "Signaling at the Plant-Soil Interface", 1st to 2nd October 2014, Bad Bevensen, Germany: Köslin-Findeklee, F. and Horst, W. J.: Are differences between oilseed-rape (*Brassica napus* L.) cultivars in nitrogen starvation-induced leaf senescence governed by leaf-inherent and/or root-derived signals?

2014 International Conference of the German Society of Plant Nutrition, 10th to 12th September 2014, Halle, Germany: Horst, W. J. and Köslin-Findeklee, F.: Genotypic differences in nitrogen efficiency of winter oilseed-rape (*Brassica napus* L.).

2013 6th European Workshop on Leaf Senescence, 14th to 18th October 2013, Versailles, France.: Köslin-Findeklee, F., Becker, M. A. Schulte auf'm Erley, G., Kunze, R., Balazadeh, S., Müller-Röber, B. and Horst, W. J.: The role of leaf senescence for genotypic differences in nitrogen efficiency of winter oilseed rape (*Brassica napus* L.).

2013 125. VDLUFA Kongress, 17th to 20th September 2013, Berlin, Germany: Köslin-Findeklee, F. and Horst, W. J.: Die Bedeutung der Blattseneszenz für Unterschiede in der Stickstoffeffizienz von Winterraps (*Brassica napus* L.).

2013 National Conference of the German Society of Plant Nutrition, 9th to 10th May 2013, Freising-Weihenstephan, Germany: Köslin-Findeklee, F. Schulte auf'm Erley, G. and Horst, W. J.: The role of leaf senescence for genotypic differences in nitrogen efficiency in winter oilseed-rape (*Brassica napus* L.).

2011 Colloquium of Plant Sciences, 8th February 2011, Graz, Austria: Köslin-Findeklee, F. and Horst, W. J.: The role of leaf senescence for genotypic differences in nitrogen efficiency of winter oilseed-rape (*Brassica napus* L.).

Poster presentations

2014 International Conference of the German Society of Plant Nutrition, 10th to 12th September 2014, Halle, Germany: Köslin-Findeklee, F., Becker, M. A., Roitsch, T. and Horst, W. J.: Differences in nitrogen starvation-induced leaf senescence between winter oilseed-rape cultivars are governed by leaf-inherent rather than by root-mediated factors.

2013 National Conference of the German Society of Plant Nutrition, 9th to 10th May 2013, Freising-Weihenstephan, Germany: Becker, M. A., Köslin-Findeklee, F. and Horst, W. J.: Identification of marker genes specific for nitrogen starvation induced leaf senescence and suitable to detected genotypic differences in oilseed rape (*Brassica napus* L.).

2012 International Conference of the German Society of Plant Nutrition, 5th to 8th September 2012, Bonn, Germany: Köslin-Findeklee, F., Balazadeh, S., Müller-Röber, B. and Horst W. J.: The role of transcription factors for genotypic differences in nitrogen deficiency-induced leaf senescence in oilseed rape (*Brassica napus* L.).

2012 International Conference of the German Society of Plant Nutrition, 5th to 8th September 2012, Bonn, Germany: Becker, M. A., Meyer, A., Köslin-Findeklee, F. and Horst, W. J.: Role of leaf-inherent and root-localized factors for genotypic differences in nitrogen deficiency-induced leaf senescence in oilseed rape (*Brassica napus* L.).

2012 National Conference of the Austraian Society of Plant Biology, 7th to 10th June 2012, Lienz, Austria: Luschin-Ebengreuth, N., Köslin-Findeklee, F., Pfeifhofer, H., Franzaring J., Fangmeier, A., Horst, W. J. and Roitsch, T.: Relation between metabolic control of leaf senescence by carbohydrates and nitrogen metabolism.

2011 Joint National Conference of the German Society of Plant Nutrition and the Society of Crop Sciences, 27th to 29th September 2011, Kiel, Germany: Köslin-Findeklee, F., Parra-Londono, S., Luschin-Ebengreut, N., Schulte auf'm Erley, G., Roitsch, T. and Horst, W. J.: The role of salicylic acid in the onset and development of leaf senescence under N starvation in winter oilseed-rape (*Brassica napus* L.) genotypes differing in N efficiency.

Acknowledgement

First of all, I would like to express my heartfelt gratitude to **Prof. Dr. Walter J. Horst**, for giving me the opportunity to study in the Institute of Plant Nutrition and specifically to work on an interesting project in such a dynamic subject. His inspiring enthusiasm, tireless supervision, kind and manifold supports through all stages of my study have helped me to successfully accomplish this work.

I am grateful to **Prof. Dr. Thomas Roitsch** and **Prof. Dr. Nicolaus von Wirén** for their willingness to be the co-referees. In the same way I am also grateful to **Prof. Dr. Hans-Peter Braun** and **Prof. Dr. Manfred K. Schenk** for pleasantly accepting the request to be examiners.

Many thanks to **Martin A. Becker, Andreas Meyer**, **Markus Niehaus**, **Sebastian Parra-Londono** and **Maike Stumpf,** who contributed with their B. Sc. and M. Sc. theses to the completion of my work.

In the same way I am thankful to **Hartmut Wieland** and **Änne Blanke** for their excellent technical support.

Also many thanks to **Ingrid Dusy** for her excellent support of administrative matters.

I also thank all colleagues particularly **Martin Duschyk** of the Institute of Plant Nutrition for sharing good time together during the last five years.

I extend my thanks to all cooperators within the **Deutsche Forschungsgemeinschaft** research group **DFG948** "Nitrogen uptake, metabolism and remobilization in leaves during plant senescence", particularly **Prof. Dr. Reinhard Kunze** (Institute of Biology, Free University Berlin) for supporting and enable the microarray analysis, **Prof. Dr. Bernd Müller-Röber**, **Dr. Salma Balazadeh** and **Dr. Muhammad Arif** (Max-Planck-Institute of Molecular Plant Physiology, Potsdam) for supporting and enable the qRT-PCR platform, **Prof. Dr. Thomas Roitsch** and **PD Dr. Eric van der Graaff** (Department of Plant and Environmental Sciences, University Copenhagen) for phytohormone analysis, **Dr. Amine Abbadi**, **Dr. Andreas Girke** (Norddeutsche Pflanzenzucht Hans-Georg Lembke KG) and **Dr. Gerhard Baumgärtel** (Landwirtschaftskammer Niedersachsen) for execution of the field experiments.

Finally, I would like to thank my parents **Ute** and **Armin Köslin** and my brother **Florian Köslin** for giving me a constant support. Last but not least, my special thanks and lots of love go to my wife, **Katharina Findeklee**, for her love, patience, understanding, constant support and encouragement during the whole study period.

Erklärung zur Dissertation

gemäß §6(1) der Promotionsordnung der Naturwissenschaftlichen Fakultät der Gottfried Wilhelm Leibniz Universität Hannover für die Promotion zum Dr. rer. nat.

Hierdurch erkläre ich, dass ich meine Dissertation mit dem Titel:

The Role of Leaf Senescence in Relation to Nitrogen Uptake and Translocation to the Reproductive Plant Organs for Cultivar Differences in Nitrogen Efficiency in Winter Oilseed-Rape (*Brassica napus* L.)

selbständig verfasst und die benutzten Hilfsmittel und Quellen sowie gegebenenfalls die zu Hilfeleistungen herangezogenen Institutionen vollständig angegeben habe. Die Dissertation wurde nicht schon als Masterarbeit, Diplomarbeit oder andere Prüfungsarbeit verwendet.

_____.

(Unterschrift)